

Inverse Problems and Data Assimilation

With Connections to Machine Learning

Daniel Sanz-Alonso [‡], Andrew Stuart [#] and Armeen Taeb [‡]

[‡] Department of Statistics, University of Chicago

[#] Department of Computing and Mathematical Sciences, Caltech

[‡] Seminar for Statistics, ETH Zürich

Introduction

Overview of the Notes

The aim of these notes is to provide a clear and concise mathematical introduction to the subjects of Inverse Problems and Data Assimilation, and their inter-relations, together with bibliographic pointers to literature in this area that goes into greater depth. The target audiences are advanced undergraduates and beginning graduate students in the mathematical sciences, together with researchers in the sciences and engineering who are interested in the systematic underpinnings of methodologies widely used in their disciplines. The notes were first developed out of Caltech course ACM 159 (now ACM/IDS 154) in Fall 2017, substantially modified for the University of Chicago course STAT 31550 in Winter 2019, and now the notes form the basis of courses taught regularly in both institutions.

In its most basic form, inverse problem theory is the study of how to estimate model parameters from data. Often the data provide indirect information about these parameters, corrupted by noise. The theory of inverse problems, however, is much richer than just parameter estimation. For example, the underlying theory can be used to determine the effects of noisy data on the accuracy of the solution; it can be used to determine what kind of observations are needed to accurately determine a parameter; and it can be used to study the uncertainty in a parameter estimate and, relatedly, is useful, for example, in the design of strategies for control or optimization under uncertainty, and for risk analysis. The theory thus has applications in many fields of science and engineering.

To apply the ideas in these notes, the starting point is a mathematical model mapping the unknown parameters to the observations: termed the “forward” or “direct” problem, and often a subject of research in its own right. A good forward model will not only identify how the data is dependent on parameters, but also what sources of noise or model uncertainty are present in the postulated relationship between unknown parameters and data. For example, if the desired forward problem cannot be solved analytically, then the forward model may be approximated by a simulation; in this case, discretization may be considered as a source of error. Once a relationship between model parameters, sources of error, and data is clearly defined, the inverse problem of estimating parameters from data can be addressed. The theory of inverse problems can be separated into two cases: (1) the ideal case where data is not corrupted by noise and is derived from a known perfect model; and (2) the practical case where data is incomplete and imprecise. The first case is useful for classifying inverse problems and determining if a given set of observations can, in principle, allow to fully reconstruct the model parameters; this provides insight into conditions needed for existence, uniqueness, and stability of a solution to the inverse problem. The second case is useful for the formulation of practical algorithms to learn about parameters, and uncertainties in their estimates, and will be the focus of these notes.

A model for which a solution exists, is unique, and changes continuously with input (stability) is termed “well-posed”. Conversely, a model lacking any of these properties is termed “ill-posed”. Ill-posedness is present in many inverse problems, and mitigating it

is an extensive part of the subject. Out of the different approaches to formulating an inverse problem, the Bayesian framework is arguably the most fundamental, and we adopt it in these notes. The goal of the Bayesian framework is to find a probability measure that assigns a probability to each possible solution for a parameter u , given the data y . Bayes formula states that

$$\mathbb{P}(u|y) = \frac{1}{\mathbb{P}(y)} \mathbb{P}(y|u) \mathbb{P}(u).$$

It enables calculation of the posterior probability on $u|y$, $\mathbb{P}(u|y)$, in terms of the product of the data likelihood $\mathbb{P}(y|u)$ and the prior information on the parameter encoded in $\mathbb{P}(u)$. The likelihood describes the probability of the observed data y , if the input parameter were set to be u ; it is determined by the forward model, and the structure of the noise. The normalization constant $\mathbb{P}(y)$ ensures that $\mathbb{P}(u|y)$ is a probability measure. There are four primary benefits to this framework: (1) it provides a clear theoretical setting in which the forward model choice, the description of how noise enters the data and the forward model, and a priori information on the unknown parameter are all explicit; (2) it provides information about the entire solution space for possible input parameter choices; (3) it naturally leads to quantification of uncertainty and risk in parameter estimates; (4) it is generalizable to a wide class of inverse problems, in finite and infinite dimension, and comes with a well-posedness theory mitigating the ill-posedness of a naive deterministic approach.

The first part of the notes is dedicated to studying the Bayesian framework for inverse problems. Techniques such as importance sampling and Markov Chain Monte Carlo (MCMC) methods are introduced; these methods have the desirable property that in the limit of an infinite number of samples they reproduce the full posterior distribution. Since it is often computationally intensive to implement these methods, especially in high-dimensional problems, techniques to approximate the posterior by a Dirac or a Gaussian distribution are also discussed, along with related optimization algorithms to determine the best approximation.

The second part of the notes covers data assimilation. This refers to a particular class of inverse problems in which the unknown parameter is the initial condition of a dynamical system or, in the case of stochastic dynamics, the entire sequence of subsequent states of the system, and the data comprises partial and noisy observations of the (possibly stochastic) dynamical system. A primary use of data assimilation is in forecasting, where the purpose is to provide better future estimates than can be obtained using either the data or the model alone. All the methods from the first part of the course may be applied directly, but there are other new methods which exploit the Markovian structure to update the state of the system sequentially, rather than to learn about the initial condition. (But of course knowledge of the initial condition may be used to inform the state of the system at later times.)

The third and final part of the notes describes various topics which blend the theory of inverse problems, data assimilation, and machine learning. We show how to design methods for generic inverse problems by building on some of the data assimilation ideas studied in the second part of the notes. Furthermore, whilst ideas from machine

learning appear in the first two parts of the notes, the final part overviews the main ways in which machine learning is impacting on, and has the potential to impact on, both the subjects of inverse problems and data assimilation.

Notation

Throughout the notes we use \mathbb{N} to denote the positive integers $\{1, 2, 3, \dots\}$, and \mathbb{Z}^+ to denote the non-negative integers $\mathbb{N} \cup \{0\} = \{0, 1, 2, 3, \dots\}$. The symbol I_d denotes the identity matrix on \mathbb{R}^d , and Id denotes the identity mapping. We use $|\cdot|$ to denote the Euclidean norm corresponding to the inner-product $\langle a, b \rangle = a^\top b$; we also use the notation $|\cdot|$ to denote the induced norm on matrices.

A symmetric matrix A is positive definite (resp. positive semi-definite) if $\langle u, Au \rangle$ is positive (resp. non-negative) for all $u \neq 0$. This will sometimes be denoted by $A > 0$ (resp. $A \geq 0$). For $A > 0$, we denote by $|\cdot|_A$ the weighted norm defined by $|v|_A^2 = v^\top A^{-1}v$. The corresponding weighted Euclidean inner-product is given by $\langle \cdot, \cdot \rangle_A$ and $\langle \cdot, A^{-1}\cdot \rangle$. We use \otimes to denote the outer product between two vectors: $(a \otimes b)c = \langle b, c \rangle a$. We let $B(u, \delta)$ denote the open ball of radius δ at u , in the Euclidean norm. We also use \det and Tr to denote the determinant and trace functions on matrices.

Throughout we denote by $\mathbb{P}(\cdot)$, $\mathbb{P}(\cdot | \cdot)$ the probability density function (pdf) of a random variable and its conditional pdf, respectively. We write

$$\rho(f) = \mathbb{E}^\rho[f] = \int_{\mathbb{R}^d} f(u) \rho(u) du$$

to denote expectation of $f : \mathbb{R}^d \mapsto \mathbb{R}$ with respect to pdf ρ on \mathbb{R}^d . The distribution of the random variables in these notes will often have density with respect to Lebesgue measure, but occasional use of Dirac masses will be required; we will use the notational convention that Dirac mass at point v has “density” $\delta(\cdot - v)$, also denoted by $\delta_v(\cdot)$. When a random variable u has pdf ρ we will write $u \sim \rho$. We use \Rightarrow to denote weak convergence of probability measures, that is, $\rho_n \Rightarrow \rho$ if $\rho_n(f) \rightarrow \rho(f)$ for all bounded and continuous $f : \mathbb{R}^d \mapsto \mathbb{R}$.

Acknowledgments

These notes were created in L^AT_EX by the students in ACM 159, based on lectures presented by the instructor Andrew Stuart, and on input from the course TA Armeen Taeb. The authors are very grateful to these students, without whom the notes would not exist. The individuals responsible for typesetting the notes, listed in alphabetic order, are: Blancquart, Paul; Cai, Karena; Chen, Jiajie; Cheng, Richard; Cheng, Rui; Feldstein, Jonathan; Huang, De; Idíni, Benjamin; Kovachki, Nikola; Lee, Marcus; Levy, Gabriel; Li, Liuchi; Muir, Jack; Ren, Cindy; Seylabi, Elnaz; Schäfer, Florian; Singhal, Vipul; Stephenson, Oliver; Song, Yichuan; Su, Yu; Teke, Oguzhan; Williams, Ethan; Wray, Parker; Zhan, Eric; Zhang, Shumao; Xiao, Fangzhou. Furthermore, the following students added content to the notes, beyond the materials presented by the instructors: Parker Wray – the Overview; Jiajie Chen – alternative proof of early presentations of under-determined inverse problems and smoothing in Gaussian data assimilation; Fangzhou Xiao – numerical simulation of prior, likelihood and

posterior; Elnaz Seylabi and Fangzhou Xiao – catching typographical errors in an early draft of these notes; Cindy Ren – numerical simulations to enhance understanding of importance sampling; Cindy Ren and De Huang – improving the constants in initial presentations of the approximation error of importance sampling; Richard Cheng and Florian Schäfer – illustrations to enhance understanding of the coupling argument used to study convergence of MCMC algorithms by presenting the finite state-space case; and Ethan Williams and Jack Muir – numerical simulations and illustrations of ensemble Kalman filter and extended Kalman filter that appeared in an eaerly version of these notes. The authors are also grateful to Tapio Helin (LUT University) who used the notes in his own course and provided very helpful feedback on an early draft. Finally the authors are thankful to Yuming Chen, Ruoxi Jiang, Phillip Lo, and Walter Zhang (University of Chicago) and Eitan Levin (Caltech) for their generous feedback, and to Hwanwoo Kim (University of Chicago) for making substantial improvements to the figures.

The work of Daniel Sanz-Alonso has been funded by DOE, NGIA, and NSF (USA) and by FBBVA (Spain). The work of Andrew Stuart has been funded by AFOSR, ARL, NIH, NSF, and ONR (USA), by EPSRC (UK), and by ERC (EU). The work of Armeen Taeb has been funded by the Resnick Fellowship (USA) and by the ETH Foundations of Data Science (Switzerland). This funded research has helped to shape the presentation of the material and is gratefully acknowledged.

Warning and Request This is a near-final version of a set of notes that the authors aim to publish in book form. Nonetheless, these notes are likely to contain mathematical errors, incomplete bibliographical information, inconsistencies in notation, and typographical errors. The authors would be extremely grateful for all feedback that might help eliminate any of these issues.

Contents

I	Inverse Problems	11
1	Bayesian Inverse Problems and Well-Posedness	13
1.1	Formulation of Bayesian Inverse Problems	13
1.2	Formula for Posterior pdf: Bayes Theorem	14
1.3	Well-Posedness of Bayesian Inverse Problems	17
1.3.1	Metrics on Probability Densities	18
1.3.2	Approximation Theorem	21
1.3.3	Example: Well-Posedness for Parameter Estimation in an ODE	23
1.4	Discussion and Bibliography	26
2	The Linear-Gaussian Setting	29
2.1	Derivation of the Posterior Distribution	29
2.2	Small Noise Limit of the Posterior Distribution	31
2.2.1	Overdetermined Case	32
2.2.2	Determined Case	34
2.2.3	Underdetermined Case	35
2.3	Discussion and Bibliography	37
3	Optimization Perspective	39
3.1	The Setting	39
3.2	Theory	41
3.3	Examples	42
3.4	Gradient-Based Optimization Algorithms	46
3.4.1	Gradient Flow	46
3.4.2	Gradient Descent	46
3.4.3	Stochastic Gradient Descent	49
3.5	Discussion and Bibliography	53
4	Gaussian Approximation	55
4.1	The Kullback-Leibler Divergence	55
4.2	Best Gaussian Fit by Minimizing $d_{\text{KL}}(p \pi)$	57
4.3	Best Gaussian Fit by Minimizing $d_{\text{KL}}(\pi p)$	59

4.4	Comparison between $d_{\text{KL}}(\pi p)$ and $d_{\text{KL}}(p \pi)$	60
4.5	Variational Formulation of Bayes Theorem	61
4.6	Discussion and Bibliography	62
5	Monte Carlo Sampling and Importance Sampling	65
5.1	Monte Carlo Sampling	66
5.2	Importance Sampling	70
5.3	Discussion and Bibliography	75
6	Markov Chain Monte Carlo	77
6.1	Markov Chains in \mathbb{R}^d	77
6.2	Markov Chain Sampling	79
6.3	Metropolis-Hastings Sampling	81
6.4	Invariance of the Target Distribution π	83
6.4.1	Detailed Balance and its Implication	83
6.4.2	Detailed Balance and the Metropolis-Hastings Algorithm	83
6.5	Convergence to the Target Distribution	84
6.5.1	Finite State-Space	85
6.5.2	The pCN Method	87
6.6	Discussion and Bibliography	91
II	Data Assimilation	93
7	Filtering and Smoothing Problems and Well-Posedness	95
7.1	Formulation of Filtering and Smoothing Problems	95
7.2	The Smoothing Problem	96
7.2.1	Formulation as an Inverse Problem	96
7.2.2	Formula for pdf of the Smoothing Problem	97
7.2.3	Well-Posedness of the Smoothing Problem	98
7.3	The Filtering Problem	99
7.3.1	Formula for pdf of the Filtering Problem	99
7.3.2	Well-Posedness of the Filtering Problem	101
7.3.3	Roadmap to Discrete Filtering Methods	101
7.4	Discussion and Bibliography	102
8	The Linear-Gaussian Setting	105
8.1	Kalman Filter	105
8.1.1	Kalman Filter: Algorithmic Implementation	108
8.1.2	Optimization Perspective: Mean of Kalman Filter	109
8.1.3	Optimality of Kalman Filter	111
8.2	Kalman Smoother	111
8.2.1	Defining Linear System	111
8.2.2	Kalman Smoother: Solution of the Linear System	113
8.3	Discussion and Bibliography	115

9	Optimization for Filtering and Smoothing: 3DVAR and 4DVAR	117
9.1	The Setting	117
9.2	3DVAR	118
9.2.1	3DVAR: Algorithmic Implementation	118
9.2.2	3DVAR: Long-Time Accuracy	119
9.3	4DVAR	121
9.4	Discussion and Bibliography	123
10	The Extended and Ensemble Kalman Filters	125
10.1	The Setting	125
10.2	The Extended Kalman Filter	126
10.3	Ensemble Kalman Filter	128
10.3.1	Algorithmic Implementation of EnKF	129
10.3.2	Subspace Property of EnKF	131
10.4	Discussion and Bibliography	132
11	Particle Filter	135
11.1	The Setting	135
11.2	The Bootstrap Particle Filter	136
11.3	Bootstrap Particle Filter Convergence	138
11.4	The Bootstrap Particle Filter as a Random Dynamical System	141
11.5	Discussion and Bibliography	142
12	Optimal Particle Filter	143
12.1	The Bootstrap and Optimal Particle Filters Compared	143
12.2	Implementation: Linear Observation Setting	146
12.3	“Optimality” of the Optimal Particle Filter	148
12.4	Discussion and Bibliography	151
III	Blending Inverse Problems, Data Assimilation, and Machine Learning	153
13	Blending Inverse Problems and Data Assimilation	155
13.1	Problem Setting and Objective Functions	155
13.2	Nonlinear-Least Squares Optimization	156
13.2.1	Gauss-Newton Method	156
13.2.2	Levenberg-Marquardt Method	157
13.3	Extended Kalman Methods	159
13.3.1	Iterative Extended Kalman Filter (IExKF)	160
13.3.2	Extended Kalman Inversion (ExKI)	161
13.3.3	Tikhonov Extended Kalman Inversion (TExKI)	162
13.4	Ensemble Kalman Methods	164
13.4.1	Iterative Ensemble Kalman Filter with Statistical Linearization (IEnKF-SL)	165

13.4.2	Ensemble Kalman Inversion with Statistical Linearization (EnKI-SL)	166
13.4.3	Tikhonov Ensemble Kalman Inversion with Statistical Linearization (TEnKI-SL)	167
13.5	Discussion and Bibliography	168
14	Blending Inverse Problems and Machine Learning	173
14.1	Supervised Learning	173
14.1.1	Neural Networks	174
14.1.2	Random Features	175
14.1.3	Gaussian Processes	176
14.1.4	Approximation Properties	178
14.2	Unsupervised Learning	178
14.2.1	Optimal Transport Maps	178
14.2.2	Other Transport Approaches	180
14.2.3	Autoencoders	181
14.2.4	Variational Autoencoders	182
14.2.5	Generative Adversarial Networks	184
14.2.6	Normalizing Flows	184
14.3	Learning the Forward Map	186
14.4	Learning the Prior	188
14.5	Learning the Prior to Posterior Map	190
14.6	Discussion and Bibliography	190
15	Blending Data Assimilation and Machine Learning	193
15.1	The Setting	193
15.2	The Expectation-Maximization Framework	195
15.3	Auto-Differentiable Kalman Filters	200
15.4	Discussion and Bibliography	201
	Bibliography	205
	Alphabetical Index	229

Part I

Inverse Problems

Chapter 1

Bayesian Inverse Problems and Well-Posedness

In this chapter we introduce the Bayesian approach to inverse problems in which the unknown parameter and the observed data are viewed as random variables. In this probabilistic formulation, the solution of the inverse problem is the posterior distribution on the parameter given the data. We will show that the Bayesian formulation leads to a form of well-posedness: small perturbations of the forward model or the observed data translate into small perturbations of the posterior distribution. Well-posedness requires a notion of distance between probability measures. We introduce the total variation and Hellinger distances, giving characterizations of them, and bounds relating them, that will be used throughout these notes. We prove well-posedness in the Hellinger distance.

The chapter is organized as follows. Section 1.1 introduces the formulation of Bayesian inverse problems. In Section 1.2 we derive a formula for the posterior pdf and explain how several estimators for the unknown parameter can be obtained using the posterior. Section 1.3 describes the well-posedness of the Bayesian formulation together with the necessary background on distances between probability measures. The chapter closes with bibliographical remarks in Section 1.4.

1.1 Formulation of Bayesian Inverse Problems

We consider the following setting. We let $G : \mathbb{R}^d \rightarrow \mathbb{R}^k$ define the forward model and aim to recover an unknown parameter $u \in \mathbb{R}^d$ from data $y \in \mathbb{R}^k$ given by

$$y = G(u) + \eta, \tag{1.1}$$

where $\eta \in \mathbb{R}^k$ represents observation noise. We view $(u, y) \in \mathbb{R}^d \times \mathbb{R}^k$ as a random variable, whose distribution is specified by means of the following assumption on the distribution of $(u, \eta) \in \mathbb{R}^d \times \mathbb{R}^k$ and the relationship between u , y and η postulated in equation (1.1).

Assumption 1.1. *The distribution of the random variable $(u, \eta) \in \mathbb{R}^d \times \mathbb{R}^k$ is defined by:*

- $u \sim \rho(u), u \in \mathbb{R}^d$.
- $\eta \sim \nu(\eta), \eta \in \mathbb{R}^k$.
- u and η are independent, written $u \perp \eta$.

Here ρ and ν describe the pdfs of the random variables u and η , respectively. Then $\rho(u)$ is called the *prior* pdf and, for each fixed $u \in \mathbb{R}^d$, $y|u \sim \nu(y - G(u))$ determines the *likelihood* function. In this probabilistic perspective, the solution to the inverse problem is the conditional distribution of u given y , which is called the *posterior* distribution, and will be denoted by $u|y \sim \pi^y(u)$. The posterior pdf determines, for any candidate parameter value in \mathbb{R}^d , how probable that parameter is, based on prior assumptions and the link between parameter and data, all expressed probabilistically. In particular, the posterior contains information about the level of uncertainty in the parameter recovery: for instance, large posterior covariance typically indicates that the data contains insufficient information to accurately recover the input parameter.

1.2 Formula for Posterior pdf: Bayes Theorem

Bayes theorem is a bridge connecting the prior, the likelihood and the posterior.

Theorem 1.2 (Bayes Theorem). *Let Assumption 1.1 hold, and assume that*

$$Z = Z(y) := \int_{\mathbb{R}^d} \nu(y - G(u)) \rho(u) du > 0.$$

Then $u|y \sim \pi^y(u)$, where

$$\pi^y(u) = \frac{1}{Z} \nu(y - G(u)) \rho(u). \quad (1.2)$$

Proof. Denote by $\mathbb{P}(\cdot)$ the pdf of a random variable and by $\mathbb{P}(\cdot|\cdot)$ its conditional pdf. We have

$$\begin{aligned} \mathbb{P}(u, y) &= \mathbb{P}(u|y) \mathbb{P}(y), \text{ if } \mathbb{P}(y) > 0, \\ \mathbb{P}(u, y) &= \mathbb{P}(y|u) \mathbb{P}(u), \text{ if } \mathbb{P}(u) > 0. \end{aligned}$$

Note that the marginal pdf on y is given by

$$\begin{aligned} \mathbb{P}(y) &= \int_{\mathbb{R}^d} \mathbb{P}(u, y) du \\ &= \int_{\mathbb{R}^d} \mathbb{P}(y|u) \mathbb{P}(u) du = Z > 0. \end{aligned}$$

Then

$$\mathbb{P}(u|y) = \frac{1}{\mathbb{P}(y)} \mathbb{P}(y|u) \mathbb{P}(u) = \frac{1}{\mathbb{P}(y)} \nu(y - G(u)) \rho(u) \quad (1.3)$$

for both $\mathbb{P}(u) = \rho(u) > 0$ and $\mathbb{P}(u) = \rho(u) = 0$. \square

We will often denote the likelihood function by $l(u) := \nu(y - G(u))$. We then write

$$\pi^y(u) = \frac{1}{Z} l(u) \rho(u),$$

omitting the data y in the likelihood function; when no confusion arises we will also simply write $\pi(u)$ for the posterior pdf, rather than $\pi^y(u)$.

Remark 1.3. The proof of Theorem 1.2 shows that in order to apply Bayes formula (1.2) one needs to guarantee that the normalizing constant $\mathbb{P}(y) = Z$ is positive; in other words, the marginal density of the observed data y needs to be positive. This is simply the natural assumption that the observed data could indeed have been observed, given the probabilistic conditions in Assumption 1.1. From now on it will be assumed without further notice that $\mathbb{P}(y) = Z > 0$. Finally, we remark that throughout these notes we will denote normalizing constants generically by Z , and depending on the context the normalizing constant may sometimes be interpreted as the marginal density of an underlying data set. \diamond

The posterior distribution $\pi^y(u)$ contains all the knowledge on the parameter u available in the prior and the data. In applications it is often useful, however, to summarize the posterior distribution through a few numerical values. Summarizing the posterior is particularly important if the parameter is high-dimensional, since then visualizing the posterior or detecting regions of high posterior probability is nontrivial. Two natural numerical summaries are the posterior mean and the posterior mode.

Definition 1.4. The *posterior mean estimator* of u given data y is the mean of the posterior distribution:

$$u_{\text{PM}} = \int_{\mathbb{R}^d} u \pi^y(u) du.$$

The *maximum a posteriori (MAP) estimator* of u given data y is the mode of the posterior distribution $\pi^y(u)$, defined as

$$u_{\text{MAP}} = \arg \max_{u \in \mathbb{R}^d} \pi^y(u).$$

\diamond

This maximum may not be uniquely defined, in which case we talk about *a*, rather than *the*, MAP estimator.

The importance of the MAP and the posterior mean already suggest the need to compute maxima (for the MAP estimator) and integrals (for the posterior mean) in order to extract actionable information from the Bayesian formulation of inverse problems and data assimilation. For this reason, optimization (to compute maxima) and sampling (to compute integrals) will play an important role in these notes. In practice it is often useful to quantify the uncertainty in the parameter reconstruction, and numerical summaries such as the posterior mean and the MAP estimators can be complemented by credible intervals, that is, parameter regions of prescribed posterior probability. In order to make tractable the computation of estimators and credible intervals, the posterior can be approximated by a simple distribution, such as a Gaussian or a Gaussian mixture; optimization can be used to determine such approximations. In a similar spirit, sampling may be viewed as approximating the posterior by a combination of Dirac masses to enable computation of integrals. An optimization perspective for inverse problems and data assimilation will be studied in Chapters 3 and 9, respectively, and Gaussian approximations will be discussed in Chapters 4 and 10, respectively; Dirac

approximations constructed via sampling will be studied in Chapters 5 and 6 (inverse problems) and in Chapters 11 and 12 (data assimilation).

We next consider two simple examples of a direct application of Bayes theorem.

Example 1.5 (MAP and Posterior Mean Estimators). Let $d = k = 1$, $\eta \sim \nu = \mathcal{N}(0, \gamma^2)$, and let

$$\rho(u) = \begin{cases} \frac{1}{2}, & u \in (-1, 1), \\ 0, & u \in (-1, 1)^c. \end{cases}$$

Suppose that the observation is generated by $y = u + \eta$. Using Bayes Theorem 1.2, we derive the posterior pdf

$$\pi^y(u) = \begin{cases} \frac{1}{2Z} \exp(-\frac{1}{2\gamma^2}|y - u|^2), & u \in (-1, 1), \\ 0, & u \in (-1, 1)^c, \end{cases}$$

where Z is a normalizing constant ensuring that $\int_{\mathbb{R}} \pi^y(u) du = 1$. Now we find the MAP estimator. From the explicit formula for π^y , we have

$$u_{\text{MAP}} = \arg \max_{u \in \mathbb{R}} \pi^y(u) = \begin{cases} y & \text{if } y \in (-1, 1), \\ -1 & \text{if } y \leq -1, \\ 1 & \text{if } y \geq 1. \end{cases}$$

In this example, the prior on u is supported on $(-1, 1)$ and the posterior on $u|y$ is supported on $(-1, 1)$. If the data lies in $(-1, 1)$ then the MAP estimator is the data itself; otherwise it is the extremal point of the prior support which matches the sign of the data. The posterior mean is

$$u_{\text{PM}} = \frac{1}{2Z} \int_{-1}^1 u \exp\left(-\frac{1}{2\gamma^2}|y - u|^2\right) du,$$

which may be approximated using, for instance, the sampling methods described in Chapters 5 and 6. \diamond

The following example illustrates once again the application of Bayes theorem, and shows that the posterior may concentrate near a low-dimensional manifold in the input parameter space \mathbb{R}^d . In such a case it is important to understand the geometry of the support of the posterior density, which cannot be captured by point estimation or Gaussian approximations.

Example 1.6 (Concentration of Posterior on Manifold). Let $d = 2, k = 1, \rho \in C(\mathbb{R}^2, \mathbb{R})$, and suppose that there is $\rho_{\max} > 0$ such that, for all $u \in \mathbb{R}^2$, $0 < \rho(u) \leq \rho_{\max} < \infty$. Suppose that the observation is generated by

$$\begin{aligned} y &= G(u) + \eta, \\ G(u) &= u_1^2 + u_2^2, \\ \eta &\sim \nu = \mathcal{N}(0, \gamma^2), \quad 0 < \gamma \ll 1, \end{aligned}$$

and assume that $y > 0$. Using Bayes theorem we obtain the posterior pdf

$$\pi^y(u) = \frac{1}{Z} \exp\left(-\frac{1}{2\gamma^2}|u_1^2 + u_2^2 - y|^2\right) \rho(u).$$

We now show that the posterior concentrates near the manifold defined by the circumference $\{u \in \mathbb{R}^2 : u_1^2 + u_2^2 = y\}$. Denote $A^\pm := \{u \in \mathbb{R}^2 : |u_1^2 + u_2^2 - y|^2 \leq \gamma^{2\pm\delta}\}$, for some fixed $\delta \in (0, 2)$. The set A^- is defined so that it captures most of the posterior probability, and A^+ so that it captures little of the posterior probability. They are defined this way because the observational noise has variance γ^2 ; considering a neighbourhood of the circumference which scales as γ raised to a power slightly smaller than 2 captures most of the posterior probability; considering a neighbourhood of the circumference in which the exponent is slightly larger than this captures little of the posterior probability. Define B to be the closed ball of radius $2\sqrt{y}$ centered at the origin. Let $u^+ \in A^+ \subset B$, $u^- \in (A^-)^c$ and let $\rho_{\min} = \inf_{u \in B} \rho(u)$. Since $\rho(u)$ is positive and continuous and B is compact, $\rho_{\min} > 0$. Taking the small noise limit yields

$$\frac{\pi^y(u^+)}{\pi^y(u^-)} \geq \exp\left(-\frac{1}{2}\gamma^\delta + \frac{1}{2}\gamma^{-\delta}\right) \frac{\rho_{\min}}{\rho_{\max}} \rightarrow \infty, \text{ as } \gamma \rightarrow 0^+.$$

Therefore, noting that $y > 0$, the posterior π^y concentrates, as $\gamma \rightarrow 0^+$, on the circumference with radius \sqrt{y} . \diamond

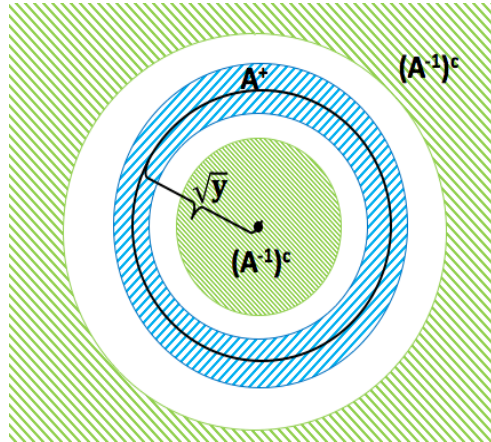


Figure 1.1 The posterior measure concentrates on a circumference with radius \sqrt{y} . Here, the blue shadow area is A^+ and the green shadow area is $(A^-)^c$.

1.3 Well-Posedness of Bayesian Inverse Problems

In this section we show that the Bayesian formulation of inverse problems leads to a form of well-posedness. More precisely, we study the sensitivity of the posterior pdf to perturbations of the forward model G . In many inverse problems the ideal forward model G is not accessible but can be approximated by some computable G_δ ; consequently π^y is replaced by π_δ^y . An example that is often found in applications,

to which the theory contained herein may be generalized, is when G is an operator acting on an infinite-dimensional space which is approximated, for the purposes of computation, by some finite-dimensional operator G_δ . We seek to prove that, under certain assumptions, the small difference between G and G_δ (forward error) leads to a similarly small difference between π^y and π_δ^y (inverse error):

Meta Theorem: Well-Posedness

$$|G - G_\delta| = O(\delta) \implies d(\pi^y, \pi_\delta^y) = O(\delta),$$

for small enough $\delta > 0$ and some metric $d(\cdot, \cdot)$ on probability densities.

This result will be formalized in Theorem 1.15 below, which shows that the $O(\delta)$ -convergence of π_δ^y with respect to some distance $d(\cdot, \cdot)$ can be guaranteed under certain assumptions on the likelihood. We will conclude the chapter by showing an example where these assumptions hold true. In order to discuss these issues we will need to introduce metrics on probability densities.

1.3.1 Metrics on Probability Densities

Here we introduce the total variation and the Hellinger distance, both of which have been used to show well-posedness results. In this chapter we will use the Hellinger distance to establish well-posedness of Bayesian inverse problems, and in Chapter 7 we employ the total variation distance to establish well-posedness of Bayesian formulations of filtering and smoothing in data assimilation.

Definition 1.7. The *total variation distance* between two pdfs π and π' is defined by

$$d_{\text{TV}}(\pi, \pi') := \frac{1}{2} \int |\pi(u) - \pi'(u)| du = \frac{1}{2} \|\pi - \pi'\|_{L^1}.$$

The *Hellinger distance* between two pdfs π and π' is defined by

$$d_{\text{H}}(\pi, \pi') := \left(\frac{1}{2} \int |\sqrt{\pi(u)} - \sqrt{\pi'(u)}|^2 du \right)^{1/2} = \frac{1}{\sqrt{2}} \|\sqrt{\pi} - \sqrt{\pi'}\|_{L^2}.$$

◇

In the rest of this subsection we will establish bounds between the Hellinger and total variation distance, and show how both distances can be used to bound the difference of expected values computed with two different densities; these results will be used in subsequent chapters. Before doing so, the next lemma motivates our choice of normalization constant $1/2$ for total variation distance and $1/\sqrt{2}$ for Hellinger distance: they are chosen so that the maximum possible distance between two densities is one. The proof also shows that π and π' have total variation and Hellinger distance equal to one if and only if they have disjoint supports, that is, if $\int \pi(u)\pi'(u)du = 0$.

Lemma 1.8. For any pdfs π and π' ,

$$0 \leq d_{\text{TV}}(\pi, \pi') \leq 1, \quad 0 \leq d_{\text{H}}(\pi, \pi') \leq 1.$$

Proof. The lower bounds follow immediately from the definitions, so we only need to prove the upper bounds. For total variation distance

$$d_{\text{TV}}(\pi, \pi') = \frac{1}{2} \int |\pi(u) - \pi'(u)| du \leq \frac{1}{2} \int \pi(u) du + \frac{1}{2} \int \pi'(u) du = 1,$$

and for Hellinger distance

$$\begin{aligned} d_{\text{H}}(\pi, \pi') &= \left(\frac{1}{2} \int \left| \sqrt{\pi(u)} - \sqrt{\pi'(u)} \right|^2 du \right)^{1/2} \\ &= \left(\frac{1}{2} \int \left(\pi(u) + \pi'(u) - 2\sqrt{\pi(u)\pi'(u)} \right) du \right)^{1/2} \\ &\leq \left(\frac{1}{2} \int (\pi(u) + \pi'(u)) du \right)^{1/2} \\ &= 1. \end{aligned}$$

□

The following result gives bounds between total variation and Hellinger distance.

Lemma 1.9. *For any pdfs π and π' ,*

$$\frac{1}{\sqrt{2}} d_{\text{TV}}(\pi, \pi') \leq d_{\text{H}}(\pi, \pi') \leq \sqrt{d_{\text{TV}}(\pi, \pi')}.$$

Proof. Using the Cauchy-Schwarz inequality

$$\begin{aligned} d_{\text{TV}}(\pi, \pi') &= \frac{1}{2} \int \left| \sqrt{\pi(u)} - \sqrt{\pi'(u)} \right| \left| \sqrt{\pi(u)} + \sqrt{\pi'(u)} \right| du \\ &\leq \left(\frac{1}{2} \int \left| \sqrt{\pi(u)} - \sqrt{\pi'(u)} \right|^2 du \right)^{1/2} \left(\frac{1}{2} \int \left| \sqrt{\pi(u)} + \sqrt{\pi'(u)} \right|^2 du \right)^{1/2} \\ &\leq d_{\text{H}}(\pi, \pi') \left(\frac{1}{2} \int (2\pi(u) + 2\pi'(u)) du \right)^{1/2} \\ &= \sqrt{2} d_{\text{H}}(\pi, \pi'). \end{aligned}$$

Notice that $|\sqrt{\pi(u)} - \sqrt{\pi'(u)}| \leq |\sqrt{\pi(u)} + \sqrt{\pi'(u)}|$ since $\sqrt{\pi(u)}, \sqrt{\pi'(u)} \geq 0$. Thus we have

$$\begin{aligned} d_{\text{H}}(\pi, \pi') &= \left(\frac{1}{2} \int \left| \sqrt{\pi(u)} - \sqrt{\pi'(u)} \right|^2 du \right)^{1/2} \\ &\leq \left(\frac{1}{2} \int \left| \sqrt{\pi(u)} - \sqrt{\pi'(u)} \right| \left| \sqrt{\pi(u)} + \sqrt{\pi'(u)} \right| du \right)^{1/2} \\ &\leq \left(\frac{1}{2} \int |\pi(u) - \pi'(u)| du \right)^{1/2} \\ &= \sqrt{d_{\text{TV}}(\pi, \pi')}. \end{aligned}$$

□

The following two lemmas show that if two densities are close in total variation or in Hellinger distance, expectations computed with respect to both densities are also close. In addition, the following lemma also provides a useful characterization of the total variation distance which will be used repeatedly throughout these notes.

Lemma 1.10. *Let f be a function such that $|f|_\infty := \sup_{u \in \mathbb{R}^d} |f(u)| < \infty$. It holds that*

$$|\mathbb{E}^\pi[f] - \mathbb{E}^{\pi'}[f]| \leq 2|f|_\infty d_{\text{TV}}(\pi, \pi').$$

Moreover, the following variational characterization of the total variation distance holds:

$$d_{\text{TV}}(\pi, \pi') = \frac{1}{2} \sup_{|f|_\infty \leq 1} |\mathbb{E}^\pi[f] - \mathbb{E}^{\pi'}[f]|. \quad (1.4)$$

Proof. For the first part of the lemma, note that

$$\begin{aligned} |\mathbb{E}^\pi[f] - \mathbb{E}^{\pi'}[f]| &= \left| \int_{\mathbb{R}^d} f(u)(\pi(u) - \pi'(u)) du \right| \\ &\leq 2|f|_\infty \cdot \frac{1}{2} \int_{\mathbb{R}^d} |\pi(u) - \pi'(u)| du \\ &= 2|f|_\infty d_{\text{TV}}(\pi, \pi'). \end{aligned}$$

This in particular shows that, for any f with $|f|_\infty = 1$,

$$d_{\text{TV}}(\pi, \pi') \geq \frac{1}{2} |\mathbb{E}^\pi[f] - \mathbb{E}^{\pi'}[f]|.$$

Our goal now is to show a choice of f with $|f|_\infty = 1$ that achieves equality. Define $f(u) := \text{sign}(\pi(u) - \pi'(u))$, so that $f(u)(\pi(u) - \pi'(u)) = |\pi(u) - \pi'(u)|$. Then it holds that $|f|_\infty = 1$, and

$$\begin{aligned} d_{\text{TV}}(\pi, \pi') &= \frac{1}{2} \int_{\mathbb{R}^d} |\pi(u) - \pi'(u)| du \\ &= \frac{1}{2} \int_{\mathbb{R}^d} f(u)(\pi(u) - \pi'(u)) du \\ &= \frac{1}{2} |\mathbb{E}^\pi[f] - \mathbb{E}^{\pi'}[f]|. \end{aligned}$$

This completes the proof of the variational characterization. \square

Lemma 1.11. *Let f be a function such that $f_2 := (\mathbb{E}^\pi[|f|^2] + \mathbb{E}^{\pi'}[|f|^2])^{\frac{1}{2}} < \infty$. It holds that*

$$|\mathbb{E}^\pi[f] - \mathbb{E}^{\pi'}[f]| \leq 2f_2 d_{\text{H}}(\pi, \pi').$$

Proof. Using the Cauchy–Schwarz inequality

$$\begin{aligned}
|\mathbb{E}^\pi[f] - \mathbb{E}^{\pi'}[f]| &= \left| \int_{\mathbb{R}^d} f(u) (\sqrt{\pi(u)} - \sqrt{\pi'(u)}) (\sqrt{\pi(u)} + \sqrt{\pi'(u)}) du \right| \\
&\leq \left(\frac{1}{2} \int |\sqrt{\pi(u)} - \sqrt{\pi'(u)}|^2 du \right)^{1/2} \left(2 \int |f(u)|^2 |\sqrt{\pi(u)} + \sqrt{\pi'(u)}|^2 du \right)^{1/2} \\
&\leq d_H(\pi, \pi') \left(4 \int |f(u)|^2 (\pi(u) + \pi'(u)) du \right)^{1/2} \\
&= 2f_2 d_H(\pi, \pi').
\end{aligned}$$

□

Remark 1.12. Note that the result for Hellinger only assumes that f is square integrable with respect to π and π' . In contrast, the result for total variation distance assumes that f is bounded, which is a stronger condition. Lemma 1.9 also demonstrates that smallness in the Hellinger metric is a more stringent condition than smallness in total variation. Our aim in the following section is to show well-posedness in some metric on probability densities. The preceding observations suggest that establishing such a result in the Hellinger metric makes a stronger statement than doing so in total variation. ◇

1.3.2 Approximation Theorem

We denote by

$$l(u) = \nu(y - G(u)) \quad \text{and} \quad l_\delta(u) = \nu(y - G_\delta(u))$$

the likelihoods associated with $G(u)$ and $G_\delta(u)$, so that

$$\pi^y(u) = \frac{1}{Z} l(u) \rho(u) \quad \text{and} \quad \pi_\delta^y(u) = \frac{1}{Z_\delta} l_\delta(u) \rho(u),$$

where $Z, Z_\delta > 0$ are the corresponding normalizing constants. Before we proceed to our main result, we make some assumptions.

Assumption 1.13. *There exist $\delta^+ > 0$ and $K_1, K_2 < \infty$ such that, for all $\delta \in (0, \delta^+)$,*

- (i) $|\sqrt{l(u)} - \sqrt{l_\delta(u)}| \leq \varphi(u)\delta$, for some $\varphi(u)$ such that $\mathbb{E}^\rho[\varphi^2(u)] \leq K_1^2$;
- (ii) $\sup_{u \in \mathbb{R}^d} (|\sqrt{l(u)}| + |\sqrt{l_\delta(u)}|) \leq K_2$.

Remark 1.14. Assumption 1.13 only involves conditions on the likelihood l and the approximate likelihood l_δ . Our presentation in this chapter emphasizes the situation in which this approximation is necessitated in order to approximate the forward model G . However, another important scenario which is covered by the theory is approximation due to perturbations of the data y . As an example, we will establish in Chapter 7 a well-posedness result that guarantees stability of Bayesian smoothing under perturbations of the data. More generally, the theoretical framework introduced here is very flexible and it may be employed to study the stability of many Bayesian formulations of inverse problems and data assimilation under a wide range of perturbations. In Chapter 14 we study two such applications in which machine learning is used to facilitate accelerated approximate evaluation of the likelihood, or to characterize the prior, approximately, from data. ◇

Now we state the main result of this section:

Theorem 1.15 (Well-Posedness of Posterior). *Under Assumption 1.13 we have*

$$d_{\text{H}}(\pi^y, \pi_\delta^y) \leq c\delta, \quad \delta \in (0, \Delta),$$

for some $\Delta > 0$ and some $c \in (0, +\infty)$ independent of δ .

Notice that this theorem together with Lemma 1.11 guarantee that expectations computed with respect to π^y and π_δ^y are order δ apart. To prove Theorem 1.15, we first show a lemma which characterizes the normalization factor Z_δ in the small δ limit.

Lemma 1.16. *Under Assumption 1.13 there exist $\Delta > 0$, $c_1, c_2 \in (0, +\infty)$ such that*

$$|Z - Z_\delta| \leq c_1\delta \quad \text{and} \quad Z, Z_\delta > c_2, \quad \text{for } \delta \in (0, \Delta).$$

Proof. Since $Z = \int l(u)\rho(u)du$ and $Z_\delta = \int l_\delta(u)\rho(u)du$ we have

$$\begin{aligned} |Z - Z_\delta| &= \left| \int (l(u) - l_\delta(u))\rho(u)du \right| \\ &\leq \left(\int |\sqrt{l(u)} - \sqrt{l_\delta(u)}|^2 \rho(u)du \right)^{1/2} \left(\int |\sqrt{l(u)} + \sqrt{l_\delta(u)}|^2 \rho(u)du \right)^{1/2} \\ &\leq \left(\int \delta^2 \varphi(u)^2 \rho(u)du \right)^{1/2} \left(\int K_2^2 \rho(u)du \right)^{1/2} \\ &\leq K_1 K_2 \delta, \quad \delta \in (0, \delta^+). \end{aligned}$$

Therefore, for $\delta \leq \Delta := \min\{\frac{Z}{2K_1K_2}, \delta^+\}$, we have

$$Z_\delta \geq Z - |Z - Z_\delta| \geq \frac{1}{2}Z.$$

The lemma follows by taking $c_1 = K_1 K_2$ and $c_2 = \frac{1}{2}Z$. □

Proof of Theorem 1.15. We break the total error into two contributions, one reflecting the difference between Z and Z_δ , and the other the difference between l and l_δ :

$$\begin{aligned} d_{\text{H}}(\pi^y, \pi_\delta^y) &= \frac{1}{\sqrt{2}} \left\| \sqrt{\pi^y} - \sqrt{\pi_\delta^y} \right\|_{L^2} \\ &= \frac{1}{\sqrt{2}} \left\| \sqrt{\frac{l\rho}{Z}} - \sqrt{\frac{l\rho}{Z_\delta}} + \sqrt{\frac{l\rho}{Z_\delta}} - \sqrt{\frac{l_\delta\rho}{Z_\delta}} \right\|_{L^2} \\ &\leq \frac{1}{\sqrt{2}} \left\| \sqrt{\frac{l\rho}{Z}} - \sqrt{\frac{l\rho}{Z_\delta}} \right\|_{L^2} + \frac{1}{\sqrt{2}} \left\| \sqrt{\frac{l\rho}{Z_\delta}} - \sqrt{\frac{l_\delta\rho}{Z_\delta}} \right\|_{L^2}. \end{aligned}$$

Using Lemma 1.16 we have, for $\delta \in (0, \Delta)$,

$$\begin{aligned} \left\| \sqrt{\frac{l\rho}{Z}} - \sqrt{\frac{l\rho}{Z_\delta}} \right\|_{L^2} &= \left| \frac{1}{\sqrt{Z}} - \frac{1}{\sqrt{Z_\delta}} \right| \left(\int l(u)\rho(u)du \right)^{1/2} \\ &= \frac{|Z - Z_\delta|}{(\sqrt{Z} + \sqrt{Z_\delta})\sqrt{Z_\delta}} \\ &\leq \frac{c_1}{2c_2}\delta, \end{aligned}$$

and

$$\left\| \sqrt{\frac{l\rho}{Z_\delta}} - \sqrt{\frac{l_\delta\rho}{Z_\delta}} \right\|_{L^2} = \frac{1}{\sqrt{Z_\delta}} \left(\int |\sqrt{l(u)} - \sqrt{l_\delta(u)}|^2 \rho(u)du \right)^{1/2} \leq \sqrt{\frac{K_1^2}{c_2}}\delta.$$

Therefore

$$d_H(\pi^y, \pi_\delta^y) \leq \frac{1}{\sqrt{2}} \frac{c_1}{2c_2} \delta + \frac{1}{\sqrt{2}} \sqrt{\frac{K_1^2}{c_2}} \delta = c\delta,$$

with $c = \frac{1}{\sqrt{2}} \frac{c_1}{2c_2} + \frac{K_1}{\sqrt{2}c_2}$, which is independent of δ . \square

1.3.3 Example: Well-Posedness for Parameter Estimation in an ODE

Many inverse problems arise from differential equations with unknown input parameters. Here we consider a simple but typical example where $G(u)$ comes from the solution of an ordinary differential equation (ODE), which needs to be solved numerically. Let $x(t)$ be the solution to the initial value problem

$$\frac{dx}{dt} = F(x; u), \quad x(0) = 0, \tag{1.5}$$

where $F : \mathbb{R}^k \times \mathbb{R}^d \rightarrow \mathbb{R}^k$ is a function such that $F(x; u)$ and the partial Jacobian $D_x F(x; u)$ are uniformly bounded with respect to (x, u) , i.e.

$$|F(x; u)|, |D_x F(x; u)| < F_{\max}, \quad \text{for all } (x, u) \in \mathbb{R}^k \times \mathbb{R}^d,$$

for some constant F_{\max} , and thus $F(x; u)$ is Lipschitz in x in that, for all $u \in \mathbb{R}^d$,

$$|F(x; u) - F(x'; u)| \leq F_{\max}|x - x'|, \quad \text{for all } x, x' \in \mathbb{R}^k.$$

Note that $u \in \mathbb{R}^d$ defines parametric dependence of the vector field defining the differential equation.

Now consider the inverse problem setting

$$y = G(u) + \eta,$$

where

$$G(u) := x(1) = x(t)|_{t=1},$$

and $\eta \sim \mathcal{N}(0, \gamma^2 I_k)$. We assume that the exact mapping $G(u)$ is replaced by some numerical approximation $G_\delta(u)$. In particular, $G_\delta(u)$ is given by using the forward Euler method to solve the ODE (1.5). Define $X_0 = 0$ and

$$X_{\ell+1} = X_\ell + \delta F(X_\ell; u), \quad \ell \geq 0,$$

where $\delta = \frac{1}{L}$ for some large integer L . Finally define $G_\delta(u) := X_L$.

In what follows, we will prove that $G_\delta(u)$ is uniformly bounded and close to $G(u)$ when δ is small, and that G and G_δ both satisfy the same global bound. Then we will use these results to show that Assumption 1.13 is satisfied. Therefore, we can apply Theorem 1.15 to this example to establish that the approximate posterior π_δ^y , defined by approximate forward model G_δ , is close to the true posterior π^y with exact forward model G .

In showing that Assumption 1.13 is satisfied we use Lemmas 1.17 and 1.18 below. Recall that $\eta \sim \mathcal{N}(0, \gamma^2 I_k)$, and thus

$$\begin{aligned} \sqrt{l(u)} &= \sqrt{\nu(y - G(u))} = \frac{1}{(2\pi)^{k/4} \gamma^{k/2}} \exp\left(-\frac{1}{4\gamma^2} |y - G(u)|^2\right), \\ \sqrt{l_\delta(u)} &= \sqrt{\nu(y - G_\delta(u))} = \frac{1}{(2\pi)^{k/4} \gamma^{k/2}} \exp\left(-\frac{1}{4\gamma^2} |y - G_\delta(u)|^2\right). \end{aligned}$$

- For Assumption 1.13(i) notice that the function e^{-w} is Lipschitz for $w > 0$, with Lipschitz constant 1. Therefore we have

$$\begin{aligned} \left| \sqrt{l(u)} - \sqrt{l_\delta(u)} \right| &\leq \frac{1}{(2\pi)^{k/4} \gamma^{k/2}} \cdot \frac{1}{4\gamma^2} \cdot \left| |y - G(u)|^2 - |y - G_\delta(u)|^2 \right| \\ &= \frac{1}{(2\pi)^{k/4} \gamma^{k/2}} \cdot \frac{1}{4\gamma^2} \cdot |2y - G(u) - G_\delta(u)| |G(u) - G_\delta(u)| \\ &\leq \frac{1}{(2\pi)^{k/4} \gamma^{k/2}} \cdot \frac{1}{4\gamma^2} \cdot (2|y| + 2F_{\max}) c\delta \\ &= \tilde{c}\delta. \end{aligned}$$

That is to say, Assumption 1.13(i) is satisfied with $\varphi(u) = \tilde{c}$ and $\int_{\mathbb{R}^d} \varphi^2(u) \rho(u) du = \tilde{c}^2 < \infty$.

- Assumption 1.13(ii) is satisfied, since

$$\begin{aligned} \sqrt{l(u)} &= \frac{1}{(2\pi)^{k/4} \gamma^{k/2}} \exp\left(-\frac{1}{4\gamma^2} |y - G(u)|^2\right) \leq \frac{1}{(2\pi)^{k/4} \gamma^{k/2}}, \\ \sqrt{l_\delta(u)} &= \frac{1}{(2\pi)^{k/4} \gamma^{k/2}} \exp\left(-\frac{1}{4\gamma^2} |y - G_\delta(u)|^2\right) \leq \frac{1}{(2\pi)^{k/4} \gamma^{k/2}}. \end{aligned}$$

The preceding verification of Assumption 1.13 used the following two lemmas, and the first of these uses the Gronwall inequality which follows them. Define $t_\ell = \ell\delta$, $x_\ell = x(t_\ell)$. The following lemma gives an estimate on the error generated from using the forward Euler method.

Lemma 1.17. *Let $E_\ell := x_\ell - X_\ell$. Then there is $c < \infty$ independent of δ such that*

$$|E_\ell| \leq c\delta, \quad 0 \leq \ell \leq L.$$

In particular,

$$|G(u) - G_\delta(u)| = |E_L| \leq c\delta.$$

Proof. For simplicity of exposition we consider the case $k = 1$; the case $k > 1$ is almost identical, simply requiring the integral form for the remainder term in the Taylor expansion. Using Taylor expansion in the case $k = 1$, there is $\xi_\ell \in [t_\ell, t_{\ell+1}]$ such that

$$\begin{aligned} x_{\ell+1} &= x_\ell + \delta \frac{dx}{dt}(t_\ell) + \frac{\delta^2}{2} \frac{d^2x}{dt^2}(\xi_\ell) \\ &= x_\ell + \delta F(x_\ell; u) + \frac{\delta^2}{2} D_x F(x(\xi_\ell); u) F(x(\xi_\ell); u). \end{aligned}$$

Thus we have

$$\begin{aligned} |E_{\ell+1}| &= |x_{\ell+1} - X_{\ell+1}| \\ &= |x_\ell - X_\ell + \delta(F(x_\ell; u) - F(X_\ell; u)) + \frac{\delta^2}{2} D_x F(x(\xi_\ell); u) F(x(\xi_\ell); u)| \\ &\leq |x_\ell - X_\ell| + \delta |F(x_\ell; u) - F(X_\ell; u)| + \frac{\delta^2}{2} |D_x F(x(\xi_\ell); u)| |F(x(\xi_\ell); u)| \\ &\leq |E_\ell| + \delta F_{\max} |E_\ell| + \frac{\delta^2}{2} F_{\max}^2. \end{aligned}$$

Noticing that $|E_0| = 0$, the discrete Gronwall inequality (Theorem 1.19) gives

$$\begin{aligned} |E_\ell| &\leq (1 + \delta F_{\max})^\ell |E_0| + \frac{(1 + \delta F_{\max})^\ell - 1}{\delta F_{\max}} \cdot \frac{\delta^2}{2} F_{\max}^2 \\ &\leq \left(\left(1 + \frac{F_{\max}}{L}\right)^L - 1 \right) \cdot \frac{F_{\max} \delta}{2} \\ &\leq \frac{(e^{F_{\max}} - 1) F_{\max}}{2} \delta. \end{aligned}$$

The lemma follows by taking $c = \frac{(e^{F_{\max}} - 1) F_{\max}}{2}$. □

Lemma 1.18. *For any $u \in \mathbb{R}^d$,*

$$|G(u)|, |G_\delta(u)| \leq F_{\max}.$$

Proof. For $G(u)$ we use that $F(x; u)$ is uniformly bounded, so that

$$|G(u)| = |x(1)| = \left| \int_0^1 F(x(t); u) dt \right| \leq \int_0^1 |F(x(t); u)| dt \leq F_{\max}.$$

As for $G_\delta(u)$, we first notice that

$$|X_{\ell+1}| = |X_\ell + \delta F(X_\ell; u)| \leq |X_\ell| + \delta |F(X_\ell; u)| \leq |X_\ell| + \delta F_{\max},$$

and by induction

$$|X_\ell| \leq |X_0| + \ell \delta F_{\max} = \ell \delta F_{\max}.$$

In particular,

$$|G_\delta(u)| = |X_L| \leq L \delta F_{\max} = F_{\max}.$$

□

The following discrete Gronwall inequality is used several times in these notes, and is stated and proved here for completeness.

Theorem 1.19 (Discrete Gronwall Inequality). *Let a positive sequence $\{Z_\ell\}_{\ell=0}^L$ satisfy*

$$Z_{\ell+1} \leq C Z_\ell + D, \quad \forall \ell = 0, \dots, L-1$$

for some constants C, D with $C > 0$. Then

$$Z_\ell \leq \frac{D}{1-C}(1 - C^\ell) + Z_0 C^\ell \quad \forall \ell = 0, \dots, L, \quad C \neq 1$$

and

$$Z_\ell \leq \ell D + Z_0 \quad \forall \ell = 0, \dots, L, \quad C = 1.$$

Proof. The proof is by induction. We start with the case $C \neq 1$. The result holds for $\ell = 0$. Assume it is true for $\ell < L$. Then, using the defining inequality,

$$Z_{\ell+1} \leq \frac{CD}{1-C}(1 - C^\ell) + Z_0 C^{\ell+1} + D.$$

Rearranging yields

$$Z_{\ell+1} \leq \frac{D}{1-C}(1 - C^{\ell+1}) + Z_0 C^{\ell+1}$$

and the result follows by induction.

When $C = 0$ we again note that the result holds for $\ell = 0$. Assume it is true for $\ell < L$. Then, using the defining inequality with $C = 1$,

$$Z_{\ell+1} \leq \ell D + Z_0 + D = (\ell + 1)D + Z_0$$

and the result follows by induction. □

1.4 Discussion and Bibliography

The book by Kaipio and Somersalo [161] provides an introduction to the Bayesian approach to inverse problems, especially in the context of differential equations, and the book [43] gives an introduction to Bayesian scientific computing. An overview of the subject of Bayesian inverse problems in differential equations, with a perspective informed by the geophysical sciences, is given in the book by Tarantola [298] (see, especially, Chapter 5). For non-statistical approaches to inverse problems we refer to the books [300, 89, 309] and the lecture notes [18, 213].

The subject of Bayesian inverse problems may be developed beyond the specific setting of equation (1.1) to study problems of the form

$$y = G(u, \eta).$$

Our emphasis on additive noise η , often assumed to be Gaussian, simplifies some algorithms and enables us to be explicit about some formulae, but is not fundamental in any way. We refer to [85] for well-posedness theory and a study of MAP estimation with multiplicative noise. In addition, the setting of equation (1.1) presupposes that the forward model G is given to us, but in some cases the forward model itself may need to be learned from data, a topic that will be considered in Chapter 14.

In the paper [292] the Bayesian approach to regularization is reviewed, developing a function space viewpoint on the subject; a similar development of this approach is described in [180, 181]. A well-posedness theory and some algorithmic approaches which are used when adopting the Bayesian approach to inverse problems are introduced. The function space viewpoint on the subject is developed in more detail in the lecture notes [66]. An application of this function space methodology to a large-scale geophysical inverse problem is considered in [205]. The paper [193] demonstrates the potential for the use of dimension reduction techniques from control theory within statistical inverse problems.

We refer to [113] for further study on the subject of metrics, and other distance-like functions, on probability measures. The first published paper to discuss stability and well-posedness of the Bayesian inverse problem is [207], in which the Kullback-Liebler divergence (see Chapter 4) is employed. Related results on stability and well-posedness, but using other distances and divergences, may be found in [182]. The articles [292, 66] study well-posedness of Bayesian inverse problems in the Hellinger metric, with respect to perturbations in the data; papers [59, 132] consider stability of the posterior distribution with respect to numerical approximation of partial differential equations appearing in the forward model. The papers [143, 142] discuss generalizations of the well-posedness theory to various classes of specific non-Gaussian priors. On the other hand, [153] contains an interesting set of examples where the Meta Theorem stated in this chapter fails in the sense that, whilst well-posedness holds, the posterior is Hölder with exponent less than one, rather than Lipschitz, with respect to perturbations.

The Bayesian approach to inverse problems builds on, and benefits from, the vast literature on Bayesian statistics. The paper [97] provides a historical overview of the development and popularization of Bayesian statistics, starting with the introduction of Bayes formula in 1763 [20] and emphasizing the leading role of Savage [274] in axiomatizing and popularizing the subjective view of probability pioneered by de Finetti [68]. We refer to [111] for a recent and comprehensive textbook on Bayesian methodology. See [222] for an overview of Bayesian inversion and, in particular, statistical consistency results in this context.

A topic of debate in Bayesian statistics, and specifically in the Bayesian approach to inverse problems, is how to construct prior probability measures from available prior information, which is typically not described probabilistically. Generative model techniques for machine learning of prior distributions from data will be discussed in

Chapter 14. The papers [233, 234] demonstrate that this is an important question: different priors, both consistent with available prior information, can lead to wildly different Bayesian inference when computing posterior expectations: what the authors term *Bayesian brittleness*. Arguably this issue may be dealt with through application of the scientific method: a given prior is postulated, posterior predictions are made and data acquired subsequent to posterior inference may be used to evaluate the Bayesian probabilistic model employed, including the prior. The body of work on Bayesian brittleness builds on related analysis in the context of forward uncertainty quantification [232], a topic concerned with propagating uncertainty on parameters through a model into predictions. The subject of uncertainty quantification, both the forward and inverse varieties, is overviewed in [294, 281].

Chapter 2

The Linear-Gaussian Setting

Recall the inverse problem of estimating an unknown parameter $u \in \mathbb{R}^d$ from data $y \in \mathbb{R}^k$ under the model assumption

$$y = G(u) + \eta. \quad (2.1)$$

In this chapter we study the linear-Gaussian setting, where the forward model $G(\cdot)$ is linear and both the prior on u and the distribution of the observation noise η are Gaussian. This setting is highly amenable to analysis and arises frequently in applications. Moreover, as we will see throughout these notes, many methods employed in nonlinear or non-Gaussian settings build on ideas from the linear-Gaussian case by performing linearization or invoking Gaussian approximations. After establishing a formula for the posterior pdf in Section 2.1, we investigate in Section 2.2 the effect that the choice of prior has on our solution by quantifying the spread of the posterior distribution in the small noise (approaching zero) limit. This investigation provides intuitive understanding concerning the impact of the prior for overdetermined, determined, and underdetermined regimes, corresponding to $d < k$, $d = k$, and $d > k$, respectively. Extensions of the theory and references to the literature are discussed in Section 2.3.

The following will be assumed throughout this chapter.

Assumption 2.1. *The relationship between unknown $u \in \mathbb{R}^d$, data $y \in \mathbb{R}^k$, and noise $\eta \in \mathbb{R}^k$ defined by equation (2.1) holds. Moreover,*

- *Linearity of the forward model: $G(u) = Au$, for some $A \in \mathbb{R}^{k \times d}$.*
- *Gaussian prior: $u \sim \rho(u) = \mathcal{N}(\hat{m}, \hat{C})$, where \hat{C} is positive definite.*
- *Gaussian noise: $\eta \sim \nu(\eta) = \mathcal{N}(0, \Gamma)$, where Γ is positive definite.*
- *u and η are independent: $u \perp \eta$.*

2.1 Derivation of the Posterior Distribution

Under Assumption 2.1 the likelihood on y given u is Gaussian,

$$y|u \sim \mathcal{N}(Au, \Gamma). \quad (2.2)$$

Therefore, using Bayes formula (1.2) we see that the posterior $\pi^y(u)$ is given by

$$\begin{aligned}\pi^y(u) &= \frac{1}{Z} \nu(y - Au) \rho(u) \\ &= \frac{1}{Z} \exp\left(-\frac{1}{2}|y - Au|_\Gamma^2\right) \exp\left(-\frac{1}{2}|u - \hat{m}|_{\hat{C}}^2\right) \\ &= \frac{1}{Z} \exp\left(-\frac{1}{2}|y - Au|_\Gamma^2 - \frac{1}{2}|u - \hat{m}|_{\hat{C}}^2\right) \\ &= \frac{1}{Z} \exp(-J(u)),\end{aligned}$$

with

$$J(u) = \frac{1}{2}|y - Au|_\Gamma^2 + \frac{1}{2}|u - \hat{m}|_{\hat{C}}^2. \quad (2.3)$$

Note that here

$$\log l(u) = -\frac{1}{2}|y - Au|_\Gamma^2. \quad (2.4)$$

Since the posterior pdf can be written as the exponential of a quadratic in u it follows that the posterior is Gaussian. Its mean and covariance are given in the following result.

Theorem 2.2 (Posterior is Gaussian). *Under Assumption 2.1 the posterior distribution is Gaussian,*

$$u|y \sim \pi^y(u) = \mathcal{N}(m, C). \quad (2.5)$$

The posterior mean m and covariance C are given by the following formulae:

$$m = (A^\top \Gamma^{-1} A + \hat{C}^{-1})^{-1} (A^\top \Gamma^{-1} y + \hat{C}^{-1} \hat{m}), \quad (2.6)$$

$$C = (A^\top \Gamma^{-1} A + \hat{C}^{-1})^{-1}. \quad (2.7)$$

Proof. Since $\pi^y(u) = \frac{1}{Z} \exp(-J(u))$ with $J(u)$ given by (2.3), a quadratic function of u , it follows that the posterior is Gaussian. Denoting the mean and variance of $\pi^y(u)$ by m and C , we can write $J(u)$ in the following form

$$J(u) = \frac{1}{2}|u - m|_C^2 + q, \quad (2.8)$$

where the term q does not depend on u . Now matching the coefficients of the quadratic and linear terms in equations (2.3) and (2.8), we get

$$\begin{aligned}C^{-1} &= A^\top \Gamma^{-1} A + \hat{C}^{-1}, \\ C^{-1}m &= A^\top \Gamma^{-1} y + \hat{C}^{-1} \hat{m}.\end{aligned}$$

Therefore equations (2.6) and (2.7) follow. \square

We saw in the previous chapter that the posterior mean estimator and the MAP estimator are typically different. However equation (2.8) shows that in the current linear-Gaussian setting the posterior mean m minimizes $J(u)$ given in (2.3). Thus the MAP estimator and the posterior mean coincide.

Corollary 2.3 (Characterization of Bayes Estimators). *The posterior mean and MAP estimators under Assumptions 2.1 agree, and are given by $u_{\text{MAP}} = u_{\text{PM}} = m$ defined in equation (2.6).*

Furthermore the formula (2.3) demonstrates that the posterior mean is found as a compromise between maximizing the likelihood (by making the *loss* term $\frac{1}{2}|y - Au|_{\Gamma}^2$ small) and minimizing deviations from the prior mean (by making the *regularization* term $\frac{1}{2}|u - \hat{m}|_{\hat{C}}^2$ small). The relative importance given to both objectives is determined by the relative size of the prior covariance \hat{C} and the noise covariance Γ . An important feature of the linear-Gaussian setting is that the posterior covariance C does not depend on the data y ; this is not true in general.

We conclude this subsection with an example.

Example 2.4. Let $\Gamma = \gamma^2 I$, $\hat{C} = \sigma^2 I$, $\hat{m} = 0$, and set $\lambda = \frac{\gamma^2}{\sigma^2}$. Then

$$J_{\lambda}(u) := \gamma^2 J(u) = \frac{1}{2}|y - Au|^2 + \frac{\lambda}{2}|u|^2.$$

Since m minimizes $J_{\lambda}(\cdot)$ it follows that

$$(A^{\top} A + \lambda I)m = A^{\top} y. \quad (2.9)$$

◇

Example 2.4 provides a link between Bayesian inversion and optimization approaches to inversion: $J_{\lambda}(u)$ can be seen as the objective function in a linear regression model with a regularizer $\frac{\lambda}{2}|u|^2$, as used in ridge regression. Equation (2.9) for m is exactly the normal equation with regularizer in the least-squares problem. In fact, in the general linear-Gaussian setting of Assumption 2.1, equation (2.6) can also be viewed as a generalized normal equation. This perspective helps us understand the structure of Bayesian regularization by linking it to the deep understanding of optimization approaches to inverse problems. A more extensive account of the optimization perspective and its interplay with Bayesian formulations will be given in the following chapter.

2.2 Small Noise Limit of the Posterior Distribution

In this section we study the small observation noise limit of the posterior in the linear-Gaussian setting. While most of the ideas and results can be extended beyond this setting, explicit calculations that are possible in the linear-Gaussian setting provide helpful intuition. Throughout this section we assume the following.

Assumption 2.5. *In addition to Assumption 2.1 (the linear-Gaussian setting), we assume that $\eta := \gamma\eta_0$, where $\eta_0 \sim \mathcal{N}(0, \Gamma_0)$; thus $\Gamma = \gamma^2\Gamma_0$.*

Note that substituting $\Gamma = \gamma^2\Gamma_0$ into (2.6) and (2.7) we obtain that

$$m = (A^{\top}\Gamma_0^{-1}A + \gamma^2\hat{C}^{-1})^{-1}(A^{\top}\Gamma_0^{-1}y + \gamma^2\hat{C}^{-1}\hat{m}), \quad (2.10)$$

$$C = \gamma^2(A^{\top}\Gamma_0^{-1}A + \gamma^2\hat{C}^{-1})^{-1}. \quad (2.11)$$

In the next three subsections we study the behavior of the posterior mean m and covariance C as $\gamma \rightarrow 0^+$ —the small noise limit. We remark that m , C , and the posterior π^y depend on the noise level γ , but we will not make explicit said dependence in our notation. We separately consider the overdetermined, determined, and underdetermined regimes. We recall that \Rightarrow denotes weak convergence of probability measures. We will use repeatedly that weak convergence of Gaussian distributions is equivalent to the convergence of their means and covariances. In particular, the weak limit of a sequence of Gaussians with means converging to m^+ and covariance matrices converging to the zero matrix is a Dirac mass δ_{m^+} .

2.2.1 Overdetermined Case

We start with the overdetermined case $d < k$.

Theorem 2.6 (Small Noise Limit of Posterior Distribution – Overdetermined). *Suppose that Assumption 2.5 holds, that $\text{Null}(A) = 0$ and that $d < k$. Then, in the limit $\gamma \rightarrow 0^+$,*

$$\pi^y \Rightarrow \delta_{m^+},$$

where m^+ is the solution of the least-squares problem

$$m^+ = \arg \min_{u \in \mathbb{R}^d} |\Gamma_0^{-1/2}(y - Au)|^2. \quad (2.12)$$

Proof. Since $\text{Null}(A) = 0$ and Γ_0 is invertible we deduce that there is $\alpha > 0$ such that, for all $u \in \mathbb{R}^d$,

$$\langle u, A^\top \Gamma_0^{-1} A u \rangle = |\Gamma_0^{-1/2} A u|^2 \geq \alpha |u|^2.$$

Thus $A^\top \Gamma_0^{-1} A$ is positive definite (and hence invertible). It follows that as $\gamma \rightarrow 0^+$, the posterior covariance converges to the zero matrix, $C \rightarrow 0$, and the posterior mean satisfies the limit

$$m \rightarrow m^* = (A^\top \Gamma_0^{-1} A)^{-1} A^\top \Gamma_0^{-1} y.$$

This proves the weak convergence of π^y to δ_{m^*} . It remains to characterize m^* . Since $\text{Null}(A) = 0$, the minimizers of the scaled loss¹

$$\mathcal{L}(u) := \frac{1}{2} |\Gamma_0^{-1/2}(y - Au)|^2$$

are unique and satisfy the normal equations $A^\top \Gamma_0^{-1} A u = A^\top \Gamma_0^{-1} y$. Hence m^* solves the desired least-squares problem and coincides with m^+ given in (2.12). \square

We have shown that in the overdetermined case where $A^\top \Gamma_0^{-1} A$ is invertible, the small observational noise limit leads to a posterior which is a Dirac, centered at the solution of the least-squares problem (2.12). Therefore, in this limit the prior plays no role in the Bayesian inference.

¹Note that this is a rescaling by γ^2 of the negative log-likelihood from equation (2.4).

Theorem 2.7 (Posterior Consistency – Overdetermined). *Suppose that the assumptions of Theorem 2.6 hold and that the data satisfies*

$$y = Au^\dagger + \gamma\eta_0^\dagger, \quad \text{for fixed } u^\dagger \in \mathbb{R}^d, \eta_0^\dagger \in \mathbb{R}^k. \quad (2.13)$$

Then, for any sequence $M(\gamma) \rightarrow \infty$ as $\gamma \rightarrow 0^+$,

$$\mathbb{P}^{\pi^\gamma}(|u - u^\dagger|^2 > M(\gamma)\gamma^2) \rightarrow 0, \quad (2.14)$$

where \mathbb{P}^{π^γ} denotes probability under the posterior distribution.

Remark 2.8. For any $\varepsilon > 0$, set $M(\gamma) = \frac{\varepsilon^2}{\gamma^2}$ in Theorem 2.10 to obtain

$$\mathbb{P}^{\pi^\gamma}(|u - u^\dagger| > \varepsilon) \rightarrow 0.$$

This shows that the posterior probability concentrates around the truth in the small noise limit. \diamond

Proof of Theorem 2.7. Throughout this proof we let c be a constant independent of γ that may change from line to line, and we denote by \mathbb{E} expectation with respect to the posterior distribution, which is Gaussian with mean m and covariance C given by equations (2.10) and (2.11). Denote

$$m^* = (A^\top \Gamma_0^{-1} A)^{-1} A^\top \Gamma_0^{-1} y$$

as in the proof of the previous theorem. We have that

$$\mathbb{E}[|u - u^\dagger|^2] \leq c \left(\mathbb{E}[|u - m|^2] + |m - m^*|^2 + |m^* - u^\dagger|^2 \right). \quad (2.15)$$

We now bound each of the three terms in the right-hand side.

For the first one,

$$\begin{aligned} \mathbb{E}[|u - m|^2] &= \mathbb{E}[(u - m)^\top (u - m)] = \mathbb{E}[\text{Tr}[(u - m) \otimes (u - m)]] \\ &= \text{Tr} \mathbb{E}[(u - m) \otimes (u - m)] \\ &= \text{Tr}(C) \leq \gamma^2 \text{Tr}[(A^\top \Gamma_0^{-1} A)^{-1}]. \end{aligned}$$

For the second term, note that

$$\begin{aligned} (A^\top \Gamma_0^{-1} A) m^* &= A^\top \Gamma_0^{-1} y, \\ (A^\top \Gamma_0^{-1} A + \gamma^2 \hat{C}^{-1}) m &= A^\top \Gamma_0^{-1} y + \gamma^2 \hat{C}^{-1} \hat{m}. \end{aligned}$$

Therefore

$$m - m^* = \gamma^2 (A^\top \Gamma_0^{-1} A)^{-1} (\hat{C}^{-1} \hat{m} - \hat{C}^{-1} m).$$

Since m converges it is bounded, and so there is $c > 0$ such that

$$|m - m^*|^2 \leq c\gamma^4.$$

Finally, for the third term we write

$$\begin{aligned} m^* &= (A^\top \Gamma_0^{-1} A)^{-1} A^\top \Gamma_0^{-1} A u^\dagger + \gamma (A^\top \Gamma_0^{-1} A)^{-1} A^\top \Gamma_0^{-1} \eta_0^\dagger \\ &= u^\dagger + \gamma (A^\top \Gamma_0^{-1} A)^{-1} A^\top \Gamma_0^{-1} \eta_0^\dagger, \end{aligned}$$

which gives

$$|m^* - u^\dagger|^2 \leq c\gamma^2.$$

Using Markov inequality and the three bounds above,

$$\mathbb{P}^{\pi^y}(|u - u^\dagger|^2 > M(\gamma)\gamma^2) \leq \frac{\mathbb{E}[|u - u^\dagger|^2]}{M(\gamma)\gamma^2} \leq \frac{c}{M(\gamma)} \rightarrow 0, \text{ as } \gamma \rightarrow 0^+.$$

□

2.2.2 Determined Case

As a byproduct of the proof of Theorem 2.6, we can determine the limiting behavior of π^y in the boundary case $d = k$.

Theorem 2.9 (Small Noise Limit of Posterior Distribution – Determined). *Suppose that Assumption 2.5 holds, $\text{Null}(A) = 0$, and $d = k$. Then, in the small noise limit $\gamma \rightarrow 0^+$,*

$$\pi^y \Rightarrow \delta_{A^{-1}y}.$$

Proof. In the proof of Theorem 2.6, the assumption $d < k$ is used only in that A is not a square matrix and thus A, A^\top are not invertible. Denote by (m, C) the mean and variance of the posterior $u|y$. Using the same argument, we have $C \rightarrow 0$ and

$$m \rightarrow m^* = (A^\top \Gamma_0^{-1} A)^{-1} A^\top \Gamma_0^{-1} y.$$

Using that A, A^\top are square invertible matrices we obtain

$$m^* = (A^{-1} \Gamma_0 (A^\top)^{-1}) A^\top \Gamma_0^{-1} y = A^{-1} y.$$

Therefore, $\pi^y(u) \Rightarrow \delta_{m^*} = \delta_{A^{-1}y}$.

□

Note that here, as in the overdetermined case, the prior plays no role in the small noise limit. Moreover, it can be shown as above that posterior consistency holds. The proof is very similar to that in the overdetermined case and therefore omitted.

Theorem 2.10 (Posterior Consistency – Determined). *Suppose that the assumptions of Theorem 2.9 hold, and that the data satisfies*

$$y = A u^\dagger + \gamma \eta_0^\dagger, \quad \text{for fixed } u^\dagger, \eta_0^\dagger \in \mathbb{R}^d. \quad (2.16)$$

Then, for any sequence $M(\gamma) \rightarrow \infty$ as $\gamma \rightarrow 0^+$,

$$\mathbb{P}^{\pi^y}(|u - u^\dagger|^2 > M(\gamma)\gamma^2) \rightarrow 0. \quad (2.17)$$

2.2.3 Underdetermined Case

Finally we consider the underdetermined case $d > k$. We assume that $A \in \mathbb{R}^{k \times d}$ with $\text{Rank}(A) = k$ and write

$$A = (A_0 \ 0)Q^\top = (A_0 \ 0)(Q_1 \ Q_2)^\top = A_0Q_1^\top, \quad (2.18)$$

with $A_0 \in \mathbb{R}^{k \times k}$ an invertible matrix, $Q = (Q_1 \ Q_2) \in \mathbb{R}^{d \times d}$ an orthogonal matrix so that $Q^\top Q = I$, $Q_1 \in \mathbb{R}^{d \times k}$, $Q_2 \in \mathbb{R}^{d \times (d-k)}$. We have the following result:

Theorem 2.11 (Small Noise Limit of Posterior Distribution – Underdetermined). *Suppose that Assumption 2.5 holds, that $\text{Rank}(A) = k$, and $d > k$. In the small noise limit $\gamma \rightarrow 0^+$,*

$$\pi^y \Rightarrow \mathcal{N}(m^+, C^+),$$

where

$$\begin{aligned} m^+ &= \hat{C}Q_1(Q_1^\top \hat{C}Q_1)^{-1}A_0^{-1}y + Q_2(Q_2^\top \hat{C}^{-1}Q_2)^{-1}Q_2^\top \hat{C}^{-1}\hat{m}, \\ C^+ &= Q_2(Q_2^\top \hat{C}^{-1}Q_2)^{-1}Q_2^\top. \end{aligned}$$

Since $\text{Rank}(C^+) = \text{Rank}(Q_2) = d - k < d$ this theorem demonstrates that, in the small observational noise limit, the posterior has no uncertainty in a subspace of dimension k , but retains uncertainty in a subspace of dimension $d - k$. As a consequence there is no posterior consistency in the underdetermined case.

Example 2.12 (Small Noise Limit – Underdetermined). To help understand the result in Theorem 2.11, we consider a simple explicit example. Assume that $A = (A_0 \ 0) \in \mathbb{R}^{k \times d}$, $\Gamma = \gamma^2 \Gamma_0 = \gamma^2 I_k$, $\hat{C} = I_d$, $\hat{m} = 0$. Let $u = (u_1, u_2)^\top \sim \mathcal{N}(0, I_d)$, with $u_1 \in \mathbb{R}^k$, $u_2 \in \mathbb{R}^{d-k}$. The data then satisfies

$$y = Au + \eta = A_0 u_1 + \eta, \quad \eta \sim \mathcal{N}(0, \gamma^2 I_k).$$

The posterior $u|y$ is $\pi^y(u) = \frac{1}{Z_\gamma} \exp(-J_\gamma(u))$, where

$$\begin{aligned} J_\gamma(u) &= \frac{1}{2\gamma^2}|y - A_0 u_1|^2 + \frac{1}{2}|u|^2 \\ &= \left(\frac{1}{2\gamma^2}|y - A_0 u_1|^2 + \frac{1}{2}|u_1|^2 \right) + \frac{1}{2}|u_2|^2. \end{aligned} \quad (2.19)$$

It is clear that

$$\pi^y(u_1) \Rightarrow \delta_{A_0^{-1}y}(u_1).$$

Once u_1 is fixed as $A_0^{-1}y$, the first term in (2.19) is a constant $\frac{1}{2}|A_0^{-1}y|^2$. Since u_1 and u_2 are independent we can derive, formally, the limiting posterior as follows

$$\pi^y(u) \Rightarrow \delta_{A_0^{-1}y}(u_1) \otimes \frac{1}{Z} \exp\left(-\frac{1}{2}|u_2|^2\right) = \delta_{A_0^{-1}y}(u_1) \otimes \mathcal{N}(0, I_{d-k}),$$

where $Z = \int_{\mathbb{R}^{d-k}} \exp(-\frac{1}{2}|u_2|^2) du_2$. In fact, this is exactly the limiting posterior measure given in Theorem 2.11. \diamond

To prove Theorem 2.11, we use the following decomposition of the identity I_d .

Lemma 2.13. *Let $\hat{C} \in \mathbb{R}^{d \times d}$ be invertible and $Q = [Q_1 \ Q_2]$ be an orthogonal matrix with $Q_1 \in \mathbb{R}^{d \times k}$, $Q_2 \in \mathbb{R}^{d \times (d-k)}$. We have the following decomposition of I_d*

$$I_d = \hat{C}Q_1(Q_1^\top \hat{C}Q_1)^{-1}Q_1^\top + Q_2(Q_2^\top \hat{C}^{-1}Q_2)^{-1}Q_2^\top \hat{C}^{-1}. \quad (2.20)$$

Proof. Denote by R the right-hand side of (2.20). Since Q is orthogonal, we have $Q_1^\top Q_2 = 0$, $Q_2^\top Q_1 = 0$ and thus

$$Q_1^\top (R - I) = 0, \quad Q_2^\top \hat{C}^{-1} (R - I) = 0.$$

If $B := (Q_1 \ \hat{C}^{-1}Q_2)$ is full rank, the above identities imply that $B^\top (R - I) = 0$ and thus $R = I$. Note that

$$Q^\top B = \begin{bmatrix} Q_1^\top \\ Q_2^\top \end{bmatrix} [Q_1 \ \hat{C}^{-1}Q_2] = \begin{bmatrix} I_k & Q_1^\top \hat{C}^{-1}Q_2 \\ 0 & Q_2^\top \hat{C}^{-1}Q_2 \end{bmatrix}.$$

Since the last matrix is invertible, B is invertible and the proof is complete. \square

Proof of Theorem 2.11. Using (2.20) we can decompose u as follows

$$u = \underbrace{\hat{C}Q_1(Q_1^\top \hat{C}Q_1)^{-1}}_S \underbrace{Q_1^\top u}_{u_1} + \underbrace{Q_2(Q_2^\top \hat{C}^{-1}Q_2)^{-1}}_T \underbrace{Q_2^\top \hat{C}^{-1}u}_{u_2} = Su_1 + Tu_2.$$

Here u_1 and u_2 are Gaussian with $u_2 \sim \mathcal{N}(Q_2^\top \hat{C}^{-1}\hat{m}, Q_2^\top \hat{C}^{-1}Q_2)$. The identity

$$\text{Cov}(u_1, u_2) = Q_1^\top \text{Cov}(u, u) \hat{C}^{-1}Q_2 = Q_1^\top Q_2 = 0$$

shows that u_1 and u_2 are independent, written $u_1 \perp u_2$. From (2.18), we have

$$y = Au + \eta = A_0Q_1^\top u + \eta = A_0u_1 + \eta. \quad (2.21)$$

Since $u \perp \eta$ and $u_1 \perp u_2$, we have that $u_2 \perp y, u_1$. We apply conditional probability to yield

$$\pi^y(u_1, u_2) := \mathbb{P}(u_1, u_2|y) = \mathbb{P}(u_2) \mathbb{P}(u_1|y).$$

Equation (2.21) and Theorem 2.9 shows that $\mathbb{P}(u_1|y) \Rightarrow \delta_{A_0^{-1}y}(u_1)$ as the noise vanishes, that is, as $\gamma \rightarrow 0^+$. Note that $u_2 \perp u_1$ and $u_2 \perp y$. The limiting posterior measure $(u_1, u_2)|y$ is

$$\pi^y(u_1, u_2) \Rightarrow \mathbb{P}(u_2) \otimes \delta_{A_0^{-1}y}(u_1) \quad (2.22)$$

as $\gamma \rightarrow 0^+$. Recall $u = Su_1 + Tu_2$ and $u_2 \sim \mathcal{N}(Q_2^\top \hat{C}^{-1}\hat{m}, Q_2^\top \hat{C}^{-1}Q_2)$. The mean and variance of the limiting posterior measure $u|y$ is

$$\begin{aligned} m^+ &= \mathbb{E}[Su_1 + Tu_2|y] = SA_0^{-1}y + T\mathbb{E}[u_2] = SA_0^{-1}y + TQ_2^\top \hat{C}^{-1}\hat{m}, \\ C^+ &= \text{Cov}(Su_1 + Tu_2|y) = \text{Cov}(Tu_2) = TQ_2^\top \hat{C}^{-1}Q_2T^\top = Q_2(Q_2^\top \hat{C}^{-1}Q_2)^{-1}Q_2^\top. \end{aligned}$$

We have thus completed the proof. \square

Equation (2.22) shows that in the limit of zero observational noise, the uncertainty is only in the variable u_2 . Since $\text{Span}(T) = \text{Span}(Q_2)$ and $u = SA_0^{-1}y + Tu_2$, the uncertainty we observed is in $\text{Span}(Q_2)$. The prior plays a role in the posterior measure, in the limit of zero observational noise, but only in the variables u_2 .

2.3 Discussion and Bibliography

The linear setting plays, for several reasons, a central role in the study of inverse problems. First, linear inverse problems are ubiquitous in applications, and are challenging to solve when the matrix defining the linear forward model is ill-conditioned, or when the system is severely underdetermined. Second, in the linear-Gaussian setting explicit solutions are available; these explicit solutions can be used to give insight into the solution of nonlinear inverse problems. Underlying the derivation of these formulae is the fact, shown in this chapter, that a Gaussian likelihood function supplemented with a Gaussian prior leads to a posterior that is again Gaussian. In statistical terms, this constitutes an example of a *conjugate prior* [111], namely a choice of prior for a given likelihood such that the posterior belongs to the same family as the prior. A third reason for the central importance of linear inverse problems is that they arise naturally in sequential data assimilation, as we will see in the second part of these notes. The paper [100], which concerns the linear-Gaussian setting, was arguably the first to formulate Bayesian inversion in function space, for the specific problem of determining the initialization of the heat equation from the solution at later times. The paper [190] studied the linear-Gaussian setting more generally.

In this chapter we have studied several small noise limits, and established a basic form of posterior consistency. While intuitively small observation noise would seem desirable in the reconstruction of the unknown parameter, perhaps counterintuitively it often makes the computational solution to the inverse problem more challenging. A concrete manifestation of this phenomenon is analyzed in the context of importance sampling in [5]. For a treatment of posterior consistency in infinite dimensions we refer to [174, 3, 221], and for the consistency problem in the classical statistical setting to the books [115, 75]. In certain large data regimes, the Bernstein-von Mises theorem [79] guarantees that the Bayesian posterior solution is approximately Gaussian [221, 224, 116] and that the prior distribution plays a negligible role in the posterior, thus providing theoretical support to the Bayesian approach. We emphasize, however, that in the underdetermined inverse problem setting one cannot expect the conclusions to hold, as demonstrated in this chapter. Furthermore, recent work [223] demonstrates specific phenomena, including potential obstacles to consistency theorems, that may result in the setting of infinite-dimensional Bayesian inversion. For non-statistical optimization-based approaches to inverse problems, and consistency in particular, see [89] and the references therein.

Chapter 3

Optimization Perspective

In this chapter we explore the properties of Bayesian inversion from the perspective of an optimization problem which corresponds to maximizing the posterior probability: that is, to finding a maximum a posteriori (MAP) estimator, or mode of the posterior distribution. We demonstrate the properties of the point estimator resulting from this optimization problem, showing its positive and negative attributes, the latter motivating our work in the following three chapters. We also introduce, and study, basic gradient-based optimization algorithms.

The chapter is organized as follows. We first introduce the problem setting in Section 3.1. Two theoretical results are presented in Section 3.2. The first shows that the MAP estimator is attained under appropriate assumptions, while the second provides an interpretation of MAP estimation in terms of maximizing the probability of infinitesimally small balls. Section 3.3 contains several examples that illustrate some possible limitations of MAP estimation. Gradient descent and stochastic gradient descent algorithms are described in Section 3.4. Both of these algorithms are important examples of gradient-based optimization algorithms, which we interpret as arising from time-discretization of an underlying differential equation. The chapter closes in Section 3.5 with bibliographical remarks.

3.1 The Setting

Once again we work in the inverse problem setting of finding $u \in \mathbb{R}^d$ from $y \in \mathbb{R}^k$ given by

$$y = G(u) + \eta$$

with noise $\eta \sim \nu$ and prior $u \sim \rho$, as in Assumption 1.1. The posterior pdf $\pi^y(u)$ on $u|y$ is given by Theorem 1.2 and has the form

$$\pi^y(u) = \frac{1}{Z} \nu(y - G(u)) \rho(u).$$

Generalizing the definition from the previous chapter, concerning only the Gaussian setting, we define a *loss function*

$$L(u) = -\log \nu(y - G(u)),$$

and a *regularizer*

$$R(u) = -\log \rho(u).$$

Note that the loss is equal to the negative log-likelihood: $L(u) = -\log l(u)$. When added together, these two functions of u comprise an *objective function* of the form

$$J(u) = L(u) + R(u).$$

Furthermore

$$\pi^y(u) = \frac{1}{Z} \nu(y - G(u)) \rho(u) \propto e^{-J(u)}.$$

We see that minimizing the objective function $J(\cdot)$ is equivalent to maximizing the posterior pdf $\pi^y(\cdot)$. Therefore, recalling Definition 1.4, the MAP estimator can be rewritten in terms of J as follows:

$$\begin{aligned} u_{\text{MAP}} &= \arg \max_{u \in \mathbb{R}^d} \pi^y(u) \\ &= \arg \min_{u \in \mathbb{R}^d} J(u). \end{aligned}$$

We will provide conditions under which the MAP estimator is attained in Theorem 3.5 and we will give an interpretation of MAP estimators in terms of maximizing the probability of infinitesimal balls in Theorem 3.8. This interpretation can be used to generalize the definition of MAP estimators to measures that do not possess a Lebesgue density.

Example 3.1 (MAP Estimator – Linear-Gaussian Setting). Consider the linear-Gaussian setting of Assumption 2.1. Then, since the posterior is Gaussian, its mode agrees with its mean, which is given by m as defined in Theorem 2.2. \diamond

Example 3.2 (Loss Function – Gaussian Observational Noise). If $\eta = \mathcal{N}(0, \Gamma)$, then $\nu(y - G(u)) \propto \exp(-\frac{1}{2}|y - G(u)|_\Gamma^2)$. So the loss in this case is $L(u) = \frac{1}{2}|y - G(u)|_\Gamma^2$, a Γ -weighted ℓ_2 loss. \diamond

Example 3.3 (ℓ_2 Regularizer – Gaussian Prior). If we have prior $\rho(u) = \mathcal{N}(0, \hat{C})$, then ignoring u -independent normalization factors, which appear as constant shifts in $J(\cdot)$, we may take the regularizer as $R(u) = \frac{1}{2}|u|_{\hat{C}}^2$. In particular, if $\hat{C} = \lambda^{-1}I$, then $R(u) = \frac{\lambda}{2}|u|^2$, an ℓ_2 regularizer. \diamond

If we combine Example 3.2 and Example 3.3, we obtain a canonical objective function

$$J(u) = \frac{1}{2}|y - G(u)|_\Gamma^2 + \frac{\lambda}{2}|u|^2.$$

To connect with future discussions, here λ corresponds to prior precision, and may be learned from data: an example of a *hierarchical* formulation of Bayesian inversion.

Example 3.4 (ℓ_1 Regularizer – Laplace Prior). As an alternative to the ℓ_2 regularizer, consider $u = (u_1, \dots, u_d)$ with u_i having prior distribution i.i.d. Laplace. Then $\rho(u) \propto \exp(-\lambda \sum_{i=1}^d |u_i|) = \exp(-\lambda|u|_1)$. In this case $R(u) = \lambda|u|_1$, an ℓ_1 regularizer.

If we combine this prior with the weighted ℓ_2 loss above, then we obtain the objective function

$$J(u) = \frac{1}{2} \|y - G(u)\|_1^2 + \lambda \|u\|_1.$$

Even though this objective function promotes sparse solutions, samples from the underlying posterior distribution are typically not sparse. \diamond

3.2 Theory

For any optimization problem for an objective function with a finite infimum, it is of interest to determine whether the infimum is attained. We have the following result which shows that, under suitable conditions on J , the infimum of J is attained and hence that the formulation of the MAP estimator through maximization of π^y (equivalently minimization of J) is well-defined.

Theorem 3.5 (Attainable MAP Estimator). *Assume that J is non-negative, continuous and that $J(u) \rightarrow \infty$ as $\|u\| \rightarrow \infty$. Then J attains its infimum. Therefore, the MAP estimator of u based on the posterior $\pi^y(u) \propto \exp(-J(u))$ is attained.*

Proof. By the assumed growth and non-negativity of J , there is R such that $\inf_{u \in \mathbb{R}^d} J(u) = \inf_{u \in B(0, R)} J(u)$, where (recall) $B(0, R)$ denotes the closed ball of radius R around the origin. Since J is assumed to be continuous, its infimum over $B(0, R)$ is attained and the proof is complete. \square

Remark 3.6. Suppose that:

1. $G \in C(\mathbb{R}^d, \mathbb{R}^k)$, i.e. G is a continuous function;
2. the objective function $J(u)$ has ℓ_2 loss as defined in Example 3.2 and ℓ_p regularizer $R(u) = \frac{\lambda}{p} \|u\|_p^p$, $p \in [1, \infty)$.

Then the assumptions on J in Theorem 3.5 are satisfied. This shows that if G is continuous, the infimum of J defined with ℓ_2 loss and ℓ_p regularizer is attained at the MAP estimator of the corresponding Bayesian problem with posterior pdf proportional to $\exp(-J(u))$. \diamond

Remark 3.7. Notice that the assumption that $J(u) \rightarrow \infty$ is not restrictive: this condition needs to hold in order to be able to normalize $\pi^y(u) \propto \exp(-J(u))$ into a pdf, which is implicitly assumed in the second part of the theorem statement. \diamond

Intuitively the MAP estimator maximizes posterior probability. We make this precise in the following theorem which links the objective function $J(\cdot)$ to small ball probabilities.

Theorem 3.8 (Objective Function and Posterior Probability). *Under the same assumptions as in Theorem 3.5, let*

$$\alpha(u, \delta) := \int_{v \in B(u, \delta)} \pi^y(v) dv = \mathbb{P}^{\pi^y}(B(u, \delta))$$

be the posterior probability of a ball with radius δ centered at u . Then, for all $u, u' \in \mathbb{R}^d$, we have

$$\lim_{\delta \rightarrow 0} \frac{\alpha(u, \delta)}{\alpha(u', \delta)} = e^{J(u') - J(u)}.$$

Proof. Let $u, u' \in \mathbb{R}^d$ and let $\epsilon > 0$. By continuity of J we have that, for all δ sufficiently small,

$$\begin{aligned} e^{-J(u) - \epsilon} &\leq e^{-J(v)} \leq e^{-J(u) + \epsilon} && \text{for all } v \in B(u, \delta), \\ e^{-J(u') - \epsilon} &\leq e^{-J(v)} \leq e^{-J(u') + \epsilon} && \text{for all } v \in B(u', \delta). \end{aligned}$$

Therefore, for all δ sufficiently small,

$$\begin{aligned} B_\delta e^{-J(u) - \epsilon} &\leq \int_{v \in B(u, \delta)} e^{-J(v)} dv \leq B_\delta e^{-J(u) + \epsilon}, \\ B_\delta e^{-J(u') - \epsilon} &\leq \int_{v \in B(u', \delta)} e^{-J(v)} dv \leq B_\delta e^{-J(u') + \epsilon}, \end{aligned}$$

where B_δ is the Lebesgue measure of a ball with radius δ . Taking the ratio of α 's and using the above bounds we obtain that, for all δ sufficiently small,

$$e^{J(u') - J(u) - 2\epsilon} \leq \frac{\alpha(u, \delta)}{\alpha(u', \delta)} \leq e^{J(u') - J(u) + 2\epsilon}.$$

Since $\epsilon > 0$ is arbitrary, the desired result follows. \square

Remark 3.9. This theorem shows that maximizing the probability of an infinitesimally small ball is the same as minimizing the objective function $J(\cdot)$. This is intuitive in finite dimensions, but the proof above generalizes beyond measures which possess a Lebesgue density, and may be used in infinite dimensions. \diamond

3.3 Examples

By means of examples we now probe the question of whether or not the MAP estimator captures useful information about the posterior distribution.

Example 3.10 (Summarizing Single-Peaked Posterior). If the posterior is single-peaked, such as a Gaussian or a Laplace distribution, as shown in Figure 3.1, the MAP estimator, i.e. minimizer of the objective function, reasonably summarizes the most likely value of the unknown parameter. \diamond

We next consider several examples where a point estimator—or a δ -radius ball with small δ —fails to adequately summarize the posterior distribution.

Example 3.11 (Summarizing Multiple-Peaked Posterior). If the posterior is rather unevenly distributed, such as a slab-and-spike distribution, as shown in Figure 3.2, then it is less clear that the MAP estimator usefully summarizes the posterior. For example, for the

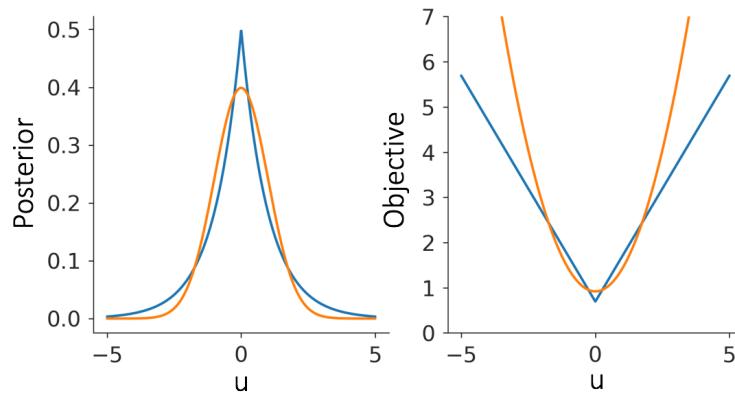


Figure 3.1 Posterior (left) and objective function (right) for $\mathcal{N}(0, 1)$ posterior (orange) and $\text{Laplace}(0, 1)$ posterior (blue).

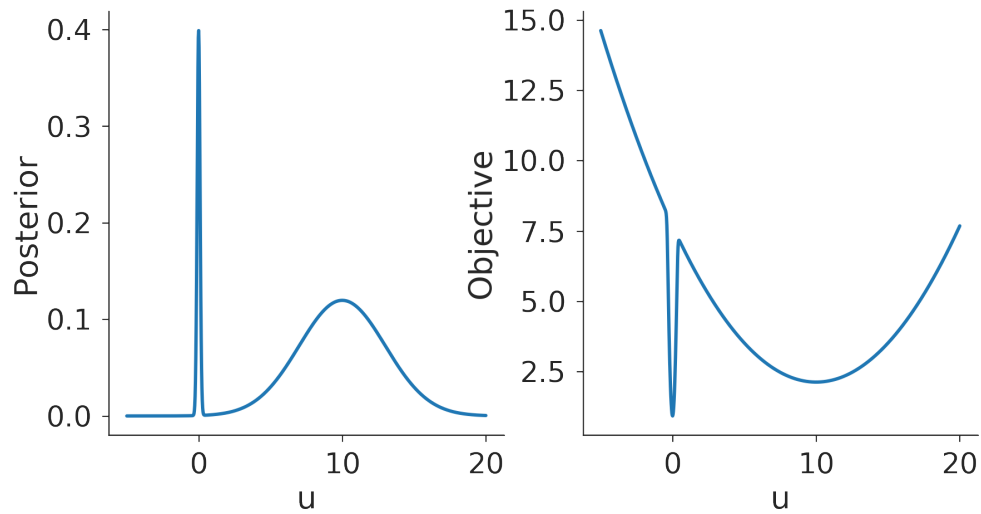


Figure 3.2 Posterior (left) and objective function (right) for a posterior that is a sum of two Gaussian distributions, $\mathcal{N}(0, 0.1^2)$ with probability 0.1 and $\mathcal{N}(10, 3^2)$ with probability 0.9.

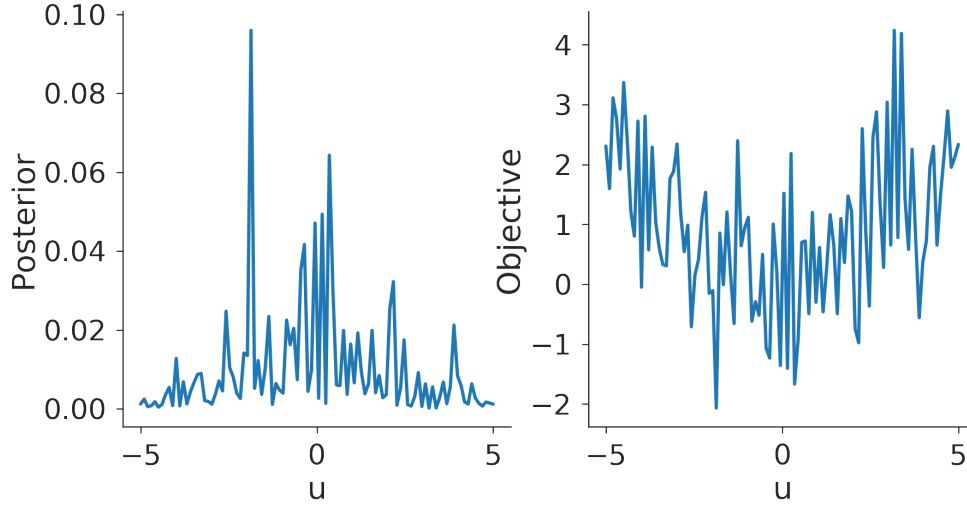


Figure 3.3 Posterior (left) and objective function (right) from an objective function that is very rough in the small scale, but contains a regular pattern on the larger scale. This specific example is generated by white noise summed with a quadratic function for the objective function, and the posterior is computed from the objective function.

case in Figure 3.2 we may want the solution output of our Bayesian problem to be a weighted average of two Gaussian distributions, or two point estimators each with a separate mean located at one of the two minima of the objective functions, and weight describing the probability mass associated with each of those two points. \diamond

Example 3.12 (Summarizing Rough Posteriors). In addition to a multiple-peak posterior, there are cases where the objective function and the associated posterior pdf are simply very rough. In these cases, the small-scale roughness should be ignored, while the large-scale variation should be captured. For example, the objective function in Figure 3.3 is very rough and has a unique minimizer at a point far from 0. However, it also has a larger-scale pattern: it tends to be smaller around 0, while larger away from 0. The MAP estimator cannot capture this large scale pattern, as it is found by minimizing the objective function. It is arguably the case that $u = 0$ is a better point estimate. An alternative way to interpret this phenomenon is that there is a natural “temperature” to this problem, in the sense that variations lower than this temperature could be viewed as random noise that do not capture meaningful information. \diamond

The preceding examples suggest that multi-peak distributions, or multi-minimum objective functions, can cause problems for MAP estimation. Next we illustrate that if the dimension d of the parameter $u \in \mathbb{R}^d$ is high, then a single point estimator, even if a MAP estimator, is typically not a good summary of the posterior.

Example 3.13 (Summarizing High-Dimensional Posterior). We consider what is the “typical size” of a vector u drawn from the standard Gaussian distribution $\mathcal{N}(0, I)$, as the dimension increases. In Figure 3.4 we display the empirical density of the norm of such

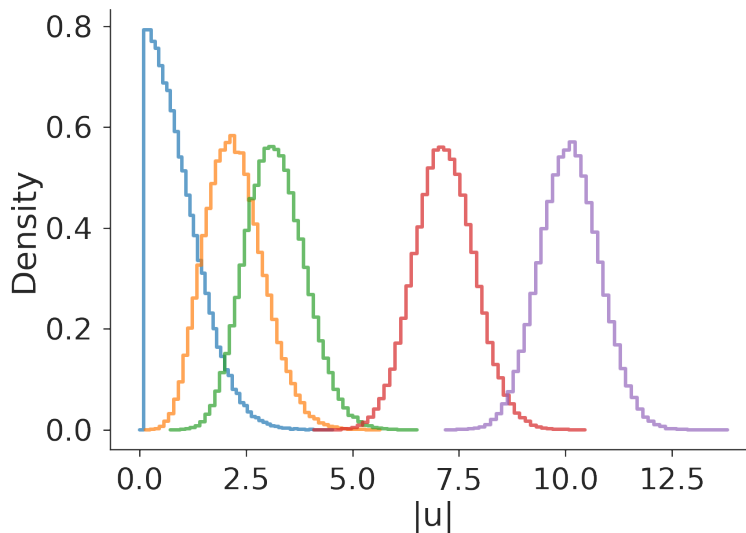


Figure 3.4 Empirical density of ℓ_2 norm of $\mathcal{N}(0, I)$ random vectors for various dimension: $d = 1$ (blue), $d = 5$ (orange), $d = 10$ (green), $d = 50$ (red), and $d = 100$ (purple). The empirical density is obtained from 10000 samples for each distribution.

random vectors. We can see that at low dimensions, such as when $d = 1$, obtaining a value close to the mode $u = 0$ is highly likely. In higher dimensions, however, the probability for a vector from this distribution to have a small ℓ_2 -norm becomes increasingly small as d grows. For example, let us consider the probability for the norm to be less than 5. Then $\mathbb{P}(|u| < 5)$ is 0.99999943 when $d = 1$, 0.99986 when $d = 5$, 0.99465 when $d = 10$, 0.001192 when $d = 50$, and 1.135×10^{-15} when $d = 100$. So we see that, as the dimension increases, with probability close to 1 a sample from the posterior would have a norm far from 0. Indeed, for $d = 1000$, the 5th and 95th percentiles are respectively 30.3464 and 32.7823. This means when $d = 1000$, we most likely will find a vector with size around 31, not 0. Another way to see this is that, since the components u_i of u are i.i.d. standard unit Gaussians we have that, by the strong law of large numbers,

$$\frac{1}{d} \sum_{i=1}^d u_i^2 \rightarrow 1$$

as $d \rightarrow \infty$ almost surely. Thus, with high probability, the ℓ_2 -norm is of size \sqrt{d} . This example suggests that in high dimension, a point estimator may not capture enough information about the density. \diamond

The preceding examples demonstrate that MAP estimators should be treated with caution as they may not capture the desired posterior information in many cases. This motivates the study of alternative ways —beyond MAP estimators— to capture information from the posterior distribution. One such approach is to fit one or several Gaussian distributions to the posterior by minimizing an appropriate distance-like measure between distributions. This is the topic of the next chapter. However, in the

remainder of this chapter we discuss gradient-based methods for minimization. These may be useful for MAP estimation, and also for fitting Gaussian approximations.

3.4 Gradient-Based Optimization Algorithms

In this section we discuss algorithms for the minimization of $J : \mathbb{R}^d \mapsto \mathbb{R}$. Algorithms for the optimization of functions of this type are numerous, and vary considerably in type. In order to focus our discussion, we devote our attention entirely to gradient-based algorithms. These are organized around a single important principle, and are also of interest due to their use in parameter estimation arising in machine learning (a form of inverse problem).

3.4.1 Gradient Flow

Our starting point is the differential equation

$$\frac{du}{dt} = -DJ(u), \quad u(0) = u_0. \quad (3.1)$$

A straightforward calculation shows that

$$\frac{d}{dt}(J(u)) = \left\langle DJ(u), \frac{du}{dt} \right\rangle = -|DJ(u)|^2. \quad (3.2)$$

This calculation is at the core of gradient-based optimization algorithms. Since the time-derivative of $u(t)$ gives the tangent to the trajectory, it demonstrates that evolving in the direction of the negative gradient of $J(u)$ will cause $J(u(t))$ to be non-increasing as a function of time; indeed $J(u(t))$ will actually decrease until u is at a critical point of $J(\cdot)$: a point at which the gradient is zero, including local minima, local maxima and saddle points.

For any $K \in \mathbb{R}^{d \times d}$, that we will assume positive definite in what follows, we may also consider the *preconditioned* gradient flow

$$\frac{du}{dt} = -KDJ(u), \quad u(0) = u_0. \quad (3.3)$$

3.4.2 Gradient Descent

In order to turn the gradient flow (3.3) into an optimization algorithm, we discretize it by the Euler method with variable time-step $\alpha_\ell > 0$.

Algorithm 3.1 Gradient Descent Algorithm

- 1: **Input:** Objective function $J : \mathbb{R}^d \rightarrow \mathbb{R}$, positive definite matrix K , initialization $u_0 \in \mathbb{R}^d$, number of steps L , rule for choosing the step-sizes $\{\alpha_\ell\}_{\ell=0}^{L-1}$.
2: For $\ell = 0, 1, \dots, L-1$ do:

$$u_{\ell+1} = u_\ell - \alpha_\ell K D J(u_\ell).$$

- 3: **Output:** Deterministic iterates u_0, u_1, \dots, u_L .
-

It is natural to ask how α_ℓ should be chosen. In order to get insight into this issue, we study in detail the case where $K = I$ and $J(u)$ is quadratic. The latter condition ensures that the iteration for u_ℓ is linear in the case of fixed α_ℓ ; it is however nonlinear when α_ℓ is adapted, as it is here, on the basis of u_ℓ .

Let $A \in \mathbb{R}^{d \times d}$ be positive definite, let $b \in \mathbb{R}^d$, and define

$$J(u) = \frac{1}{2} |b - Au|_A^2. \quad (3.4)$$

This strictly convex function has minimum u^* which is solution of the linear system

$$Au^* = b. \quad (3.5)$$

The gradient flow (3.2) gives the linear differential equation

$$\frac{du}{dt} = b - Au$$

and has unique globally attracting fixed point at u^* .

The resulting discrete time-step algorithm is

$$u_{\ell+1} = u_\ell + \alpha_\ell (b - Au_\ell).$$

The first question we ask is how α_ℓ should be chosen to maximize the decrease in $J(\cdot)$ in one step of the algorithm. We address this in the next lemma and then, using this optimal time-step, we study the convergence properties of the algorithm. With this goal in mind, it is helpful to define the *residual function* $r : \mathbb{R}^d \rightarrow \mathbb{R}^d$ by $r(u) = b - Au$. Given the sequence $\{u_\ell\}$ we may then define the *residual vector* $r_\ell = r(u_\ell)$. Then $J(u) = \frac{1}{2} |r(u)|_A^2$, $J(u_\ell) = \frac{1}{2} |r_\ell|_A^2$ and

$$u_{\ell+1} = u_\ell + \alpha_\ell r_\ell.$$

Lemma 3.14. *Choosing*

$$\alpha_\ell = \frac{|r_\ell|^2}{|r_\ell|_{A^{-1}}^2}$$

leads to the maximal decrease in $J(\cdot)$ and to the algorithm

$$u_{\ell+1} = u_\ell + \frac{|r_\ell|^2}{|r_\ell|_{A^{-1}}^2} r_\ell. \quad (3.6)$$

Proof. We have

$$\begin{aligned} Au_{\ell+1} &= Au_{\ell} + \alpha_{\ell} Ar_{\ell}, \\ b &= b, \end{aligned}$$

so that subtracting gives

$$r_{\ell+1} = r_{\ell} - \alpha_{\ell} Ar_{\ell}.$$

From this it follows that

$$J(u_{\ell+1}) = J(u_{\ell}) - \alpha_{\ell} |r_{\ell}|^2 + \frac{1}{2} \alpha_{\ell}^2 |r_{\ell}|_{A^{-1}}^2. \quad (3.7)$$

The right-hand side is quadratic in α_{ℓ} and minimized at the prescribed choice of α_{ℓ} . \square

Theorem 3.15 (Conditioning of A and Decrease of J). *Let A have maximal and minimal eigenvalues $\lambda_{\max} \geq \lambda_{\min} > 0$, respectively. Then*

$$J(u_{\ell+1}) \leq \left(1 - \frac{\lambda_{\min}}{\lambda_{\max}}\right) J(u_{\ell}). \quad (3.8)$$

Proof. Substituting the optimal choice of α_{ℓ} into equation (3.7) gives

$$\begin{aligned} J(u_{\ell+1}) &= J(u_{\ell}) - \frac{1}{2} \frac{|r_{\ell}|^4}{|r_{\ell}|_{A^{-1}}^2} \\ &= J(u_{\ell}) - \frac{|r_{\ell}|^4}{|r_{\ell}|_{A^{-1}}^2 |r_{\ell}|_A^2} J(u_{\ell}). \end{aligned}$$

Applying the result of Lemma 3.17 below gives the desired result. \square

Remark 3.16. Inequality (3.8) suggests slow convergence of the algorithm for matrices A which have a large condition number, i.e. for which $\lambda_{\max} \gg \lambda_{\min}$. In principle this can be ameliorated by preconditioning the algorithm by choosing $K = A^{-1}$ so that the preconditioned steepest descent iteration becomes

$$u_{\ell+1} = u_{\ell} + \alpha_{\ell} (A^{-1}b - u_{\ell}).$$

The optimal choice of α_{ℓ} for this iteration becomes $\alpha_{\ell} = 1$, which gives $u_{\ell+1} = A^{-1}b$. Thus, the algorithm converges in one step, regardless of the initial condition. However, implementing the algorithm with $K = A^{-1}$ would require computation of $A^{-1}b$; the goal of the descent algorithm is, of course, to avoid computation of A^{-1} in the first place. This discussion illustrates nonetheless the potential practical advantage of preconditioning using a positive definite matrix $K \approx A^{-1}$ whose action on vectors can nonetheless be computed much more cheaply than that of A^{-1} itself. \diamond

Lemma 3.17. *For any $u \in \mathbb{R}^d$,*

$$\frac{|u|^4}{|u|_{A^{-1}}^2 |u|_A^2} \geq \frac{\lambda_{\min}}{\lambda_{\max}}.$$

Proof. Since A is assumed to be positive definite, the eigenvalue problem for A has solutions with the form

$$\begin{aligned} A\varphi_i &= \lambda_i\varphi_i, \quad i = 1, \dots, d, \\ \langle \varphi_i, \varphi_j \rangle &= \delta_{ij}, \quad i, j = 1, \dots, d, \end{aligned}$$

where we may assume the ordering

$$0 < \lambda_{\min} := \lambda_1 \leq \dots \leq \lambda_d =: \lambda_{\max}.$$

Expanding $u \in \mathbb{R}^d$ in this eigenbasis, we have

$$u = \sum_{i=1}^d u_i \varphi_i$$

with $u_i = \langle u, \varphi_i \rangle$. Now, noting that

$$|u|^2 = \sum_{i=1}^d u_i^2, \quad |u|_{A^{-1}}^2 = \sum_{i=1}^d \lambda_i u_i^2, \quad |u|_A^2 = \sum_{i=1}^d \frac{u_i^2}{\lambda_i},$$

we get

$$\begin{aligned} |u|^2 &= \sum_{i=1}^d u_i^2 \geq \lambda_{\min} |u|_A^2, \\ |u|_{A^{-1}}^2 &= \sum_{i=1}^d \lambda_i u_i^2 \leq \lambda_{\max} |u|^2. \end{aligned}$$

The desired result follows. □

3.4.3 Stochastic Gradient Descent

Here we consider optimizing a stochastically defined objective function. This concerns the setting where

$$J(u) = \int_B F(u, z) \zeta(z) dz, \tag{3.9}$$

$B \subseteq \mathbb{R}^{d_z}$, and ζ is the pdf of a random variable $z \in B$. The goal is optimization of $J(u)$.

Stochastic gradient descent is designed to numerically solve this optimization problem in cases where explicit evaluation of $J(u)$, and its gradient $DJ(u)$, is not possible because doing so involves an integration over B . It is assumed, however, that $D_u F(u, z)$ can be evaluated for any fixed $z \in B \subseteq \mathbb{R}^{d_z}$. The proposed algorithm is then the following:

Algorithm 3.2 Stochastic Gradient Descent Algorithm

- 1: **Input:** Objective function J defined implicitly by (3.9), positive definite matrix K , initialization $u^{(0)} \in \mathbb{R}^d$, number of steps L , rule for choosing the step-sizes $\{\alpha_\ell\}_{\ell=0}^{L-1}$.
 - 2: For $\ell = 0, 1, \dots, L-1$ do:
 $u^{(\ell+1)} = u^{(\ell)} - \alpha_\ell K D_u F(u^{(\ell)}, z^{(\ell)})$ with $z^{(\ell)} \sim \zeta$ i.i.d.
 - 3: **Output:** Random iterates $u^{(0)}, u^{(1)}, \dots, u^{(L)}$.
-

The output of the algorithm defines an (in general) inhomogeneous Markov chain; it will be homogeneous if α_ℓ is constant in ℓ . Markov chains are discussed in more detail in Chapter 6. In what follows we will show the convergence of the algorithm in a simple setting, amenable to a concrete analysis. We will also motivate the importance of the algorithm in a machine learning context.

Our convergence analysis will rely on the following assumption.

Assumption 3.18. *The objective function J in (3.9) satisfies:*

- (i) *There exists c_1 such that, for all $u \in \mathbb{R}^d$, $\sup_{z \in B} |D_u F(u, z)|^2 \leq c_1$.*
- (ii) *There exists $c_2 > 0$ such that, for all $u, v \in \mathbb{R}^d$,*

$$J(v) \geq J(u) + \langle DJ(u), v - u \rangle + \frac{c_2}{2} |u - v|^2. \quad (3.10)$$

Note that item (i) in Assumption 3.18 implies a Lipschitz condition on F over its second argument, while the second item assumes strong convexity of J . In particular, this second condition implies that, if J is sufficiently smooth, its Hessian satisfies $D^2 J \geq c_2 I$, that is, for all $u \in \mathbb{R}^d$ the matrix $D^2 J(u) - c_2 I$ is positive definite.

Theorem 3.19 (Convergence of Stochastic Gradient Descent). *Suppose that Assumption 3.18 holds. Suppose further that the step-sizes are positive with $\alpha_\ell \rightarrow 0$ and $\sum_{\ell=0}^{\infty} \alpha_\ell = \infty$. Then the objective function J has a unique minimizer u^* and the output of Algorithm 3.2 satisfies $\mathbb{E}[|u^{(\ell)} - u^*|^2] \rightarrow 0$ as $\ell \rightarrow \infty$.*

Proof. The existence and uniqueness of the minimizer u^* of J follows by the strong convexity in Assumption 3.18 item (ii). Denote $e_\ell = \mathbb{E}[|u^{(\ell)} - u^*|^2]$. Then, from the definition of the stochastic gradient descent updates, we have that

$$\begin{aligned} e_{\ell+1} &= \mathbb{E}[|u^{(\ell)} - u^* - \alpha_\ell D_u F(u^{(\ell)}, z^{(\ell)})|^2] \\ &= e_\ell + \alpha_\ell^2 \mathbb{E}[|D_u F(u^{(\ell)}, z^{(\ell)})|^2] - 2\alpha_\ell \mathbb{E}[\langle u^{(\ell)} - u^*, D_u F(u^{(\ell)}, z^{(\ell)}) \rangle]. \end{aligned} \quad (3.11)$$

By the law of total expectation and the definition of J in (3.9), we can rewrite the last expectation in the right-hand side as

$$\mathbb{E}\left[\mathbb{E}[\langle u^{(\ell)} - u^*, D_u F(u^{(\ell)}, z^{(\ell)}) \rangle \mid u^{(1)}, \dots, u^{(\ell)}, z^{(1)}, \dots, z^{(\ell-1)}]\right] = \mathbb{E}[\langle u^{(\ell)} - u^*, DJ(u^{(\ell)}) \rangle]. \quad (3.12)$$

Therefore, using Assumption 3.18 items (i) and (ii) to bound the second and third terms in the right-hand side of (3.11), we deduce that

$$e_{\ell+1} \leq (1 - \alpha_\ell c_2)e_\ell + \alpha_\ell^2 c_1.$$

It follows that, for any $\epsilon > 0$,

$$e_{\ell+1} - \epsilon \leq (1 - \alpha_\ell c_2)(e_\ell - \epsilon) + \alpha_\ell(\alpha_\ell c_1 - \epsilon c_2).$$

Note that, for all sufficiently large ℓ , $\alpha_\ell(\alpha_\ell c_1 - \epsilon c_2) < 0$. Thus we obtain that, for all sufficiently large ℓ ,

$$e_{\ell+1} - \epsilon \leq (1 - \alpha_\ell c_2)(e_\ell - \epsilon).$$

Iterating this inequality gives that, for some ℓ sufficiently large and all $m \in \mathbb{N}$,

$$e_{\ell+m} - \epsilon \leq \prod_{j=0}^{m-1} (1 - \alpha_{\ell+j} c_2)(e_\ell - \epsilon).$$

Recall that for $x \in (0, 1)$ we have that $\log(1 - x) \leq -x$ (a proof can be found in Chapter 4, Lemma 4.3). Now notice that, as $m \rightarrow \infty$,

$$0 \leq \prod_{j=0}^{m-1} (1 - \alpha_{\ell+j} c_2) \leq \exp\left(\sum_{j=0}^{m-1} -\alpha_{\ell+j} c_2\right) \rightarrow 0 \quad (3.13)$$

since by assumption $\sum_{\ell=0}^{\infty} \alpha_\ell = \infty$. Thus $e_{\ell+m} \leq \epsilon$ for all m large enough, and since ϵ is arbitrary the desired result follows. \square

Example 3.20 (Stochastic Gradient Descent in Machine Learning). Although the original motivation for the algorithm was settings in which $DJ(u)$ is not explicitly calculable, the methodology has gained importance in machine learning optimization tasks where the motivation is different. Consider an objective function defined by

$$J(u) = \frac{1}{2} \sum_{i=1}^{d_z} |y^i - G^i(u)|^2,$$

where each $y^i \in \mathbb{R}^k$ represents data arising from a forward model G^i . We may write this objective in the form of equation (3.9) as follows. Define

$$F(u, z) = \frac{d_z}{2} \sum_{i=1}^{d_z} z_i |y^i - G^i(u)|^2$$

with $z := (z_1, \dots, z_{d_z}) \in \mathbb{R}^{d_z}$. Define $e^i := (0, \dots, 1, \dots, 0)^\top$, the i -th unit vector and let

$$\zeta(z) = \frac{1}{d_z} \sum_{i=1}^{d_z} \delta(z - e^i).$$

Then

$$J(u) = \int_B F(u, z) \zeta(z) dz$$

with B any bounded set containing all the unit vectors $\{e^i\}_{i=1}^{d_z}$. This is because if $z \sim \zeta$, then $\mathbb{E}[z] = d_z^{-1}(1, \dots, 1)^\top \in \mathbb{R}^{d_z}$.

In this setting the stochastic gradient descent algorithm becomes

$$\begin{aligned} i(\ell) &\sim \mathbf{u}(\{1, \dots, d_z\}) \text{ i.i.d.} \\ u^{(\ell+1)} &= u^{(\ell)} + \alpha_\ell d_z D G^{i(\ell)}(u^{(\ell)})^\top (y^{i(\ell)} - G^{i(\ell)}(u^{(\ell)})), \end{aligned} \quad (3.14)$$

where the notation signifies that $i(\ell)$ is chosen uniformly at random from the index set $\{1, \dots, d_z\}$. In the context of machine learning this algorithm has several potential advantages over standard gradient descent: i) if d_z is massive (large data sets) then it is not necessary to hold the entirety of $DJ(u)$ in memory at any one time; ii) if the data is received in a streaming fashion then the algorithm can be implemented in a non-random fashion where the indices $i(\ell)$ are traversed systematically as the components of the data are received; (iii) it is observed empirically that the randomness induced by sampling terms from the summand defining $DJ(u)$ promotes improved optimization for nonconvex $J(u)$, in comparison with standard gradient descent, because the randomness allows escape from local minima and allows for more rapid traversing of saddle-point neighbourhoods. \diamond

We now consider the setting of Example 3.20 in which $G^i(u) = A^i u$ for some positive definite matrix $A^i \in \mathbb{R}^{d \times d}$, $y^i \in \mathbb{R}^d$ and we modify the definition of J so that each term employs a different norm:

$$J(u) = \frac{1}{2} \sum_{i=1}^{d_z} |y^i - A^i u|_{A^i}^2.$$

We define

$$\bar{y} = \frac{1}{d_z} \sum_{i=1}^{d_z} y^i, \quad \bar{A} = \frac{1}{d_z} \sum_{i=1}^{d_z} A^i.$$

A straightforward calculation reveals that \bar{A} is positive definite and $J(u)$ has a unique minimizer u^* solving the equation $\bar{A}u^* = \bar{y}$.

In this setting the analog of the algorithm from (3.14) becomes

$$u^{(\ell+1)} = u^{(\ell)} + \alpha_\ell (y^{i(\ell)} - A^{i(\ell)} u^{(\ell)}), \quad (3.15)$$

where $i(\ell)$ is chosen uniformly at random from $\{1, \dots, d_z\}$ i.i.d. at every step, and independently from $u^{(\ell)}$. This gives an (in general inhomogeneous) Markov chain. Theorem 3.19 concerning stochastic gradient descent made the assumption that the time-step α_ℓ decreases to zero with increasing ℓ . Here we choose a fixed time-step α leading to a homogeneous Markov chain; we prove a positive result about the convergence of the algorithm in an average sense.

Theorem 3.21 (Convergence of Stochastic Gradient Descent – Constant Step-Size). *Let $\alpha_\ell = \alpha > 0$ and assume that, in (3.15), $\lim_{\ell \rightarrow \infty} \mathbb{E}[u^{(\ell)}]$ exists. Then the limit is given by u^\star .*

Proof. Take expectation in (3.15) conditional on knowing $u^{(\ell)}$ to obtain

$$\begin{aligned} \mathbb{E}[u^{(\ell+1)} | u^{(\ell)}] &= u^{(\ell)} + \alpha \left(\mathbb{E}[y^{i(\ell)}] - \mathbb{E}[A^{i(\ell)} u^{(\ell)}] \right) \\ &= u^{(\ell)} + \alpha \left(\bar{y} - \bar{A} u^{(\ell)} \right). \end{aligned}$$

Taking expectation over $u^{(\ell)}$ gives

$$\mathbb{E}[u^{(\ell+1)}] = \mathbb{E}[u^{(\ell)}] + \alpha \left(\bar{y} - \bar{A} \mathbb{E}[u^{(\ell)}] \right).$$

Taking the limit $\ell \rightarrow \infty$ and assuming $\lim_{\ell \rightarrow \infty} \mathbb{E}[u^{(\ell)}]$ exists and is given by u^\dagger yields

$$u^\dagger = u^\dagger + \alpha (\bar{y} - \bar{A} u^\dagger).$$

Hence $\bar{A} u^\dagger = \bar{y}$ and by the invertibility of \bar{A} it follows that $u^\dagger = u^\star$. \square

3.5 Discussion and Bibliography

Standard textbooks on optimization include [227, 74, 33]. The optimization perspective on inversion predates the development of the Bayesian approach as a computational tool, because it is typically far cheaper to implement. The subject of classical regularization techniques for inversion is discussed in [89]. The concept of MAP estimators, which links probability to optimization, is discussed in the books [161, 298] in the finite-dimensional setting. The paper [67] studies this connection precisely: it defines the MAP estimator for infinite-dimensional Bayesian inverse problems, and the corresponding variational formulation, in the setting of Gaussian priors and Gaussian noise. The paper [138] studies related ideas, but in the non-Gaussian setting, and [4] generalizes the variational formulation of MAP estimators to non-Gaussian priors that are sparsity promoting. Recent work sets MAP estimators for PDE-based inverse problems within the existing framework of statistical estimation theory [225]. The paper [299] shows an example of optimization based inversion in a large-scale geophysical application.

A discussion of gradient-based descent in both continuous and discrete time may be found in [293]. Stochastic analogues of (3.2) may be used to sample the probability distribution $\exp(-\beta J(u))$ and an introduction to this subject may be found in [238]. The idea of using *stochastic approximation* for solving nonlinear equations defined via an expectation was introduced in the paper [262]. The specific analysis in the case of such equations defined as a gradient, and in particular the statement and proof of a result closely related to Theorem 3.19, may be found in [170]. The link to machine learning, described in Example 3.20, is overviewed in [119]. The paper [32] provides an accessible introduction to optimization methods for large-scale machine learning.

Chapter 4

Gaussian Approximation

Recall the inverse problem of finding u from y given by (1.1), and the Bayesian formulation which follows from Assumption 1.1. In the previous chapter we explored the idea of obtaining a point estimator using an optimization perspective arising from maximizing the posterior pdf. We related this idea to finding the center of a ball of radius δ with maximal probability in the limit $\delta \rightarrow 0^+$. Whilst the idea is intuitively appealing, and reduces the complexity of Bayesian inference from determination of a pdf to determination of a single point, the approach has a number of limitations, in particular for noisy, multi-peaked or high-dimensional posterior distributions; the examples in the previous chapter illustrated these limitations.

In this chapter we again adopt an optimization approach to the problem of Bayesian inference, but instead seek a Gaussian distribution $p = \mathcal{N}(\mu, \Sigma)$ that minimizes some distance-like measure from the posterior $\pi^y(u)$. However, rather than using a metric to define the distance, we use the Kullback-Leibler divergence introduced in Section 4.1. Since this divergence is not symmetric, we obtain two distinct minimization problems described, in turn, in Sections 4.2 and 4.3. Both approaches are compared in Section 4.4. In Section 4.5 we show how Bayes theorem itself can be formulated through a closely related minimization principle. The chapter closes in Section 4.6 with extensions and bibliographical remarks.

4.1 The Kullback-Leibler Divergence

Definition 4.1. Let $\pi, \pi' > 0$ be two pdfs on \mathbb{R}^d .¹ The *Kullback-Leibler divergence*, also known as *relative entropy*, of π with respect to π' is defined by

$$\begin{aligned} d_{\text{KL}}(\pi \| \pi') &:= \int_{\mathbb{R}^d} \log \left(\frac{\pi(u)}{\pi'(u)} \right) \pi(u) du \\ &= \mathbb{E}^{\pi} \left[\log \left(\frac{\pi}{\pi'} \right) \right] \\ &= \mathbb{E}^{\pi'} \left[\log \left(\frac{\pi}{\pi'} \right) \frac{\pi}{\pi'} \right]. \end{aligned}$$

◇

¹The definition extends to situations where the support of π' is not the whole of \mathbb{R}^d , provided π is absolutely continuous with respect to π' .

Kullback-Leibler is a divergence in that $d_{\text{KL}}(\pi\|\pi') \geq 0$, with equality if and only if $\pi = \pi'$. From the definition it is clear that $d_{\text{KL}}(\pi\|\pi') = 0$ if $\pi = \pi'$; that it is otherwise strictly positive is proved in Lemma 4.3 below, as a consequence of the analogous property for the Hellinger or total variation distances. However, unlike Hellinger and total variation it does not define a metric. In particular, the Kullback-Leibler divergence is not symmetric: in general

$$d_{\text{KL}}(\pi\|\pi') \neq d_{\text{KL}}(\pi'\|\pi),$$

a fact that will be important in this chapter. Nevertheless, it is useful for at least four reasons: (1) it provides an upper bound for many distances, as illustrated in Lemma 4.3 below; (2) its logarithmic structure allows explicit computations that are difficult using actual distances; (3) it satisfies many convenient analytical properties such as being convex in both arguments and lower-semicontinuous in the topology of weak convergence; and (4) it has an information theoretic and physical interpretation.

Example 4.2. Consider two Gaussian densities p_1 and p_2 , both in dimension d , with means m_1, m_2 and covariance matrices Σ_1, Σ_2 . Then

$$d_{\text{KL}}(p_1\|p_2) = \frac{1}{2} \left(\log \frac{\det \Sigma_2}{\det \Sigma_1} - d + |m_1 - m_2|_{\Sigma_2}^2 + \text{Tr}(\Sigma_2^{-1} \Sigma_1) \right).$$

In particular, if p_2 is the standard unit Gaussian, then

$$d_{\text{KL}}(p_1\|p_2) = \frac{1}{2} \left(-\log \det \Sigma_1 - d + |m_1|^2 + \text{Tr}(\Sigma_1) \right).$$

◇

The following lemma establishes upper-bounds on total variation and Hellinger distances in terms of the Kullback-Leibler divergence. Note that as a corollary we obtain a proof of the fact that $d_{\text{KL}}(\pi\|\pi') > 0$ if $\pi \neq \pi'$.

Lemma 4.3. *The Kullback-Leibler divergence provides the following upper bounds for Hellinger and total variation distance:*

$$d_{\text{H}}(\pi, \pi')^2 \leq \frac{1}{2} d_{\text{KL}}(\pi\|\pi'), \quad d_{\text{TV}}(\pi, \pi')^2 \leq d_{\text{KL}}(\pi\|\pi').$$

Proof. The second inequality follows from the first one by Lemma 1.9; thus we prove only the first inequality. Consider the function $\varphi : \mathbb{R}^+ \mapsto \mathbb{R}$ defined by

$$\varphi(x) = x - 1 - \log x.$$

Note that

$$\begin{aligned} \varphi'(x) &= 1 - \frac{1}{x}, \\ \varphi''(x) &= \frac{1}{x^2}, \\ \varphi(\infty) &= \varphi(0) = \infty. \end{aligned}$$

Thus the function is convex on its domain. As the minimum of φ is attained at $x = 1$, and as $\varphi(1) = 0$, we deduce that $\varphi(x) \geq 0$ for all $x \in (0, \infty)$. Hence,

$$\begin{aligned} x - 1 &\geq \log x && \text{for all } x \geq 0, \\ \sqrt{x} - 1 &\geq \frac{1}{2} \log x && \text{for all } x \geq 0. \end{aligned}$$

We can use this last inequality to bound the Hellinger distance:

$$\begin{aligned} d_{\text{H}}(\pi, \pi')^2 &= \frac{1}{2} \int \left(1 - \sqrt{\frac{\pi'}{\pi}}\right)^2 \pi du \\ &= \frac{1}{2} \int \left(1 + \frac{\pi'}{\pi} - 2\sqrt{\frac{\pi'}{\pi}}\right) \pi du \\ &= \int \left(1 - \sqrt{\frac{\pi'}{\pi}}\right) \pi du \leq -\frac{1}{2} \int \log\left(\frac{\pi'}{\pi}\right) \pi du = \frac{1}{2} d_{\text{KL}}(\pi \| \pi'). \end{aligned}$$

□

4.2 Best Gaussian Fit by Minimizing $d_{\text{KL}}(p \| \pi)$

In this section we prove the existence of a best Gaussian approximation $p = \mathcal{N}(\mu, \Sigma)$ to a given pdf π in the sense that $d_{\text{KL}}(p \| \pi)$ is minimized. As part of our analysis, we will show that Gaussian pdfs p that minimize $d_{\text{KL}}(p \| \pi)$ can be found by solving a stochastic optimization algorithm to determine optimal mean and covariance. Therefore, the stochastic gradient descent algorithm studied in Chapter 3 provides a natural method to find a best Gaussian fit. While the existence of a minimizer and the applicability of stochastic gradient descent apply more broadly, we focus our discussion on the case where $\pi = \pi^y$ is a posterior distribution satisfying the following assumption:

Assumption 4.4. *The posterior distribution $\pi(u) = \frac{1}{Z} \exp(-L(u))\rho(u)$ satisfies:*

- *The loss function $L(u)$ is non-negative and bounded above.*
- *The prior is a centered isotropic Gaussian: $\rho(u) = \mathcal{N}(0, \lambda^{-1}I)$.*

Let \mathcal{A} be the set of Gaussian distributions on \mathbb{R}^d with positive definite covariance,

$$\mathcal{A} = \{\mathcal{N}(\mu, \Sigma) : \mu \in \mathbb{R}^d, \Sigma \in \mathbb{R}^{d \times d} \text{ positive definite}\}.$$

We have the following theorem, which establishes the existence of a best Gaussian approximation. We remark, however, that minimizers need not be unique. Note that \mathcal{A} is an open set since the set of positive definite matrices is open. It is thus implicit in the theorem that the infimum is indeed attained with positive definite covariance.

Theorem 4.5 (Best Gaussian Approximation). *Under Assumption 4.4, there exists at least one probability distribution $p \in \mathcal{A}$ at which the infimum*

$$\inf_{p \in \mathcal{A}} d_{\text{KL}}(p \| \pi)$$

is attained.

Proof. The Kullback-Leibler divergence can be computed explicitly as

$$\begin{aligned} d_{\text{KL}}(p \| \pi) &= \mathbb{E}^p[\log p] - \mathbb{E}^p[\log \pi] \\ &= \mathbb{E}^p \left[-\frac{1}{2} |u - \mu|_{\Sigma}^2 - \frac{1}{2} \log((2\pi)^d \det \Sigma) + \mathbf{L}(u) + \frac{\lambda}{2} |u|^2 + \log Z \right]. \end{aligned}$$

Note that Z is the normalization constant for π and is independent of p , and hence of μ and Σ . We can represent a random variable $u \sim p$ by writing $u = \mu + \Sigma^{1/2} \xi$, where $\xi \sim \mathcal{N}(0, I)$, and hence

$$|u|^2 = |\mu|^2 + |\Sigma^{1/2} \xi|^2 + 2\langle \mu, \Sigma^{1/2} \xi \rangle.$$

Using this we obtain

$$d_{\text{KL}}(p \| \pi) = -\frac{d}{2} - \frac{d}{2} \log(2\pi) - \frac{1}{2} \log \det \Sigma + \mathbb{E}^p[\mathbf{L}(u)] + \frac{\lambda}{2} |\mu|^2 + \frac{\lambda}{2} \text{tr}(\Sigma) + \log Z.$$

Define

$$\begin{aligned} J(\mu, \Sigma) &= \frac{\lambda}{2} |\mu|^2 + \frac{\lambda}{2} \text{tr}(\Sigma) - \frac{1}{2} \log \det \Sigma + \mathbb{E}^p[\mathbf{L}(u)], \\ J_0(\mu, \Sigma) &= \frac{\lambda}{2} |\mu|^2 + \frac{\lambda}{2} \text{tr}(\Sigma) - \frac{1}{2} \log \det \Sigma. \end{aligned}$$

Note that since \mathbf{L} is assumed to be bounded above, $J \rightarrow \infty$ if and only if $J_0 \rightarrow \infty$. Furthermore, writing positive definite $\Sigma = QDQ^\top$ where Q is orthogonal and D is diagonal with non-negative entries $\{\sigma_i\}_{i=1}^d$ we find that

$$\begin{aligned} J(\mu, \Sigma) &= \frac{\lambda}{2} |\mu|^2 + \frac{1}{2} \sum_{i=1}^d \left(\lambda \sigma_i - \log(\sigma_i) \right) + \mathbb{E}^p[\mathbf{L}(u)], \\ J_0(\mu, \Sigma) &= \frac{\lambda}{2} |\mu|^2 + \frac{1}{2} \sum_{i=1}^d \left(\lambda \sigma_i - \log(\sigma_i) \right) \end{aligned}$$

For any Σ , $J_0(\mu, \Sigma) \rightarrow \infty$ (and hence $J(\mu, \Sigma) \rightarrow \infty$) as $|\mu| \rightarrow \infty$. Furthermore, for any μ and any i , $J_0(\mu, \Sigma) \rightarrow \infty$ (and hence $J(\mu, \Sigma) \rightarrow \infty$) as $\sigma_i \rightarrow 0^+$ or $\sigma_i \rightarrow \infty$. Now define, for $\Sigma = QDQ^\top$ as above,

$$\tilde{\mathcal{A}} := \{(\mu, \Sigma) : \mu \in \mathbb{R}^d, Q \in \mathbb{R}^{d \times d} : Q^\top Q = I, |\mu| \leq M, r \leq \sigma_i \leq R \forall i\}.$$

Note that $J(0, I) < \infty$. Thus there are $M, r, R > 0$ such that the infimum of $J(\mu, \Sigma)$ over $\mu \in \mathbb{R}^d$ and positive definite Σ is equal to the infimum of $J(\mu, \Sigma)$ over the closed and bounded set $\tilde{\mathcal{A}}$. Since J is continuous in $\tilde{\mathcal{A}}$ it achieves its infimum, and the proof is complete. \square

Remark 4.6 (Minimizing $d_{\text{KL}}(p||\pi)$ with Stochastic Gradient Descent). The proof of Theorem 4.5 shows that a best Gaussian approximation $p \in \mathcal{A}$ to π can be found by minimizing the objective

$$\begin{aligned} J(\mu, \Sigma) &= \mathbb{E}^{\xi \sim \mathcal{N}(0, I)} \left[\frac{\lambda}{2} |\mu|^2 + \frac{\lambda}{2} \text{tr}(\Sigma) - \frac{1}{2} \log \det \Sigma + \mathbf{L}(\mu + \Sigma^{1/2} \xi) \right] \\ &= \int_{\mathbb{R}^d} F(u, z) \zeta(z) dz, \end{aligned}$$

where $u = (\mu, \Sigma)$, $\zeta = \mathcal{N}(0, I)$, and

$$F(u, z) = \frac{\lambda}{2} |\mu|^2 + \frac{\lambda}{2} \text{tr}(\Sigma) - \frac{1}{2} \log \det \Sigma + \mathbf{L}(\mu + \Sigma^{1/2} z).$$

Thus, this optimization problem can be solved using the stochastic gradient descent algorithm described in Chapter 3. \diamond

4.3 Best Gaussian Fit by Minimizing $d_{\text{KL}}(\pi||p)$

In this section we show that the best Gaussian approximation in Kullback-Leibler with respect to its second argument is unique and given by moment matching.

Theorem 4.7 (Best Gaussian Approximation by Moment Matching). *Assume that $\bar{\mu} := \mathbb{E}^\pi[u]$ is finite and that $\bar{\Sigma} := \mathbb{E}^\pi[(u - \bar{\mu}) \otimes (u - \bar{\mu})]$ is positive definite. Then the infimum*

$$\inf_{p \in \mathcal{A}} d_{\text{KL}}(\pi||p)$$

is attained at the element in \mathcal{A} with mean $\bar{\mu}$ and covariance $\bar{\Sigma}$.

Proof. By definition

$$d_{\text{KL}}(\pi||p) = -\mathbb{E}^\pi[\log p] + \mathbb{E}^\pi[\log \pi]. \quad (4.1)$$

Since the second term does not involve p , we study minimization of

$$\begin{aligned} -\mathbb{E}^\pi[\log p] &= -\mathbb{E}^\pi \left[\log \left(\frac{1}{\sqrt{(2\pi)^d \det \Sigma}} \exp \left(-\frac{1}{2} |u - \mu|_\Sigma^2 \right) \right) \right] \\ &= \frac{1}{2} \mathbb{E}^\pi [|u - \mu|_\Sigma^2] + \frac{1}{2} \log \det \Sigma + \frac{d}{2} \log 2\pi. \end{aligned}$$

Let $\Omega = \Sigma^{-1}$. Then our task is equivalent to minimizing the following function of μ and Ω :

$$J(\mu, \Omega) = \frac{1}{2} \mathbb{E}^\pi [\langle u - \mu, \Omega(u - \mu) \rangle] - \frac{1}{2} \log \det \Omega.$$

First we find the critical points of J by taking its first order partial derivative with respect to μ and Ω and setting both to zero:

$$\begin{aligned} \partial_\mu J &= -\mathbb{E}^\pi[\Omega(u - \mu)] = 0; \\ \partial_\Omega J &= \frac{1}{2} \partial_\Omega (\mathbb{E}^\pi[(u - \mu) \otimes (u - \mu) : \Omega]) - \frac{1}{2 \det \Omega} \partial_\Omega \det \Omega \\ &= \frac{1}{2} \mathbb{E}^\pi[(u - \mu) \otimes (u - \mu)] - \frac{1}{2} \Omega^{-1} = 0; \end{aligned}$$

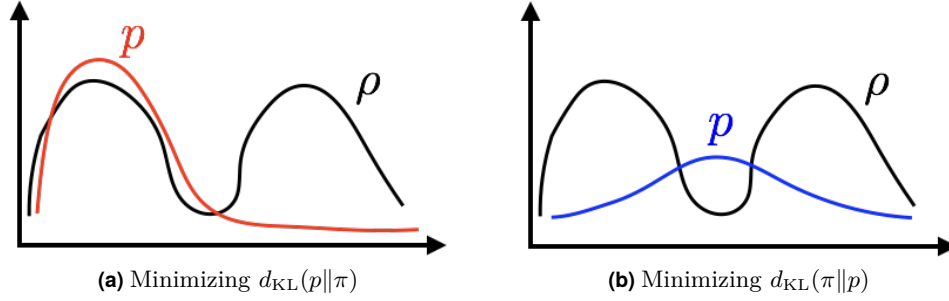


Figure 4.1 (a) Minimizing $d_{\text{KL}}(p||\pi)$ can lead to serious information loss while (b) minimizing $d_{\text{KL}}(\pi||p)$ ensures a comprehensive consideration of all components of π .

here we have used the relation $\partial_{\Omega} \det \Omega = \det \Omega \cdot \Omega^{-1}$. Solving the above two equations gives us the critical point, expressed in terms of mean and covariance,

$$(\bar{\mu}, \bar{\Sigma}) = (\mathbb{E}^{\pi}[u], \mathbb{E}^{\pi}[(u - \bar{\mu}) \otimes (u - \bar{\mu})]).$$

The fact that the critical point $(\bar{\mu}, \bar{\Sigma}^{-1})$ is a minimizer of J follows because J is convex. Indeed, note that J is the sum of two convex functions: a positive definite quadratic form and a negative log-determinant. \square

Remark 4.8 (Minimizing $d_{\text{KL}}(\pi||p)$ with Monte Carlo). Theorem 4.7 shows that the Gaussian $p \in \mathcal{A}$ closest to π in the sense of minimizing $d_{\text{KL}}(\pi||p)$ is the Gaussian with the same mean and covariance $(\bar{\mu}, \bar{\Sigma})$ as π . Both mean and covariance can be computed using Monte Carlo methods, a family of algorithms designed to compute expected values with respect to a given target distribution using samples. Monte Carlo algorithms will be studied in Chapter 5. \diamond

4.4 Comparison between $d_{\text{KL}}(\pi||p)$ and $d_{\text{KL}}(p||\pi)$

It is instructive to compare the two different minimization problems, both leading to a “best Gaussian”, that we described in the preceding two sections. We write the two relevant divergences as follows and then explain the nomenclature:

$$\begin{aligned} d_{\text{KL}}(p||\pi) &= \mathbb{E}^p \left[\log \left(\frac{p}{\pi} \right) \right] = \mathbb{E}^p [\log p] - \mathbb{E}^p [\log \pi], \quad \text{“Mode-seeking”} \\ d_{\text{KL}}(\pi||p) &= \mathbb{E}^{\pi} \left[\log \left(\frac{\pi}{p} \right) \right] = \mathbb{E}^{\pi} [\log \pi] - \mathbb{E}^{\pi} [\log p]. \quad \text{“Mean-seeking”} \end{aligned}$$

Note that when minimizing $d_{\text{KL}}(p||\pi)$ we want $\log \frac{p}{\pi}$ to be small in regions of high probability under p , which can happen when $p \simeq \pi$ or when p is much smaller than π . This illustrates the fact that minimizing $d_{\text{KL}}(p||\pi)$ may miss out components of π . For example, in Figure 4.1(a) π is a bimodal distribution but minimizing $d_{\text{KL}}(p||\pi)$ over Gaussians p can only give a single mode approximation which is achieved by matching one of the modes; we may think of this as “mode-seeking”. In contrast, when

minimizing $d_{\text{KL}}(\pi\|p)$ over Gaussians p we want $\log \frac{\pi}{p}$ to be small where p appears as the denominator. This implies that wherever π has some mass we must let p also have some mass there in order to keep $\frac{\pi}{p}$ as close as possible to one. Therefore, the minimization is carried out by allocating the mass of p in a way such that on average the divergence between p and π attains its minimum, as shown in Figure 4.1(b); hence the label “mean-seeking.” Different applications will favor different choices between the mean and mode seeking approaches to Gaussian approximation.

4.5 Variational Formulation of Bayes Theorem

This chapter has been concerned with finding the best Gaussian approximation to a measure with respect to Kullback-Leibler divergences. Bayes Theorem 1.2 itself can be formulated through a closely related minimization principle. Consider a posterior $\pi^y(u)$ in the following form:

$$\pi^y(u) = \frac{1}{Z} \exp(-L(u)) \rho(u),$$

where $\rho(u)$ is the prior, $L(u)$ is the negative log-likelihood, and Z the normalization constant. We assume here for exposition that all pdfs are positive. Dropping the superscript y from π^y for notational simplicity, we express $d_{\text{KL}}(p\|\pi)$ in terms of the prior as follows:

$$\begin{aligned} d_{\text{KL}}(p\|\pi) &= \int_{\mathbb{R}^d} \log\left(\frac{p}{\pi}\right) p \, du \\ &= \int_{\mathbb{R}^d} \log\left(\frac{p \rho}{\rho \pi}\right) p \, du \\ &= \int_{\mathbb{R}^d} \log\left(\frac{p}{\rho} \exp(L(u)) Z\right) p \, du \\ &= d_{\text{KL}}(p\|\rho) + \mathbb{E}^p[L(u)] + \log Z. \end{aligned}$$

If we define

$$\mathcal{J}(p) = d_{\text{KL}}(p\|\rho) + \mathbb{E}^p[L(u)],$$

then we have the following:

Theorem 4.9 (Bayes Theorem as an Optimization Principle). *The posterior distribution π is given by the following minimization principle:*

$$\pi = \operatorname{argmin}_{p \in \mathcal{P}} \mathcal{J}(p),$$

where \mathcal{P} contains all pdfs on \mathbb{R}^d .

Proof. Note that

$$d_{\text{KL}}(p\|\pi) = \mathcal{J}(p) + \log Z.$$

Since Z is the normalization constant for π and is independent of p , the minimizer of $d_{\text{KL}}(p\|\pi)$ over $p \in \mathcal{P}$ will also be the minimizer of $\mathcal{J}(p)$. Since the unique global minimizer of $d_{\text{KL}}(p\|\pi)$ is attained at $p = \pi$ the result follows. \square

The posterior distribution π is the minimizer of $\mathcal{J}(p)$ over all pdfs. However, we can approximate π by minimizing $\mathcal{J}(p)$ over a subset of all pdfs. The following example of this connects to earlier parts of the chapter; further discussion on other computational methods and theoretical insights that stem from viewing Bayes theorem as an optimization problem may be found in the conclusion Section 4.6.

Example 4.10 (Optimization over Gaussians). If we approximate π by minimizing $\mathcal{J}(p)$ over Gaussians then we obtain the methodology studied in Section 4.2. \diamond

4.6 Discussion and Bibliography

The definition of the Kullback-Leibler divergence, and upper-bounds in terms of probability metrics, can be found in [113]. For a basic introduction to variational Bayesian methods, including the moment-matching version of Gaussian approximation, see [27]. The idea of approximating a target distribution π by minimizing the Kullback-Leibler divergence within a family of admissible distributions is popular in probabilistic machine learning. Variational Bayesian methods [158, 313] minimize $d_{\text{KL}}(p||\pi)$; in contrast expectation propagation methods [214], which seek a factorized approximate distribution, proceed by minimizing $d_{\text{KL}}(\pi||p)$. We refer to [313, 28] for accessible introductions to variational Bayesian methods and further pointers to the literature.

In this chapter we have focused on Gaussian approximations, but other families of admissible distributions can be considered. The family of admissible distributions should in practice be large enough to allow for accurate approximation of the target distribution, while also allowing for efficient optimization. Gaussian approximations are useful in Bayesian inverse problems and are invoked by many data assimilation algorithms, as we shall see in Chapter 10. In probabilistic machine learning it is common to invoke mean-field rather than Gaussian approximations, and a variety of efficient optimization algorithms are available in this context [27]. Recent works that employ variational inference techniques for the solution of inverse problems include [6, 183].

The problem of finding a Gaussian approximation of a general finite-dimensional probability distribution is studied in [199], and infinite-dimensional formulations are considered in [244] and the companion paper [243]. Gaussian approximation of small noise diffusions are studied in [270]. The approximation in Theorem 4.5 consists of a single Gaussian distribution. If the posterior has more than one mode, a single Gaussian may not be appropriate. For an approximation composed of Gaussian mixtures, the reader is referred to [199]. The paper [108] highlights how minimization of Kullback-Leibler divergence arises naturally in the optimization of local entropy and heat regularized costs in deep learning.

The formulation of Bayes theorem as an optimization principle is well known; see the book [201] and the paper [19] for clear expositions of this subject. There are at least three advantages of viewing Bayes theorem as an optimization problem. First, the variational formulation provides a natural way to approximate the posterior by restricting the minimization problem to distributions satisfying some computationally desirable property. For instance, variational Bayesian methods often restrict the minimization to densities with a factorizable structure implied by independence with respect to the

components of the unknown u ; similarly, in Section 4.2 we have studied restriction to the class of Gaussian distributions. Second, variational formulations allow to show convergence of posterior distributions indexed by some parameters using techniques from calculus of variations. For instance, the papers [109] and [106] exploit the variational formulation of Bayes theorem to establish convergence of Bayesian procedures. Third, variational formulations provide natural paths, defined by a gradient flow, towards the posterior. Understanding these flows and their rates of convergence is helpful in the design and choice of sampling algorithms [107].

For more information about the properties of the exponential family we refer to [226], and for background on matrix calculations that were used in this chapter we refer to [239].

Chapter 5

Monte Carlo Sampling and Importance Sampling

In this chapter we introduce Monte Carlo sampling and importance sampling. These are two general techniques for estimating expectations with respect to a given pdf π . Monte Carlo generates independent samples from π and combines them with equal weights, whilst importance sampling uses independent samples, weighted appropriately, from a different distribution. In quantifying the error in Monte Carlo and importance sampling we will use a distance on random probability measures that reduces to total variation in the case of deterministic probability measures; and we will introduce the χ^2 divergence.

In Bayesian inverse problems, we are typically unable to directly generate samples from the posterior distribution π^y itself, so that Monte Carlo sampling is not viable; however, importance sampling may be used. For example, it is often possible to generate samples from the prior; importance sampling can then be used to reweight samples from the prior distribution, to approximate posterior expectations.

Recall that for any pdf p and function $\varphi : \mathbb{R}^d \rightarrow \mathbb{R}$, we denote

$$p(\varphi) = \mathbb{E}^p[\varphi(u)] = \int_{\mathbb{R}^d} \varphi(u)p(u) du. \quad (5.1)$$

Thus we view the pdf p as a linear functional on the space of real-valued functions on \mathbb{R}^d . Our task in this chapter is to evaluate $\pi(f)$ for target distribution π on \mathbb{R}^d and for a given test function $f : \mathbb{R}^d \rightarrow \mathbb{R}$. Thus, we are interested in computing

$$\pi(f) = \int_{\mathbb{R}^d} f(u)\pi(u) du. \quad (5.2)$$

Monte Carlo sampling approximates this integral using samples from the target π .

To describe importance sampling, we note that for any pdf ρ such that the support of π is contained in the support of ρ , equation (5.2) can be rewritten as

$$\pi(f) = \int_{\mathbb{R}^d} f(u) \left(\frac{\pi(u)}{\rho(u)} \right) \rho(u) du = \rho(fw), \quad (5.3)$$

where

$$w(u) = \frac{\pi(u)}{\rho(u)}.$$

We assume that the ratio $\pi(u)/\rho(u)$ is only known up to a normalization constant and write

$$w(u) = \frac{\pi(u)}{\rho(u)} = \frac{1}{Z} l(u), \quad (5.4)$$

where the unknown normalizing constant is defined by $Z = \rho(l)$. Noting that $w(u) = Z^{-1}l(u)$, we obtain from (5.3)

$$\pi(f) = \frac{\rho(fl)}{\rho(l)}. \quad (5.5)$$

Importance sampling methods are based on approximating the two integrals on the right-hand side of this identity with Monte Carlo, using samples from ρ . Note that it is not necessary to know Z to implement this method.

A particular application of importance sampling in the context of Bayes theorem is the setting where ρ is the prior, π the posterior and g the likelihood. However the importance sampling method is not restricted to this splitting of the posterior into a product of likelihood and prior; and indeed, depending on the specific test function f of interest, the importance sampling method may be far from optimal if applied with this choice of ρ .

To summarize, Monte Carlo approximates $\pi(f)$ using (5.2) and samples from π ; importance sampling approximates $\pi(f) = \rho(fw)$ using (5.5) and samples from ρ . Underlying the approximations of integrals are approximations of measures. For this reason, it is convenient in this chapter to generalize the concept of pdf to include Dirac mass distributions. A Dirac mass at v will be viewed as having pdf $\delta(\cdot - v)$ where $\delta(\cdot)$ integrates to one and takes the value zero everywhere except at the origin. This Dirac mass is also sometimes written as $\delta_v(\cdot)$.

This chapter is organized as follows. We first introduce and analyze Monte Carlo sampling in Section 5.1. Importance sampling is then studied in Section 5.2. We close in Section 5.3 with pointers to the extant literature on this subject.

5.1 Monte Carlo Sampling

Monte Carlo sampling applies when it is possible to generate i.i.d. samples $u^{(n)} \sim \pi$, $1 \leq n \leq N$. The method approximates the target distribution π by a sum of Dirac masses located at the samples $u^{(n)}$, each given equal weight $1/N$. This leads to the Monte Carlo estimator π_{MC}^N of π given by

$$\pi_{MC}^N := \frac{1}{N} \sum_{n=1}^N \delta(u - u^{(n)}). \quad (5.6)$$

We summarize this simple procedure in the following algorithm:

Algorithm 5.1 Monte Carlo Sampling Algorithm

- 1: **Input:** Target distribution π , number of samples N .
 - 2: Sample $u^{(n)} \sim \pi$ i.i.d. $n \in \{1, \dots, N\}$.
 - 3: **Output:** Target approximation $\pi \approx \pi_{\text{MC}}^N := \frac{1}{N} \sum_{n=1}^N \delta(u - u^{(n)})$.
-

This algorithm leads to the following estimator of $\pi(f)$:

$$\pi_{\text{MC}}^N(f) = \frac{1}{N} \sum_{n=1}^N f(u^{(n)}), \quad u^{(n)} \sim \pi \quad \text{i.i.d.}$$

We are interested in determining whether the estimator $\pi_{\text{MC}}^N(f)$ of $\pi(f)$ is accurate regardless of the specific test function f . For this reason, we seek to understand whether the Monte Carlo estimator π_{MC}^N is a good approximation to π in a suitable metric. This perspective will also be useful in analyzing importance sampling in this chapter, and when analyzing sequential methods for data assimilation in Chapters 11 and 12. Note that π_{MC}^N is a *random* probability measure due to sampling, and so in order to formalize this question we need a distance between random probability measures. To this end, for random probability measures π and π' , we define

$$d(\pi, \pi') = \sup_{|f|_\infty \leq 1} \left(\mathbb{E} \left[(\pi(f) - \pi'(f))^2 \right] \right)^{1/2}, \quad (5.7)$$

where the expectation is taken over the random variable, in our case the randomness from sampling π . It is possible to show that $d(\cdot, \cdot)$ indeed defines a distance between random probability measures. Furthermore, when π, π' are deterministic, then we have $d(\pi, \pi') = 2d_{\text{TV}}(\pi, \pi')$. Using this distance between random probability measures, we have the following result.

Theorem 5.1 (Monte Carlo Error). *For $f : \mathbb{R}^d \rightarrow \mathbb{R}$ denote $|f|_\infty := \sup_{u \in \mathbb{R}^d} |f(u)|$. We have*

$$\begin{aligned} \sup_{|f|_\infty \leq 1} \left| \mathbb{E} \left[\pi_{\text{MC}}^N(f) - \pi(f) \right] \right| &= 0, \\ d(\pi_{\text{MC}}^N, \pi)^2 &\leq \frac{1}{N}. \end{aligned}$$

Proof. To prove the first result, namely that the estimator is unbiased, we use linearity of the expected value and that $u^{(n)} \sim \pi$:

$$\begin{aligned} \mathbb{E} \left[\pi_{\text{MC}}^N(f) \right] &= \mathbb{E} \left[\frac{1}{N} \sum_{n=1}^N f(u^{(n)}) \right] \\ &= \frac{1}{N} N \pi(f) = \pi(f) = \mathbb{E}[\pi(f)]. \end{aligned}$$

Therefore the supremum over $|f|_\infty \leq 1$ is a supremum over a quantity that is zero, for any f , and the result follows.

For the second result, note that since $\pi_{\text{MC}}^N(f)$ is unbiased, its variance agrees with its mean squared error. Now using that the $u^{(n)} \sim \pi$ are independent we deduce that

$$\begin{aligned}\text{Var}\left[\pi_{\text{MC}}^N(f)\right] &= \text{Var}\left[\frac{1}{N} \sum_{n=1}^N f(u^{(n)})\right] \\ &= \frac{1}{N^2} N \text{Var}_{\pi}[f] = \frac{1}{N} \text{Var}_{\pi}[f].\end{aligned}$$

For $|f|_{\infty} \leq 1$, we have

$$\text{Var}_{\pi}[f] = \pi(f^2) - \pi(f)^2 \leq \pi(f^2) \leq 1,$$

and therefore

$$\sup_{|f|_{\infty} \leq 1} \left| \mathbb{E} \left[\left(\pi_{\text{MC}}^N(f) - \pi(f) \right)^2 \right] \right| = \sup_{|f|_{\infty} \leq 1} \left| \frac{1}{N} \text{Var}_{\pi}[f] \right| \leq \frac{1}{N}.$$

□

The theorem shows that the Monte Carlo estimator π_{MC}^N is an unbiased approximation for the posterior π and that, by choosing N large enough, expectation of any bounded function f can in principle be approximated by Monte Carlo sampling to arbitrary accuracy. Furthermore, although the convergence is slow with respect to N – the mean squared error decays like N^{-1} so the typical error only decays like $N^{-1/2}$ – there is no dependence on the dimension of the problem or on the properties of f , other than its supremum. Moreover, the proof of Theorem 5.1 shows that, in fact, the Monte Carlo error in the approximation of $\pi(f)$ is determined by the variance of f under π .

Example 5.2 (Approximation of an Integral). Let $f : \mathbb{R} \rightarrow \mathbb{R}$ be a sigmoid function defined on \mathbb{R} and shown in Figure 5.1(a) below as the blue solid curve. For the target distribution π we take a mixture of two Gaussians found by choosing from $\mathcal{N}(-5, 1)$ with probability $1/10$ and from $\mathcal{N}(5, 1)$ with probability $9/10$. We wish to approximate the expected value, under π , of $f(u) \times \mathbb{I}_{[a,b]}(u)$ where

$$\mathbb{I}_{[a,b]}(u) = \begin{cases} 1 & \text{if } u \in [a, b], \\ 0 & \text{otherwise.} \end{cases}$$

We use Monte Carlo sampling to generate N random samples $u^{(1)}, \dots, u^{(N)}$ and compute the error between the actual integral and the Monte Carlo estimator. The integral and estimator are in the form:

$$\begin{aligned}\pi(f) &= \int_a^b f(u) \pi(u) \, du, \\ \pi_{\text{MC}}^N(f) &= \frac{1}{N} \sum_{n=1}^N f(u^{(n)}) \mathbb{I}_{[a,b]}(u^{(n)}).\end{aligned}$$

The results of a set of numerical experiments with $a = -5, b = 5$ and varying N are shown in Figure 5.1(b). A randomly chosen subset of the samples used when $N = 100$ is displayed in Figure 5.1(a); only samples in $[-5, 5]$ are shown since other samples do not contribute to the estimator in this case. ◇

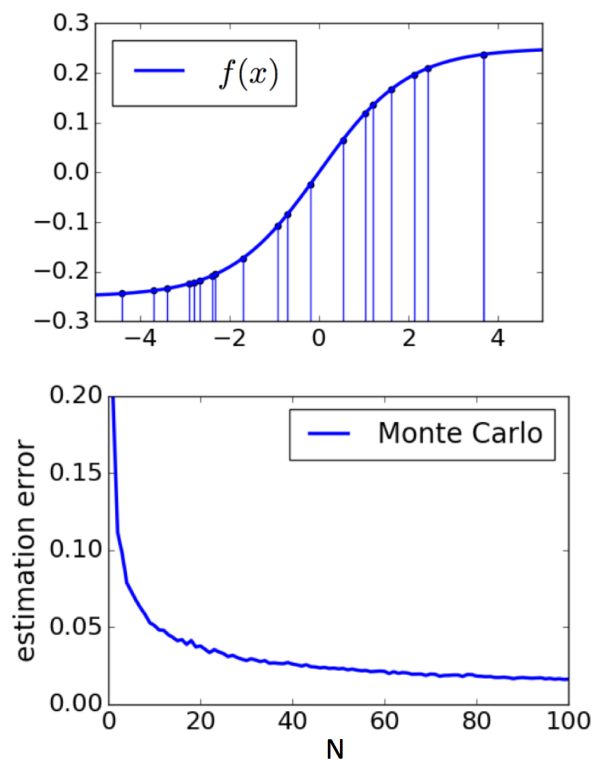


Figure 5.1 Large sample size N reduces the estimation error by the Monte Carlo method.

5.2 Importance Sampling

Monte Carlo sampling can only be used when it is possible to sample from the desired target distribution π . When it is not possible to sample from π , we can draw samples from another *proposal* distribution ρ instead. Consider π as in equation (5.4). Given a test function $f : \mathbb{R}^d \rightarrow \mathbb{R}$ we can rewrite its expectation with respect to π in terms of expected values with respect to ρ as in equation (5.5). Approximating the numerator and the denominator using Monte Carlo with samples from ρ gives

$$\begin{aligned}\pi(f) &\approx \sum_{n=1}^N w^{(n)} f(u^{(n)}), \quad u^{(n)} \sim \rho \text{ i.i.d.} \\ &= \pi_{\text{IS}}^N(f),\end{aligned}$$

where

$$w^{(n)} := \frac{l(u^{(n)})}{\sum_{m=1}^N l(u^{(m)})}, \quad \pi_{\text{IS}}^N := \sum_{n=1}^N w^{(n)} \delta(u - u^{(n)}).$$

Thus, given N samples $u^{(1)}, \dots, u^{(N)}$ generated i.i.d. according to ρ , we can estimate π with the *particle approximation measure* π_{IS}^N .

Algorithm 5.2 Importance Sampling Algorithm

- 1: **Input:** Target distribution $\pi(u) = \frac{1}{Z} l(u) \rho(u)$, proposal distribution ρ , number of samples N .
- 2: Sample $u^{(n)} \sim \rho$ i.i.d. $n \in \{1, \dots, N\}$.
- 3: Compute

$$w^{(n)} := \frac{l(u^{(n)})}{\sum_{m=1}^N l(u^{(m)})}.$$

- 4: **Output:** Target approximation $\pi \approx \pi_{\text{IS}}^N := \sum_{n=1}^N w^{(n)} \delta(u - u^{(n)})$.
-

We emphasize that implementation of this algorithm does not assume knowledge of the normalizing constant Z , but only that g can be evaluated and that ρ can be sampled from. In particular, note that the algorithm is invariant under $g \mapsto \lambda g$ for any scalar λ . Algorithm 5.2 leads to the following estimator of $\pi(f)$:

$$\pi_{\text{IS}}^N(f) = \sum_{n=1}^N w^{(n)} f(u^{(n)}), \quad u^{(n)} \sim \rho \text{ i.i.d.}$$

Example 5.3 (Change of Measurement). We consider a similar set-up as in Example 5.2, integrating a sigmoid function, shown in blue in Figure 5.2, with respect to a pdf π which is bimodal, shown in red in Figure 5.2; we again restrict the support of the desired integral. We estimate the integral using importance sampling based on N random

samples $u^{(1)}, \dots, u^{(N)}$ from the measure $\rho = \mathcal{N}(\mu, \sigma^2)$, shown in green in Figure 5.2. The estimator of the integral is given by

$$\pi_{\text{IS}}^N(f) = \sum_{n=1}^N w^{(n)} f(u^{(n)}) \mathbb{1}_{[a,b]}(u^{(n)}),$$

$$w^{(n)} = \frac{l(u^{(n)})}{\sum_{m=1}^N l(u^{(m)})}.$$

Here g is a function proportional to the ratio of the densities of π and ρ . If $\pi(u^{(n)}) > \rho(u^{(n)})$, the samples should have been denser, so we raise the weight on $f(u^{(n)})$ in proportion to $\frac{\pi(u^{(n)})}{\rho(u^{(n)})} > 1$. If $\pi(u^{(n)}) < \rho(u^{(n)})$, the samples should have been less dense, so we lower the weight on $f(u^{(n)})$ in proportion to $\frac{\pi(u^{(n)})}{\rho(u^{(n)})} < 1$. \diamond

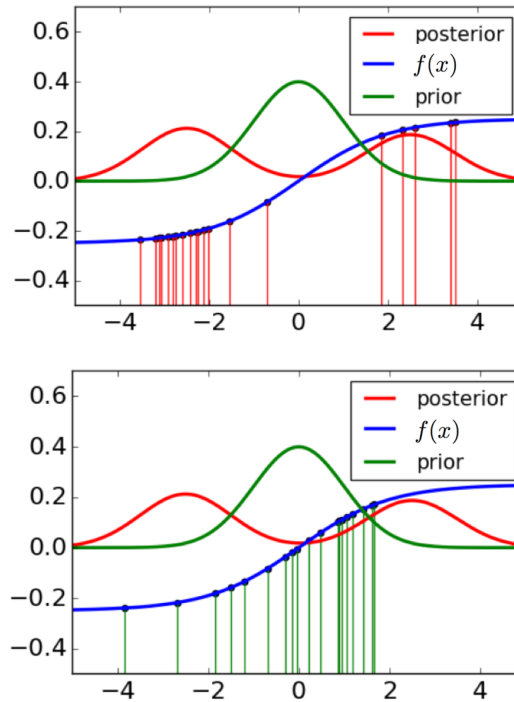


Figure 5.2 importance sampling is a change of measure via the importance weights. The red curve shows a bimodal distribution π and the green curve shows a Gaussian distribution ρ . The blue curve is the function to be integrated, on its support $[-5, 5]$. The upper figure shows samples from the posterior π itself; these would be used for Monte Carlo sampling; the lower curve shows samples from the prior ρ , as used for importance sampling. The importance weights capture and compensate for the difference of sampling from these two distributions.

We now introduce the χ^2 divergence between probability distributions, and discuss

some of its properties, before going on to use it to quantify the accuracy of importance sampling.

Definition 5.4. Let $\pi, \pi' > 0$ be two pdfs on \mathbb{R}^d .¹ The χ^2 divergence of π with respect to π' is

$$d_{\chi^2}(\pi \| \pi') := \int_{\mathbb{R}^d} \left(\frac{\pi(u)}{\pi'(u)} - 1 \right)^2 \pi'(u) du. \quad (5.8)$$

◇

The χ^2 divergence is not a distance as it is, in general, not symmetric; it is, however, distance-like and captures the closeness of the two distributions; this is analogous to the Kullback-Leibler divergence defined in the preceding chapter. The next lemma shows that the χ^2 divergence may be used to upper bound the Kullback-Leibler divergence and therefore, by Lemma 4.3, also the total variation and Hellinger distances.

Lemma 5.5. *The χ^2 divergence provides the following upper bounds for the Kullback-Leibler divergence:*

$$d_{\text{KL}}(\pi \| \pi') \leq \log(d_{\chi^2}(\pi \| \pi') + 1), \quad d_{\text{KL}}(\pi \| \pi') \leq d_{\chi^2}(\pi \| \pi').$$

Proof. The second inequality is a direct consequence of the first one, noting that, for $x \geq 0$, $\log(x + 1) \leq x$. To prove the first inequality note that by Jensen inequality

$$\begin{aligned} d_{\text{KL}}(\pi \| \pi') &= \int_{\mathbb{R}^d} \log\left(\frac{\pi(u)}{\pi'(u)}\right) \pi(u) du \\ &\leq \log\left(\int_{\mathbb{R}^d} \frac{\pi(u)}{\pi'(u)} \frac{\pi(u)}{\pi'(u)} \pi'(u) du\right) \\ &= \log(d_{\chi^2}(\pi \| \pi') + 1), \end{aligned}$$

where for the last equality we used that

$$\begin{aligned} d_{\chi^2}(\pi \| \pi') &= \int_{\mathbb{R}^d} \left(\frac{\pi(u)}{\pi'(u)} - 1 \right)^2 \pi'(u) du \\ &= \int_{\mathbb{R}^d} \left(\frac{\pi(u)}{\pi'(u)} \right)^2 \pi'(u) du - 2 \int_{\mathbb{R}^d} \left(\frac{\pi(u)}{\pi'(u)} \right) \pi'(u) du + \int_{\mathbb{R}^d} \pi'(u) du \\ &= \int_{\mathbb{R}^d} \left(\frac{\pi(u)}{\pi'(u)} \right)^2 \pi'(u) du - 1. \end{aligned}$$

□

The next result shows that, similarly as for Monte Carlo sampling, the mean squared error of $\pi_{\text{IS}}^N(f)$ as an estimator of $\pi(f)$ is order N^{-1} . However, there are two main differences: the estimator is now biased, and the constant in the mean squared error depends on the χ^2 divergence between the target and the proposal.

¹The definition extends to situations where the support of π' is not the whole of \mathbb{R}^d , provided π is absolutely continuous with respect to π' .

Theorem 5.6 (Importance Sampling Error). *We have*

$$\sup_{|f|_\infty \leq 1} \left| \mathbb{E} \left[\pi_{\text{IS}}^N(f) - \pi(f) \right] \right| \leq 2 \frac{1 + d_{\chi^2}(\pi \| \rho)}{N},$$

$$d(\pi_{\text{IS}}^N, \pi)^2 \leq 4 \frac{1 + d_{\chi^2}(\pi \| \rho)}{N}.$$

Proof. The proof of the first item (bias) uses the second item (variance). Nonetheless, we start with the proof for the bias, because bias and variance are often thought of, conceptually, in that order. Given

$$\pi(u) = \frac{1}{Z} l(u) \rho(u) = \frac{1}{\rho(l)} l(u) \rho(u),$$

the proof of Lemma 5.5 shows that

$$d_{\chi^2}(\pi \| \rho) = \frac{\rho(l^2)}{\rho(l)^2} - 1.$$

To ease the notation we introduce

$$\zeta := \frac{\rho(l^2)}{\rho(l)^2}.$$

We rewrite

$$\pi(f) = \frac{\rho(lf)}{\rho(l)} \simeq \frac{\rho_{\text{MC}}^N(lf)}{\rho_{\text{MC}}^N(l)} = \pi_{\text{IS}}^N(f).$$

Then we have

$$\begin{aligned} \pi_{\text{IS}}^N(f) - \pi(f) &= \pi_{\text{IS}}^N(f) - \frac{\rho(lf)}{\rho(l)} \\ &= \frac{\pi_{\text{IS}}^N(f) (\rho(l) - \rho_{\text{MC}}^N(l))}{\rho(l)} - \frac{(\rho(lf) - \rho_{\text{MC}}^N(lf))}{\rho(l)}. \end{aligned} \tag{5.9}$$

The expectation of the second term is zero and hence

$$\begin{aligned} \left| \mathbb{E} \left[\pi_{\text{IS}}^N(f) - \pi(f) \right] \right| &= \frac{1}{\rho(l)} \left| \mathbb{E} \left[\pi_{\text{IS}}^N(f) (\rho(l) - \rho_{\text{MC}}^N(l)) \right] \right| \\ &\leq \frac{1}{\rho(l)} \left| \mathbb{E} \left[(\pi_{\text{IS}}^N(f) - \pi(f)) (\rho(l) - \rho_{\text{MC}}^N(l)) \right] \right|, \end{aligned}$$

since $\mathbb{E} [\rho(l) - \rho_{\text{MC}}^N(l)] = 0$. Using the Cauchy-Schwarz inequality, the second result from this theorem (whose proof follows) and Theorem 5.1 we have, for all $|f|_\infty \leq 1$,

$$\begin{aligned} \left| \mathbb{E} \left[\pi_{\text{IS}}^N(f) - \pi(f) \right] \right| &\leq \frac{1}{\rho(l)} \left(\mathbb{E} \left[(\pi_{\text{IS}}^N(f) - \pi(f))^2 \right] \right)^{1/2} \left(\mathbb{E} \left[(\rho(l) - \rho_{\text{MC}}^N(l))^2 \right] \right)^{1/2} \\ &\leq \frac{1}{\rho(l)} \left(\frac{4\zeta}{N} \right)^{1/2} \left(\frac{\rho(l^2)}{N} \right)^{1/2} = \frac{2\zeta}{N}. \end{aligned}$$

We now prove the second result. We use the splitting of $\pi_{\text{IS}}^N(f) - \pi(f)$ into the sum of two terms as derived in equation (5.9). Using Theorem 5.1, the basic inequality $(a - b)^2 \leq 2(a^2 + b^2)$ and that for all $|f|_\infty \leq 1$, $|\pi_{\text{IS}}^N(f)| \leq 1$, we have, for all $|f|_\infty \leq 1$,

$$\begin{aligned}
& \left| \mathbb{E} \left[\left(\pi_{\text{IS}}^N(f) - \pi(f) \right)^2 \right] \right| \\
& \leq \frac{2}{\rho(l)^2} \left(\mathbb{E} \left[\left(\pi_{\text{IS}}^N(f) \right)^2 \left(\rho(l) - \rho_{\text{MC}}^N(l) \right)^2 \right] + \mathbb{E} \left[\left(\rho(lf) - \rho_{\text{MC}}^N(lf) \right)^2 \right] \right) \\
& \leq \frac{2}{\rho(l)^2} \left(\mathbb{E} \left[\left(\rho(l) - \rho_{\text{MC}}^N(l) \right)^2 \right] + \mathbb{E} \left[\left(\rho(lf) - \rho_{\text{MC}}^N(lf) \right)^2 \right] \right) \\
& = \frac{2}{\rho(l)^2 N} (\text{Var}_\rho[l] + \text{Var}_\rho[lf]) \\
& \leq \frac{2}{\rho(l)^2 N} (\rho(l^2) + \rho(l^2 f^2)) \\
& \leq \frac{4\rho(l^2)}{\rho(l)^2 N} = \frac{4\zeta}{N}.
\end{aligned}$$

Therefore,

$$d(\pi_{\text{IS}}^N, \pi)^2 = \sup_{|f|_\infty \leq 1} \left| \mathbb{E} \left[\left(\pi_{\text{IS}}^N(f) - \pi(f) \right)^2 \right] \right| \leq \frac{4\zeta}{N}.$$

□

Remark 5.7. In Theorem 5.6 we measure the quality of π_{IS}^N as an approximation of the target π by considering the worst-case bias and mean squared error over the class of bounded test functions $\{f : \mathbb{R}^d \rightarrow \mathbb{R} : |f|_\infty = 1\}$. We show that worst-case error upper-bounds can be obtained in terms of the χ^2 divergence between the target and the proposal, quantifying the intuitive fact that, over a broad *class* of test functions, the performance of importance sampling depends on the closeness between target and proposal. Note, however, that for a *specific* function f careful choice of ρ in the importance sampling methodology may lead to considerable improvement over Monte Carlo sampling.

Unlike Monte Carlo, the importance sampling estimator $\pi_{\text{IS}}^N(f)$ is biased for $\pi(f)$. The theorem shows, however, that the bias decays at a rate that is twice that of the standard deviation, and so for large N the mean squared error is dominated by the variance. As for Monte Carlo, the rate of convergence of the variance is governed by the inverse of N , and the dimension d does not directly appear in the upper-bound. However for importance sampling to be accurate (with a limited number of samples N) it is important that target and proposal are close in χ^2 divergence, a condition that will not be typically satisfied in high dimensions. ◇

Example 5.8 (Explicit Bound for a Linear-Gaussian Inverse Problem). Let $a \in \mathbb{R}$ be given, and consider the one-dimensional inverse problem

$$y = au + \eta, \quad \eta \sim \mathcal{N}(0, \gamma^2),$$

supplemented with a Gaussian prior $u \sim \rho(u) = \mathcal{N}(0, \hat{c}^2)$. Defining

$$l(u) := \exp\left(-\frac{a^2}{2\gamma^2}u^2 + \frac{ay}{\gamma^2}u\right)$$

we can write the posterior distribution $\pi(u)$ in the form (5.4), namely

$$\pi(u) = \frac{1}{Z} l(u) \rho(u).$$

Setting $\delta^2 := a^2 \hat{c}^2 / \gamma^2$ a direct calculation shows that

$$\begin{aligned} \rho(l) &= \frac{1}{\sqrt{\delta^2 + 1}} \exp\left(\frac{1}{2} \frac{\delta^2 y^2}{a^2 \hat{c}^2 + \gamma^2}\right), \\ \rho(l^2) &= \frac{1}{\sqrt{2\delta^2 + 1}} \exp\left(\frac{2\delta^2 y^2}{2a^2 \hat{c}^2 + \gamma^2}\right), \end{aligned}$$

and so, noting that $\frac{y}{\sqrt{a^2 \hat{c}^2 + \gamma^2}} \sim \mathcal{N}(0, 1)$ under our model, we obtain that

$$\begin{aligned} \zeta &= \frac{\rho(l^2)}{\rho(l)^2} \\ &= \frac{\delta^2 + 1}{\sqrt{2\delta^2 + 1}} \exp\left(\frac{\delta^2}{2\delta^2 + 1} z^2\right), \quad z \sim \mathcal{N}(0, 1). \end{aligned}$$

Theorem 5.6 then guarantees that

$$d(\pi_{\text{IS}}^N, \pi)^2 \leq \frac{4\zeta}{N}.$$

It is illustrative to note that ζ —and hence the χ^2 -divergence between the posterior and the prior— is an increasing function of $\delta^2 = a^2 \hat{c}^2 / \gamma^2$. This is intuitive, since (i) larger a and \hat{c}^2 make the prior less informative; and (ii) smaller γ makes the data more informative. In either of these two limiting regimes we expect the posterior to become further away from the prior. \diamond

5.3 Discussion and Bibliography

A classic reference on the Monte Carlo method is [129]. Recent textbooks covering both methodological and theoretical aspects of Monte Carlo methods include [195, 263]. In practice, a wide range of probabilities, integrals and summations can be approximated by the Monte Carlo method. An advantage of Monte Carlo methods is that the convergence rate is independent of the dimension of the vector space supporting the random variable; indeed the $N^{-1/2}$ rate can be obtained for infinite-dimensional problems, in principle. A caveat of Monte Carlo methods is that they converge slowly. A faster convergence rate can be attained using quasi-random, low discrepancy sequences rather than random samples from the target. These quasi-random points can be suitably chosen in order to provide greater uniformity than random or pseudo-random sequences. The convergence

theory, practical limitations, and scalability to high dimension of the resulting *quasi-Monte Carlo* methods are overviewed in [41, 77, 280]. The subject of multi-level Monte Carlo (MLMC) has made the use of Monte Carlo methods practical in new areas of application; see [114] for an overview. The methodology applies when approximating expectations over infinite-dimensional spaces, and distributes the computational budget over different levels of approximation, with the goal of optimizing the cost per unit error, noting that the latter balances sampling and approximation based sources.

Importance sampling is reviewed in [302]. The methodology was first developed as an approach to reduce the variance of Monte Carlo integration [160, 159]. The chapter notes [11] give a comparison of Monte Carlo and importance sampling with examples. Early investigations of importance sampling focused on the following question: given a test function f , how should one choose the proposal ρ so that the estimator $\pi_{\text{IS}}^N(f)$ of $\pi(f)$ has a small mean squared error? This question has led to a plethora of algorithms for simulation of rare events, which is still a very active area of research. The presentation in this chapter closely follows the papers [5, 271], which study importance sampling from the perspective of filtering and sequential importance resampling. In this context, it is important to guarantee the accuracy of the importance sampling estimator $\pi_{\text{IS}}^N(f) \approx \pi(f)$ for a variety of test functions. This can be achieved by ensuring that π_{IS}^N is close to π , as shown in Theorem 5.6. In order for importance sampling to be accurate for a wide family of test functions, target and proposal need to be sufficiently close, since otherwise the *effective sample size* will be low [5, 271, 206]. Necessary sample size results for importance sampling in terms of several divergences between target and proposal are established in [268, 52]. The papers [40, 166] consider advanced importance sampling via adaptive algorithms. Some recent adaptive methods are based on the idea of finding the proposal distribution within some parametric family that is closest to the target distribution in an appropriate sense [265, 7, 73].

Chapter 6

Markov Chain Monte Carlo

In this chapter we study Markov chain Monte Carlo (MCMC), a methodology that delivers approximate samples from a given *target* distribution π . The methodology applies to settings in which π is the posterior distribution in (1.2), but it is also widely used in numerous applications beyond Bayesian inference. As with Monte Carlo and importance sampling, MCMC may be viewed as approximating the target distribution by a sum of Dirac masses, thus allowing the approximation of expectations with respect to the target. Implementation of Monte Carlo presupposes that independent samples from the target can be obtained. Importance sampling and MCMC bypass this restrictive assumption: importance sampling by appropriately weighting independent samples from a proposal distribution, and MCMC by drawing correlated samples from a Markov kernel that has the target as invariant distribution.

The concepts of Markov kernel and invariant distribution will hence play a central role in this chapter and we start in Section 6.1 with a recap of the elements of this theory needed in the remainder of the chapter. Then in Section 6.2 we provide a general discussion of Markov chain sampling, which assumes the existence of an ergodic Markov chain, with a kernel from which samples may be drawn iteratively, with invariant distribution equal to the target π . Following that, in Section 6.3 we discuss Metropolis-Hastings sampling which assumes the existence of a Markov kernel from which samples may readily be drawn, and then uses a correction mechanism to obtain a new Markov chain with invariant distribution equal to the target π . The relationship between Metropolis-Hastings sampling and Markov chain sampling is analogous to the relationship between importance sampling and Monte Carlo sampling. After introducing the general Metropolis-Hastings methodology, and showing its invariance with respect to the target distribution in Section 6.4, we will specify to the case where π is a posterior distribution given via Bayes theorem from the product of the likelihood function and the prior distribution. In this context, we will analyze in Section 6.5 the convergence of the pCN algorithm, which uses the prior and the likelihood separately as part of its design, and is prototypical of many useful Metropolis-Hastings methods. The chapter closes in Section 6.6 with extensions and bibliographical remarks.

6.1 Markov Chains in \mathbb{R}^d

We recall that $p : \mathbb{R}^d \times \mathbb{R}^d \rightarrow \mathbb{R}$ is called a *Markov kernel* if,

- (i) $p(u, v) \geq 0$ for all $(u, v) \in \mathbb{R}^d \times \mathbb{R}^d$; and
- (ii) $\int_{\mathbb{R}^d} p(u, v) dv = 1$ for all $u \in \mathbb{R}^d$.

Thus if $p : \mathbb{R}^d \times \mathbb{R}^d \rightarrow \mathbb{R}$ is a Markov kernel, then $p(u, \cdot) : \mathbb{R}^d \rightarrow \mathbb{R}^+$ is a pdf on \mathbb{R}^d . We also recall that π is an *invariant distribution* of the Markov kernel $p(u, v)$ if, for any $v \in \mathbb{R}^d$,

$$\int_{\mathbb{R}^d} \pi(u) p(u, v) du = \pi(v). \quad (6.1)$$

A *sample path* of the Markov chain generated by kernel p is defined as follows: given initial distribution π_0 , generate $\{u^{(n)}\}_{n \in \mathbb{Z}^+}$ inductively:

$$\begin{aligned} u^{(0)} &\sim \pi_0, \\ u^{(n+1)} &\sim p(u^{(n)}, \cdot), \quad n \in \mathbb{Z}^+. \end{aligned}$$

Note that $\{u^{(n)}\}_{n \in \mathbb{Z}^+}$ is a random sequence and hence, for each $n \in \mathbb{Z}^+$, there is a marginal distribution on $u^{(n)}$, denoted π_n ; in later discussions correlations between $u^{(n)}$ and $u^{(m)}$ for $n \neq m$ will also be relevant. The following result is fundamental.

Lemma 6.1. *Let π be an invariant distribution of the Markov kernel p . Let $\{u^{(n)}\}_{n \in \mathbb{Z}^+}$ be a sample path generated with kernel p and initial distribution $\pi_0 = \pi$. Then it follows that $u^{(n)} \sim \pi$ for all $n \in \mathbb{Z}^+$.*

Proof. By induction it suffices to show that if $\pi_n = \pi$ then $\pi_{n+1} = \pi$. Let A denote an arbitrary subset in \mathbb{R}^d . We first note that

$$\mathbb{P}(u^{(n+1)} \in A | u^{(n)}) = \int_A p(u^{(n)}, v) dv.$$

Thus, using $\pi_n = \pi$, exchanging the order of integration and using the invariance of π with respect to kernel p , we find that

$$\begin{aligned} \pi_{n+1}(A) &= \mathbb{P}(u^{(n+1)} \in A) \\ &= \mathbb{E}^{u^{(n)} \sim \pi_n} [\mathbb{P}(u^{(n+1)} \in A | u^{(n)})] \\ &= \int_{\mathbb{R}^d} \pi_n(u) \left(\int_A p(u, v) dv \right) du \\ &= \int_{\mathbb{R}^d} \pi(u) \left(\int_A p(u, v) dv \right) du \\ &= \int_A \left(\int_{\mathbb{R}^d} \pi(u) p(u, v) du \right) dv \\ &= \int_A \pi(v) dv \\ &= \pi(A). \end{aligned}$$

Since A is arbitrary the proof is complete. □

In the following it will be useful to compute expectations with respect to the distribution on sample paths $\mathbf{u} = \{u^{(n)}\}_{n \in \mathbb{Z}^+}$ implied by the Markov kernel p and initial distribution π_0 . To this end we let \mathbb{E} denote expectation with respect to the distribution on sample paths and define, for real-valued functions f and g on the sample paths,

$$\begin{aligned}\text{Var}(f(\mathbf{u})) &:= \mathbb{E}[(f(\mathbf{u}) - \mathbb{E}(f))^2], \\ \text{Cov}(f(\mathbf{u}), g(\mathbf{u})) &:= \mathbb{E}[(f(\mathbf{u}) - \mathbb{E}(f))(g(\mathbf{u}) - \mathbb{E}(g))].\end{aligned}$$

We will be particularly interested in the case in which the initial distribution of the Markov chain is π ; the preceding lemma shows that each element $u^{(n)}$ of the sample path \mathbf{u} is then distributed according to π . We then write $\mathbb{E}^{u^{(0)} \sim \pi}$. If, abusing notation, f and g depend only on a single element $u^{(n)}$ of \mathbf{u} , then we have

$$\begin{aligned}\text{Var}(f(u^{(n)})) &:= \text{Var}_\pi(f(u)) := \pi((f(u) - \pi(f))^2), \\ \text{Cov}(f(u^{(n)}), g(u^{(m)})) &:= \mathbb{E}^{u^{(0)} \sim \pi}[(f(u^{(n)}) - \pi(f))(g(u^{(m)}) - \pi(g))].\end{aligned}$$

6.2 Markov Chain Sampling

The idea of MCMC is simple to state: given a target distribution π , find a Markov kernel that can be sampled from and has π as its invariant distribution. Samples $\{u^{(n)}\}_{n=1}^N$ drawn iteratively from the kernel may be used to approximate posterior expectations. The samples are given uniform weights $1/N$ but, in contrast to standard Monte Carlo, they are not independent and they are not drawn exactly from the target π . However, if the chain is guaranteed to satisfy *sample path ergodicity*, then the resulting estimator for $\pi(f)$ is asymptotically unbiased and satisfies a central limit theorem for suitable test functions f . We display the algorithm, define the estimator and then state a theorem summarizing convergence.

Algorithm 6.1 Markov Chain Sampling Algorithm

- 1: **Input:** Target distribution π , initial distribution π_0 , Markov kernel $q(u, v)$ with invariant distribution π , number of samples N .
 - 2: **Initial Draw:** Draw initial sample $u^{(0)} \sim \pi_0$.
 - 3: **Subsequent Samples:** For $n = 0, 1, \dots, N - 1$ do:
 1. Sample $u^{(n+1)} \sim q(u^{(n)}, \cdot)$.
 - 4: **Output:** Target approximation $\pi \approx \pi_{\text{MCMC}}^N := \frac{1}{N} \sum_{n=1}^N \delta(u - u^{(n)})$.
-

The estimator for $\pi(f)$ resulting from Algorithm 6.1 is then

$$\pi_{\text{MCMC}}^N(f) = \frac{1}{N} \sum_{n=1}^N f(u^{(n)}).$$

Recall the notation Var , Cov and $\mathbb{E}^{u^{(0)} \sim \pi}$ from the previous section. We then have the following result concerning the error in this estimator.

Theorem 6.2 (MCMC Error). *Let $f : \mathbb{R}^d \rightarrow \mathbb{R}$ satisfy $\text{Var}_\pi[f] = 1$. We have*

$$\begin{aligned}\mathbb{E}^{u^{(0)} \sim \pi} [\pi_{\text{MCMC}}^N(f) - \pi(f)] &= 0, \\ \mathbb{E}^{u^{(0)} \sim \pi} \left[\left(\pi_{\text{MCMC}}^N(f) - \pi(f) \right)^2 \right] &= \frac{\tau_N^2(f)}{N},\end{aligned}$$

where

$$\tau_N^2(f) = 1 + 2 \sum_{m=1}^{N-1} \frac{N-m}{N} \text{Cov}(f(u^{(0)}), f(u^{(m)})).$$

In particular,

$$\lim_{N \rightarrow \infty} N \mathbb{E}^{u^{(0)} \sim \pi} \left[\left(\pi_{\text{MCMC}}^N(f) - \pi(f) \right)^2 \right] = \tau^2(f),$$

where

$$\tau^2(f) = 1 + 2 \sum_{m=1}^{\infty} \text{Cov}(f(u^{(0)}), f(u^{(m)})),$$

provided that the series converges.

Proof. First note that, under the assumptions that $u^{(0)} \sim \pi$ and that the kernel q has invariant distribution π , it follows that $u^{(n)} \sim \pi$ for all $n \geq 1$. Therefore, π_{MCMC}^N is unbiased for $\pi(f)$ by linearity of expectation. Now we characterize the mean squared error of π_{MCMC}^N , which agrees with its variance:

$$\begin{aligned}\mathbb{E}^{u^{(0)} \sim \pi} \left[\left(\pi_{\text{MCMC}}^N(f) - \pi(f) \right)^2 \right] &= \text{Var}[\pi_{\text{MCMC}}^N(f)] \\ &= \frac{1}{N^2} \left[\sum_{n=1}^N \text{Var}[f(u^{(n)})] + 2 \sum_{n=1}^{N-1} \sum_{m>n}^{N-1} \text{Cov}(f(u^{(n)}), f(u^{(m)})) \right] \\ &= \frac{1}{N^2} \left[N + 2 \sum_{n=1}^{N-1} \sum_{m=1}^{N-n} \text{Cov}(f(u^{(n)}), f(u^{(n+m)})) \right] \\ &= \frac{1}{N} \left[1 + \frac{2}{N} \sum_{m=1}^{N-1} \sum_{n=1}^{N-m} \text{Cov}(f(u^{(n)}), f(u^{(n+m)})) \right] \\ &= \frac{1}{N} \left[1 + \frac{2}{N} \sum_{m=1}^{N-1} \sum_{n=1}^{N-m} \text{Cov}(f(u^{(0)}), f(u^{(m)})) \right] \\ &= \frac{1}{N} \left[1 + 2 \sum_{m=1}^{N-1} \frac{N-m}{N} \text{Cov}(f(u^{(0)}), f(u^{(m)})) \right] \\ &= \frac{\tau_N^2(f)}{N}.\end{aligned}$$

The final result follows by the dominated convergence theorem. \square

Remark 6.3. Suppose that $\text{Var}_\pi[f] = 1$. If, for $1 \leq n \leq N$, $u^{(n)} \sim \pi$ are independent, then we have that

$$\text{Var} \left[\frac{1}{N} \sum_{n=1}^N f(u^{(n)}) \right] = \frac{1}{N},$$

as we saw in the proof of Theorem 5.1 for standard Monte Carlo. Thus if the *auto-correlations* $\text{Cov}(f(u^{(0)}), f(u^{(m)}))$ are positive, then the ergodic average will be less accurate than estimated from an i.i.d. sample. This is because positively correlated random variables have redundant information so are less informative than i.i.d. random variables. On the other hand, if the correlations are negative ergodic averages may be more accurate than a direct Monte Carlo estimator with i.i.d. samples.

The theorem is stated in the idealized (and unrealistic) setting in which the Markov chain starts at the desired target distribution. In general ergodicity is needed to ensure that chains initialized far from stationarity will converge to the desired target. Controlling the size of $\tau^2(f)$ and ensuring rapid convergence to stationarity are the two primary design goals when constructing Markov chains invariant with respect to π . \diamond

Addressing the design and analysis of MCMC methods in generality and depth is beyond the scope of a single chapter; entire books are devoted to this subject. We will restrict our discussion to a particular class of MCMC methods, known as Metropolis-Hastings algorithms. We will prove that the desired target distribution is invariant for the Metropolis-Hastings kernel, and we will show *geometric ergodicity* of the pCN Metropolis-Hastings algorithm, meaning that the distribution π_n of the n -th sample approaches the invariant distribution exponentially fast in total variation distance. The idea is illustrated in Figure 6.1: after an initial number of *burn-in* steps the samples from the chain start to concentrate in regions where the target distribution has the greatest mass. We will not discuss sample path ergodicity, noting simply that a general abstract theory exists to deduce it from geometric ergodicity.

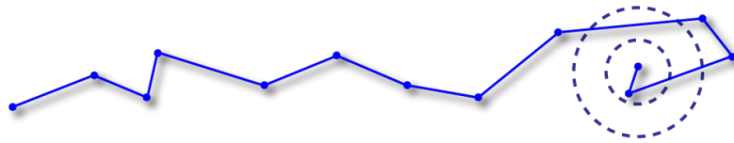


Figure 6.1 The Markov chain samples points from distribution π_n at step n , and the sampling distribution converges towards the target distribution π whose high density regions are represented by the dashed circles.

6.3 Metropolis-Hastings Sampling

Here we outline the Metropolis-Hastings algorithm. The algorithm has two ingredients: a *proposal kernel* $q(u, v)$, which is a Markov transition kernel; and an acceptance probability $a(u, v)$ that will be used to convert the proposal kernel into a kernel $p_{\text{MH}}(u, v)$ for which the given target π is an invariant distribution. Given the n -th sample $u^{(n)}$, we generate $u^{(n+1)}$ by drawing v^* from the distribution $q(u^{(n)}, \cdot)$. The result is accepted, which means setting $u^{(n+1)} = v^*$, with probability $a(u^{(n)}, v^*)$; it is rejected, meaning

$u^{(n+1)} = u^{(n)}$, with the remaining probability $1 - a(u^{(n)}, v^*)$. The acceptance probability is given by

$$a(u, v) = \min\left(\frac{\pi(v)q(v, u)}{\pi(u)q(u, v)}, 1\right). \quad (6.2)$$

Algorithm 6.2 Metropolis-Hastings Algorithm

- 1: **Input:** Target distribution π , initial distribution π_0 , Markov kernel $q(u, v)$, number of samples N .
- 2: **Initial Draw:** Draw initial sample $u^{(0)} \sim \pi_0$.
- 3: **Subsequent Samples:** For $n = 0, 1, \dots, N - 1$ do:
 1. Sample $v^* \sim q(u^{(n)}, \cdot)$.
 2. Calculate the acceptance probability $a_n := a(u^{(n)}, v^*)$.
 3. Update

$$u^{(n+1)} = \begin{cases} v^*, & \text{with probability } a_n, \\ u^{(n)}, & \text{with probability } 1 - a_n. \end{cases}$$

- 4: **Output:** Target approximation $\pi \approx \pi_{\text{MH}}^N := \frac{1}{N} \sum_{n=1}^N \delta(u - u^{(n)})$.
-

The estimator resulting from Algorithm 6.2 for $\pi(f)$ is then

$$\pi_{\text{MH}}^N(f) = \frac{1}{N} \sum_{n=1}^N f(u^{(n)}).$$

The Metropolis-Hastings algorithm implicitly defines a Markov kernel $p_{\text{MH}}(u, \cdot)$ which specifies the density of the $(n + 1)$ -th sample given that the n -th sample is located at u . For $u \neq v$, the Metropolis-Hastings kernel has the following simple expression in terms of the proposal kernel and the acceptance probability

$$p_{\text{MH}}(u, v) = a(u, v)q(u, v); \quad (6.3)$$

this expression may be deduced noting that in order to move from u to a new location v , the move needs to be proposed and accepted.

Remark 6.4. We note the following concerning the Metropolis-Hastings algorithm.

- In order to implement the Metropolis-Hastings algorithm one needs to be able to sample from the proposal kernel $q(u, \cdot)$ and evaluate the acceptance probability $a(u, v)$. Importantly, the target distribution only appears in the acceptance probability $a(u, v)$, and only the ratio $\pi(v)/\pi(u)$ is involved. Therefore the Metropolis-Hastings algorithm may be implemented for target distributions that are only specified up to an unknown normalizing constant.

- If $q(u, v) = q(v, u)$ the acceptance probability simplifies to $\min(1, \pi(v)/\pi(u))$. This is the setting in which the original *Metropolis algorithm* was introduced. In such a case, moves to regions of higher target density are always accepted, while moves to regions of smaller but non-zero target density are accepted with positive probability in order to ensure exploration of the target space. The quantity $\pi(u)q(u, v)$ should be viewed as a joint distribution on the pair (u, v) with u distributed according to the invariant distribution and $v|u$ then defined by the Markov kernel. In the general *Metropolis-Hastings algorithm setting*, when q is not necessarily symmetric, the method favors moves that are easier to be reversed, in the sense that $\pi(v)q(v, u) > \pi(u)q(u, v)$.
- The Metropolis-Hastings algorithm is extremely flexible due to the freedom in the choice of proposal kernel $q(u, v)$. For this algorithm the ergodic behavior, and size of $\tau^2(\cdot)$, is heavily dependent on the choice of proposal kernel.
- The accept-reject step may be implemented by drawing, independently from the proposal, a uniformly distributed random variable θ_n in the interval $[0, 1]$. Recall a_n as defined in Algorithm 6.1. If $\theta_n \in [0, a_n]$ then the proposal is accepted ($u^{(n+1)} = v^*$); it is rejected ($u^{(n+1)} = u^{(n)}$) otherwise.

◇

6.4 Invariance of the Target Distribution π

In this section we show that the target π is an invariant distribution for the Metropolis-Hastings kernel. We start by introducing the notion of detailed balance and showing that it implies invariance. We then prove that the Metropolis-Hastings kernel satisfies detailed balance with respect to π , and hence π is invariant.

6.4.1 Detailed Balance and its Implication

A Markov kernel $p(u, v)$ satisfies *detailed balance* with respect to π if, for any $u, v \in \mathbb{R}^d$,

$$\pi(u)p(u, v) = \pi(v)p(v, u).$$

Detailed balance of $p(u, v)$ with respect to π implies that π is an invariant distribution for $p(u, v)$. To see this, note that if $p(u, v)$ satisfies detailed balance with respect to π , then

$$\int_{\mathbb{R}^d} \pi(u)p(u, v) du = \pi(v) \int_{\mathbb{R}^d} p(v, u) du = \pi(v).$$

Invariance guarantees that, if the chain is distributed according to π at a given step, then it will also be distributed according to π in the following step. Detailed balance guarantees that the in/out probability flux between any two states is preserved; this is a stronger condition, which implies invariance.

6.4.2 Detailed Balance and the Metropolis-Hastings Algorithm

The following theorem establishes the detailed balance of the Metropolis-Hastings kernel with respect to the target π ; it implies, as a consequence, that the target is an invariant distribution for the Metropolis-Hastings kernel.

Theorem 6.5 (Metropolis-Hastings and Detailed Balance). *The Metropolis-Hastings kernel satisfies detailed balance with respect to the distribution π .*

Proof. We need to show that, for any $u, v \in \mathbb{R}^d$,

$$\pi(u)p_{\text{MH}}(u, v) = \pi(v)p_{\text{MH}}(v, u). \quad (6.4)$$

We let v^* denote the point proposed from kernel $q(u, \cdot)$, calculate the joint probability distribution of (u, v^*, v) and then integrate out v^* in order to identify $\pi(u)p_{\text{MH}}(u, v)$. We first note that the random variable $v|u, v^*$ has density

$$\delta_{v^*}(v)a(u, v^*) + \delta_u(v)(1 - a(u, v^*)). \quad (6.5)$$

The density of (u, v^*) is found from the product of the density of $v^*|u$ and the density of u and is hence given by

$$q(u, v^*)\pi(u). \quad (6.6)$$

Multiplying (6.5) and (6.6) gives the density of (u, v^*, v) and integrating out v^* gives the density of (u, v) , namely

$$\begin{aligned} \pi(u)p_{\text{MH}}(u, v) &= \pi(u)q(u, v)a(u, v) + \pi(u)\delta_u(v)\beta(u), \\ \beta(u) &= \int_{\mathbb{R}^d} (1 - a(u, v^*))q(u, v^*)dv^*. \end{aligned}$$

Now note that

$$\begin{aligned} q(u, v)a(u, v) &= \min \left(\frac{\pi(v)q(v, u)}{\pi(u)q(u, v)}, 1 \right) q(u, v) \\ &= \frac{1}{\pi(u)} \times \min \left(\pi(u)q(u, v), \pi(v)q(v, u) \right). \end{aligned}$$

Thus, invoking symmetry,

$$\pi(u)q(u, v)a(u, v) = \min \left(\pi(u)q(u, v), \pi(v)q(v, u) \right) = \pi(v)q(v, u)a(v, u).$$

It is then apparent that $\pi(u)p_{\text{MH}}(u, v)$ is symmetric with respect to the pair (u, v) , establishing (6.4) and completing the proof. \square

Invariance of the Metropolis-Hastings kernel p_{MH} with respect to π implies that if the initial sample is drawn from the target ($\pi_0 = \pi$), then all subsequent samples are also distributed according to the target ($\pi_n = \pi$).

6.5 Convergence to the Target Distribution

In the previous section we showed that if we initialize the Metropolis-Hastings algorithm with distribution π , all samples produced by the algorithm will be distributed according to π . But the motivation for the Metropolis-Hastings algorithm is that we are not able to directly sample from π . Our aim in this section is to show that, for certain Metropolis-Hastings methods, the law π_n of the n -th sample converges to π regardless

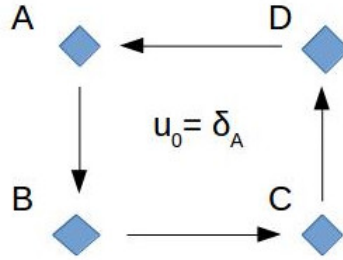


Figure 6.2 The arrows represent transitions with probability one in a four state Markov chain. The invariant distribution is the uniform distribution but for $\pi_0 = \delta_A$, we have $\pi_1 = \delta_B, \pi_2 = \delta_C, \pi_3 = \delta_D, \pi_4 = \delta_A$, etc. Here π_n does not converge to a limit distribution.

of the initial distribution π_0 . This is a strong form of *ergodic* behavior which does not hold in general, as illustrated by the chain depicted in Figure 6.2.

In order to understand the mechanisms behind ergodicity we will first consider Markov chains with finite state-space. We then study a specific Metropolis-Hastings algorithm, known as the pCN (for *preconditioned Crank-Nicolson*) method, which applies to targets π defined by their density with respect to a Gaussian distribution.

6.5.1 Finite State-Space

We consider a Markov chain on the finite state-space $S = \{1, \dots, d\}$. The Markov kernel described earlier becomes a $d \times d$ *transition matrix* P with non-negative entries $p(i, j)$ satisfying

$$\sum_{j \in S} p(i, j) = 1.$$

The invariant distribution becomes $d \times 1$ column vector π , with non-negative entries which sum to one, satisfying

$$\pi^\top = \pi^\top P. \quad (6.7)$$

Such an invariant distribution always exists but is not, in general, unique. The distribution at each step of the Markov chain is the $d \times 1$ column vector π_n satisfying

$$\pi_{n+1}^\top = \pi_n^\top P, \quad (6.8)$$

where π_0 is the initial distribution of the chain. Ergodicity may be defined as convergence of the sequence π_n to limit π as $n \rightarrow \infty$; this is related to the eigenvalue 1 of P having algebraic and geometric multiplicity one. We now illustrate a *coupling* approach to proving ergodicity and then, in the next subsection, generalize the methodology to study the pCN method on the continuous state-space \mathbb{R}^d .

Theorem 6.6 (Ergodicity in Finite State-Space). *Let $\{u^{(n)}\}_{n \in \mathbb{Z}^+}$ be a Markov chain with state-space $S = \{1, \dots, d\}$, transition matrix P and initial distribution π_0 . Assume that there is $\varepsilon > 0$ such that*

$$\min_{(i,j) \in S \times S} p(i, j) \geq \frac{\varepsilon}{d}. \quad (6.9)$$

Then there is a unique solution π to (6.7) within the class of probability vectors on S . Furthermore, the following convergence result holds for iteration (6.8):

$$d_{\text{TV}}(\pi_n, \pi) \leq (1 - \varepsilon)^n. \quad (6.10)$$

Proof. First note that the Markov matrix P is a continuous map from the space of probability distributions on S into itself; it thus continuously maps a compact, convex set into itself. By Brouwer's fixed point theorem it follows that P has a fixed point in this space, ensuring that an invariant distribution π solving (6.7) exists. We will now show that for any invariant distribution π equation (6.10) holds, which also implies the uniqueness of the invariant distribution within the class of probability vectors.

Let π be an invariant distribution, a probability vector on S . Proving convergence to equilibrium amounts to “forgetting the past”, to show that the long time behavior of the Markov chain does not depend on the initial distribution π_0 and in fact converges to π . In general, $u^{(n+1)}$ will be strongly dependent on $u^{(n)}$, but the condition given in (6.9) implies that there is always some residual chance that the chain jumps to any new state, at each step, independently of where it is currently located, $u^{(n)}$. This residual probability of the chain to make a “totally random” move will be shown to diminish the stochastic dependence on $u^{(0)}$ as n increases.

To formalize this idea, let b_n be i.i.d. Bernoulli random variables with $\mathbb{P}(b_n = 1) = \varepsilon$ and $\mathbb{P}(b_n = 0) = 1 - \varepsilon$; furthermore assume that the sequence $\{b_n\}$ is independent of the randomness defining draws from $\{p(u^{(n)}, \cdot)\}$. Define r to be the uniform transition kernel with equal probability of transitioning to each state in S : $r(i, j) = d^{-1}$ for all $(i, j) \in S \times S$.

Using the lower bound on p we may define a new Markov chain $\{w^{(n)}\}_{n \in \mathbb{Z}^+}$ as follows:

$$w^{(n+1)} \sim \begin{cases} s(w^{(n)}, \cdot), & \text{for } b_n = 0, \\ r(w^{(n)}, \cdot), & \text{for } b_n = 1, \end{cases} \quad (6.11)$$

where

$$s(i, j) := \frac{p(i, j) - \varepsilon r(i, j)}{1 - \varepsilon}.$$

We make two observations about this construction. First, the lower bound of ε/d on $p(i, j)$ means that the probability transition matrix s is well-defined; secondly the fact that $r(i, j)$ is independent of i is key as it means that sampling explicitly forgets the current state whenever $b_n = 1$. We may now compute

$$\begin{aligned} \mathbb{P}(w^{(n+1)} = j | w^{(n)} = i) &= \varepsilon \mathbb{P}(w^{(n+1)} = j | w^{(n)} = i, b_n = 1) \\ &\quad + (1 - \varepsilon) \mathbb{P}(w^{(n+1)} = j | w^{(n)} = i, b_n = 0) \\ &= \varepsilon r(i, j) + p(i, j) - \varepsilon r(i, j) \\ &= p(i, j). \end{aligned}$$

Thus the kernel defined by (14.11) is equivalent in law to that defined by matrix P . However, by introducing the ancillary random variables b_n , we have made explicit the

concept of “forgetting the past entirely, with a small probability” at every step. We may now use this to complete the proof. Let $f : S \mapsto \mathbb{R}$ be an arbitrary test function with $|f|_\infty \leq 1$ and $\tau := \min(n \in \mathbb{N} : b_n = 1)$. Then, regardless of how $w^{(0)}$ is initialized,

$$\begin{aligned} \mathbb{E}[f(w^{(n)})] &= \mathbb{E}[f(w^{(n)}) | \tau \geq n] \mathbb{P}(\tau \geq n) + \sum_{l=0}^{n-1} \mathbb{E}[f(w^{(n)}) | \tau = l] \mathbb{P}(\tau = l) \\ &= \underbrace{\mathbb{E}[f(w^{(n)}) | \tau \geq n] \mathbb{P}(\tau \geq n)}_{|\cdot| \leq (1-\varepsilon)^n} + \underbrace{\sum_{l=0}^{n-1} \mathbb{E}^{w^{(0)} \sim u(\cdot)}[f(w^{(n-l)})] \mathbb{P}(\tau = l)}_{\text{independent of original initial distribution}}, \end{aligned}$$

where u denotes the uniform distribution on S .

Now consider two Markov chains $\{w^{(n)}\}$ and $\{w'^{(n)}\}$ with kernel (14.11), the first initialized from π_0 and the second from an invariant distribution π ; denote their distributions at time n by π_n and π'_n , respectively. The law of $w^{(n)}$ agrees with the law π_n of the original chain $u^{(n)}$ when initialized at π_0 ; on the other hand, for the second chain it follows from invariance that $\pi'_n = \pi$. We will use the variational characterization of the total variation distance established in Lemma 1.10. Employing the preceding identity and noting that the contribution which is independent of the initial distribution will cancel in the two different Markov chains, we obtain

$$d_{\text{TV}}(\pi_n, \pi'_n) = \frac{1}{2} \sup_{|f|_\infty \leq 1} |\mathbb{E}^{\pi_n}[f(u)] - \mathbb{E}^{\pi'_n}[f(u)]| \leq (1 - \varepsilon)^n.$$

Since $\pi'_n = \pi$ the desired result follows. \square

Before extending the above argument to a setting with continuous state-space, we make two remarks:

Remark 6.7. The coupling proof we have just exhibited may be generalized in a number of ways; in particular:

- The distribution r does not need to be uniform; it was only chosen so for convenience. What is important is that $r(i, j)$ is lower bounded, independently of i , for all j . Adapting r to the matrix P at hand, might in some cases greatly improve the above bound —a larger ε might be identified.
- Convergence to equilibrium can also be shown if condition (6.9) holds with P replaced by the n -step transition Markov matrix P^n . Again, for some chains this may yield faster bounds on the convergence to equilibrium.

\diamond

6.5.2 The pCN Method

The coupling argument used in the previous subsection for Markov chains with finite state-space may also be employed to study ergodicity of Markov chains on a continuous state-space. To illustrate this we consider a particular Metropolis-Hastings algorithm,

the pCN method, applied to a specific Bayesian inverse problem setting. Before we get into the details of this setting, we describe the idea behind the pCN method at a high level. The idea is this. If the desired target distribution has the form

$$\pi(u) = \frac{1}{Z} \tilde{l}(u) \tilde{\rho}(u) \quad (6.12)$$

and if the Metropolis-Hastings proposal kernel q satisfies detailed balance with respect to $\tilde{\rho}$, then (6.2) simplifies to give

$$a(u, v) = \min\left(\frac{\tilde{\rho}(v) \tilde{l}(v) q(v, u)}{\tilde{\rho}(u) \tilde{l}(u) q(u, v)}, 1\right) = \min\left(\frac{\tilde{l}(v)}{\tilde{l}(u)}, 1\right). \quad (6.13)$$

We will apply and study this idea in the case where $\tilde{\rho}$ is a Gaussian distribution, in which case it is straightforward to construct a proposal kernel that satisfies detailed balance with respect to $\tilde{\rho}$. This scenario arises naturally in Bayesian inverse problems where the prior is either a Gaussian, or it is naturally expressed via density which is the product of a Gaussian with another function. We now formalize the inverse problem setting that we consider by imposing certain assumptions on the likelihood and the prior, and then relate both to the functions \tilde{l} and $\tilde{\rho}$ in equation (6.12).

Assumption 6.8. *We make the following assumptions on the Bayesian inverse problem:*

- *Bounded likelihood: there are $l^-, l^+ > 0$ such that, for all $u \in \mathbb{R}^d$,*

$$0 < l^- < l(u) < l^+.$$
- *Truncated Gaussian prior: there is a compact set $B \subset \mathbb{R}^d$ and of positive Lebesgue measure such that $\rho(u) \propto \mathbb{1}_B(u) z(u)$, where z is the pdf of Gaussian $\mathcal{N}(0, \hat{C})$.*

Under Assumption 6.8 we obtain for the posterior density

$$\pi(u) \propto l(u) \mathbb{1}_B(u) z(u),$$

which is of the form in equation (6.12) with $\tilde{l}(u) = l(u) \mathbb{1}_B(u)$ and $\tilde{\rho}(u) = z(u)$.

The pCN method is a Metropolis-Hastings algorithm with proposal kernel

$$q(u, \cdot) \sim \mathcal{N}\left((1 - \beta^2)^{1/2} u, \beta^2 \hat{C}\right), \quad (6.14)$$

where $\beta \in (0, 1]$ is a user-specified parameter that should be tuned to obtain an acceptance probability that, on average, stays away from 0 or 1—for example one that is approximately 1/2. Thus, given the sample $u^{(n)}$, the pCN proposes a new sample

$$v^* \sim \left(1 - \beta^2\right)^{1/2} u^{(n)} + \beta \xi^{(n)}, \quad \xi^{(n)} \sim \mathcal{N}(0, \hat{C}),$$

which only requires to sample a Gaussian. Note that

$$\mathbb{E}\left[v^*(v^*)^\top\right] = (1 - \beta^2) \mathbb{E}\left[u^{(n)}(u^{(n)})^\top\right] + \beta^2 \hat{C},$$

demonstrating that if $u^{(n)} \sim \mathcal{N}(0, \hat{C})$ then the proposal satisfies $v^* \sim \mathcal{N}(0, \hat{C})$ as well. The following lemma shows the stronger result that the proposal kernel satisfies detailed balance with respect to z .

Lemma 6.9. *The proposal kernel (6.14) satisfies detailed balance with respect to the pdf z of Gaussian $\mathcal{N}(0, \hat{C})$.*

Proof. Recall the notation for the covariance weighted inner-product and resulting norm described in the introduction to these notes. We need to show that $z(v)q(v, u)$ is symmetric in u and v . By direct calculation,

$$\begin{aligned} -\log(z(v)q(v, u)) &= \frac{1}{2}|v|_{\hat{C}}^2 + \frac{1}{2\beta^2}\left|u - (1 - \beta^2)^{1/2}v\right|_{\hat{C}}^2 \\ &= \left(\frac{1}{2} + \frac{(1 - \beta^2)}{2\beta^2}\right)|v|_{\hat{C}}^2 + \frac{1}{2\beta^2}|u|_{\hat{C}}^2 - \frac{(1 - \beta^2)^{1/2}}{\beta^2}\langle u, v \rangle_{\hat{C}} \\ &= \frac{1}{2\beta^2}(|v|_{\hat{C}}^2 + |u|_{\hat{C}}^2) - \frac{(1 - \beta^2)^{1/2}}{\beta^2}\langle u, v \rangle_{\hat{C}}. \end{aligned}$$

□

We now display the pCN algorithm applied in the setting of Assumption 6.8 and describe how it leads to an estimator of $\pi(f)$. The expression for the acceptance probability in Algorithm 6.3 follows from equation (6.13) using Lemma 6.9 and noting that π_0 being supported on B implies that $u^{(n)} \in B$ for all n , as any proposed move out of B will be rejected. Thus $\mathbb{1}_B(u)$ may be dropped from the formula for the acceptance probability in equation (6.13).

Algorithm 6.3 pCN Algorithm

- 1: **Input:** Tuning parameter $\beta \in (0, 1)$, covariance \hat{C} , bounded set B , likelihood function g , initial distribution π_0 supported on B , number of samples N .
- 2: **Initial Draw:** Draw initial sample $u^{(0)} \sim \pi_0$.
- 3: **Subsequent Samples:** For $n = 0, 1, \dots, N - 1$ do:

1. Sample $v^* \sim \mathcal{N}\left((1 - \beta^2)^{1/2}u^{(n)}, \beta^2\hat{C}\right)$.
2. Calculate the acceptance probability $a_n := a(u^{(n)}, v^*)$ where

$$a(u, v) = \min\left(\frac{l(v)}{l(u)}\mathbb{1}_B(v), 1\right).$$

3. Update

$$u^{(n+1)} = \begin{cases} v^*, & \text{with probability } a_n, \\ u^{(n)}, & \text{with probability } 1 - a_n. \end{cases}$$

- 4: **Output:** Target approximation $\pi \approx \pi_{\text{pCN}}^N := \frac{1}{N} \sum_{n=1}^N \delta(u - u^{(n)})$.
-

The estimator for $\pi(f)$ resulting from Algorithm 6.3 is then

$$\pi_{\text{pCN}}^N(f) = \frac{1}{N} \sum_{n=1}^N f(u^{(n)}).$$

We can now prove ergodicity using similar techniques to those employed in the previous subsection in the finite state-space setting. The main idea is that, restricted to the bounded set B , the probability density of the transition kernel is bounded away from zero by some ε . Splitting off a “forgetful part” that is triggered with probability ε then yields the result.

Theorem 6.10 (Ergodicity for pCN Method). *Assume that we apply the pCN method to sample from a posterior density π arising from Assumptions 6.8 with initial condition drawn from any density supported on B . Then there exists a constant $\varepsilon \in (0, 1)$ such that*

$$d_{\text{TV}}(\pi_n, \pi) \leq (1 - \varepsilon)^n,$$

where π_n is the law of the n -th sample from the pCN Metropolis-Hastings algorithm.

Proof of Theorem 6.10. Note again that since $u^{(0)} \in B$ we have $u^{(n)} \in B$ for all $n \geq 1$. Note further that since B is compact and q is continuous in both of its arguments, there is $q^- > 0$ such that, for any $u, v \in B$,

$$q(u, v) \geq q^-.$$

Let p be the Markov kernel defined by the pCN Metropolis-Hastings algorithm. It follows that, for $u, v \in B$,

$$\begin{aligned} p(u, v) &\geq q(u, v)a(u, v) \\ &\geq q^- \frac{g^-}{g^+} =: \varepsilon \text{Leb}(B), \end{aligned}$$

where the last equation defines ε and $\text{Leb}(B)$ denotes the Lebesgue measure of B (which is assumed to be positive). Analogously to the discrete proof, we now define b_n to be i.i.d. Bernoulli random variables with $\mathbb{P}(b_n = 1) = \varepsilon$, independently of all other randomness, and consider the transition rule

$$u^{(n+1)} \sim \begin{cases} s(u^{(n)}, \cdot), & \text{for } b_n = 0, \\ r(\cdot), & \text{for } b_n = 1, \end{cases}$$

where r denotes the uniform distribution on B and, for $A \subset B$ and $u \in B$,

$$s(u, A) := \frac{p(u, A) - \varepsilon r(A)}{1 - \varepsilon}.$$

Just as in the discrete case, one can check that the resulting Markov kernel is equal to the pCN Metropolis-Hastings kernel $p(\cdot, \cdot)$. Furthermore, exponential convergence is then deduced in exactly the same way as in the discrete case. \square

6.6 Discussion and Bibliography

The idea of sampling a target distribution π by means of a π -invariant Markov chain was introduced in the statistical physics community in [211], where a symmetric proposal kernel was used. Hastings introduced a powerful generalization of the method in [136] which allowed for asymmetric proposal kernels. The Bayesian methodology [111], and in particular MCMC-based exploration of the posterior, became practical as a result of advances in computer power and became widely adopted for many sampling problems arising in science and engineering.

The book [103] is a useful basic introduction to MCMC and the book [38] presents state of the art as of 2010. The paper [60] overviews the pCN method and related MCMC algorithms specifically designed for inverse problems and other sampling problems in high-dimensional state-spaces. The book [194] describes the coupling method in a general setting. The book [212] contains a wide-ranging presentation of Markov chains, and their long-time behavior, including ergodicity and coupling. Furthermore, the book describes the general framework for going from convergence of expectations in (possibly weighted) total variation distances to sample path ergodicity and almost sure convergence of time averages, a topic we did not cover in this chapter. The paper [209] describes the coupling technique in the context of stochastic differential equations and their approximations.

The tuning of parameters in MCMC, such as the parameter β appearing in the pCN method, is key to their success. If the goal of the MCMC sampling method is to approximate the expectation of a given test function f , then the aim of parameter tuning is to minimize the integrated auto-correlation $\tau^2(f)$ defined in Theorem 6.2. In general different f will lead to different optimal proposal parameter choices; however, for a wide class of high-dimensional target distributions and specific proposal kernels there are generic rules of thumb, independent of f , for tuning parameters in the proposal [264]. This universality often arises from using suboptimal algorithms and, for specific problems, can be circumvented by using tailored proposals. For example, for target measures that have a density with respect to a Gaussian, the pCN proposal is preferable to the random walk Metropolis proposal, as demonstrated in [60, 128, 109].

Part II

Data Assimilation

Chapter 7

Filtering and Smoothing Problems and Well-Posedness

In this chapter we introduce data assimilation problems in which the model of interest, and the data associated with it, have a time-ordered nature. We distinguish between the filtering problem (on-line) in which the data is incorporated sequentially as it comes in, and the smoothing problem (off-line) which is a specific instance of the inverse problems that have been the subject of the preceding chapters. We formulate the filtering and smoothing problems in Section 7.1. After that, we focus on the smoothing problem in Section 7.2 and describe its interpretation as an inverse problem. This interpretation will allow us to seamlessly apply to the smoothing problem the well-posedness theory for inverse problems developed in Chapter 1. Section 7.3 is concerned with the on-line filtering problem. We will establish well-posedness of the filtering problem in total variation distance as a corollary of the well-posedness of the smoothing problem. We will also provide a roadmap for the filtering methods that will be introduced in subsequent chapters, highlighting the settings in which they will be presented. Section 7.4 closes with extensions and bibliographical remarks.

7.1 Formulation of Filtering and Smoothing Problems

Consider the *stochastic dynamics model* given by

$$\begin{aligned} v_{j+1} &= \Psi(v_j) + \xi_j, \quad j \in \mathbb{Z}^+, \\ v_0 &\sim \mathcal{N}(m_0, C_0), \quad \xi_j \sim \mathcal{N}(0, \Sigma) \text{ i.i.d.}, \end{aligned}$$

where we assume that v_0 is independent of the sequence $\{\xi_j\}$; this is often written as $v_0 \perp \{\xi_j\}$. Now we add the *data model* given by

$$\begin{aligned} y_{j+1} &= h(v_{j+1}) + \eta_{j+1}, \quad j \in \mathbb{Z}^+, \\ \eta_j &\sim \mathcal{N}(0, \Gamma) \text{ i.i.d.}, \end{aligned}$$

where we assume that $\{\eta_j\} \perp v_0$ for all j and $\eta_k \perp \xi_j$ for all j, k . The following will be assumed in the remainder of these notes.

Assumption 7.1. *The matrices C_0 , Σ and Γ are positive definite. Further, we have $\Psi \in C(\mathbb{R}^d, \mathbb{R}^d)$ and $h \in C(\mathbb{R}^d, \mathbb{R}^k)$.*

We define, for a given and fixed integer J ,

$$V := \{v_0, \dots, v_J\}, Y := \{y_1, \dots, y_J\}, \text{ and } Y_j := \{y_1, \dots, y_j\}.$$

The sequence V is often termed the *signal* and the sequence Y the *data*.

Definition 7.2. The *smoothing problem* is to find the probability density $\Pi(V) := \mathbb{P}(V|Y) = \mathbb{P}(\{v_0, \dots, v_J\}|\{y_1, \dots, y_J\})$ on $\mathbb{R}^{d(J+1)}$ for some fixed integer J . We refer to Π as the *smoothing distribution*. \diamond

Definition 7.3. The *filtering problem* is to find, and update sequentially in j , the probability densities $\pi_j(v_j) := \mathbb{P}(v_j|Y_j) = \mathbb{P}(v_j|\{y_1, \dots, y_j\})$ on \mathbb{R}^d for $j = 1, \dots, J$. We refer to π_j as the *filtering distribution at time j* . \diamond

The key conceptual issue to appreciate concerning the filtering problem, in comparison with the smoothing problem, is that interest is focused on characterizing, or approximating, a sequence of probability distributions, defined in an iterative fashion as the data is acquired sequentially.

Remark 7.4. We note the following identity:

$$\int \Pi(v_0, \dots, v_J) dv_0 dv_1 \dots dv_{J-1} = \pi_J(v_J).$$

This expresses the fact that the marginal of the smoothing distribution at time J corresponds to the filtering distribution at time J . Note also that, for $j < J$, in general

$$\int \Pi(v_0, \dots, v_J) dv_0 \dots dv_{j-1} dv_{j+1} \dots dv_J \neq \pi_j(v_j),$$

since the expression on the left-hand side of the equation depends on data Y_J , whereas that on the right-hand side depends only on Y_j , and $j < J$. \diamond

7.2 The Smoothing Problem

7.2.1 Formulation as an Inverse Problem

If we define

$$\eta := \{\eta_1, \dots, \eta_J\}$$

and

$$G(V) := \{h(v_1), \dots, h(v_J)\},$$

then the data model can be written in the form of the inverse problem (1.1):

$$Y = G(V) + \eta.$$

The stochastic dynamics model provides a prior probabilistic description of V , which may then be used to formulate a Bayesian version of the inverse problem of finding V from Y .

7.2.2 Formula for pdf of the Smoothing Problem

The smoothing distribution can be found by combining a prior on v and a likelihood function using Bayes theorem. The prior is the probability distribution on v implied by the distribution of v_0 and the stochastic dynamics model; the likelihood function is defined by the data model. We now derive the prior and the likelihood separately.

The prior distribution can be derived as follows:

$$\begin{aligned}\mathbb{P}(V) &= \mathbb{P}(v_J, v_{J-1}, \dots, v_0) \\ &= \mathbb{P}(v_J | v_{J-1}, \dots, v_0) \mathbb{P}(v_{J-1}, \dots, v_0) \\ &= \mathbb{P}(v_J | v_{J-1}) \mathbb{P}(v_{J-1}, \dots, v_0).\end{aligned}$$

The third equality comes from the Markov, or memoryless, property which follows from the independence of the elements of the sequence $\{\xi_j\}$. By induction, we have

$$\begin{aligned}\mathbb{P}(V) &= \mathbb{P}(v_0) \prod_{j=0}^{J-1} \mathbb{P}(v_{j+1} | v_j) \\ &= \frac{1}{Z_\rho} \exp(-R(V)) \\ &=: \rho(V),\end{aligned}$$

where $Z_\rho > 0$ is a normalizing constant and

$$R(V) := \frac{1}{2} |v_0 - m_0|_{C_0}^2 + \frac{1}{2} \sum_{j=0}^{J-1} |v_{j+1} - \Psi(v_j)|_\Sigma^2.$$

The likelihood function, which incorporates the measurements gathered from observing the system, depends only on the measurement model and may be derived as follows:

$$\begin{aligned}\mathbb{P}(Y|V) &= \prod_{j=0}^{J-1} \mathbb{P}(y_{j+1} | v_0, \dots, v_J) \\ &= \prod_{j=0}^{J-1} \mathbb{P}(y_{j+1} | v_{j+1}) \\ &\propto \exp(-L(V; Y)),\end{aligned}$$

where the loss function is given by

$$L(V; Y) := \frac{1}{2} \sum_{j=0}^{J-1} |y_{j+1} - h(v_{j+1})|_\Gamma^2.$$

The factorization of $\mathbb{P}(Y|V)$ in terms of the product of the $\mathbb{P}(y_{j+1} | v_{j+1})$ follows from the independence of the elements of $\{\eta_j\}$ and the fact that the observation at time $j+1$ depends only on the state at time $j+1$.

Using Bayes Theorem 1.2 we find the smoothing distribution by combining the likelihood and the prior

$$\begin{aligned}\Pi(V) &\propto \mathbb{P}(Y|V) \mathbb{P}(V) \\ &= \frac{1}{Z} \exp(-R(V) - L(V; Y)).\end{aligned}$$

Note that $V \in \mathbb{R}^{d(J+1)}$ and $Y \in \mathbb{R}^{kJ}$.

7.2.3 Well-Posedness of the Smoothing Problem

Now we study the well-posedness of the smoothing problem with respect to perturbations in the data. To this end, we consider two smoothing distributions corresponding to different observed data sequences Y, Y' :

$$\begin{aligned}\Pi(V) &:= \mathbb{P}(V|Y) = \frac{1}{Z} \exp(-R(V) - L(V; Y)), \\ \Pi'(V) &:= \mathbb{P}(V|Y') = \frac{1}{Z'} \exp(-R(V) - L(V; Y')).\end{aligned}$$

We make the following assumptions:

Assumption 7.5. *There is a finite non-negative constant R such that the data Y, Y' and the observation function h satisfy:*

- $|Y|, |Y'| \leq R$;
- Letting $\varphi(V) := \left(\sum_{j=1}^J (|h(v_j)|^2)\right)^{1/2}$, it holds that $\mathbb{E}^\rho[\varphi^2(V)] < \infty$.

The following theorem shows well-posedness of the smoothing problem.

Theorem 7.6 (Well-Posedness of Smoothing). *Under Assumption 7.5, there is $\kappa \in [0, \infty)$ independent of Y and Y' such that*

$$d_H(\Pi, \Pi') \leq \kappa |Y - Y'|.$$

Proof. We show that the proof of Theorem 1.15, which established well-posedness for Bayesian inverse problems under Assumption 1.13, applies in the smoothing context as well. To do so, we rewrite the problem in the same notation used in Chapter 1, and show that Assumption 7.5 above implies Assumption 1.13. Write

$$\begin{aligned}\Pi(V) &= \frac{1}{Z} \exp(-L(V; Y)) \rho(V) = \frac{1}{Z} l(V; Y) \rho(V), \\ \Pi'(V) &= \frac{1}{Z'} \exp(-L(V; Y')) \rho(V) = \frac{1}{Z'} l(V; Y') \rho(V),\end{aligned}$$

where $Z, Z' > 0$ are normalization constants. Here $|Y - Y'|$ plays the role of δ in Theorem 1.15. Since the likelihood $l(V; Y) := \exp(-L(V; Y))$ and $L(V; Y)$ is positive we have that

$$\sup_v \left| \sqrt{l(V; Y)} \right| + \left| \sqrt{l(V; Y')} \right| \leq 2,$$

and so Assumption 1.13 (ii) is satisfied. To see that Assumption 1.13 (i) is also satisfied, note that e^{-x} is Lipschitz-1. Therefore, using the Cauchy-Schwarz inequality and some algebraic manipulations, there is κ independent of Y and Y' such that

$$\begin{aligned}
 \left| \sqrt{l(V, Y)} - \sqrt{l(V; Y')} \right| &\leq \frac{1}{2} \left| L(V; Y) - L(V; Y') \right| \\
 &= \frac{1}{2} \left| \sum_{j=0}^{J-1} \frac{1}{2} \left(|y_{j+1} - h(v_{j+1})|_{\Gamma}^2 - |y'_{j+1} - h(v_{j+1})|_{\Gamma}^2 \right) \right| \\
 &\leq \kappa \sum_{j=0}^{J-1} |y_{j+1} - y'_{j+1}|_{\Gamma} |y_{j+1} + y'_{j+1} - 2h(v_{j+1})|_{\Gamma} \\
 &\leq \kappa |Y - Y'| \varphi(V),
 \end{aligned}$$

where φ is defined in Assumption 7.5. This shows that under Assumption 7.5 the likelihood function of the smoothing problem satisfies Assumption 1.13 with $\delta = |Y - Y'|$; Theorem 7.6 follows from Theorem 1.15. \square

7.3 The Filtering Problem

7.3.1 Formula for pdf of the Filtering Problem

Filtering concerns the iterative updating of distributions, as new data arrives. We recall that we denote the filtering distribution at time j by $\pi_j = \mathbb{P}(v_j | Y_j)$, and we now introduce $\hat{\pi}_{j+1} = \mathbb{P}(v_{j+1} | Y_j)$. Then, we decompose in two steps the updating of the filtering distribution from time j to time $j+1$:

$$\begin{aligned}
 \text{Prediction Step:} \quad & \hat{\pi}_{j+1} = \mathcal{P}\pi_j. \\
 \text{Analysis Step:} \quad & \pi_{j+1} = \mathcal{A}_j \hat{\pi}_{j+1}.
 \end{aligned} \tag{7.3}$$

The combination of the prediction and analysis steps is shown schematically in Figure 7.1 and leads to the update

$$\pi_{j+1} = \mathcal{A}_j \mathcal{P} \pi_j,$$

where \mathcal{P} is a Markov map and \mathcal{A}_j is a likelihood map (Bayes theorem) that we define in what follows.

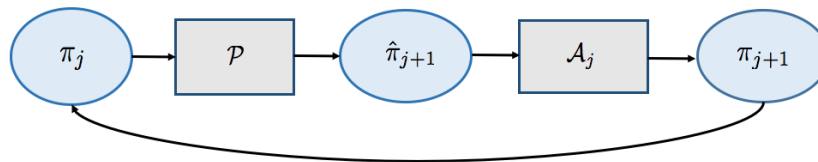


Figure 7.1 Prediction and analysis steps combined.

We first derive the map \mathcal{P} , which is sometimes termed *prediction*. By the Markov property of the stochastic dynamics model, we have

$$\begin{aligned}
 \hat{\pi}_{j+1}(v_{j+1}) &= \mathbb{P}(v_{j+1}|Y_j) \\
 &= \int_{\mathbb{R}^d} \mathbb{P}(v_{j+1}|Y_j, v_j) \mathbb{P}(v_j|Y_j) dv_j \\
 &= \int_{\mathbb{R}^d} \mathbb{P}(v_{j+1}|v_j) \mathbb{P}(v_j|Y_j) dv_j \\
 &= \int_{\mathbb{R}^d} \mathbb{P}(v_{j+1}|v_j) \pi_j(v_j) dv_j \\
 &= \frac{1}{(2\pi)^{d/2}(\det \Sigma)^{1/2}} \int_{\mathbb{R}^d} \exp\left(-\frac{1}{2}|v_{j+1} - \Psi(v_j)|_{\Sigma}^2\right) \pi_j(v_j) dv_j.
 \end{aligned} \tag{7.4}$$

This defines the operator \mathcal{P} ; the prediction step is shown schematically in Figure 7.2. Note that \mathcal{P} is independent of step j because the Markov chain defined by the stochastic dynamics model is time-homogeneous. In the absence of data, the distribution of v_j simply evolves through repeated application of \mathcal{P} .

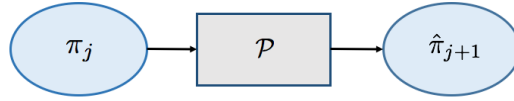


Figure 7.2 Prediction step.

Now we derive the likelihood map \mathcal{A}_j , which is sometimes called *analysis*. Note that the prediction step does not make use of the new observation y_{j+1} , which is assimilated in the analysis step through application of Bayes theorem, as follows:

$$\begin{aligned}
 \pi_{j+1}(v_{j+1}) &= \mathbb{P}(v_{j+1}|Y_{j+1}) \\
 &= \mathbb{P}(v_{j+1}|Y_j, y_{j+1}) \\
 &= \frac{\mathbb{P}(y_{j+1}|v_{j+1}, Y_j) \mathbb{P}(v_{j+1}|Y_j)}{\mathbb{P}(y_{j+1}|Y_j)} \\
 &= \frac{\mathbb{P}(y_{j+1}|v_{j+1}) \mathbb{P}(v_{j+1}|Y_j)}{\mathbb{P}(y_{j+1}|Y_j)} \\
 &= \frac{\exp(-\frac{1}{2}|y_{j+1} - h(v_{j+1})|_{\Gamma}^2) \hat{\pi}_{j+1}(v_{j+1})}{\int_{\mathbb{R}^d} \exp(-\frac{1}{2}|y_{j+1} - h(v_{j+1})|_{\Gamma}^2) \hat{\pi}_{j+1}(v_{j+1}) dv_{j+1}}.
 \end{aligned} \tag{7.5}$$

This defines the map \mathcal{A}_j through multiplication by the likelihood, and then normalization to a probability measure. The analysis update is shown schematically in Figure 7.3. It depends on j because the data y_{j+1} appears in the equation and this will change with each set of measurements.

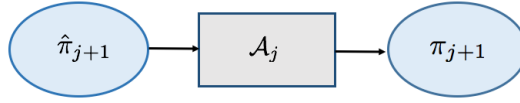


Figure 7.3 Update step.

7.3.2 Well-Posedness of the Filtering Problem

Now we establish the well-posedness of the filtering problem. We let

$$\pi_J = \mathbb{P}(v_J|Y), \quad \pi'_J = \mathbb{P}(v_J|Y')$$

be two filtering distributions arising from observed data $Y = Y_J$ and $Y' = Y'_J$. As noted in Remark 7.4, the filtering distribution at time J is the J -th marginal of the smoothing distribution; using this observation, the well-posedness of the filtering problem is a direct consequence of the well-posedness of the smoothing problem in the Hellinger distance. However, for the filtering problem this approach only gives well-posedness in the (weaker) total variation distance.

Corollary 7.7 (Well-posedness of Filtering). *Under Assumption 7.5, there exists $\kappa = \kappa(R)$ such that $d_{\text{TV}}(\pi_J, \pi'_J) \leq \kappa|Y - Y'|$.*

Proof. Let Π, Π' be the smoothing distributions $\Pi = \mathbb{P}(V|Y)$ and $\Pi' = \mathbb{P}(V|Y')$. We note that there exists κ such that $d_{\text{TV}}(\Pi, \Pi') \leq \kappa|Y - Y'|$ by Theorem 7.6 and by the fact that the Hellinger distance bounds the total variation distance (Lemma 1.9). Let $f : \mathbb{R}^d \rightarrow \mathbb{R}$ and $F : \mathbb{R}^{d(J+1)} \rightarrow \mathbb{R}$. Then

$$\begin{aligned} d_{\text{TV}}(\pi_J, \pi'_J) &= \frac{1}{2} \sup_{|f|_\infty \leq 1} \left| \mathbb{E}^{\pi_J}[f(v_J)] - \mathbb{E}^{\pi'_J}[f(v_J)] \right| \\ &= \frac{1}{2} \sup_{|f|_\infty \leq 1} \left| \mathbb{E}^\Pi[f(v_J)] - \mathbb{E}^{\Pi'}[f(v_J)] \right| \\ &\leq \frac{1}{2} \sup_{|F|_\infty \leq 1} \left| \mathbb{E}^\Pi[F(V)] - \mathbb{E}^{\Pi'}[F(V)] \right| \\ &= d_{\text{TV}}(\Pi, \Pi') \\ &\leq \kappa|Y - Y'|. \end{aligned}$$

Here the first inequality follows from the fact that $\{|f| \leq 1\}$ can be viewed as a subset of $\{|F| \leq 1\}$. \square

7.3.3 Roadmap to Discrete Filtering Methods

There are several filtering methods for performing the prediction and analysis steps. Some methods can be applied generally to nonlinear problems. However, others require a linear dynamics model ($\Psi(\cdot) = M\cdot$) and/or linear observations ($h(\cdot) = H\cdot$). Some of the methods provably approximate the filtering distributions, while some just estimate

Kalman Filter	$\Psi(\cdot) = M \cdot$	$h(\cdot) = H \cdot$	P	Chapter 8
3DVAR	General Ψ	$h(\cdot) = H \cdot$	S	Chapter 9
Extended Kalman Filter	General Ψ	$h(\cdot) = H \cdot$	S	Chapter 10
Ensemble Kalman Filter	General Ψ	$h(\cdot) = H \cdot$	S	Chapter 10
Bootstrap Particle Filter	General Ψ	General h	P	Chapter 11
Optimal Particle Filter	General Ψ	$h(\cdot) = H \cdot$	P	Chapter 12

Table 7.1 Summary of the filtering methods considered in the following chapters, along with the settings in which they will be presented.

the state using covariance information to weight the relative importance of predictions based on the dynamics model and on the data model.

The applicability of the methods that will be studied in the following chapters is summarized in Table 7.1, with respect to linearity/nonlinearity of the dynamics and the observation model. Furthermore **P** is used to denote methods which provably approximate the filtering distributions π_j in certain large particle limit; **S** denotes methods which only attempt to estimate the state using the data. Some of these constraints on the setting in which they apply can be relaxed, but the list above describes the methods as will be presented in these notes. Furthermore, extended and ensemble Kalman filters can accurately represent the filtering distributions in situations where approximate Gaussianity holds; this may be induced by small noise and/or by large data.

7.4 Discussion and Bibliography

The book [185] gives a mathematical introduction to data assimilation; for further information on the smoothing problem as presented here, see Section 2.3 in that book; for further information on the filtering problem as presented here, see Section 2.4. The books [2, 259, 15, 273, 17, 63, 95] and the review paper [258] give alternative foundational presentations of the subject. The books [164, 228, 203, 45] study data assimilation in the context of weather forecasting, oil reservoir simulation, turbulence modeling, and geophysical sciences, respectively.

In this chapter, we have assumed throughout that Σ , the model covariance, is positive definite. In applications, the stochastic dynamics model can be interpreted as arising from discretization of a stochastic differential equation governing the evolution of the state. Even if the underlying signal is governed by a deterministic map Ψ , the use of a *stochastic* dynamics model can help account for errors in the modeling of this deterministic map. However, the case where $\Sigma \equiv 0$ is also of interest as it corresponds to deterministic dynamics without model error. In this case we again define

$$\eta := \{\eta_1, \dots, \eta_J\}$$

and then define

$$G_0(v_0) := \left\{ h(\Psi^{(1)}(v_0)), h(\Psi^{(2)}(v_0)) \dots, h(\Psi^{(J)}(v_0)) \right\},$$

where $\Psi^{(j)}$ denotes Ψ composed with itself j times. Then the data model can be written in the form of the following inverse problem for the determination of the initial condition of the dynamical system:

$$Y = G_0(v_0) + \eta.$$

The Gaussian assumption $v_0 \sim \mathcal{N}(m_0, C_0)$ provides a prior model for a Bayesian formulation of this problem. We refer to the book chapter [126] for the derivation of the posterior distribution in other related settings, including dynamical systems defined by ordinary and stochastic differential equations with discrete and continuous observations.

To streamline the presentation, throughout Part II of these notes we assume to have access to maps Ψ and h , and covariance matrices C_0 , Σ , and Γ defining the dynamics and data models. In practice, however, models only reflect imperfectly the evolution of the system and the relationship between signal and data. For this reason, an important challenge in data assimilation is the identification and correction of model errors, and the estimation of model parameters, along with the state, from data. Several recent efforts that leverage machine learning to address model error in dynamical systems are reviewed in [191]. Relatedly, several recent frameworks are emerging to blend data assimilation with machine learning to obtain model corrections or surrogate models for the dynamics, including [55, 31, 34, 122, 177]. Some of these ideas will be discussed in Chapter 15 of these notes.

Chapter 8

The Linear-Gaussian Setting

Recall the stochastic dynamics and data models introduced in the previous chapter:

$$\begin{aligned} v_{j+1} &= \Psi(v_j) + \xi_j, & \xi_j &\sim \mathcal{N}(0, \Sigma) \text{ i.i.d.}, \\ y_{j+1} &= h(v_{j+1}) + \eta_{j+1}, & \eta_j &\sim \mathcal{N}(0, \Gamma) \text{ i.i.d.}, \end{aligned} \tag{8.1}$$

with $v_0 \sim \mathcal{N}(m_0, C_0)$, C_0, Σ and Γ positive definite and $v_0 \perp \{\xi_j\} \perp \{\eta_j\}$. Here we study the filtering and smoothing problems under the assumption that both the state-transition function $\Psi(\cdot)$ and the observation function $h(\cdot)$ are linear. Throughout, we will assume the following:

Assumption 8.1. *The stochastic dynamics and the data models defined by equation (8.1) hold with linear $\Psi(\cdot)$ and $h(\cdot)$:*

- *Linear dynamics:* $v_{j+1} = Mv_j + \xi_j$ for some $M \in \mathbb{R}^{d \times d}$.
- *Linear observation:* $y_{j+1} = Hv_{j+1} + \eta_{j+1}$ for some $H \in \mathbb{R}^{k \times d}$.

We will be mostly concerned with the case where $d > k$. Under the *linear-Gaussian* assumption, the filtering and smoothing distributions are Gaussian and therefore are fully characterized by their mean and covariance. We consider first the *Kalman filter* in Section 8.1, which gives explicit formulae for the iterative update of the mean and covariance of the filtering distribution, and then in Section 8.2 the *Kalman smoother*, which characterizes the smoothing distribution. Section 8.3 closes this chapter with bibliographical remarks. While the Kalman filter and the Kalman smoother only characterize the filtering and smoothing distributions in the linear-Gaussian setting, their importance extends beyond this setting, as will be demonstrated in the next two chapters.

8.1 Kalman Filter

The *filtering problem* is to estimate the state at time j given the data from the past up to the present time j . That is, we want to determine the pdf $\pi_j = \mathbb{P}(v_j | Y_j)$, where $Y_j := \{y_1, \dots, y_j\}$. We define $\hat{\pi}_{j+1} = \mathbb{P}(v_{j+1} | Y_j)$ and recall the evolution

$$\pi_{j+1} = \mathcal{A}_j \mathcal{P} \pi_j, \quad \pi_0 = \mathcal{N}(m_0, C_0),$$

which can be decomposed in terms of the prediction and analysis steps (7.3). Note that \mathcal{P} does not depend on j because the same Markov chain defined by the state dynamics governs each prediction step, whereas \mathcal{A}_j depends on j because at each step j the likelihood sees different data. The linear dynamics assumption implies that applying the operator \mathcal{P} to a Gaussian distribution gives again a Gaussian, and the linear observation assumption implies that applying the operator \mathcal{A}_j to a Gaussian gives again a Gaussian. Therefore we have the following:

Theorem 8.2 (Gaussianity of Filtering Distributions). *Under Assumption 8.1, π_0 , $\{\pi_{j+1}\}_{j \in \mathbb{Z}^+}$ and $\{\hat{\pi}_{j+1}\}_{j \in \mathbb{Z}^+}$ are all Gaussian distributions.*

As a consequence, the filtering distributions can be entirely characterized by their mean and covariance. We write

$$\begin{aligned}\hat{\pi}_{j+1} &= \mathbb{P}(v_{j+1}|Y_j) = \mathcal{N}(\hat{m}_{j+1}, \hat{C}_{j+1}), & (\text{prediction}) \\ \pi_{j+1} &= \mathbb{P}(v_{j+1}|Y_{j+1}) = \mathcal{N}(m_{j+1}, C_{j+1}), & (\text{analysis})\end{aligned}$$

and aim to find update formulae for these means and covariances. The Kalman filter achieves this.

Theorem 8.3 (Characterization of the Kalman Filter). *Suppose that Assumption 8.1 holds. Then, for all $j \in \mathbb{Z}^+$, C_j is positive definite and*

$$\hat{m}_{j+1} = Mm_j, \quad (8.2a)$$

$$\hat{C}_{j+1} = MC_jM^\top + \Sigma, \quad (8.2b)$$

$$C_{j+1}^{-1} = (MC_jM^\top + \Sigma)^{-1} + H^\top \Gamma^{-1} H, \quad (8.2c)$$

$$C_{j+1}^{-1}m_{j+1} = (MC_jM^\top + \Sigma)^{-1}Mm_j + H^\top \Gamma^{-1}y_{j+1}. \quad (8.2d)$$

Proof. The proof proceeds by breaking the Kalman filter step above into the prediction and the analysis steps. We first derive the update formulae, assuming that C_j and \hat{C}_{j+1} are positive definite; we conclude with an inductive proof that this is indeed the case.

Prediction: The mean and variance of the prediction step may be calculated as follows. The mean is given by:

$$\begin{aligned}\hat{m}_{j+1} &= \mathbb{E}[v_{j+1}|Y_j] \\ &= \mathbb{E}[Mv_j + \xi_j|Y_j] \\ &= M\mathbb{E}[v_j|Y_j] + \mathbb{E}[\xi_j|Y_j] \\ &= Mm_j,\end{aligned}$$

where we used that ξ_j and Y_j are independent. The covariance is given by

$$\begin{aligned}\hat{C}_{j+1} &= \mathbb{E}[(v_{j+1} - \hat{m}_{j+1}) \otimes (v_{j+1} - \hat{m}_{j+1})|Y_j] \\ &= \mathbb{E}[M(v_j - m_j) \otimes M(v_j - m_j)|Y_j] + \mathbb{E}[\xi_j \otimes \xi_j|Y_j] \\ &\quad + \mathbb{E}[\xi_j \otimes M(v_j - m_j)|Y_j] + \mathbb{E}[M(v_j - m_j) \otimes \xi_j|Y_j] \\ &= M\mathbb{E}[(v_j - m_j) \otimes (v_j - m_j)|Y_j]M^\top + \Sigma \\ &= MC_jM^\top + \Sigma,\end{aligned}$$

where we used that ξ_j and v_j are independent. Thus in the linear-Gaussian setting the prediction operator \mathcal{P} from $\pi_j = \mathcal{N}(m_j, C_j)$ to $\hat{\pi}_{j+1} = \mathcal{N}(\hat{m}_{j+1}, \hat{C}_{j+1})$ is given by

$$\begin{aligned}\hat{m}_{j+1} &= Mm_j, \\ \hat{C}_{j+1} &= MC_jM^\top + \Sigma.\end{aligned}$$

Analysis: The analysis step may be derived as follows, using Bayes Theorem 1.2:

$$\begin{aligned}\mathbb{P}(v_{j+1}|Y_{j+1}) &= \mathbb{P}(v_{j+1}|y_{j+1}, Y_j) \\ &\propto \mathbb{P}(y_{j+1}|v_{j+1}, Y_j) \mathbb{P}(v_{j+1}|Y_j) \\ &= \mathbb{P}(y_{j+1}|v_{j+1}) \mathbb{P}(v_{j+1}|Y_j).\end{aligned}$$

This gives

$$\begin{aligned}\mathbb{P}(v_{j+1}|Y_{j+1}) &\propto \exp\left(-\frac{1}{2}|v_{j+1} - m_{j+1}|_{\hat{C}_{j+1}}^2\right) \\ &\propto \exp\left(-\frac{1}{2}|y_{j+1} - Hv_{j+1}|_\Gamma^2\right) \exp\left(-\frac{1}{2}|v_{j+1} - \hat{m}_{j+1}|_{\hat{C}_{j+1}}^2\right) \\ &= \exp\left(-\frac{1}{2}|y_{j+1} - Hv_{j+1}|_\Gamma^2 - \frac{1}{2}|v_{j+1} - \hat{m}_{j+1}|_{\hat{C}_{j+1}}^2\right).\end{aligned}\tag{8.3}$$

Taking logarithms and matching quadratic and linear terms in v_{j+1} from either side of this identity gives the update operator \mathcal{A}_j from $\hat{\pi}_{j+1} = \mathcal{N}(\hat{m}_{j+1}, \hat{C}_{j+1})$ to $\pi_{j+1} = \mathcal{N}(m_{j+1}, C_{j+1})$:

$$\begin{aligned}C_{j+1}^{-1} &= \hat{C}_{j+1}^{-1} + H^\top \Gamma^{-1} H, \\ C_{j+1}^{-1} m_{j+1} &= \hat{C}_{j+1}^{-1} \hat{m}_{j+1} + H^\top \Gamma^{-1} y_{j+1}.\end{aligned}$$

Combining the prediction operator \mathcal{P} and update operator \mathcal{A}_j yields the desired update formulae.

Positive-definiteness: It remains to show that $C_j > 0$ for all $j \in \mathbb{Z}^+$. We will use induction. By assumption the result holds true for $j = 0$. Assume that it is true for C_j . For the prediction operator \mathcal{P} we have, for $u \neq 0$,

$$\begin{aligned}\langle u, \hat{C}_{j+1} u \rangle &= \langle u, MC_j M^\top u \rangle + \langle u, \Sigma u \rangle \\ &= \langle M^\top u, C_j M^\top u \rangle + \langle u, \Sigma u \rangle \\ &\geq \langle u, \Sigma u \rangle \\ &> 0,\end{aligned}$$

where we used that $C_j > 0$ and $\Sigma > 0$. Therefore $\hat{C}_{j+1}, \hat{C}_{j+1}^{-1} > 0$. Then for the update operator \mathcal{A}_j :

$$\begin{aligned}\langle u, C_{j+1}^{-1} u \rangle &= \langle u, \hat{C}_{j+1}^{-1} u \rangle + \langle u, H^\top \Gamma^{-1} H u \rangle \\ &= \langle u, \hat{C}_{j+1}^{-1} u \rangle + \langle H u, \Gamma^{-1} H u \rangle \\ &\geq \langle u, \hat{C}_{j+1}^{-1} u \rangle \\ &> 0,\end{aligned}$$

where we used that $\Gamma > 0$. Therefore, $C_{j+1}, C_{j+1}^{-1} > 0$, which concludes the proof. \square

Remark 8.4. The previous proof reveals two interesting facts about the structure of the Kalman filter updates. The first is that the covariance update does not involve the observed data; this can be thought of as a consequence of the fact that the posterior covariance in the linear-Gaussian setting for inverse problems does not depend on the observed data, as noted in Chapter 2. The second is that the update formulae for the covariance are linear in the prediction step, but nonlinear in the analysis step; specifically the analysis step is linear in the precisions (inverse covariances). \diamond

8.1.1 Kalman Filter: Algorithmic Implementation

We now rewrite the Kalman filter in an alternative form, which can be advantageous for algorithmic implementation. This formulation is summarized in Algorithm 8.1 below and it is written in terms of covariance matrices instead of precision matrices.

Algorithm 8.1 Kalman Filter Algorithm

- 1: **Input:** Initial distribution $\pi_0 = \mathcal{N}(m_0, C_0)$ with $m_0 \in \mathbb{R}^d$, $C_0 \in \mathbb{R}^{d \times d}$.
- 2: For $j = 0, 1, \dots, J - 1$ do the following prediction and analysis steps:
- 3: **Prediction:**

$$\hat{m}_{j+1} = Mm_j, \quad (8.4)$$

$$\hat{C}_{j+1} = MC_jM^\top + \Sigma, \quad (8.5)$$

- 4: **Analysis:**

$$\begin{aligned} m_{j+1} &= \hat{m}_{j+1} + K_{j+1}d_{j+1}, \\ C_{j+1} &= (I - K_{j+1}H)\hat{C}_{j+1}, \end{aligned} \quad (8.6)$$

where

$$\begin{aligned} d_{j+1} &= y_{j+1} - H\hat{m}_{j+1}, \\ S_{j+1} &= H\hat{C}_{j+1}H^\top + \Gamma, \\ K_{j+1} &= \hat{C}_{j+1}H^\top S_{j+1}^{-1}. \end{aligned} \quad (8.7)$$

- 5: **Output:** Predicted distributions $\hat{\pi}_{j+1} = \mathcal{N}(\hat{m}_{j+1}, \hat{C}_{j+1})$ and filtering distributions $\pi_{j+1} = \mathcal{N}(m_{j+1}, C_{j+1})$, $j = 0, 1, \dots, J - 1$.
-

Importantly, the formulation in Theorem 8.3 involves a matrix inversion in the state-space \mathbb{R}^d while the one given in Algorithm 8.1 requires only inversion in the data space \mathbb{R}^k to compute S_{j+1}^{-1} . In many applications the observation space dimension is much smaller than the state-space dimension ($k \ll d$), and then the formulation given in this section is much cheaper to compute than the one given in Theorem 8.3.

The vector d_{j+1} is known as the *innovation* and the matrix K_{j+1} as the *Kalman gain*. Note that d_{j+1} measures the mismatch of the predicted state from the given data.

Combining the form of d_{j+1} and \hat{m}_{j+1} shows that the update formula for the Kalman mean can be written as

$$m_{j+1} = (I - K_{j+1}H)\hat{m}_{j+1} + K_{j+1}y_{j+1}, \quad \hat{m}_{j+1} = Mm_j. \quad (8.8)$$

This update formula has the very natural interpretation that the mean update is formed as a linear combination of the evolution of the noise-free dynamics and of the data. Equations (8.6) and (8.8) show that the Kalman gain K_{j+1} determines the weight given to the new observation y_{j+1} in the state estimation. The update formula (8.8) may be also derived from an optimization perspective, the topic of the next subsection.

The fact that the analysis update given by Algorithm 8.1 agrees with the one derived in Theorem 8.3 can be established using the following lemma:

Lemma 8.5 (Woodbury Matrix Identity). *Let $A \in \mathbb{R}^{p \times p}$, $U \in \mathbb{R}^{p \times q}$, $B \in \mathbb{R}^{q \times q}$, $V \in \mathbb{R}^{q \times p}$. If $A, B > 0$, then $A + UBV$ is invertible and*

$$(A + UBV)^{-1} = A^{-1} - A^{-1}U(B^{-1} + VA^{-1}U)^{-1}VA^{-1}.$$

Now, to see the agreement between the characterization in terms of precision matrices in Theorem 8.3 and the covariance characterization in (8.6) and (8.7), note that Lemma 8.5 applied to (8.2c) gives

$$\begin{aligned} C_{j+1} &= \hat{C}_{j+1} - \hat{C}_{j+1}H^\top(\Gamma + H\hat{C}_{j+1}H^\top)^{-1}H\hat{C}_{j+1} \\ &= \left(I - \hat{C}_{j+1}H^\top(\Gamma + H\hat{C}_{j+1}H^\top)^{-1}H\right)\hat{C}_{j+1} \\ &= (I - \hat{C}_{j+1}H^\top S_{j+1}^{-1}H)\hat{C}_{j+1} \\ &= (I - K_{j+1}H)\hat{C}_{j+1}, \end{aligned}$$

as desired.

8.1.2 Optimization Perspective: Mean of Kalman Filter

Since π_{j+1} is Gaussian, its mean agrees with its mode. Thus, formulae (8.3) implies that

$$\begin{aligned} m_{j+1} &= \operatorname{argmax}_v \pi_{j+1}(v) \\ &= \operatorname{argmin}_v J(v), \end{aligned}$$

where

$$J(v) := \frac{1}{2}|y_{j+1} - Hv|_\Gamma^2 + \frac{1}{2}|v - \hat{m}_{j+1}|_{\hat{C}_{j+1}}^2.$$

In other words, m_{j+1} is chosen to fit both the observed data y_{j+1} and the predictions \hat{m}_{j+1} as well as possible. The covariances Γ and \hat{C}_{j+1} determine the relative weighting between the two quadratic terms. The solution of the minimization problem is given by (8.8), as may be verified by direct differentiation of J .

An alternative derivation which is helpful in more sophisticated contexts is to cast the problem in terms of constrained minimization. Write $v' = v - \hat{m}_{j+1}$, $y' = y_{j+1} - H\hat{m}_{j+1}$ and $C' = \hat{C}_{j+1}$. Then minimization of J may be reformulated as

$$m_{j+1} = \hat{m}_{j+1} + \operatorname{argmin}_{v'} \left(\frac{1}{2} |y' - Hv'|_{\Gamma}^2 + \frac{1}{2} \langle v', b \rangle \right),$$

where the minimization is now subject to the constraint $C'b = v'$. Using Lagrange multipliers we write

$$l(v') = \frac{1}{2} |y' - Hv'|_{\Gamma}^2 + \frac{1}{2} \langle v', b \rangle + \langle \lambda, C'b - v' \rangle; \quad (8.9)$$

computing the derivative and setting to zero gives

$$\begin{aligned} -H^{\top} \Gamma^{-1} (y' - Hv') + \frac{1}{2} b - \lambda &= 0, \\ \frac{1}{2} v' + C' \lambda &= 0, \\ v' - C' b &= 0. \end{aligned}$$

The last two equations imply that $C'(2\lambda + b) = 0$. Thus we set $\lambda = -\frac{1}{2}b$ and drop the second equation, replacing the first by

$$-H^{\top} \Gamma^{-1} (y' - HC'b) + b = 0.$$

Solving for b gives

$$\begin{aligned} v &= \hat{m}_{j+1} + v' \\ &= \hat{m}_{j+1} + C'b \\ &= \hat{m}_{j+1} + C'(H^{\top} \Gamma^{-1} HC' + I)^{-1} H^{\top} \Gamma^{-1} y' \\ &= \hat{m}_{j+1} + C'(H^{\top} \Gamma^{-1} HC' + I)^{-1} H^{\top} \Gamma^{-1} (y_{j+1} - H\hat{m}_{j+1}) \\ &= (I - K_{j+1}H) \hat{m}_{j+1} + K_{j+1} y_{j+1}, \end{aligned}$$

where we have defined

$$K_{j+1} = C'(H^{\top} \Gamma^{-1} HC' + I)^{-1} H^{\top} \Gamma^{-1}.$$

It remains to show that K_{j+1} agrees with the definition given in (8.7). To see this we note that if we choose S to be any matrix satisfying $K_{j+1} = C'H^{\top}S^{-1}$, then

$$H^{\top} S^{-1} = (H^{\top} \Gamma^{-1} HC' + I)^{-1} H^{\top} \Gamma^{-1}$$

so that

$$(H^{\top} \Gamma^{-1} HC' + I) H^{\top} = H^{\top} \Gamma^{-1} S.$$

Thus

$$H^{\top} \Gamma^{-1} HC' H^{\top} + H^{\top} = H^{\top} \Gamma^{-1} S$$

which may be achieved by choosing any S so that

$$\Gamma^{-1} (HC' H^{\top} + \Gamma) = \Gamma^{-1} S$$

and multiplication by Γ gives the desired formula for S .

8.1.3 Optimality of Kalman Filter

The following theorem states that the Kalman filter gives the best estimator of the mean in an online setting. In the following, \mathbb{E} denotes expectation with respect to all randomness present in the problem statement, through the initial condition, the noisy dynamical evolution, and the noisy data. Furthermore $\mathbb{E}[\cdot | Y_j]$ denotes conditional expectation, given the data Y_j up to time j .

Theorem 8.6 (Optimality of Kalman Filter). *Let $\{m_j\}$ be the sequence computed using the Kalman filter, and $\{z_j\}$ be any sequence in \mathbb{R}^d such that z_j is Y_j measurable.¹ Then, for all $j \in \mathbb{N}$,*

$$\mathbb{E} \left[|v_j - m_j|^2 \mid Y_j \right] \leq \mathbb{E} \left[|v_j - z_j|^2 \mid Y_j \right].$$

Proof. Note that m_j and z_j are fixed and non-random, given Y_j . Thus we have:

$$\begin{aligned} \mathbb{E} \left[|v_j - z_j|^2 \mid Y_j \right] &= \mathbb{E} \left[|v_j - m_j + m_j - z_j|^2 \mid Y_j \right] \\ &= \mathbb{E} \left[|v_j - m_j|^2 + 2 \langle v_j - m_j, m_j - z_j \rangle + |m_j - z_j|^2 \mid Y_j \right] \\ &= \mathbb{E} \left[|v_j - m_j|^2 \mid Y_j \right] + 2 \langle \mathbb{E} [v_j - m_j \mid Y_j], m_j - z_j \rangle + |m_j - z_j|^2 \\ &= \mathbb{E} \left[|v_j - m_j|^2 \mid Y_j \right] + 2 \langle \mathbb{E} [v_j \mid Y_j] - m_j, m_j - z_j \rangle + |m_j - z_j|^2 \\ &= \mathbb{E} \left[|v_j - m_j|^2 \mid Y_j \right] + 0 + |m_j - z_j|^2 \\ &\geq \mathbb{E} \left[|v_j - m_j|^2 \mid Y_j \right]. \end{aligned}$$

The fifth step follows since $m_j = \mathbb{E} [v_j \mid Y_j]$. □

8.2 Kalman Smoother

We next discuss the Kalman smoother, which refers to the smoothing problem in the linear-Gaussian setting of Assumption 8.1. As with the Kalman filter, it is possible to solve the problem explicitly because the smoothing distribution is itself a Gaussian. The explicit formulae computed help to build intuition about the smoothing distribution more generally. We recall Remark 7.4, which implies that the filtering distribution at time $j = J$ determines the marginal of the Kalman smoother on its last coordinate. However, the filtering distributions do not determine the Kalman smoother in its entirety.

8.2.1 Defining Linear System

Let $V = \{v_0, \dots, v_J\}$ and $Y = \{y_1, \dots, y_J\}$. Using Bayes Theorem 1.2 and the fact that $\{\xi_j\}$, $\{\eta_j\}$ are mutually independent i.i.d. sequences, independent of v_0 , we have

$$\mathbb{P}(V|Y) \propto \mathbb{P}(Y|V) \mathbb{P}(V) = \prod_{j=1}^J \mathbb{P}(y_j|v_j) \times \prod_{j=0}^{J-1} \mathbb{P}(v_{j+1}|v_j) \times \mathbb{P}(v_0).$$

¹For practical purposes, this means z_j is a fixed non-random function of given observed Y_j .

Noting that

$$v_{j+1}|v_j \sim \mathcal{N}(Mv_j, \Sigma), \quad y_j|v_j \sim \mathcal{N}(Hv_j, \Gamma)$$

the smoothing distribution can be expressed as

$$\mathbb{P}(V|Y) \propto \exp(-J(V)), \quad (8.11)$$

where

$$J(V) := \frac{1}{2}|v_0 - m_0|_{C_0}^2 + \frac{1}{2} \sum_{j=0}^{J-1} |v_{j+1} - Mv_j|_{\Sigma}^2 + \frac{1}{2} \sum_{j=0}^{J-1} |y_{j+1} - Hv_{j+1}|_{\Gamma}^2. \quad (8.12)$$

Theorem 8.7 (Characterization of the Kalman Smoother). *Suppose that Assumption 8.1 holds. Then $\mathbb{P}(V|Y)$ is Gaussian with a block tridiagonal precision matrix $\Omega > 0$ and mean m solving $\Omega m = r$, where*

$$\Omega = \begin{bmatrix} \Omega_{0,0} & \Omega_{0,1} & & & & & \\ \Omega_{1,0} & \Omega_{1,1} & \dots & & & 0 & \\ 0 & \dots & \dots & & & & \\ & 0 & \dots & \dots & \dots & & \\ & & & \dots & \Omega_{J-1,J-1} & \Omega_{J-1,J} & \\ & & & & \Omega_{J,J-1} & \Omega_{J,J} & \end{bmatrix} \quad (8.13)$$

with

$$\begin{aligned} \Omega_{0,0} &= C_0^{-1} + M^\top \Sigma^{-1} M, \\ \Omega_{j,j} &= \Sigma^{-1} + M^\top \Sigma^{-1} M + H^\top \Gamma^{-1} H, \quad 1 \leq j \leq J-1, \\ \Omega_{J,J} &= \Sigma^{-1} + H^\top \Gamma^{-1} H, \\ \Omega_{j,j+1} &= -\Sigma^{-1} M, \quad 0 \leq j \leq J-1, \\ r_0 &= C_0^{-1} m_0, \\ r_j &= H^\top \Gamma^{-1} y_j, \quad 1 \leq j \leq J. \end{aligned}$$

Proof. We may write $J(V) = \frac{1}{2}|\Omega^{1/2}(V - m)|^2 + q$ with q independent of V , by definition. Note that Ω is then the Hessian of $J(V)$, and differentiating in equation (8.12) we obtain that

$$\begin{aligned} \Omega_{0,0} &= \partial_{v_0}^2 J(V) = C_0^{-1} + M^\top \Sigma^{-1} M, \\ \Omega_{j,j} &= \partial_{v_j}^2 J(V) = \Sigma^{-1} + M^\top \Sigma^{-1} M + H^\top \Gamma^{-1} H, \\ \Omega_{J,J} &= \partial_{v_J}^2 J(V) = \Sigma^{-1} + H^\top \Gamma^{-1} H, \\ \Omega_{j-1,j} &= \partial_{v_{j-1}, v_j}^2 J(V) = -\Sigma^{-1} M. \end{aligned}$$

Otherwise, for all other values of indices $\{k, l\}$, $\Omega_{k,l} = 0$. This proves that the matrix Ω has a block tridiagonal structure.

Now we focus on finding m . We have that $\nabla_V J(V) = \Omega(V - m)$, so that $-\nabla_V J(V)|_{V=0} = \Omega m$. Thus, we find r as

$$\begin{aligned} r_0 &= -\nabla_{v_0} J(V)|_{V=0} = -(-C_0^{-1}m_0) = C_0^{-1}m_0, \\ r_j &= -\nabla_{v_j} J(V)|_{V=0} = -(-H^\top \Gamma^{-1}y_j) = H^\top \Gamma^{-1}y_j. \end{aligned}$$

We have shown that Ω is symmetric and that $\Omega \geq 0$; to prove that Ω is a precision matrix, we need to show that $\Omega > 0$. Take, for the sake of argument, $Y = 0$ and $m_0 = 0$ in equation (8.12), so that every term in the expansion of $J(V)$ involves V . It is evident that in such case $J(V) = V^\top \Omega V$. Suppose that $V^\top \Omega V = 0$ for some nonzero V . Then by positive-definiteness of C_0 , Σ , and Γ , it must be that $v_0 = 0$ and $v_{j+1} = Mv_j$ for $j = 0, 1, \dots, J$. Thus we must have $V = 0$. This proves that Ω is positive definite. \square

Remark 8.8. Since the smoothing distribution in the linear-Gaussian setting is itself Gaussian, its mean agrees with its mode. Therefore, the posterior mean found above is the unique minimizer of $J(V)$, that is, the MAP estimator. \diamond

8.2.2 Kalman Smoother: Solution of the Linear System

The mean of the Kalman smoother may be obtained by Gaussian elimination, as summarized in the following algorithm.

Algorithm 8.2 Kalman Smoother by Gaussian Elimination

- 1: **Input:** Initial distribution $\pi_0 = \mathcal{N}(m_0, C_0)$ with $m_0 \in \mathbb{R}^d$, $C_0 \in \mathbb{R}^{d \times d}$.
- 2: **Row reduction:** Define a matrix sequence $\{\Omega_j\}$:

$$\begin{aligned} \Omega_0 &= \Omega_{0,0}, \\ \Omega_{j+1} &= \Omega_{j+1,j+1} - M^\top \Sigma^{-1} \Omega_j^{-1} \Sigma^{-1} M, \quad j = 0, \dots, J-1; \end{aligned} \quad (8.14)$$

and vector sequence $\{z_j\}$:

$$\begin{aligned} z_0 &= C_0^{-1}m_0, \\ z_{j+1} &= H^\top \Gamma^{-1}y_{j+1} - M^\top \Sigma^{-1} \Omega_j^{-1} z_j. \end{aligned}$$

- 3: **Back-substitution:** Read off m_J by solving the equation $\Omega_J m_J = z_J$. Perform back-substitution to obtain

$$\Omega_j m_j = z_j - \Omega_{j,j+1} m_{j+1}, \quad j = J-1, \dots, 1.$$

- 4: **Output:** Mean $m = \{m_j\}_{j=0}^J$ of the Kalman smoother.
-

Note that m_J found this way coincides with the mean of the Kalman filter at $j = J$. The rest of this chapter is devoted to proving the following proposition:

Proposition 8.9. *The matrices $\{\Omega_j\}$ in (8.14) are positive definite.*

Proof. The proof of this theorem relies on the following two lemmas:

Lemma 8.10. *If*

$$X := \begin{bmatrix} X_1 & \times & \times & \times \\ \times & X_2 & \times & \times \\ \times & \times & \dots & \times \\ \times & \times & \times & X_d \end{bmatrix}$$

is positive definite, then X_i is positive definite for all $i \in \{1, \dots, d\}$.

Lemma 8.11. *Let B be a block lower (or upper) triangular matrix with identity on the diagonal. Then B is an invertible matrix.*

Using Lemma 8.10, we deduce that $\Omega_0 = \Omega_{0,0}$ is positive definite. Consider the matrix $B \in \mathbb{R}^{d(J+1) \times d(J+1)}$ defined as

$$B = \begin{bmatrix} I & 0 & 0 \\ -\Omega_{1,0}\Omega_0^{-1} & I & \dots \\ 0 & \dots & 0 & I \end{bmatrix}.$$

We compute

$$B\Omega B^\top = \begin{bmatrix} \Omega_0 & 0 & & 0 \\ 0 & \Omega_1 & \Omega_{1,2} & \dots & 0 \\ & \Omega_{2,1} & \Omega_{2,2} & \dots & \\ 0 & & & \Omega_{J-1,J-1} & \Omega_{J-1,J} \\ 0 & & & \Omega_{J,J-1} & \Omega_{J,J} \end{bmatrix}.$$

By Lemma 8.10, the matrix

$$\tilde{\Omega} = \begin{bmatrix} \Omega_1 & \Omega_{1,2} & \dots & 0 \\ \Omega_{2,1} & \Omega_{2,2} & \dots & \\ & & \Omega_{J-1,J-1} & \Omega_{J-1,J} \\ & & \Omega_{J,J-1} & \Omega_{J,J} \end{bmatrix}$$

is positive definite, and so is Ω_0 .

Lemma 8.10 and the positive-definiteness of $\tilde{\Omega}$ imply that Ω_1 is positive definite. Therefore, by Lemma 8.11 the matrix

$$B_2 = \begin{bmatrix} I & 0 & 0 \\ -\Omega_{2,1}\Omega_1^{-1} & I & \dots \\ & \dots & 0 & I \\ 0 & & & \end{bmatrix}$$

is invertible. Thus we have

$$B_2 \tilde{\Omega} B_2^\top = \begin{bmatrix} \Omega_1 & 0 & & & 0 \\ 0 & \Omega_2 & \Omega_{2,3} & \dots & \\ & \Omega_{3,2} & \Omega_{3,3} & & 0 \\ & & & \Omega_{J-1,J-1} & \Omega_{J-1,J} \\ 0 & & & \Omega_{J,J-1} & \Omega_{J,J} \end{bmatrix},$$

giving the positive-definiteness of Ω_2 . Iterating the argument shows that all the Ω_j are positive definite. \square

8.3 Discussion and Bibliography

The original paper of Kalman [162] is arguably the first systematic presentation of a methodology to combine models with data. The continuous time analogue of that work may be found in [163]. We refer to [254, 110, 10, 185, 259, 15, 273] for further background on the linear-Gaussian setting and for alternative derivations and expressions of the Kalman update formulae. Kalman filters and smoothers are the cornerstones of numerous data assimilation algorithms for filtering and smoothing, some of which will be studied in the next two chapters. The book [135] overviews the subject in the context of time-series analysis and economics. The optimality of the Kalman filter is described in [10]. The paper [269] contains an application of the optimality property of the Kalman filter (which applies beyond the linear-Gaussian setting to the mean of the filtering distribution in quite general settings). A link between the standard implementation of the Kalman smoother and Gauss-Newton methods for MAP estimation is made in [21]. For further details on the Kalman smoother, in both discrete and continuous time, see [185] and [127]. We refer to [177] for a machine learning approach to learn linear (and nonlinear) dynamics and data models using deep learning.

Chapter 9

Optimization for Filtering and Smoothing: 3DVAR and 4DVAR

This chapter demonstrates the use of optimization, namely the 3DVAR and 4DVAR methodologies, to obtain information from the filtering and smoothing distributions. We emphasize that the methods we present in this chapter do not provide approximations of the filtering and smoothing distributions; they simply provide estimates of the signal, given data, in the filtering (on-line) and smoothing (off-line) data scenarios. Their relationship to the filtering and smoothing distributions is analogous to the relationship of MAP estimation to the full Bayesian posterior distribution. In the previous chapter we showed how the mean of the Kalman filter could be derived through an optimization principle, once the predictive covariance is known; this idea is generalized to nonlinear forward models to obtain 3DVAR. On the other hand, 4DVAR is defined directly as a MAP estimator.

Here “VAR” refers to variational, and encodes the concept of optimization. The 3D and 4D, respectively, refer to three Euclidean spatial dimensions and to three Euclidean spatial dimensions plus a time dimension; this nomenclature reflects the historical derivation of these problems in the geophysical sciences, but the specific structure of fields over three-dimensional Euclidean space plays no role in the generalized form of the methods described here. The key distinction is that 3DVAR solves a sequence of optimization problems at each point in time (hence is an on-line filtering method); in contrast, 4DVAR solves an optimization problem which involves data distributed over time (and is an off-line smoothing method).

This chapter is organized as follows. We introduce the problem setting in Section 9.1. 3DVAR and 4DVAR are considered, in turn, in Sections 9.2 and 9.3. Section 9.4 closes with extensions and bibliographical remarks.

9.1 The Setting

3DVAR borrows from the Kalman filter optimization principle outlined in Subsection 8.1.2, but substitutes a fixed given covariance for the predictive covariance. Throughout we consider the setting, commonly occurring in applications, in which the dynamics model is nonlinear, but the observation function is linear. We thus have a discrete-time

Kalman Filter	3DVAR
$m_{j+1} = \arg \min_v J(v)$	$m_{j+1} = \arg \min_v J(v)$
$J(v) = \frac{1}{2} y_{j+1} - Hv _\Gamma^2 + \frac{1}{2} v - \hat{m}_{j+1} _{\hat{C}_{j+1}}^2$	$J(v) = \frac{1}{2} y_{j+1} - Hv _\Gamma^2 + \frac{1}{2} v - \hat{m}_{j+1} _{\hat{C}}^2$
$\hat{m}_{j+1} = Mm_j$	$\hat{m}_{j+1} = \Psi(m_j)$
$m_{j+1} = (I - K_{j+1}H)\hat{m}_{j+1} + K_{j+1}y_{j+1}$	$m_{j+1} = (I - KH)\hat{m}_{j+1} + Ky_{j+1}$

Table 9.1 Comparison of Kalman filter and 3DVAR update formulae.

dynamical system with noisy state transitions and noisy observations given by

Stochastic Dynamics Model: $v_{j+1} = \Psi(v_j) + \xi_j, \quad j \in \mathbb{Z}^+.$

Data Model: $y_{j+1} = Hv_{j+1} + \eta_{j+1}, \quad j \in \mathbb{Z}^+, \text{ for some } H \in \mathbb{R}^{k \times d}.$

Probabilistic Structure: $v_0 \sim \mathcal{N}(m_0, C_0), \quad \xi_j \sim \mathcal{N}(0, \Sigma), \quad \eta_j \sim \mathcal{N}(0, \Gamma).$

Probabilistic Structure: $v_0 \perp \{\xi_j\} \perp \{\eta_j\}$ independent.

9.2 3DVAR

We introduce 3DVAR by analogy with the update formula (8.8) for the Kalman filter, and its derivation through optimization from Subsection 8.1.2. The primary differences between 3DVAR and the Kalman filter mean update are that $\Psi(\cdot)$ can be nonlinear for 3DVAR, and that for 3DVAR we have no closed update formula for the covariances. To deal with this second issue 3DVAR uses a fixed predicted covariance, independent of time j , and pre-specified. The resulting minimization problem, and its solution, is described in Table 9.1, making the analogy with the Kalman filter.

Note that the minimization itself is of a quadratic functional, and so may be solved by means of linear algebra. The constraint formulation used for the Kalman filter, in Subsection 8.1.2, may also be applied and used to derive the mean update formula.

9.2.1 3DVAR: Algorithmic Implementation

The 3DVAR filtering method is fully described in the following algorithm.

Algorithm 9.1 3DVAR

- 1: **Input:** Initial mean $m_0 \in \mathbb{R}^d$ and fixed predictive covariance $\hat{C} \in \mathbb{R}^{d \times d}$.
- 2: For $j = 0, 1, \dots, J - 1$ do the following prediction and analysis steps:
- 3: **Prediction:**

$$\hat{m}_{j+1} = \Psi(m_j). \quad (9.1)$$

- 4: **Analysis:**

$$m_{j+1} = (I - KH)\hat{m}_{j+1} + Ky_{j+1}. \quad (9.2)$$

- 5: **Output:** Estimates $\{m_j\}_{j=1}^J$ of the signal.
-

The Kalman gain K for 3DVAR is fixed, because the predicted covariance \hat{C} is fixed. Precisely we have, by analogy with the Kalman filter, the following formulae for the 3DVAR gain matrix K :

$$\begin{aligned} S &= H\hat{C}H^\top + \Gamma, \\ K &= \hat{C}H^\top S^{-1}. \end{aligned}$$

The method also delivers an implied analysis covariance $C = (I - KH)\hat{C}$. Note that the resulting algorithm which maps m_j to m_{j+1} may be specified directly in terms of the gain K , without need to introduce \hat{C} , C , and S . In the remainder of this section we simply view K as fixed and given. In this setting we show that the 3DVAR algorithm produces accurate state estimation under vanishing noise assumptions in the dynamics/data model.

9.2.2 3DVAR: Long-Time Accuracy

We will make the following assumptions on the dynamics/data model:

Assumption 9.1. *Consider the dynamics/data model under the assumptions that $\xi_j \equiv 0$, $\Gamma = \gamma^2 \Gamma_0$, $|\Gamma_0| = 1$ and assume that the data y_{j+1} used in the 3DVAR algorithm is found from observing a true signal v_j^\dagger given by*

$$\begin{aligned} \text{Dynamics Model: } v_{j+1}^\dagger &= \Psi(v_j^\dagger), \quad j \in \mathbb{Z}^+. \\ \text{Data Model: } y_{j+1} &= Hv_{j+1}^\dagger + \gamma\eta_{j+1,0}^\dagger, \quad j \in \mathbb{Z}^+. \end{aligned}$$

With this assumption of noise-free dynamics ($\xi_j \equiv 0$) we deduce that the 3DVAR filter produces output which, asymptotically, has an error of the same size as the observational noise error γ . The key additional assumption in the theorem that allows this deduction is a relationship between the Kalman gain K and the derivative $D\Psi(\cdot)$

of the dynamics model. Encoded in the assumption are two ingredients: that the observation function H is rich enough in principle to learn enough components of the system to synchronize the whole system; and that K is designed cleverly enough to effect this synchronization. The proof of the theorem is simply using these two ingredients and then controlling the small stochastic perturbations, arising from noisy observations in Assumption 9.1.

Theorem 9.2 (Accuracy of 3DVAR). *Let Assumption 9.1 hold with $\eta_{j,0}^\dagger \sim \mathcal{N}(0, \Gamma_0)$ an i.i.d. sequence. Assume that, for the gain matrix K appearing in the 3DVAR method, there exists a norm $\|\cdot\|$ on \mathbb{R}^d and constant $\lambda \in (0, 1)$ such that, for all $v \in \mathbb{R}^d$,*

$$\|(I - KH)D\Psi(v)\| \leq \lambda.$$

Then, there is a constant $c > 0$ such that the 3DVAR algorithm satisfies the following large-time asymptotic error bound:

$$\limsup_{j \rightarrow \infty} \mathbb{E}[\|m_j - v_j^\dagger\|] \leq \frac{c\gamma}{1 - \lambda},$$

where the expectation is taken with respect to the sequence $\{\eta_{j,0}^\dagger\}$.

Proof. We have

$$\begin{aligned} v_{j+1}^\dagger &= \Psi(v_j^\dagger), \\ m_{j+1} &= (I - KH)\Psi(m_j) + Ky_{j+1}, \end{aligned}$$

and hence that

$$\begin{aligned} v_{j+1}^\dagger &= (I - KH)\Psi(v_j^\dagger) + KH\Psi(v_j^\dagger), \\ m_{j+1} &= (I - KH)\Psi(m_j) + KH\Psi(v_j^\dagger) + \gamma K\eta_{j+1,0}^\dagger. \end{aligned}$$

Define $e_j = m_j - v_j^\dagger$. By subtracting the evolution equation for v_j^\dagger from that for m_j we obtain, using the mean value theorem,

$$\begin{aligned} e_{j+1} &= m_{j+1} - v_{j+1}^\dagger \\ &= (I - KH)(\Psi(m_j) - \Psi(v_j^\dagger)) + \gamma K\eta_{j+1,0}^\dagger \\ &= \left((I - KH) \int_0^1 D\Psi(sm_j + (1-s)v_j^\dagger) ds \right) e_j + \gamma K\eta_{j+1,0}^\dagger. \end{aligned}$$

As a result, by the triangle inequality,

$$\begin{aligned} \|e_{j+1}\| &\leq \left\| \left(\int_0^1 (I - KH)D\Psi(sm_j + (1-s)v_j^\dagger) ds \right) e_j \right\| + \|\gamma K\eta_{j+1,0}^\dagger\| \\ &\leq \left(\int_0^1 \|(I - KH)D\Psi(sm_j + (1-s)v_j^\dagger)\| ds \right) \|e_j\| + \|\gamma K\eta_{j+1,0}^\dagger\| \\ &\leq \lambda \|e_j\| + \gamma \|K\eta_{j+1,0}^\dagger\|. \end{aligned}$$

Taking expectations on both sides, we obtain, for $c := \mathbb{E}[\|K\eta_{j+1,0}^\dagger\|] > 0$,

$$\begin{aligned}\mathbb{E}[\|e_{j+1}\|] &\leq \lambda \mathbb{E}[\|e_j\|] + \gamma \mathbb{E}[\|K\eta_{j+1,0}^\dagger\|] \\ &\leq \lambda \mathbb{E}[\|e_j\|] + \gamma c.\end{aligned}\tag{9.3}$$

Using the discrete Gronwall inequality of Theorem 1.19 we have that:

$$\begin{aligned}\mathbb{E}[\|e_j\|] &\leq \lambda^j \mathbb{E}[\|e_0\|] + \sum_{i=0}^{j-1} c \lambda^i \gamma \\ &\leq \lambda^j \mathbb{E}[\|e_0\|] + c \gamma \frac{1 - \lambda^j}{1 - \lambda},\end{aligned}\tag{9.4}$$

where $e_0 = m_0 - v_0$. Since $\lambda < 1$, the desired statement follows. \square

9.3 4DVAR

Recall that 3DVAR differs from 4DVAR because, whilst also based on an optimization principle, 4DVAR is applied in a distributed fashion over all data in the time interval $j = 1, \dots, J$; in contrast 3DVAR is applied sequentially from time $j - 1$ to time j , for $j = 1, \dots, J$. We consider two forms of the methodology: *weak constraint 4DVAR* (*w4DVAR*), in which the fact that the dynamics model contains randomness is accounted for in the optimization; and *4DVAR* (sometimes known as *strong constraint 4DVAR*), which can be derived from w4DVAR in the limit of $\Sigma \rightarrow 0$ (no randomness in the dynamics).

The objective function minimized in w4DVAR is

$$J(V) = \frac{1}{2} |v_0 - m_0|_{C_0}^2 + \frac{1}{2} \sum_{j=0}^{J-1} |v_{j+1} - \Psi(v_j)|_{\Sigma}^2 + \frac{1}{2} \sum_{j=0}^{J-1} |y_{j+1} - H v_{j+1}|_{\Gamma}^2, \tag{9.5}$$

where $V = \{v_j\}_{j=0}^J \in \mathbb{R}^{d(J+1)}$, $Y = \{y_j\}_{j=1}^J \in \mathbb{R}^{kJ}$, $v_j \in \mathbb{R}^d$, $y_j \in \mathbb{R}^k$, H is the observation function, Σ is the random dynamical system covariance, Γ is the data noise covariance, and m_0 and C_0 are the mean and covariance of the initial state. The three terms in the objective function enforce, in turn, information about the initial condition v_0 , the dynamics model, and the data model. Note that, because Ψ is nonlinear, the objective is not quadratic and cannot be optimized in closed form. Implementation of the 4DVAR smoothing algorithm involves therefore using a suitable numerical optimization algorithm; a brief discussion of some guiding principles for the construction of gradient-based optimization methods can be found in Chapter 3, but whole books are devoted to this subject. In contrast, each step of 3DVAR requires solution of a quadratic optimization problem, tractable in closed form.

Theorem 9.3 (Minimizer Exists for w4DVAR). *Assume that Ψ is bounded and continuous. Then J has a minimizer, which is a MAP estimator for the smoothing problem.*

Proof. Recall Theorem 3.5, which shows that the MAP estimator based on the smoothing distribution $\mathbb{P}(V|Y) \propto \exp(-J(V))$ is attained provided that J is guaranteed to be

non-negative, continuous, and satisfy $J(V) \rightarrow \infty$ as $|V| \rightarrow \infty$. Now, the objective J defined by equation (9.5) is clearly non-negative, and it is continuous since Ψ is assumed to be continuous. It remains to show that $J(V) \rightarrow \infty$ as $|V| \rightarrow \infty$. Let R be a bound for Ψ , so that $|\Psi(v_j)|_\Sigma \leq R$ for all $v_j \in \mathbb{R}^d$. Then, since

$$J(V) \geq \frac{1}{2}|v_0|_{C_0}^2 - |v_0|_{C_0}|m_0|_{C_0} + \frac{1}{2} \sum_{j=0}^{J-1} (|v_{j+1}|_\Sigma^2 - 2R|v_{j+1}|_\Sigma),$$

it follows that $J(V) \rightarrow \infty$ as $|V| \rightarrow \infty$ and the proof is complete. \square

We now consider the vanishing dynamical noise limit of w4DVAR. This is to minimize

$$J_0(V) = \frac{1}{2}|v_0 - m_0|_{C_0}^2 + \frac{1}{2} \sum_{j=0}^{J-1} |y_{j+1} - H v_{j+1}|_\Gamma^2$$

subject to the hard constraint that

$$v_{j+1} = \Psi(v_j), \quad j = 0, \dots, J-1.$$

This is 4DVAR. Note that by using the constraint, 4DVAR can be written as a minimization over v_0 , rather than over the entire sequence $\{v_j\}_{j=0}^J$ as is required in w4DVAR.

We let J_σ denote the objective function J from w4DVAR in the case where Σ is replaced by $\sigma^2 \Sigma_0$. Roughly speaking, the following result shows that minimizers of J_σ converge as $\sigma \rightarrow 0^+$ to points in $\mathbb{R}^{k(J+1)}$ which satisfy the hard constraint associated with 4DVAR.

Theorem 9.4 (Small Signal Noise Limit of w4DVAR). *Suppose that Ψ is bounded and continuous and let V^σ be a minimizer of J_σ . Then as $\sigma \rightarrow 0^+$ there is a convergent subsequence of V^σ with limit V^* satisfying $v_{j+1}^* = \Psi(v_j^*)$.*

Proof. Throughout this proof c is a constant which may change from instance to instance, but is independent of σ . Consider $V \in \mathbb{R}^{d(J+1)}$ defined by $v_0 = m_0$ and $v_{j+1} = \Psi(v_j)$. Then V is bounded, as $\Psi(\cdot)$ is bounded, and the bound is independent of σ . Furthermore

$$J_\sigma(V) = \frac{1}{2} \sum_{j=0}^{J-1} |y_{j+1} - H v_{j+1}|_\Gamma^2 \leq c,$$

where c is independent of σ . It follows that

$$J_\sigma(V^\sigma) \leq J_\sigma(V) \leq c.$$

Thus

$$\begin{aligned} \frac{1}{2}|v_{j+1}^\sigma - \Psi(v_j^\sigma)|_{\Sigma_0}^2 &= \frac{\sigma^2}{2}|v_{j+1}^\sigma - \Psi(v_j^\sigma)|_\Sigma^2 \leq \sigma^2 J_\sigma(V^\sigma) \leq \sigma^2 c, \\ \frac{1}{2}|v_0^\sigma - m_0|_{C_0}^2 &\leq J_\sigma(V^\sigma) \leq c. \end{aligned}$$

Since Ψ is bounded, these bounds imply that $|V^\sigma|$ is bounded above independently of σ . Therefore, there is a limit $V^* : V^\sigma \rightarrow V^*$ along a subsequence. By continuity

$$0 \leq \frac{1}{2}|v_{j+1}^* - \Psi(v_j^*)|_{\Sigma_0}^2 \leftarrow \frac{1}{2}|v_{j+1}^\sigma - \Psi(v_j^\sigma)|_{\Sigma_0}^2 \leq \sigma^2 c.$$

Letting $\sigma \rightarrow 0^+$ we obtain that $v_{j+1}^* = \Psi(v_j^*)$. □

9.4 Discussion and Bibliography

The 3DVAR and 4DVAR methodologies, in the context of weather forecasting, are discussed in [196] and [98], respectively. The implementation of these methodologies by the Met Office is overviewed in [197, 255]. The accuracy analysis presented here is similar to that which first appeared in the papers [36, 215] and was developed further in [184, 269, 186]. It arises from considering stochastic perturbations of the seminal work of Titi and collaborators, exemplified by the paper [137]. In all of these works, particular emphasis is placed in estimating the state of deterministic chaotic dynamical systems from partial and noisy observations [179, 237, 236, 35, 229]. For an overview of variational data assimilation methods, and their links to problems in physics and mechanics, see the book [2] and the references therein; see also the paper [37].

Chapter 10

The Extended and Ensemble Kalman Filters

In this chapter we describe the Extended Kalman Filter (ExKF)¹ and the Ensemble Kalman Filter (EnKF). The ExKF approximates the predictive covariance by linearization, while the EnKF approximates it by the empirical covariance of a collection of particles. The ExKF is a provably accurate approximation of the filtering distribution if the dynamics are approximately linear and small noise is present in both signal and data, in which case the filtering distribution is well approximated by a Gaussian. In such settings, the EnKF can also provide a good approximation of the filtering distribution if a sufficiently large number of particles is used. For problems where the filtering distributions are not well approximated by Gaussians, ExKF and EnKF can still be successful online optimizers for state estimation; they may be thought of as generalizations of 3DVAR in which the model covariance, which weights the model contribution to the optimization problem solved at every step, is updated on the basis of linearized (ExKF) or ensemble (EnKF) information.

This chapter is organized as follows. We introduce the problem setting in Section 10.1. The ExKF and EnKF are described, in turn, in Sections 10.2 and 10.3. We close in Section 10.4 with extensions and bibliographical remarks.

10.1 The Setting

Throughout this chapter we consider the setting in which 3DVAR was introduced and may be applied: the dynamics model is nonlinear, but the observation function is linear. For purposes of exposition we summarize it again here:

$$\begin{aligned} v_{j+1} &= \Psi(v_j) + \xi_j, & \xi_j &\sim \mathcal{N}(0, \Sigma) \text{ i.i.d.}, \\ y_{j+1} &= H v_{j+1} + \eta_{j+1}, & \eta_j &\sim \mathcal{N}(0, \Gamma) \text{ i.i.d.}, \end{aligned}$$

with $v_0 \sim \mathcal{N}(m_0, C_0)$ independent of the independent i.i.d. sequences $\{\xi_j\}$ and $\{\eta_j\}$. Throughout this chapter we assume that $v_j \in \mathbb{R}^d$, $y_j \in \mathbb{R}^k$.

¹The extended Kalman filter is often termed the EKF in the literature, a terminology introduced before the existence of the EnKF; we find it useful to write ExKF to unequivocally distinguish it from the EnKF.

Kalman Filter	ExKF
$m_{j+1} = \arg \min_v J(v)$	$m_{j+1} = \arg \min_v J(v)$
$J(v) = \frac{1}{2} y_{j+1} - Hv _{\Gamma}^2 + \frac{1}{2} v - \hat{m}_{j+1} _{\hat{C}_{j+1}}^2$	$J(v) = \frac{1}{2} y_{j+1} - Hv _{\Gamma}^2 + \frac{1}{2} v - \hat{m}_{j+1} _{\hat{C}_{j+1}}^2$
$\hat{m}_{j+1} = Mm_j$	$\hat{m}_{j+1} = \Psi(m_j)$
\hat{C}_{j+1} update exact	\hat{C}_{j+1} update by linearization
$m_{j+1} = (I - K_{j+1}H)\hat{m}_{j+1} + K_{j+1}y_{j+1}$	$m_{j+1} = (I - K_{j+1}H)\hat{m}_{j+1} + K_{j+1}y_{j+1}$

Table 10.1 Comparison of Kalman filter and ExKF update formulae.

10.2 The Extended Kalman Filter

This method is derived by applying the Kalman methodology, using linearization to propagate the covariance C_j to the predictive covariance \hat{C}_{j+1} . Table 10.1 summarizes the idea, and in what follows we calculate the formulae required in full detail.

We first recall the Kalman filter update formulae and their derivation. We have

$$\hat{v}_{j+1} = Mv_j + \xi_j, \quad v_j \sim \mathcal{N}(m_j, C_j), \quad \xi_j \sim \mathcal{N}(0, \Sigma). \quad (10.1)$$

From this we deduce, by taking expectations, that

$$\hat{m}_{j+1} = \mathbb{E}[\hat{v}_{j+1} | Y_j] = \mathbb{E}[Mv_j + \xi_j | Y_j] = \mathbb{E}[Mv_j | Y_j] + \mathbb{E}[\xi_j | Y_j] = Mm_j. \quad (10.2)$$

The covariance update is derived as follows:

$$\begin{aligned}
\hat{C}_{j+1} &= \mathbb{E}[(\hat{v}_{j+1} - \hat{m}_{j+1}) \otimes (\hat{v}_{j+1} - \hat{m}_{j+1}) | Y_j] \\
&= \mathbb{E}[(M(v_j - m_j) + \xi_j) \otimes (M(v_j - m_j) + \xi_j) | Y_j] \\
&= \mathbb{E}[(M(v_j - m_j)) \otimes (M(v_j - m_j)) | Y_j] + \mathbb{E}[\xi_j \otimes \xi_j | Y_j] \\
&\quad + \mathbb{E}[(M(v_j - m_j)) \otimes \xi_j | Y_j] + \mathbb{E}[\xi_j \otimes (M(v_j - m_j)) | Y_j] \\
&= M \mathbb{E}[(v_j - m_j) \otimes (v_j - m_j) | Y_j] M^\top + \Sigma \\
&= MC_j M^\top + \Sigma.
\end{aligned} \quad (10.3)$$

For the ExKF, the prediction map Ψ is no longer linear. But since ξ_j is independent of Y_j and v_j , we obtain

$$\hat{m}_{j+1} = \mathbb{E}[\Psi(v_j) + \xi_j | Y_j] = \mathbb{E}[\Psi(v_j) | Y_j] + \mathbb{E}[\xi_j | Y_j] = \mathbb{E}[\Psi(v_j) | Y_j].$$

If we assume that the fluctuations of v_j around its mean m_j (conditional on data) are small, then a reasonable approximation is to take $\Psi(v_j) \approx \Psi(m_j)$ so that

$$\hat{m}_{j+1} = \Psi(m_j). \quad (10.4)$$

For the predictive covariance we use linearization; we have

$$\begin{aligned}
\hat{C}_{j+1} &= \mathbb{E}[(\hat{v}_{j+1} - \hat{m}_{j+1}) \otimes (\hat{v}_{j+1} - \hat{m}_{j+1}) | Y_j] \\
&= \mathbb{E}[(\Psi(v_j) - \Psi(m_j) + \xi_j) \otimes (\Psi(v_j) - \Psi(m_j) + \xi_j) | Y_j] \\
&= \mathbb{E}[(\Psi(v_j) - \Psi(m_j)) \otimes (\Psi(v_j) - \Psi(m_j)) | Y_j] + \Sigma \\
&\approx D\Psi(m_j) \mathbb{E}[(v_j - m_j) \otimes (v_j - m_j) | Y_j] D\Psi(m_j)^\top + \Sigma,
\end{aligned}$$

and so, again assuming that fluctuations of v_j around its mean m_j (conditional on data) are small, we invoke the approximation

$$\hat{C}_{j+1} = D\Psi(m_j) C_j D\Psi(m_j)^\top + \Sigma. \quad (10.5)$$

To be self-consistent, Σ itself should be small. We next summarize the steps of the ExKF.

Algorithm 10.1 Extended Kalman Filter

- 1: **Input:** Initial mean $m_0 \in \mathbb{R}^d$ and covariance $C_0 \in \mathbb{R}^{d \times d}$.
- 2: For $j = 0, 1, \dots, J-1$ do the following prediction and analysis steps:
- 3: **Prediction:**

$$\hat{m}_{j+1} = \Psi(m_j), \quad (10.6)$$

$$\hat{C}_{j+1} = D\Psi(m_j) C_j D\Psi(m_j)^\top + \Sigma. \quad (10.7)$$

- 4: **Analysis:**

$$\begin{aligned}
m_{j+1} &= (I - K_{j+1}H) \hat{m}_{j+1} + K_{j+1}y_{j+1}, \\
C_{j+1} &= (I - K_{j+1}H) \hat{C}_{j+1}.
\end{aligned} \quad (10.8)$$

- 5: **Output:** Predictive means $\{\hat{m}_j\}_{j=1}^J$ and covariances $\{\hat{C}_j\}_{j=1}^J$, and analysis means $\{m_j\}_{j=1}^J$ and covariances $\{C_j\}_{j=1}^J$.
-

Note that the Kalman gain K_{j+1} in equation (10.8) is defined in the same way as for the Kalman filter, namely

$$K_{j+1} = \hat{C}_{j+1} H^\top S_{j+1}^{-1}, \quad S_{j+1} = H \hat{C}_{j+1} H^\top + \Gamma.$$

Thus, the analysis step is the same as for the Kalman filter. However, for the ExKF the maps $C_j \mapsto \hat{C}_{j+1} \mapsto C_{j+1}$ depend on the observed data through the dependence of the predictive covariance on the filter mean. To be self-consistent with the “small fluctuations around the mean” assumptions made in the derivation of the ExKF, Σ and Γ should both be small.

The analysis step can also be defined by

$$\begin{aligned} C_{j+1}^{-1} &= \hat{C}_{j+1}^{-1} + H^\top \Gamma^{-1} H, \\ m_{j+1} &= \arg \min_v J(v), \end{aligned}$$

where

$$J(v) = \frac{1}{2} |y_{j+1} - H v|_\Gamma^2 + \frac{1}{2} |v - \hat{m}_{j+1}|_{\hat{C}_{j+1}}^2 \quad (10.9)$$

and $\hat{m}_{j+1}, \hat{C}_{j+1}$ are calculated as above in the prediction step (10.6). The constraint formulation of the minimization problem, derived for the Kalman filter in Section 8.1.2, may also be used to derive the update formulae above.

10.3 Ensemble Kalman Filter

When the dynamical system is in high dimension, evaluation and storage of the predictive covariance, and in particular the Jacobian required for the update formula (10.5), becomes computationally inefficient and expensive for the ExKF. The EnKF was developed to overcome this issue. The basic idea is to maintain an ensemble of particles, and to use their empirical covariance within a Kalman-type update. The method is summarized in Table 10.2. It may be thought of as an ensemble 3DVAR technique in which a collection of particles are generated similarly to 3DVAR, but interact through an ensemble estimate of their covariance.

In the basic form which we present here, the EnKF is applied when Ψ is nonlinear, while the observation function H is linear. The N particles used at step j are denoted $\{v_j^{(n)}\}_{n=1}^N$. They are all given equal weight so it is possible, in principle, to make an approximation to the filtering distribution of the form

$$\pi_j^N(v_j) \approx \frac{1}{N} \sum_{n=1}^N \delta(v_j - v_j^{(n)}).$$

This approximation can in principle be accurate if N is sufficiently large and the filtering distributions are approximately Gaussian. In problems where approximate Gaussianity of the filtering distribution fails—for instance due to strong nonlinearity of Ψ and large observation noise—EnKF is better understood as a sequential optimization method, similar in spirit to 3DVAR, as described in the introduction to the chapter.

The state of all the particles at time $j+1$ are predicted to give $\{\hat{v}_{j+1}^{(n)}\}_{n=1}^N$ using the dynamical model. The resulting empirical covariance is then used to define an objective function which is minimized in order to perform the analysis step and obtain $\{v_{j+1}^{(n)}\}_{n=1}^N$. The updates are denoted schematically by

$$\{v_j^{(n)}\}_{n=1}^N \mapsto \{\hat{v}_{j+1}^{(n)}\}_{n=1}^N \mapsto \{v_{j+1}^{(n)}\}_{n=1}^N.$$

The idea of the EnKF is summarized in Table 10.2 below, which is followed by a full description of the algorithm.

Kalman Filter	EnKF
$m_{j+1} = \arg \min_v J(v)$	$v_{j+1}^{(n)} = \arg \min_v J_n(v)$
$J(v) = \frac{1}{2} y_{j+1} - Hv _\Gamma^2 + \frac{1}{2} v - \hat{m}_{j+1} _{\hat{C}_{j+1}}^2$	$J_n(v) = \frac{1}{2} y_{j+1}^{(n)} - Hv _\Gamma^2 + \frac{1}{2} v - \hat{v}_{j+1}^{(n)} _{\hat{C}_{j+1}}^2$
$\hat{m}_{j+1} = Mm_j$	$\hat{v}_{j+1}^{(n)} = \Psi(v_j^{(n)}) + \xi_j^{(n)}$
\hat{C}_{j+1} update exact	\hat{C}_{j+1} update by ensemble estimate
$m_{j+1} = (I - K_{j+1}H)\hat{m}_{j+1} + K_{j+1}y_{j+1}$	$v_{j+1}^{(n)} = (I - K_{j+1}H)\hat{v}_{j+1}^{(n)} + K_{j+1}y_{j+1}^{(n)}$

Table 10.2 Comparison of Kalman filter and EnKF update formulae.

10.3.1 Algorithmic Implementation of EnKF

We next summarize the steps of the EnKF:

Algorithm 10.2 Ensemble Kalman Filter

- 1: **Input:** Ensemble size N . Initial ensemble $\{v_0^{(n)}\}_{n=1}^N$. Parameter $s \in \{0, 1\}$.
- 2: For $j = 0, 1, \dots, J - 1$ do the following prediction and analysis steps:
- 3: **Prediction:**

$$\begin{aligned}
\xi_j^{(n)} &\sim \mathcal{N}(0, \Sigma), \quad \text{i.i.d.}, \quad n = 1, \dots, N, \\
\hat{v}_{j+1}^{(n)} &= \Psi(v_j^{(n)}) + \xi_j^{(n)}, \quad n = 1, \dots, N, \\
\hat{m}_{j+1} &= \frac{1}{N} \sum_{n=1}^N \hat{v}_{j+1}^{(n)}, \\
\hat{C}_{j+1} &= \frac{1}{N} \sum_{n=1}^N (\hat{v}_{j+1}^{(n)} - \hat{m}_{j+1}) \otimes (\hat{v}_{j+1}^{(n)} - \hat{m}_{j+1}).
\end{aligned} \tag{10.10}$$

- 4: **Analysis:**

$$\begin{aligned}
\eta_{j+1}^{(n)} &\sim \mathcal{N}(0, \Gamma), \quad n = 1, \dots, N, \\
y_{j+1}^{(n)} &= y_{j+1} + s\eta_{j+1}^{(n)}, \quad n = 1, \dots, N, \\
v_{j+1}^{(n)} &= (I - K_{j+1}H)\hat{v}_{j+1}^{(n)} + K_{j+1}y_{j+1}^{(n)}, \quad n = 1, \dots, N.
\end{aligned} \tag{10.11}$$

- 5: **Output:** Ensembles $\{v_j^{(n)}\}_{n=1}^N$, $j = 0, 1, \dots, J$.
-

Once again the Kalman gain K_{j+1} in equation (10.11) is defined in the same way as for the Kalman filter, namely

$$K_{j+1} = \hat{C}_{j+1}H^\top S_{j+1}^{-1}, \quad S_{j+1} = H\hat{C}_{j+1}H^\top + \Gamma.$$

However \hat{C}_{j+1} is estimated in a novel fashion, using an ensemble of particles; this is the key innovation behind the EnKF. The parameter s may be chosen to be 0 or

1. The choice $s = 1$ is natural when aiming at approximating the Kalman filter in linear-Gaussian settings; in such case the $y_{j+1}^{(n)}$ are referred to as *perturbed observations*. The choice $s = 0$ is natural if viewing the algorithm as a sequential optimizer in problems where the filtering distributions are not well approximated by Gaussians.

The analysis step may be written as

$$v_{j+1}^{(n)} = \arg \min_v J_n(v), \quad (10.12)$$

where

$$J_n(v) := \frac{1}{2} |y_{j+1}^{(n)} - Hv|_\Gamma^2 + \frac{1}{2} |v - \hat{v}_{j+1}^{(n)}|_{\hat{C}_{j+1}}^2 \quad (10.13)$$

and the predictive mean and covariance are given by (10.10). Note that \hat{C}_{j+1} is typically not invertible as it is a rank N matrix and N is usually less than the dimension d of the space on which \hat{C}_{j+1} acts; this is since the typical use of ensemble methods is for high-dimensional state-space estimation, with a small ensemble size. The minimizing solution can be found by regularizing \hat{C}_{j+1} by adding ϵI for $\epsilon > 0$, deriving the update equations as above, and then letting $\epsilon \rightarrow 0^+$. Alternatively, the constraint formulation of the minimization problem, derived for the Kalman filter in Subsection 8.1.2, may also be used to derive the update formulae above.

The following theorem explains why perturbing the observations with $s = 1$ may be favored when aiming at approximating the Kalman filter in (close to) linear-Gaussian settings. Setting $s = 1$ ensures that if each prediction particle $\hat{v}_{j+1}^{(n)}$ is distributed according to a non-degenerate Gaussian predictive distribution $\mathcal{N}(\hat{m}_{j+1}, \hat{C}_{j+1})$, then, in the linear Gaussian setting, each analysis particle $\hat{v}_{j+1}^{(n)}$ will be Gaussian distributed with mean and covariance given by the filtering distribution found by the Kalman filter formulae. This is achieved by updating each particle minimizing an objective defined using a randomization of the likelihood function.

Theorem 10.1 (Perturbed Observation EnKF — Randomized Likelihood Viewpoint). *Suppose that $\hat{v}_{j+1}^{(n)} \sim \mathcal{N}(\hat{m}_{j+1}, \hat{C}_{j+1})$ with \hat{C}_{j+1} positive definite. Let $v_{j+1}^{(n)}$ be the minimizer of*

$$J_n(v) := \frac{1}{2} |y_{j+1} + \eta_{j+1}^{(n)} - Hv|_\Gamma^2 + \frac{1}{2} |v - \hat{v}_{j+1}^{(n)}|_{\hat{C}_{j+1}}^2, \quad \eta_{j+1}^{(n)} \sim \mathcal{N}(0, \Gamma), \quad (10.14)$$

where $\hat{v}_{j+1}^{(n)}$ and $\eta_{j+1}^{(n)}$ are independent. Then $v_{j+1}^{(n)} \sim \mathcal{N}(m_{j+1}, C_{j+1})$, where m_{j+1} and C_{j+1} are defined by

$$m_{j+1} = \hat{m}_{j+1} + K_{j+1}(y_{j+1} - H\hat{m}_{j+1}), \quad (10.15)$$

$$C_{j+1} = (I - K_{j+1}H)\hat{C}_{j+1}, \quad (10.16)$$

and

$$K_{j+1} := \hat{C}_{j+1}H^\top(H\hat{C}_{j+1}H^\top + \Gamma)^{-1}.$$

Proof. The minimizer of (10.14) is given by

$$v_{j+1}^{(n)} = \hat{v}_{j+1}^{(n)} + K_{j+1}(y_{j+1} + \eta_{j+1}^{(n)} - H\hat{v}_{j+1}^{(n)}) \quad (10.17)$$

$$= C_{j+1} \left\{ \hat{C}_{j+1}^{-1} \hat{v}_{j+1}^{(n)} + H^\top \Gamma^{-1} (y_{j+1} + \eta_{j+1}^{(n)}) \right\}, \quad (10.18)$$

where C_{j+1} is defined in (10.16) and the equivalence between (10.17) and (10.18) follows from the equivalence of precision and covariance characterizations of the Kalman filter in Theorem 8.3 and equations (8.6) and (8.7). Notice that (10.17) and (10.18) show that $v_{j+1}^{(n)}$ can be written as a linear combination of Gaussian random variables, so $v_{j+1}^{(n)}$ is Gaussian. We next show that its mean and covariance are given by (10.15) and (10.16).

First, from (10.17) we deduce that

$$\begin{aligned}\mathbb{E}[v_{j+1}^{(n)}] &= \mathbb{E}[\hat{v}_{j+1}^{(n)} + K_{j+1}(y_{j+1} + \eta_{j+1}^{(n)} - H\hat{v}_{j+1}^{(n)})] \\ &= \hat{m}_{j+1} + K_{j+1}(y_{j+1} - H\hat{m}_{j+1}),\end{aligned}$$

where we used that by assumption $\mathbb{E}[\hat{v}_{j+1}^{(n)}] = \hat{m}_{j+1}$ and that $\mathbb{E}[\eta_{j+1}^{(n)}] = 0$.

Second, from (10.18) we deduce that

$$\begin{aligned}\mathbb{E}[(v_{j+1}^{(n)} - m_{j+1}) \otimes (v_{j+1}^{(n)} - m_{j+1})] &= C_{j+1}\hat{C}_{j+1}^{-1}C_{j+1} + C_{j+1}H^\top\Gamma^{-1}HC_{j+1} \\ &= C_{j+1}(\hat{C}_{j+1}^{-1} + H^\top\Gamma^{-1}H)C_{j+1} \\ &= C_{j+1},\end{aligned}$$

where we used that $C_{j+1}^{-1} = \hat{C}_{j+1}^{-1} + H^\top\Gamma^{-1}H$ by the equivalent characterization of the Kalman filter covariance in Theorem 8.3 and equations (8.6) and (8.7). \square

10.3.2 Subspace Property of EnKF

We now give another way to think of, and exploit in algorithms, the low rank property of \hat{C}_{j+1} . Note that $J_n(v)$ is undefined unless

$$v - \hat{v}_{j+1}^{(n)} = \hat{C}_{j+1}a$$

for some $a \in \mathbb{R}^d$. From the structure of \hat{C}_{j+1} it follows that

$$v = \hat{v}_{j+1}^{(n)} + \frac{1}{N} \sum_{m=1}^N b_m(\hat{v}_{j+1}^{(m)} - \hat{m}_{j+1}) \quad (10.19)$$

for some unknown vector $b = \{b_m\}_{m=1}^N \in \mathbb{R}^N$ to be determined. Note that both a and b depend on the ensemble member n , but we suppress that dependence from the notation. This form for v can be substituted into (10.13) to obtain a functional $l_n(b)$ to be minimized over $b \in \mathbb{R}^N$. We re-emphasize that N will typically be much smaller than d , the state-space dimension. Once b is determined it may be substituted back into (10.19) to obtain the solution to the minimization problem.

To dig a little deeper into this calculation, we define

$$e^{(m)} = \hat{v}_{j+1}^{(m)} - \hat{m}_{j+1}$$

and note that then

$$\hat{C}_{j+1} = \frac{1}{N} \sum_{m=1}^N e^{(m)} \otimes e^{(m)}.$$

Since

$$\hat{C}_{j+1}a = \frac{1}{N} \sum_{m=1}^N b_m e^{(m)}$$

we deduce that

$$b_m = \langle e^{(m)}, a \rangle.$$

Now note that

$$\frac{1}{2} |v - \hat{v}_{j+1}^{(n)}|_{\hat{C}_{j+1}}^2 = \frac{1}{2} \langle a, \hat{C}_{j+1}a \rangle = \frac{1}{2N} \sum_{m=1}^N b_m^2.$$

Therefore, defining

$$F_n(b) := \frac{1}{2} \left| y_{j+1}^{(n)} - H\hat{v}_{j+1}^{(n)} - \frac{1}{N} \sum_{m=1}^N b_m H(\hat{v}_{j+1}^{(n)} - \hat{m}_{j+1}) \right|_{\Gamma}^2 + \frac{1}{2N} \sum_{m=1}^N b_m^2 \quad (10.20)$$

we have proved the following:

Theorem 10.2 (Implementation of EnKF in N -Dimensional Subspace). *Given the prediction defined by (10.10), the Kalman update formulae (10.11) may be found by minimizing $F_n(b)$ with respect to b and substituting into (10.19).*

10.4 Discussion and Bibliography

In this chapter we have considered a derivative-based filtering algorithm (ExKF) and an ensemble-based filtering algorithm (EnKF). Extended and ensemble Kalman algorithms for the smoothing problem are also available, see e.g. [94, 21]. The development and theory of the ExKF is documented in the text [156]. A methodology for analyzing evolving probability distributions with small variance, and establishing the validity of the Gaussian approximation, is described in [270]. The use of the ExKF for weather forecasting was proposed in [112]. However, the dimension of the state-space in most geophysical applications renders the ExKF impractical. The EnKF provided an innovation with far reaching consequences in geophysical applications, because it allowed for the use of partial empirical correlation information, without the computation of the full covariance. An overview of ensemble Kalman methods may be found in the book [92], including a historical perspective on the subject, originating from papers of Evensen and Van Leeuwen in the mid 1990s [91, 93]; a similar idea was also developed by Houtekamer within the Canadian meteorological service, around the same time; [144, 145]. An overview of ensemble Kalman methods, adopting a unifying mean-field perspective in which $N \rightarrow \infty$, may be found in [42]. The paper [8] develops a unified non-asymptotic analysis of ensemble Kalman methods from the perspective of high-dimensional statistics, which explains why a small sample size N suffices in applications where the covariance models have moderate effective dimension.

The presentation of the EnKF as a smart optimization tool is also developed in [185], but the derivation of the update equations in a space whose dimension is that of the ensemble is not described there. The form of EnKF with perturbed observations ($s = 1$) presented on these notes is closely related to randomized maximum likelihood [53], but

other implementations of the algorithm are available, see e.g. [301, 12, 26, 203]. See also [168] for a proof of Theorem 10.1 and for further details on the connection between randomized maximum likelihood and perturbed observation EnKF. The analysis of ensemble methods is difficult and theory is only just starting to emerge. In the linear case the method converges in the large ensemble limit to the Kalman filter [117, 204, 178], but in the nonlinear case the limit does not reproduce the filtering distribution [90]. In any case, the primary advantage of ensemble methods is that they can provide good state estimation when the number of particles is *not* large; this subject is discussed in [121, 168, 303, 304, 8].

Chapter 11

Particle Filter

This chapter is devoted to the particle filter, a method that approximates the filtering distribution by a sum of Dirac masses. Particle filters provably converge to the filtering distribution as the number of particles, and hence the number of Dirac masses, approaches infinity. We focus on the bootstrap particle filter, also known as sequential importance resampling; it is linked to the material on Monte Carlo and importance sampling described in Chapter 5. We note that the Kalman filter completely characterizes the filtering distribution in the linear-Gaussian setting. The Kalman-based methods introduced in the two previous chapters apply outside the linear-Gaussian setting and are built by approximating the predictive distribution using a Gaussian ansatz, and then applying the Kalman formulae for the analysis step. The bootstrap particle filter approximates the predictive distribution by a sum of Dirac masses and, using this structure, exactly solves the analysis step. Thus, both Kalman-based methods (with linear observations) and the bootstrap particle filter use exact application of Bayes formula, but with approximate priors found by approximating the outcome of the prediction step. However, whilst Kalman-based methods use an approximation that is only valid for problems which are close to Gaussian, particle filters have the potential of recovering an accurate approximation to the filtering distribution in non-linear, non-Gaussian settings provided that the number of particles is large enough. However, an important disadvantage of particle filters is that they tend to struggle in high-dimensional problems for practically implementable particle numbers. In contrast, Kalman-based methods are robust, but harder to interpret in a rigorous fashion except for linear-Gaussian problems.

This chapter is organized as follows. We describe the problem setting in Section 11.1. We then introduce the bootstrap particle filter in Section 11.2 and analyze its convergence in Section 11.3. Section 11.4 describes how the bootstrap particle filter can be interpreted as a random dynamical system. We close in Section 11.5 with extensions and bibliographical remarks.

11.1 The Setting

Let us return to the setting in which we introduced filtering and smoothing in Chapter 7, with nonlinear stochastic dynamics and nonlinear observation function, namely the

model

$$\begin{aligned} v_{j+1} &= \Psi(v_j) + \xi_j, & \xi_j &\sim \mathcal{N}(0, \Sigma) \text{ i.i.d.}, \\ y_{j+1} &= h(v_{j+1}) + \eta_{j+1}, & \eta_j &\sim \mathcal{N}(0, \Gamma) \text{ i.i.d.}, \end{aligned}$$

with $v_0 \sim \pi_0 := \mathcal{N}(m_0, C_0)$ independent of the i.i.d. sequences $\{\xi_j\}$ and $\{\eta_j\}$. Here $\Psi(\cdot)$ drives the dynamics and $h(\cdot)$ is the observation function. Recall that we denote by $Y_j = \{y_1, \dots, y_j\}$ all the data up to time j and by π_j the pdf of $v_j|Y_j$, that is, $\pi_j = \mathbb{P}(v_j|Y_j)$. The filtering problem is to determine π_{j+1} from π_j . We may do so in two steps: first, we run forward the Markov chain generated by the stochastic dynamical system (prediction), and second, we incorporate the data by an application of Bayes theorem (analysis).

For the prediction step, we define the operator \mathcal{P} acting on a pdf π as an application of a Markov kernel defined by

$$(\mathcal{P}\pi)(v) = \int_{\mathbb{R}^d} p(u, v) \pi(u) du, \quad (11.1)$$

where $p(u, v)$ is the associated pdf of the stochastic dynamics, so that

$$p(u, v) = \frac{1}{\sqrt{(2\pi)^d \det \Sigma}} \exp\left(-\frac{1}{2}|v - \Psi(u)|_{\Sigma}^2\right).$$

Thus, we obtain

$$\mathbb{P}(v_{j+1}|Y_j) = \hat{\pi}_{j+1} = \mathcal{P}\pi_j.$$

We then define the analysis operator \mathcal{A}_j acting on a pdf π to correspond to an application of Bayes theorem, namely

$$(\mathcal{A}_j\pi)(v) = \frac{l_j(v)\pi(v)}{\int_{\mathbb{R}^d} l_j(v)\pi(v) dv}, \quad l_j(v) = \exp\left(-\frac{1}{2}|y_{j+1} - h(v)|_{\Gamma}^2\right).$$

Finally, combining the prediction and analysis steps, we obtain

$$\pi_{j+1} = \mathcal{A}_j \hat{\pi}_{j+1} = \mathcal{A}_j \mathcal{P}\pi_j.$$

We now describe a way to numerically approximate, and update, the pdfs π_j .

11.2 The Bootstrap Particle Filter

The Bootstrap Particle Filter (BPF) can be thought of as performing sequential importance resampling. Let S^N be an operator acting on a pdf π by producing an N -samples Dirac approximation of π , that is

$$(S^N\pi)(u) = \sum_{n=1}^N w_n \delta(u - u^{(n)}),$$

where $u^{(1)}, \dots, u^{(N)}$ are i.i.d samples from π that are weighted uniformly i.e. $w_n = \frac{1}{N}$. Note that $S^N\pi = \pi_{MC}^N$, as introduced in Chapter 5, equation (5.6). We will use the

operator S^N to approximate the measure produced by the Markov kernel step \mathcal{P} within the overall filtering map $\mathcal{A}_j\mathcal{P}$. Note that S^N is a *random* map taking pdfs into pdfs if we interpret weighted sums of Dirac masses as a pdf.

Let $\pi_0^N = \pi_0 = \mathcal{N}(m_0, C_0)$ and let π_j^N denote a particle approximation of the pdf π_j that we will determine in what follows. We define

$$\hat{\pi}_{j+1}^N = S^N \mathcal{P} \pi_j^N;$$

this is an approximation of $\hat{\pi}_{j+1}$ from the previous section. We then apply the operator \mathcal{A}_j to act on $\hat{\pi}_{j+1}^N$ by appropriately reconfiguring the weights w_j according to the data.

To understand this reconfiguration of the weights we use the fact that, if

$$\pi(v) = \frac{1}{N} \sum_{n=1}^N \delta(v - v^{(n)}),$$

then

$$(\mathcal{A}_j \pi)(v) = \sum_{n=1}^N w^{(n)} \delta(v - v^{(n)}),$$

where

$$\bar{w}^{(n)} = l_j(v^{(n)})$$

and the $w^{(n)}$ are found from the $\bar{w}^{(n)}$ by renormalizing them to sum to one. We use this calculation concerning the application of Bayes formula to sums of Dirac masses within the following desired approximation of the filtering update formula:

$$\pi_{j+1} \approx \pi_{j+1}^N = \mathcal{A}_j \hat{\pi}_{j+1}^N = \mathcal{A}_j S^N \mathcal{P} \pi_j^N.$$

The steps for the method are summarized in Algorithm 11.1.

Algorithm 11.1 Bootstrap Particle Filter

- 1: **Input:** Initial distribution $\pi_0^N = \pi_0$, number of particles N .
 - 2: **Particle Generation:** For $j = 0, 1, \dots, J - 1$, perform
 1. Draw $v_j^{(n)} \sim \pi_j^N$ for $n = 1, \dots, N$ i.i.d.
 2. Set $\hat{v}_{j+1}^{(n)} = \Psi(v_j^{(n)}) + \xi_j^{(n)}$ with $\xi_j^{(n)}$ i.i.d. $\mathcal{N}(0, \Sigma)$.
 3. Set $\bar{w}_{j+1}^{(n)} = \exp\left(-\frac{1}{2}|y_{j+1} - h(\hat{v}_{j+1}^{(n)})|_{\Gamma}^2\right)$.
 4. Set $w_{j+1}^{(n)} = \bar{w}_{j+1}^{(n)} / \sum_{n=1}^N \bar{w}_{j+1}^{(n)}$.
 5. Set $\pi_{j+1}^N(u) = \sum_{n=1}^N w_{j+1}^{(n)} \delta(u - \hat{v}_{j+1}^{(n)})$.
 - 3: **Output:** Particle approximations $\pi_j^N \approx \pi_j$, $j = 1, \dots, J$.
-

11.3 Bootstrap Particle Filter Convergence

We will now show that, under certain conditions, the BPF converges to the true filtering distribution in the limit $N \rightarrow \infty$. The proof is similar to that of the Lax-Equivalence Theorem from the numerical approximation of evolution equations, part of which is the statement that consistency and stability together imply convergence. For the BPF, consistency refers to a Monte Carlo error estimate, similar to that derived in the chapter on importance sampling, and stability manifests in bounds on the Lipschitz constants for the operators \mathcal{P} and \mathcal{A}_j .

Our first step is to define what we mean by convergence, that is, we need a metric on probability measures. Notice that the operators \mathcal{P} and \mathcal{A}_j are deterministic, but the operator S^N is random since it requires sampling. As a consequence, the approximate pdfs π_j^N are also random. Thus, in fact, we need a distance between random probability measures. To this end, for random pdfs π and π' , we define

$$d(\pi, \pi') = \sup_{|f|_\infty \leq 1} \left(\mathbb{E} \left[(\pi(f) - \pi'(f))^2 \right] \right)^{1/2},$$

where the expectation is taken over the random variable, in our case, the randomness from sampling with S^N . This distance between random probability measures was introduced in Chapter 5 to study Monte Carlo integration: see equation (5.7).

We now prove three lemmas which together will enable us to prove convergence of the BPF. The first shows consistency; the second and third show stability estimates for \mathcal{P} and \mathcal{A}_j , respectively.

Lemma 11.1. *For any pdf π , it holds that*

$$d(\pi, S^N \pi) \leq \frac{1}{\sqrt{N}}.$$

Proof. This is a consequence of Theorem 5.1, since $S^N \pi$ agrees with π_{MC}^N as defined in Chapter 5. \square

Now we prove a stability bound for the operator \mathcal{P} defined in equation (11.1).

Lemma 11.2. *For any pdfs π, π' , it holds that*

$$d(\mathcal{P}\pi, \mathcal{P}\pi') \leq d(\pi, \pi').$$

Proof. For $|f|_\infty \leq 1$ define a function q on \mathbb{R}^d by

$$q(v') = \int_{\mathbb{R}^d} p(v', v) f(v) dv,$$

where, recall, p denotes the transition pdf associated to the stochastic dynamics model. Note that

$$|q(v')| \leq \int_{\mathbb{R}^d} p(v', v) dv = 1,$$

and so $|q|_\infty \leq 1$. Moreover, it holds that

$$\pi(q) = (\mathcal{P}\pi)(f).$$

To see this, note that by exchanging the order of integration, we have

$$\begin{aligned} \pi(q) &= \int_{\mathbb{R}^d} q(v') \pi(v') dv' = \int_{\mathbb{R}^d} \left[\int_{\mathbb{R}^d} p(v', v) f(v) dv \right] \pi(v') dv' \\ &= \int_{\mathbb{R}^d} \left[\int_{\mathbb{R}^d} p(v', v) \pi(v') dv' \right] f(v) dv \\ &= \int_{\mathbb{R}^d} (\mathcal{P}\pi)(v) f(v) dv. \end{aligned}$$

Finally, using that $|q|_\infty \leq 1$ and $\pi(q) = (\mathcal{P}\pi)(f)$ we deduce that

$$\begin{aligned} d(\mathcal{P}\pi, \mathcal{P}\pi') &= \sup_{|f|_\infty \leq 1} \left(\mathbb{E} \left[((\mathcal{P}\pi)(f) - (\mathcal{P}\pi')(f))^2 \right] \right)^{1/2} \\ &\leq \sup_{|q|_\infty \leq 1} \left(\mathbb{E} \left[(\pi(q) - \pi'(q))^2 \right] \right)^{1/2} \\ &= d(\pi, \pi'). \end{aligned}$$

□

To prove the next lemma and the main convergence theorem of the BPF below, we will make the following assumption which encodes the idea of a bound on the observation function.

Assumption 11.3. *There exists $\kappa \in (0, 1)$ such that, for all $v \in \mathbb{R}^d$ and $j \in \{0, \dots, J-1\}$,*

$$\kappa \leq l_j(v) \leq \kappa^{-1}.$$

It may initially appear strange to use the same constant κ in the upper and lower bounds, but recall that l_j is undefined up to a multiplicative constant. Consequently, given any upper and lower bounds, l_j can be scaled to achieve the bound as stated. Relatedly, it is κ^{-2} which appears in the stability constant in the next lemma; if l_j is not scaled to produce the same constant κ in the upper and lower bounds in Assumption 11.3, then it is the ratio of the upper and lower bounds which would appear in the stability bound.

Lemma 11.4. *Let Assumption 11.3 hold. Then, for all pdfs π, π' and $j \in \{0, \dots, J-1\}$, it holds that*

$$d(\mathcal{A}_j\pi, \mathcal{A}_j\pi') \leq \frac{2}{\kappa^2} d(\pi, \pi').$$

Proof. To ease the notation, we drop the j subscripts in l_j and \mathcal{A}_j . Let $|f|_\infty \leq 1$. Following the proof of Theorem 5.6 in Chapter 5, we use the following identity:

$$\begin{aligned} (\mathcal{A}\pi)(f) - (\mathcal{A}\pi')(f) &= \frac{\pi(fl)}{\pi(l)} - \frac{\pi'(fl)}{\pi'(l)} \\ &= \frac{\pi(fl)}{\pi(l)} - \frac{\pi'(fl)}{\pi(l)} + \frac{\pi'(fl)}{\pi(l)} - \frac{\pi'(fl)}{\pi'(l)} \\ &= \frac{1}{\kappa} \left(\frac{\pi(\kappa fl) - \pi'(\kappa fl)}{\pi(l)} + \frac{\pi'(fl)}{\pi'(l)} \frac{\pi'(\kappa l) - \pi(\kappa l)}{\pi(l)} \right). \end{aligned}$$

Applying Bayes Theorem 1.2 and using that $|f|_\infty \leq 1$ gives

$$\left| \frac{\pi'(fl)}{\pi'(l)} \right| = |(\mathcal{A}\pi')(f)| \leq 1.$$

Therefore,

$$|(\mathcal{A}\pi)(f) - (\mathcal{A}\pi')(f)| \leq \frac{1}{\kappa^2} \left(|\pi(\kappa fl) - \pi'(\kappa fl)| + |\pi'(\kappa l) - \pi(\kappa l)| \right).$$

It follows that

$$\mathbb{E} \left[((\mathcal{A}\pi)(f) - (\mathcal{A}\pi')(f))^2 \right] \leq \frac{2}{\kappa^4} \left(\mathbb{E} \left[(\pi(\kappa fl) - \pi'(\kappa fl))^2 \right] + \mathbb{E} \left[(\pi'(\kappa l) - \pi(\kappa l))^2 \right] \right).$$

Since $|\kappa l| \leq 1$, we find that

$$\sup_{|f|_\infty \leq 1} \mathbb{E} \left[((\mathcal{A}\pi)(f) - (\mathcal{A}\pi')(f))^2 \right] \leq \frac{4}{\kappa^4} \sup_{|f|_\infty \leq 1} \mathbb{E} \left[(\pi(f) - \pi'(f))^2 \right],$$

and hence

$$d(\mathcal{A}\pi, \mathcal{A}\pi') \leq \frac{2}{\kappa^2} d(\pi, \pi').$$

□

Theorem 11.5 (Convergence of the BPF). *Let Assumption 11.3 hold. Then there exists a $c = c(J, \kappa)$ independent of N such that, for all $j = 1, \dots, J$,*

$$d(\pi_j, \pi_j^N) \leq \frac{c}{\sqrt{N}}.$$

Proof. Let $e_j = d(\pi_j, \pi_j^N)$. Using the triangle inequality,

$$\begin{aligned} e_{j+1} &= d(\pi_{j+1}, \pi_{j+1}^N) = d(\mathcal{A}_j \mathcal{P} \pi_j, \mathcal{A}_j S^N \mathcal{P} \pi_j^N) \\ &\leq d(\mathcal{A}_j \mathcal{P} \pi_j, \mathcal{A}_j \mathcal{P} \pi_j^N) + d(\mathcal{A}_j \mathcal{P} \pi_j^N, \mathcal{A}_j S^N \mathcal{P} \pi_j^N). \end{aligned}$$

Applying the stability bound for \mathcal{A}_j , we have

$$e_{j+1} \leq \frac{2}{\kappa^2} \left[d(\mathcal{P} \pi_j, \mathcal{P} \pi_j^N) + d(\hat{\pi}_j^N, S^N \hat{\pi}_j^N) \right],$$

where $\hat{\pi}_j^N = \mathcal{P}\pi_j^N$. By the stability bound for \mathcal{P} ,

$$d(\mathcal{P}\pi_j, \mathcal{P}\pi_j^N) \leq d(\pi_j, \pi_j^N)$$

and by the consistency bound for S^N ,

$$d(\hat{\pi}_j^N, S^N \hat{\pi}_j^N) \leq \frac{1}{\sqrt{N}}.$$

Therefore,

$$\begin{aligned} e_{j+1} &\leq \frac{2}{\kappa^2} \left(d(\pi_j, \pi_j^N) + \frac{1}{\sqrt{N}} \right) \\ &\leq \frac{2}{\kappa^2} \left(e_j + \frac{1}{\sqrt{N}} \right). \end{aligned}$$

We let $\lambda = 2/\kappa^2$ and note that $\lambda \geq 2$ since $\kappa \in (0, 1]$. Then the discrete Gronwall inequality of Theorem 1.19 gives

$$e_j \leq \lambda^j e_0 + \frac{\lambda}{\sqrt{N}} \frac{1 - \lambda^j}{1 - \lambda}.$$

Recall that $\pi_0^N = \pi_0$ hence $e_0 = 0$. Thus, letting

$$c = \frac{\lambda(1 - \lambda^J)}{1 - \lambda}$$

completes the proof since $\lambda(1 - \lambda^j)/(1 - \lambda)$ is increasing in j . \square

11.4 The Bootstrap Particle Filter as a Random Dynamical System

A nice interpretation of the BPF is to view it as a random dynamical system for a set of interacting particles $\{v_j^{(n)}\}_{n=1}^N$. To this end, a measure

$$\bar{\pi}_j^N(u) = \frac{1}{N} \sum_{n=1}^N \delta(u - v_j^{(n)}) \approx \pi_j^N(u) \approx \pi_j(u)$$

with equally weighted particles may be naturally defined after the resampling step from π_j^N . It can then be seen that the BPF updates the particle positions

$$\{v_j^{(n)}\}_{n=1}^N \mapsto \{v_{j+1}^{(n)}\}_{n=1}^N$$

via the random map

$$\begin{aligned} \hat{v}_{j+1}^{(n)} &= \Psi(v_j^{(n)}) + \xi_j^{(n)}, & \xi_j^{(n)} &\sim \mathcal{N}(0, \Sigma) \text{ i.i.d.}, \\ v_{j+1}^{(n)} &= \sum_{m=1}^N \mathbb{1}_{I_{j+1}^{(m)}}(r_{j+1}^{(n)}) \hat{v}_{j+1}^{(m)}, & r_{j+1}^{(n)} &\sim \text{Uniform}(0, 1) \text{ i.i.d.} \end{aligned}$$

Here the supports $I_j^{(m)}$ of the indicator functions have widths given by the weights appearing in $\pi_j^N(u)$. Specifically, we have

$$I_{j+1}^{(m)} = [\alpha_{j+1}^{(m-1)}, \alpha_{j+1}^{(m)}], \quad \alpha_{j+1}^{(m+1)} = \alpha_{j+1}^{(m)} + w_{j+1}^{(m)}, \quad \alpha_{j+1}^{(0)} = 0.$$

Note that, by construction, $\alpha_j^{(N)} = 1$.

Thus the underlying dynamical system on particles comprises N particles governed by two steps: (i) the underlying stochastic dynamics model, in which the particles do not interact; (ii) a resampling of the resulting collection of particles, to reflect the different weights associated with them, in which the particles do then interact. The interaction is driven by the weights which see all the particle positions, and measure their goodness of fit to the data. Note that the same particle may be replicated more than once through the resampling in (ii) and, relatedly, a particle may disappear through the resampling.

11.5 Discussion and Bibliography

Particle filters are overviewed from an algorithmic viewpoint in [81, 80], and from a more mathematical perspective in [69, 56]. A variety of ways to resample the weights are reviewed and compared in [56]. The convergence of particle filters is addressed in [64]; the clean proof presented here originates in [256] and may also be found in [185]. We refer to [62] for a review paper on convergence results for particle filters. For problems in which the dynamics evolve in relatively low-dimensional spaces they have been enormously successful. However, particle filters often perform poorly in high-dimensional systems due to the fact that the particle weight typically concentrates on one, or a small number, of particles —see [24, 284, 282]. Generalizing them so that they work for the high-dimensional problems that arise, for example, in geophysical applications, provides a major challenge [189].

Chapter 12

Optimal Particle Filter

This chapter is devoted to the Optimal Particle Filter (OPF). Like the Bootstrap Particle Filter (BPF) from the previous chapter, the OPF approximates the filtering distribution by a sum of Dirac masses. But while the BPF is conceptually derived by factorizing the update of the filtering distribution into a prediction and an analysis step, the OPF uses a different factorization which can result in improved performance.

We introduce the decomposition of the filtering update used by the OPF in Section 12.1. The setting will initially be the same as for the BPF (nonlinear stochastic dynamics and nonlinear observations), and in this general setting we will prove a convergence result, similar to that for the BPF from the previous chapter. However, we will see that the OPF cannot be implemented in the fully nonlinear case without additional approximate sampling. For this reason, we will specify in Section 12.2 to the case of linear observations, where the OPF can be implemented in a straightforward fashion, without additional approximate sampling; indeed we will see that in this setting the method may be characterized as a set of interacting 3DVAR filters. Section 12.3 discusses the sense in which the OPF has desirable properties in comparison with the BPF. We close in Section 12.4 with bibliographical remarks.

12.1 The Bootstrap and Optimal Particle Filters Compared

We initially work in the setting in which we introduced filtering and smoothing in Chapter 7, with nonlinear stochastic dynamics and nonlinear observation function, namely the model

$$\begin{aligned} v_{j+1} &= \Psi(v_j) + \xi_j, & \xi_j &\sim \mathcal{N}(0, \Sigma) \text{ i.i.d.}, \\ y_{j+1} &= h(v_{j+1}) + \eta_{j+1}, & \eta_j &\sim \mathcal{N}(0, \Gamma) \text{ i.i.d.}, \end{aligned}$$

with $v_0 \sim \pi_0 := \mathcal{N}(m_0, C_0)$ independent of the i.i.d. sequences $\{\xi_j\}$ and $\{\eta_j\}$. Here $\Psi(\cdot)$ drives the dynamics and $h(\cdot)$ is the observation function. Recall that we denote by $Y_j = \{y_1, \dots, y_j\}$ all the data up to time j and by π_j the pdf of $v_j|Y_j$, that is, $\pi_j = \mathbb{P}(v_j|Y_j)$. The filtering problem is to determine π_{j+1} from π_j .

The fundamental filtering problem that we are interested in is thus determination of $\mathbb{P}(v_{j+1}|Y_{j+1})$ from $\mathbb{P}(v_j|Y_j)$. The BPF is based on applying sampling to the outcome

of the following manipulation:

$$\begin{aligned}
\mathbb{P}(v_{j+1}|Y_{j+1}) &= \mathbb{P}(v_{j+1}|y_{j+1}, Y_j) \\
&= \frac{\mathbb{P}(y_{j+1}|v_{j+1}, Y_j) \mathbb{P}(v_{j+1}|Y_j)}{\mathbb{P}(y_{j+1}|Y_j)} \\
&= \frac{\mathbb{P}(y_{j+1}|v_{j+1}, Y_j)}{\mathbb{P}(y_{j+1}|Y_j)} \int_{\mathbb{R}^d} \mathbb{P}(v_{j+1}|v_j, Y_j) \mathbb{P}(v_j|Y_j) dv_j \\
&= \frac{\mathbb{P}(y_{j+1}|v_{j+1})}{\mathbb{P}(y_{j+1}|Y_j)} \int_{\mathbb{R}^d} \mathbb{P}(v_{j+1}|v_j) \mathbb{P}(v_j|Y_j) dv_j \\
&= \mathcal{A}_j \mathcal{P} \mathbb{P}(v_j|Y_j).
\end{aligned}$$

The Markov kernel \mathcal{P} acts on arbitrary density π by

$$\mathcal{P}\pi(v_{j+1}) = \int_{\mathbb{R}^d} \mathbb{P}(v_{j+1}|v_j) \pi(v_j) dv_j,$$

and \mathcal{A}_j acts on an arbitrary density π by application of Bayes theorem, taking into account the likelihood of the data

$$\mathcal{A}_j \pi(v_{j+1}) = \frac{1}{Z} \mathbb{P}(y_{j+1}|v_{j+1}) \pi(v_{j+1}),$$

with Z normalization to a probability density. The above manipulations are summarized by the relationship

$$\pi_{j+1} = \mathcal{A}_j \mathcal{P} \pi_j. \quad (12.1)$$

Note that in this factorization we apply a Markov kernel and then Bayes theorem. In contrast, to derive the OPF we perform the following manipulation:

$$\begin{aligned}
\mathbb{P}(v_{j+1}|Y_{j+1}) &= \int_{\mathbb{R}^d} \mathbb{P}(v_{j+1}, v_j|Y_{j+1}) dv_j \\
&= \int_{\mathbb{R}^d} \mathbb{P}(v_{j+1}|v_j, Y_{j+1}) \mathbb{P}(v_j|Y_{j+1}) dv_j \\
&= \int_{\mathbb{R}^d} \mathbb{P}(v_{j+1}|v_j, y_{j+1}, Y_j) \mathbb{P}(v_j|y_{j+1}, Y_j) dv_j \\
&= \int_{\mathbb{R}^d} \mathbb{P}(v_{j+1}|v_j, y_{j+1}) \mathbb{P}(v_j|y_{j+1}, Y_j) dv_j \\
&= \int_{\mathbb{R}^d} \mathbb{P}(v_{j+1}|v_j, y_{j+1}) \frac{\mathbb{P}(y_{j+1}|v_j, Y_j)}{\mathbb{P}(y_{j+1}|Y_j)} \mathbb{P}(v_j|Y_j) dv_j \\
&= \int_{\mathbb{R}^d} \mathbb{P}(v_{j+1}|v_j, y_{j+1}) \frac{\mathbb{P}(y_{j+1}|v_j)}{\mathbb{P}(y_{j+1}|Y_j)} \mathbb{P}(v_j|Y_j) dv_j \\
&= \mathcal{P}_j^{OPF} \mathcal{A}_j^{OPF} \mathbb{P}(v_j|Y_j),
\end{aligned}$$

with Markov kernel for particle update

$$\mathcal{P}_j^{OPF} \pi(v_{j+1}) = \int_{\mathbb{R}^d} \mathbb{P}(v_{j+1}|v_j, y_{j+1}) \pi(v_j) dv_j$$

and application of Bayes theorem to include the likelihood

$$\mathcal{A}_j^{OPF} \pi(v_j) = \frac{1}{Z} \mathbb{P}(y_{j+1}|v_j) \pi(v_j).$$

Thus we have

$$\pi_{j+1} = \mathcal{P}_j^{OPF} \mathcal{A}_j^{OPF} \pi_j. \quad (12.2)$$

Note that in the factorization given by OPF we apply Bayes theorem and then a Markov kernel, the opposite order to the BPF. Moreover the propagation mechanism is different—it sees the data through the Markov kernel \mathcal{P}_j^{OPF} —and hence the weighting of the particles is also different: the BPF weights are proportional to the likelihood $\mathbb{P}(y_{j+1}|v_{j+1})$ and the OPF weights are proportional to $\mathbb{P}(y_{j+1}|v_j)$ which may be, in general, not available in closed form. In the BPF, the evolution of the particles and the observation of the data are kept separate from each other—the Markov kernel \mathcal{P} depends only on the dynamics and not the observed data and is thus independent of j . Furthermore, sampling from the Markov kernel \mathcal{P}_j^{OPF} may not be possible and may require further approximation. In the next subsection we will see that these two issues may be overcome when the observation function is linear, and particle updates use a 3DVAR procedure. However in the remainder of this subsection we study particle approximations of (12.2), simply assuming that the OPF weights are computed exactly and that \mathcal{P}_j^{OPF} can be sampled from without approximation.

The natural particle approximation of (12.2), generalizing the BPF from the preceding chapter, is to consider the iteration

$$\pi_{j+1}^N = \mathcal{P}_j^{OPF} S^N \mathcal{A}_j^{OPF} \pi_j^N, \quad \pi_0^N = S^N \pi_0.$$

We refer to this as the OPF. It is possible to show that, under suitable assumptions, the OPF satisfies a convergence result analogous to Theorem 11.5 for the BPF. Here we will analyze a slight modification of the OPF, called the Gaussianized Optimal Particle Filter (GOPF), which reorders the resampling and propagation steps. We first write the resulting algorithm and then establish a convergence result.

The GOPF satisfies the recursion

$$\pi_{j+1}^N = S^N \mathcal{P}_j^{OPF} \mathcal{A}_j^{OPF} \pi_j^N, \quad \pi_0^N = S^N \pi_0.$$

This recursion is similar in spirit to the one we derived for the BPF, but note that the order of the analysis, sampling and prediction steps is different. Our goal now is to show a convergence result for the GOPF. We will make the following assumption, which is analogous to Assumption 11.3 in Chapter 11 for the Bootstrap filter.

Assumption 12.1. *There exists $\kappa \in (0, 1)$ such that, for all $v_j \in \mathbb{R}^d$, and for all $j \in \{0, \dots, J-1\}$,*

$$\kappa \leq \mathbb{P}(y_{j+1}|v_j) \leq \kappa^{-1}.$$

We are ready to establish a convergence result for the GOPF. The proof employs the same distance (5.7) between random probability measures used in Theorem 11.5 to establish convergence for the BPF and in Chapter 5 to study Monte Carlo and importance sampling.

Theorem 12.2 (Convergence of GOPF). *Let Assumption 12.1 hold. Then there is a $c = c(J, \kappa)$ independent of N such that, for all $j = 1 \dots, J$,*

$$d(\pi_j, \pi_j^N) \leq \frac{c}{\sqrt{N}}$$

Proof. Let $e_j = d(\pi_j, \pi_j^N)$. Then,

$$\begin{aligned} e_{j+1} &= d(\pi_{j+1}, \pi_{j+1}^N) \\ &= d(\mathcal{P}_j^{OPF} \mathcal{A}_j^{OPF} \pi_j, S^N \mathcal{P}_j^{OPF} \mathcal{A}_j^{OPF} \pi_j^N) \\ &\leq d(\mathcal{P}_j^{OPF} \mathcal{A}_j^{OPF} \pi_j, \mathcal{P}_j^{OPF} \mathcal{A}_j^{OPF} \pi_j^N) + d(\mathcal{P}_j^{OPF} \mathcal{A}_j^{OPF} \pi_j^N, S^N \mathcal{P}_j^{OPF} \mathcal{A}_j^{OPF} \pi_j^N) \\ &\leq \frac{2}{\kappa^2} e_j + \frac{1}{\sqrt{N}}, \end{aligned}$$

where we have used Lemmas 11.1, 11.2 and Lemma 11.4, replacing Assumption 11.3 by Assumption 12.1 in order to guarantee the stability of \mathcal{A}^{OPF} . The rest of the proof is identical to that of Theorem 11.5. \square

12.2 Implementation: Linear Observation Setting

In general it is not possible to implement the OPF in the fully nonlinear setting because of two computational bottlenecks:

- There may not be a closed formula for evaluating the likelihood $\mathbb{P}(y_{j+1}|v_j)$, making unfeasible the computation of the particle weights.
- It may not be possible to sample from the Markov kernel $\mathbb{P}(v_{j+1}|v_j, y_{j+1})$, making unfeasible the propagation of particles.

However, when the observation function $h(\cdot)$ is linear, i.e. $h(\cdot) = H \cdot$ for some $H \in \mathbb{R}^{k \times d}$, both bottlenecks are overcome. We thus consider the following setting, which arises in many applications:

$$\begin{aligned} v_{j+1} &= \Psi(v_j) + \xi_j, & \xi_j &\sim \mathcal{N}(0, \Sigma) \text{ i.i.d.}, \\ y_{j+1} &= H v_{j+1} + \eta_{j+1}, & \eta_j &\sim \mathcal{N}(0, \Gamma) \text{ i.i.d.}, \end{aligned}$$

with $v_0 \sim \mathcal{N}(m_0, C_0)$ and $v_0, \{\xi_j\}, \{\eta_j\}$ independent. First, note that combining the stochastic dynamics and data models we may write

$$y_{j+1} = H \Psi(v_j) + H \xi_j + \eta_{j+1},$$

which shows that the conditional distribution for y_{j+1} given v_j is

$$\mathbb{P}(y_{j+1}|v_j) = \mathcal{N}(H \Psi(v_j), S),$$

where $S = H \Sigma H^\top + \Gamma$. We will use this formula to compute the weights, thus overcoming the first computational bottleneck.

We now show that, under the linear observation assumption, \mathcal{P}_j^{OPF} is a Gaussian kernel, and hence the second computational bottleneck is overcome too. We have

$$\begin{aligned}\mathbb{P}(v_{j+1}|v_j, y_{j+1}) &\propto \mathbb{P}(y_{j+1}|v_{j+1}, v_j) \mathbb{P}(v_{j+1}|v_j) \\ &= \mathbb{P}(y_{j+1}|v_{j+1}) \mathbb{P}(v_{j+1}|v_j) \\ &\propto \exp\left(-\frac{1}{2}|y_{j+1} - Hv_{j+1}|_\Gamma^2 - \frac{1}{2}|v_{j+1} - \Psi(v_j)|_\Sigma^2\right) \\ &= \exp(-J_{\text{OPT}}(v_{j+1})).\end{aligned}$$

This is a Gaussian distribution for v_{j+1} as

$$J_{\text{OPT}}(v_{j+1}) := \frac{1}{2}|y_{j+1} - Hv_{j+1}|_\Gamma^2 + \frac{1}{2}|v_{j+1} - \Psi(v_j)|_\Sigma^2$$

is quadratic with respect to v_{j+1} .¹ Consequently, we can compute the mean m_{j+1} and covariance C (which, note, is independent of j) of this Gaussian by matching the mean and quadratic terms in the relevant quadratic forms:

$$\begin{aligned}C^{-1} &= H^\top \Gamma^{-1} H + \Sigma^{-1}, \\ C^{-1}m_{j+1} &= \Sigma^{-1}\Psi(v_j) + H^\top \Gamma^{-1}y_{j+1}.\end{aligned}$$

Then $\mathbb{P}(v_{j+1}|y_{j+1}, v_j) = \mathcal{N}(m_{j+1}, C)$. This is hence a special case of 3DVAR in which the analysis covariance is fixed at C ; note that when we derived 3DVAR we fixed the predictive covariance \hat{C} which, here, is fixed at Σ . As with the Kalman filter, and with 3DVAR, it is possible to implement the prediction step through the following mean and covariance formulae which avoid inversion in state-space, and require inversion only in data space:

$$\begin{aligned}m_{j+1} &= (I - KH)\Psi(v_j) + Ky_{j+1}, \\ C &= (I - KH)\Sigma, \\ K &= \Sigma H^\top S^{-1}, \\ S &= H\Sigma H^\top + \Gamma.\end{aligned}$$

Furthermore, as for 3DVAR, the inversion of S need only be performed once in a pre-processing step before the algorithm is run. Since the expression for $\mathbb{P}(v_{j+1}|v_j, y_{j+1})$ is Gaussian we now have the ability to sample directly from \mathcal{P}_j^{OPF} . The OPF is thus given by the following update algorithm for approximations $\pi_j^N \approx \pi_j$ in which we generalize the notational conventions used in the previous chapter to formulate particle filters as random dynamical systems:²

¹ J_{OPT} is identical to J on the right-hand side of Table 9.1, with \hat{C} replaced by Σ .

² The notation used in step 4 for the resampling step was introduced in Subsection 11.4.

Algorithm 12.1 Optimal Particle Filter

- 1: **Input:** Initial distribution $\mathbb{P}(v_0) = \pi_0$, number of particles N .
 - 2: **Initial Sampling:** Draw N particles $v_0^{(n)} \sim \pi_0$ so that $\pi_0^N = S^N \pi_0$.
 - 3: **Subsequent Sampling** For $j = 0, 1, \dots, J-1$, perform:
 1. Set $\hat{v}_{j+1}^{(n)} = (I - KH)\Psi(v_j^{(n)}) + Ky_{j+1} + \zeta_{j+1}^{(n)}$ with $\zeta_{j+1}^{(n)}$ i.i.d. $\mathcal{N}(0, C)$.
 2. Set $\bar{w}_{j+1}^{(n)} = \exp\left(-\frac{1}{2}|y_{j+1} - H\Psi(v_j^{(n)})|_S^2\right)$.
 3. Set $w_{j+1}^{(n)} = \bar{w}_{j+1}^{(n)} / \sum_{n=1}^N \bar{w}_{j+1}^{(n)}$.
 4. Set $v_{j+1}^{(n)} = \sum_{m=1}^N \mathbb{1}_{I_{j+1}^{(m)}}(r_{j+1}^{(n)}) \hat{v}_{j+1}^{(m)}$.
 5. Set $\pi_{j+1}^N(v_{j+1}) = \frac{1}{N} \sum_{n=1}^N \delta(v_{j+1} - v_{j+1}^{(n)})$.
 - 4: **Output:** Particle approximations $\pi_j^N \approx \pi_j$, $j = 1, \dots, J$.
-

The GOPF has a similar form, after a reordering of the sampling and propagation steps: ³

Algorithm 12.2 Gaussianized Optimal Particle Filter

- 1: **Input:** Initial distribution $\mathbb{P}(v_0) = \pi_0$, number of particles N .
 - 2: **Initial Sampling:** Draw N particles $v_0^{(n)} \sim \pi_0$ so that $\pi_0^N = S^N \pi_0$.
 - 3: **Subsequent Sampling** For $j = 0, 1, \dots, J-1$, perform:
 1. Set $\bar{w}_{j+1}^{(n)} = \exp\left(-\frac{1}{2}|y_{j+1} - H\Psi(v_j^{(n)})|_S^2\right)$.
 2. Set $w_{j+1}^{(n)} = \bar{w}_{j+1}^{(n)} / \sum_{n=1}^N \bar{w}_{j+1}^{(n)}$.
 3. Set $\hat{v}_j^{(n)} = \sum_{m=1}^N \mathbb{1}_{I_{j+1}^{(m)}}(r_{j+1}^{(n)}) v_j^{(m)}$.
 4. Set $v_{j+1}^{(n)} = (I - KH)\Psi(\hat{v}_j^{(n)}) + Ky_{j+1} + \zeta_{j+1}^{(n)}$ with $\zeta_{j+1}^{(n)}$ i.i.d. $\mathcal{N}(0, C)$.
 5. Set $\pi_{j+1}^N(v_{j+1}) = \frac{1}{N} \sum_{n=1}^N \delta(v_{j+1} - v_{j+1}^{(n)})$.
 - 4: **Output:** Particle approximations $\pi_j^N \approx \pi_j$, $j = 1, \dots, J$.
-

12.3 “Optimality” of the Optimal Particle Filter

Particle filter methods rely on approximating the distribution for the model by a swarm of Dirac masses; it is clear that the distribution will not be well approximated by only a small number of particles in most cases. Consequently, a performance requirement

³Here again, the resampling step 3 follows the notation introduced in Subsection 11.4.

for particle filter methods is that they do not lead to degeneracy of the particles. Resampling leads to degeneracy if a small number of particles have all the weights. Conversely, non-degeneracy may be promoted by ensuring that the weights $w_j^{(n)}$ are similar in magnitude, so that a small number of particles are not overly favored during the resampling step. This condition can be formulated as a requirement that the variance of the weights be minimized; doing this results in the OPF.

To understand this perspective we consider an arbitrary particle update kernel of the form $\pi(v_{j+1}|v_j^{(n)}, Y_{j+1})$ and we study the resulting particle filter without resampling. It is then the case that the unnormalized particle weights are updated according to the formula

$$\bar{w}_{j+1}^{(n)} = \bar{w}_j^{(n)} \frac{\mathbb{P}(y_{j+1}|v_{j+1}) \mathbb{P}(v_{j+1}|v_j^{(n)})}{\pi(v_{j+1}|v_j^{(n)}, Y_{j+1})}. \quad (12.3)$$

Theorem 12.3 (Meaning of Optimality). *The choice of $\mathbb{P}(v_{j+1}|v_j^{(n)}, y_{j+1})$ as the particle update kernel $\pi(v_{j+1}|v_j^{(n)}, Y_{j+1})$ results in the minimal variance of the weight $w_{j+1}^{(n)}$ with respect to all possible choices of the particle update kernel $\pi(v_{j+1}|v_j^{(n)}, Y_{j+1})$.*

Proof. We calculate the variance of the unnormalized weights (treated as random variables) $\bar{w}_{j+1}^{(n)}$ with respect to the transition density $\pi(v_{j+1}|v_j^{(n)}, Y_{j+1})$ and obtain

$$\begin{aligned} \text{Var}_{\pi(v_{j+1}|v_j^{(n)}, Y_{j+1})}[\bar{w}_{j+1}^{(n)}] &= \int_{\mathbb{R}^d} \left(\bar{w}_{j+1}^{(n)} \right)^2 \pi(v_{j+1}|v_j^{(n)}, Y_{j+1}) dv_{j+1} \\ &\quad - \left[\int_{\mathbb{R}^d} \bar{w}_{j+1}^{(n)} \pi(v_{j+1}|v_j^{(n)}, Y_{j+1}) dv_{j+1} \right]^2 \\ &= \left(\bar{w}_j^{(n)} \right)^2 \int_{\mathbb{R}^d} \frac{\left(\mathbb{P}(y_{j+1}|v_{j+1}) \mathbb{P}(v_{j+1}|v_j^{(n)}) \right)^2}{\pi(v_{j+1}|v_j^{(n)}, Y_{j+1})} dv_{j+1} \\ &\quad - \left(\bar{w}_j^{(n)} \right)^2 \left[\int_{\mathbb{R}^d} \mathbb{P}(y_{j+1}|v_{j+1}) \mathbb{P}(v_{j+1}|v_j^{(n)}) dv_{j+1} \right]^2 \\ &= \left(\bar{w}_j^{(n)} \right)^2 \left[\int_{\mathbb{R}^d} \frac{\left(\mathbb{P}(y_{j+1}|v_{j+1}) \mathbb{P}(v_{j+1}|v_j^{(n)}) \right)^2}{\pi(v_{j+1}|v_j^{(n)}, Y_{j+1})} dv_{j+1} - \mathbb{P}(y_{j+1}|v_j^{(n)})^2 \right]. \end{aligned}$$

Choosing $\pi(v_{j+1}|v_j^{(n)}, Y_{j+1}) = \mathbb{P}(v_{j+1}|v_j^{(n)}, y_{j+1})$, as in the OPF, we obtain

$$\begin{aligned} \text{Var}_{\mathbb{P}(v_{j+1}|v_j^{(n)}, Y_{j+1})}[\bar{w}_{j+1}^{(n)}] &= \left(\bar{w}_j^{(n)} \right)^2 \left[\int_{\mathbb{R}^d} \frac{\left(\mathbb{P}(y_{j+1}|v_{j+1}) \mathbb{P}(v_{j+1}|v_j^{(n)}) \right)^2}{\mathbb{P}(v_{j+1}|v_j^{(n)}, y_{j+1})} dv_{j+1} - \mathbb{P}(y_{j+1}|v_j^{(n)})^2 \right] \\ &= \left(\bar{w}_j^{(n)} \right)^2 \left[\mathbb{P}(y_{j+1}|v_j^{(n)})^2 - \mathbb{P}(y_{j+1}|v_j^{(n)})^2 \right] \\ &= 0. \end{aligned}$$

□

Remark 12.4. Note that directly from (12.3) we can see that choosing $\pi(v_{j+1}|v_j^{(n)}, Y_{j+1}) = \mathbb{P}(v_{j+1}|v_j^{(n)}, y_{j+1})$ gives the weight update

$$\bar{w}_{j+1}^{(n)} = \bar{w}_j^{(n)} \mathbb{P}(y_{j+1}|v_j^{(n)}),$$

which does not depend on the draw $v_{j+1} \sim \mathbb{P}(v_{j+1}|v_j^{(n)}, y_{j+1})$, and is deterministic given y_{j+1} and $v_j^{(n)}$. \diamond

Remark 12.5. The OPF is optimal in the very precise sense of the theorem. Note that no optimality criterion is asserted by this theorem with respect to iterating the particle updates, and in particular when resampling is included. The nomenclature “optimal” should thus be treated with caution. \diamond

Example 12.6 (Linear-Gaussian One-Step Filter). Recall Example 5.8 from Chapter 5. We considered a linear-Gaussian one-dimensional inverse problem with prior $\rho(u) = \mathcal{N}(0, \hat{c}^2)$ and likelihood $\mathbb{P}(y|u) = \mathcal{N}(au, \gamma^2)$, and we showed that the χ^2 divergence between the posterior π and the prior ρ is given by

$$\begin{aligned} \zeta &= d_{\chi^2}(\pi||\rho) + 1 \\ &= \frac{\delta^2 + 1}{\sqrt{2\delta^2 + 1}} \exp\left(\frac{\delta^2}{2\delta^2 + 1} z^2\right), \quad z \sim \mathcal{N}(0, 1), \end{aligned}$$

where $\delta^2 := a^2 \hat{c}^2 / \gamma^2$. It is easy to see that ζ is monotonically increasing as a function of δ . We saw in Chapter 5 that a large χ^2 divergence between target (posterior) and proposal (prior) leads to a poor approximation of the target by reweighing prior samples.

Now we consider a scalar, linear-Gaussian filtering step

$$\begin{aligned} v_1 &= \alpha v_0 + \xi, & v_0 &\sim \mathcal{N}(0, c_0^2), & \xi &\sim \mathcal{N}(0, \sigma^2), \\ y_1 &= h v_1 + \eta, & \eta &\sim \mathcal{N}(0, \gamma^2). \end{aligned}$$

In the analysis step, the BPF updates the prior $\mathbb{P}(v_1) = \mathcal{N}(0, \alpha^2 c_0^2 + \sigma^2)$ with likelihood $\mathbb{P}(y_1|v_1) = \mathcal{N}(h v_1, \gamma^2)$, while the OPF updates the prior $\mathbb{P}(v_0) = \mathcal{N}(0, c_0^2)$ with likelihood $\mathbb{P}(y_1|v_0) = \mathcal{N}(h \alpha v_0, h^2 \sigma^2 + \gamma^2)$. Both bootstrap and optimal analysis steps reweigh samples from their respective priors using their given likelihoods; since in both cases the prior is Gaussian and the observation model is linear, we are in the setting of Example 5.8. Here, the χ^2 divergence between the target and proposal for the bootstrap and optimal filters are determined by

$$\begin{aligned} \delta_{\text{BPF}} &= \frac{h^2 \alpha^2 c_0^2 + h^2 \sigma^2}{\gamma^2}, \\ \delta_{\text{OPF}} &= \frac{h^2 \alpha^2 c_0^2}{h^2 \sigma^2 + \gamma^2}. \end{aligned}$$

Clearly, $\delta_{\text{OPF}} \leq \delta_{\text{BPF}}$, which indicates that the χ^2 divergence between target and proposal is smaller for the optimal than for the bootstrap filter. In particular, note

that in the small observation noise limit $\gamma \rightarrow 0^+$, the χ^2 divergence for the bootstrap filter diverges, while for the optimal filter it remains bounded provided that $h^2\sigma^2 > 0$. In such a small observation noise regime, the OPF is clearly advantageous over the BPF. Finally, it is illustrative to see that the bootstrap and optimal filter agree and $\delta_{\text{BPF}} = \delta_{\text{OPF}}$ if there is no noise in the stochastic dynamics model, i.e. if $\sigma^2 = 0$. \diamond

12.4 Discussion and Bibliography

The OPF is discussed, and further references given, in the paper [80]; see section IID. Throughout much of this chapter we assumed Gaussian additive noise and linear observation function, in which case the prediction step is tractable; the order in which the prediction and resampling is performed can be commuted, leading to the distinction between what we term the GOPF and the OPF. The paper [80] discusses the general setting, beyond that in which Gaussian additive noise and linear observation function are assumed; the idea that the order of prediction and resampling can be commuted was observed in the general setting in [245]. The convergence of the OPF is studied in [157]. The formulation of the bootstrap and optimal particle filters as random dynamical systems may be found in [167].

The performance of the BPF is poor when the filtering distributions are far from the predictive distributions, a situation that arises in high-dimensional or small observation noise filtering settings. In such cases, the update of the weights in the analysis step of the BPF results in a degenerate distribution of weights, with the largest weight being close to 1 [24, 284, 282]. This is the issue that the OPF tries to ameliorate; the papers [283, 5, 271] show calculations which demonstrate the extent to which this amelioration is manifest in theory. In practice, further exploiting decay of correlations through *localization* is often needed. A review of local particle filters can be found in [96] and the paper [256] addresses, from a theoretical viewpoint, the question of whether localization can help to beat the curse of dimension. Attempts to bridge particle filters with ensemble Kalman filters to alleviate the curse of dimension include [101, 287], and the relation between the collapse of ensemble and particle methods is investigated in the paper [216], which also emphasizes the importance of localization.

Part III

Blending Inverse Problems, Data Assimilation, and Machine Learning

Chapter 13

Blending Inverse Problems and Data Assimilation

This chapter brings together the material in the first two parts of these notes, demonstrating how the principles and ideas underpinning the derivation of extended and ensemble Kalman filters for data assimilation can be used to design ensemble Kalman methods for inverse problems. We adopt an optimization perspective to the inverse problem and study gradient-based and ensemble algorithms for the minimization of two objective functions: a *data-misfit* objective defined by a loss function; and a *Tikhonov-Phillips* objective defined by appending the loss term with a regularization term. These objective functions will be introduced in Section 13.1, where we also show that they are particular instances of a general family of nonlinear least-squares objectives. Section 13.2 contains a short overview of Gauss-Newton and Levenberg-Marquardt optimization algorithms for nonlinear least-squares. In Section 13.3 we consider gradient-based extended Kalman methods for both objectives, highlighting their interpretation as standard Gauss-Newton and Levenberg-Marquardt optimization algorithms. Finally, in Section 13.4 we consider ensemble Kalman methods that avoid the calculation of gradients by invoking a statistical linearization defined with an ensemble of particles. The chapter closes in Section 13.5 with extensions and bibliographical remarks.

13.1 Problem Setting and Objective Functions

Recall the inverse problem of finding an unknown $u \in \mathbb{R}^d$ from data $y \in \mathbb{R}^k$, where

$$y = G(u) + \eta, \quad \eta \sim \mathcal{N}(0, \Gamma), \quad (13.1)$$

and G represents a given forward model. We consider an optimization approach to the inverse problem, seeking to recover the unknown u by minimizing a data-misfit or a Tikhonov-Phillips objective function defined, respectively, by

$$J_{\text{DM}}(u) := \frac{1}{2} |y - G(u)|_{\Gamma}^2, \quad J_{\text{TP}}(u) := \frac{1}{2} |y - G(u)|_{\Gamma}^2 + \frac{1}{2} |u - \hat{m}|_{\hat{C}}^2. \quad (13.2)$$

As discussed in Section 3.1 and the examples therein, the data-misfit objective function J_{DM} can be interpreted as a loss function and minimizing it promotes fitting the given data y ; and the Tikhonov-Phillips objective J_{TP} comprises a loss function appended with a regularization term that helps prevent overfitting the data. While in this chapter we focus on the optimization perspective, we recall that in the Bayesian perspective the

regularization term can be interpreted as the negative log-density of a Gaussian prior $\rho(u) = \mathcal{N}(\hat{m}, \hat{C})$, in which case minimizing the Tikhonov-Phillips objective is equivalent to finding the MAP estimator.

The data-misfit and Tikhonov-Phillips objectives are examples of nonlinear least-squares objectives of the general form

$$J(u) = \frac{1}{2}|r(u)|^2. \quad (13.3)$$

To see this, note first that the data-misfit objective can be written in the form

$$J_{\text{DM}}(u) = \frac{1}{2}|r_{\text{DM}}(u)|^2, \quad r_{\text{DM}}(u) := \Gamma^{-1/2}(y - G(u)). \quad (13.4)$$

Secondly, note that the Tikhonov-Phillips objective may be written in the form

$$\begin{aligned} J_{\text{TP}}(u) &= \frac{1}{2}|y - G(u)|_{\Gamma}^2 + \frac{1}{2}|u - \hat{m}|_{\hat{C}}^2 \\ &= \frac{1}{2}|z - h(u)|_Q^2, \end{aligned}$$

where

$$z := \begin{bmatrix} y \\ \hat{m} \end{bmatrix}, \quad h(u) := \begin{bmatrix} G(u) \\ u \end{bmatrix}, \quad Q := \begin{bmatrix} \Gamma & 0 \\ 0 & \hat{C} \end{bmatrix}.$$

Therefore,

$$J_{\text{TP}}(u) = \frac{1}{2}|r_{\text{TP}}(u)|^2, \quad r_{\text{TP}}(u) := Q^{-1/2}(z - h(u)). \quad (13.5)$$

Equations (13.4) and (13.5) show that both the data-misfit and the Tikhonov-Phillips objectives can be written in the general form (13.3).

13.2 Nonlinear-Least Squares Optimization

Gradient-based optimization algorithms for the nonlinear least-squares problem of minimizing (13.3) can be broadly classified into line-search and trust region methods, exemplified by the classical Gauss-Newton and Levenberg-Marquardt algorithms, respectively. We overview each of these in turn.

13.2.1 Gauss-Newton Method

The Gauss-Newton method applied to the general least-squares objective (13.3) is a line-search method which, starting from an initialization u_0 , sets

$$u_{\ell+1} = u_{\ell} + \alpha_{\ell} v_{\ell}, \quad \ell = 0, 1, \dots, L-1,$$

where v_{ℓ} is a search direction defined by

$$v_{\ell} = \arg \min_v J_{\ell}^{\text{lin}}(v), \quad J_{\ell}^{\text{lin}}(v) := \frac{1}{2}|Dr(u_{\ell})v + r(u_{\ell})|^2, \quad (13.6)$$

and $\alpha_\ell > 0$ is a user-chosen step-size parameter. Here and throughout this chapter, Dr will denote the Jacobian of r , which here is assumed to exist. However, a significant outcome of the presentation in this chapter is the derivation of ensemble Kalman formulae for the search direction update, avoiding the need for the calculation of the Jacobian; these ensemble methods can be used when the Jacobian does not exist, or is too expensive to compute.

Our presentation in Sections 13.3 and 13.4 will focus on the derivation of extended and ensemble Kalman formulae, respectively, for the search direction update. Although the choice of step-size is crucial to the efficiency of all Gauss-Newton methods, it is not the focus of these notes. Consequently we introduce algorithms viewing the number L of iterations, and the mechanism for determining the step-size schedule $\{\alpha_\ell\}_{\ell=0}^{L-1}$, as given inputs.

Remark 13.1. In practice each step-size α_ℓ is chosen adaptively based on the current state u_ℓ and search direction v_ℓ . A unifying idea shared by many sophisticated line search strategies is to find an interval of desirable step-sizes and then try out a sequence of candidates within that interval, stopping when certain conditions are satisfied. For instance, a simple condition is to require reduction of J in which case α_ℓ is required to satisfy

$$J(u_\ell + \alpha_\ell v_\ell) < J(u_\ell).$$

However, this condition is not sufficient to guarantee convergence and motivates the stronger Armijo condition: for some constant $c_1 \in (0, 1)$

$$J(u_\ell + \alpha_\ell v_\ell) \leq J(u_\ell) + c_1 \alpha_\ell \langle DJ(u_\ell), v_\ell \rangle.$$

The choice of stopping criteria and adaptive step-sizes will be further discussed in Section 13.5. \diamond

13.2.2 Levenberg-Marquardt Method

The Levenberg-Marquardt method applied to the general least-squares objective (13.3) is a trust region method which, starting from an initialization u_0 , sets

$$u_{\ell+1} = u_\ell + v_\ell, \quad \ell = 0, 1, \dots, L-1,$$

where

$$v_\ell = \arg \min_v J_\ell^{\text{lin}}(v), \quad \text{s.t. } |v|_C^2 \leq \delta_\ell, \quad J_\ell^{\text{lin}}(v) := \frac{1}{2} |Dr(u_\ell)v + r(u_\ell)|^2.$$

Similar to Gauss-Newton methods, the increment v_ℓ is defined as the minimizer of a linearized objective, but now the minimization is constrained to a ball $\{|v|_C^2 \leq \delta_\ell\}$ in which we *trust* that the objective can be replaced by its linearization. For any δ_ℓ there is an $\alpha_\ell \in (0, \infty]$ such that

$$v_\ell = \arg \min_v J_\ell^{\text{uc}}(v),$$

where

$$J_\ell^{\text{uc}}(v) = J_\ell^{\text{lin}}(v) + \frac{1}{2\alpha_\ell} |v|_C^2. \quad (13.7)$$

Objective	Optimization	Gradient Method	Ensemble Method
J_{TP}	Gauss-Newton	IExKF	IEnKF-SL
J_{DM}	Levenberg-Marquardt	ExKI	EnKI-SL
J_{TP}	Levenberg-Marquardt	TExKI	TEnKI-SL

Table 13.1 Summary of the algorithms considered in this chapter.

The parameter $\alpha_\ell \in (0, \infty]$ acts as a Lagrange multiplier and plays an analogous role to the step-size in Gauss-Newton methods. We study Levenberg-Marquardt methods from the perspective of the unconstrained minimization problem for J_ℓ^{UC} given by (13.7). Our presentation in Sections 13.3 and 13.4 will focus on the derivation of Kalman formulae for the increments v_ℓ . As for Gauss-Newton methods, we view the number L of iterations and the mechanism for determining the step-size schedule $\{\alpha_\ell\}_{\ell=0}^{L-1}$ as inputs to the algorithms we state here.

Remark 13.2. In practice, the parameter δ_ℓ is chosen adaptively, for instance by monitoring the ratio

$$s_\ell = \frac{J(u_\ell) - J(u_\ell + v_\ell)}{Q(0) - Q(v_\ell)},$$

where $Q(v)$ is a quadratic approximation to $J(u_\ell + v)$. If s_ℓ is close to 1, this indicates that the objective (13.3) can be well approximated by a quadratic in a neighborhood of size δ_ℓ around u_ℓ , and thus that the next trust region can be enlarged. On the other hand, if s_ℓ is small, we may shrink the trust region in the next iteration. The choice of stopping criteria and adaptive step-sizes will be further discussed in Section 13.5. \diamond

Note that the Levenberg-Marquardt increment is the unconstrained minimizer of a *regularized* objective. It is for this reason that we say that Levenberg-Marquardt provides an implicit regularization. This regularization helps avoid overfitting when applied to the data-misfit objective which, unlike the Tikhonov-Phillips objective, is not regularized. On the other hand, Gauss-Newton methods do not provide implicit regularization and therefore should not be applied to the data-misfit objective when solving ill-posed inverse problems. We will therefore focus on gradient and ensemble methods that arise from the following three choices of objective function and optimization algorithm (see Table 13.1):

1. Tikhonov-Phillips and Gauss-Newton, leading to Iterative Extended and Iterative Ensemble Kalman Filters (IExKF and IEnKF-SL);
2. Data-misfit and Levenberg-Marquardt, leading to Extended and Ensemble Kalman Inversion (ExKI and EnKI-SL); and
3. Tikhonov-Phillips and Levenberg-Marquardt, leading to Tikhonov Extended and Tikhonov Ensemble Kalman Inversion (TExKI and TEnKI-SL).

Gradient methods will be introduced in Section 13.3 while their ensemble counterparts will be introduced in Section 13.4.

13.3 Extended Kalman Methods

In this section we derive closed formulae for the Gauss-Newton method applied to the Tikhonov-Phillips objective J_{TP} , as well as for the Levenberg-Marquardt method applied to the data-misfit objective J_{DM} and the Tikhonov-Phillips objective J_{TP} . These formulae are the basis for the ensemble methods considered in the next section.

Since the search directions of Gauss-Newton and Levenberg-Marquardt methods are found by minimizing a linearization of the objective, it is instructive to consider first linear least-squares optimization before delving into the nonlinear setting. The following result characterizes the minimizer m of the Tikhonov-Phillips objective J_{TP} in the case of linear $G(u) = Au$. Note that it is a consequence of completing the square and is derived in the linear-Gaussian setting for inverse problems studied in Chapter 2; we record it here as it will be used extensively in this chapter.

Lemma 13.3. *It holds that*

$$\frac{1}{2}|y - Au|_{\Gamma}^2 + \frac{1}{2}|u - \hat{m}|_{\hat{C}}^2 = \frac{1}{2}|u - m|_C^2 + \beta, \quad (13.8)$$

where β does not depend on u , and

$$C^{-1} = A^{\top} \Gamma^{-1} A + \hat{C}^{-1}, \quad (13.9)$$

$$C^{-1}m = A^{\top} \Gamma^{-1} y + \hat{C}^{-1} \hat{m}. \quad (13.10)$$

Equivalently,

$$m = \hat{m} + K(y - A\hat{m}), \quad (13.11)$$

$$C = (I - KA)\hat{C}, \quad (13.12)$$

where K is the Kalman gain matrix given by

$$K = \hat{C}A^{\top}(A\hat{C}A^{\top} + \Gamma)^{-1} = CA^{\top}\Gamma^{-1}. \quad (13.13)$$

Proof. The formulae (13.9) and (13.10) follow by matching linear and quadratic coefficients in u between

$$\frac{1}{2}|u - m|_C^2 \quad \text{and} \quad \frac{1}{2}|u - \hat{m}|_{\hat{C}}^2 + \frac{1}{2}|y - Au|_{\Gamma}^2. \quad (13.14)$$

The formulae (13.11) and (13.12) as well as the equivalent expressions for the Kalman gain K in Equation (13.13) can be obtained using the Woodbury matrix identity, Lemma 8.5. \square

13.3.1 Iterative Extended Kalman Filter (IExKF)

In this subsection we introduce two ways of writing the Gauss-Newton update applied to the Tikhonov-Phillips objective J_{TP} . In order to apply the Gauss-Newton method to the Tikhonov-Phillips objective, we use (13.5). The following result is a direct consequence of Lemma 13.3.

Lemma 13.4. *The Gauss-Newton method applied to the Tikhonov-Phillips objective J_{TP} admits the characterizations:*

$$u_{\ell+1} = u_{\ell} + \alpha_{\ell} C_{\ell} \left(G_{\ell}^{\top} \Gamma^{-1} (y - G(u_{\ell})) + \hat{C}^{-1} (\hat{m} - u_{\ell}) \right), \quad (13.15)$$

and

$$u_{\ell+1} = u_{\ell} + \alpha_{\ell} \left(K_{\ell} (y - G(u_{\ell})) + (I - K_{\ell} G_{\ell}) (\hat{m} - u_{\ell}) \right), \quad (13.16)$$

where $G_{\ell} = DG(u_{\ell})$ and

$$\begin{aligned} K_{\ell} &= \hat{C} G_{\ell}^{\top} (G_{\ell} \hat{C} G_{\ell}^{\top} + \Gamma)^{-1}, \\ C_{\ell} &= (I - K_{\ell} G_{\ell}) \hat{C}. \end{aligned}$$

Proof. The search direction v_{ℓ} of Gauss-Newton for the objective J_{TP} is given by

$$v_{\ell} = \arg \min_v \frac{1}{2} |Dr_{\text{TP}}(u_{\ell})v + r_{\text{TP}}(u_{\ell})|^2 \quad (13.17)$$

$$= \arg \min_v \frac{1}{2} |z - h(u_{\ell}) - Dh(u_{\ell})v|_Q^2 \quad (13.18)$$

$$= \arg \min_v \left\{ \frac{1}{2} |y - G(u_{\ell}) - DG(u_{\ell})v|_{\Gamma}^2 + \frac{1}{2} |v - (\hat{m} - u_{\ell})|_{\hat{C}}^2 \right\}. \quad (13.19)$$

Applying Lemma 13.3, using formulae (13.10) and (13.12), we deduce that

$$v_{\ell} = C_{\ell} \left(G_{\ell}^{\top} \Gamma^{-1} (y - G(u_{\ell})) + \hat{C}^{-1} (\hat{m} - u_{\ell}) \right),$$

which establishes the characterization (13.15). The equivalence between (13.15) and (13.16) follows from the identity (13.13), which implies that $C_{\ell} G_{\ell}^{\top} \Gamma^{-1} = K_{\ell}$ and $C_{\ell} \hat{C}^{-1} = I - K_{\ell} G_{\ell}$. \square

We refer to the Gauss-Newton method applied to J_{TP} as the Iterative Extended Kalman Filter (IExKF) algorithm. Discussion of how to choose the step-sizes adaptively can be found in Section 13.5.

Algorithm 13.1 Iterative Extended Kalman Filter (IExKF)

1: **Input:** Initialization $u_0 = \hat{m}$, rule for choosing the step-sizes $\{\alpha_\ell\}_{\ell=0}^{L-1}$.

2: For $\ell = 0, 1, \dots, L-1$ do:

1. Set $K_\ell = \hat{C}G_\ell^\top(G_\ell\hat{C}G_\ell^\top + \Gamma)^{-1}$, $G_\ell = DG(u_\ell)$.

2. Set

$$u_{\ell+1} = u_\ell + \alpha_\ell \left(K_\ell(y - G(u_\ell)) + (I - K_\ell G_\ell)(\hat{m} - u_\ell) \right). \quad (13.20)$$

3: **Output:** u_1, u_2, \dots, u_L .

The next proposition shows that in the linear case, if $\alpha_\ell = 1$ for all $\ell \geq 0$, IExKF finds the minimizer of the objective (13.2) in one iteration, and further iterations still stay at the minimizer.

Proposition 13.5. *Suppose that $G(u) = Au$ is linear and that $\alpha_\ell = 1$ for all $\ell \geq 0$. Then the output of Algorithm 13.1 satisfies*

$$u_\ell = m, \quad \ell = 1, 2, \dots$$

where m is the minimizer of the Tikhonov-Phillips objective (13.2).

Proof. In the linear case we have

$$G_\ell = A, \quad K_\ell = K = \hat{C}A^\top(A\hat{C}A^\top + \Gamma)^{-1}, \quad \ell = 0, 1, \dots$$

Therefore, update (13.20) simplifies as

$$u_{\ell+1} = \hat{m} + K(y - A\hat{m}), \quad \ell = 0, 1, \dots$$

This implies that, for all $\ell \geq 1$, it holds that $u_\ell = m$ with m defined in (13.11). \square

13.3.2 Extended Kalman Inversion (ExKI)

In this subsection we study the application of the Levenberg-Marquardt algorithm to the data-misfit objective J_{DM} . In order to apply the Levenberg-Marquardt method to the data-misfit objective J_{DM} , recall that this objective can be written in standard nonlinear least-squares form:

$$J_{\text{DM}}(u) = \frac{1}{2}|r_{\text{DM}}(u)|^2, \quad r_{\text{DM}}(u) := \Gamma^{-1/2}(y - G(u)). \quad (13.21)$$

Lemma 13.6. *The Levenberg-Marquardt method applied to the data-misfit objective J_{DM} admits the following characterization:*

$$u_{\ell+1} = u_\ell + K_\ell(y - G(u_\ell)), \quad (13.22)$$

where

$$K_\ell = \alpha_\ell \hat{C}G_\ell^\top(\alpha_\ell G_\ell \hat{C}G_\ell^\top + \Gamma)^{-1}, \quad G_\ell = DG(u_\ell).$$

Proof. Note that the increment v_ℓ is defined as the unconstrained minimizer of

$$\begin{aligned} J_{\text{DM},\ell}^{\text{UC}}(v) &= \frac{1}{2} |Dr_{\text{DM}}(u_\ell)v + r_{\text{DM}}(u_\ell)|^2 + \frac{1}{2\alpha_\ell} |v|_{\widehat{C}}^2 \\ &= \frac{1}{2} |y - G(u_\ell) - DG(u_\ell)v|_\Gamma^2 + \frac{1}{2\alpha_\ell} |v|_{\widehat{C}}^2. \end{aligned} \quad (13.23)$$

The result follows from Lemma 13.3. \square

The previous lemma motivates the following Extended Kalman Inversion (ExKI) algorithm. Discussion of how to choose the step-sizes adaptively can be found in Section 13.5.

Algorithm 13.2 Extended Kalman Inversion (ExKI)

- 1: **Input:** Initialization $u_0 = \widehat{m}$, rule for choosing the step-sizes $\{\alpha_\ell\}_{\ell=0}^{L-1}$.
- 2: For $\ell = 0, 1, \dots, L-1$ do:

1. Set $K_\ell = \alpha_\ell \widehat{C} G_\ell^\top (\alpha_\ell G_\ell \widehat{C} G_\ell^\top + \Gamma)^{-1}$, $G_\ell = DG(u_\ell)$.
2. Set

$$u_{\ell+1} = u_\ell + K_\ell (y - G(u_\ell)). \quad (13.24)$$

- 3: **Output:** u_1, u_2, \dots, u_L .
-

When $\alpha_0 = 1$, the following linear-case result shows that ExKI reaches the minimizer of J_{TP} in one iteration. However, in contrast to IExKF, further iterations of ExKI will typically no longer agree with the minimizer of J_{TP} .

Proposition 13.7. *Suppose that $G(u) = Au$ is linear and $\alpha_0 = 1$. Then the output of Algorithm 13.2 satisfies*

$$u_1 = \arg \min_u J_{\text{TP}}(u),$$

where J_{TP} is the Tikhonov-Phillips objective (13.2).

Proof. The proof is identical to that of Proposition 13.5, noting that in the linear case $u_{\ell+1} = u_\ell + K(y - Au_\ell)$. \square

13.3.3 Tikhonov Extended Kalman Inversion (TExKI)

In this subsection we describe the application of the Levenberg-Marquardt algorithm to the Tikhonov-Phillips objective J_{TP} .

Lemma 13.8. *The Levenberg-Marquardt method applied to the Tikhonov-Phillips objective J_{TP} admits the following characterization:*

$$u_{\ell+1} = u_\ell + K_\ell (z - h(u_\ell)),$$

where

$$K_\ell = \alpha_\ell \widehat{C} H_\ell^\top (\alpha_\ell H_\ell \widehat{C} H_\ell^\top + Q)^{-1}, \quad H_\ell = Dh(u_\ell).$$

Proof. Note that the increment v_ℓ is defined as the unconstrained minimizer of

$$\mathbf{J}_{\text{TP},\ell}^{\text{UC}}(v) = \mathbf{J}_{\text{TP},\ell}^\ell(v) + \frac{1}{2\alpha_\ell}|v|_{\hat{C}}^2 \quad (13.25)$$

$$= \frac{1}{2}|z - h(u_\ell) - Dh(u_\ell)v|_Q^2 + \frac{1}{2\alpha_\ell}|v|_{\hat{C}}^2. \quad (13.26)$$

This has the form of Equation (13.23), replacing y with z , G with h , and Γ with Q . \square

The previous lemma motivates the following Tikhonov Extended Kalman Inversion (TExKI) algorithm. Discussion of how to choose the step-sizes adaptively can be found in Section 13.5.

Algorithm 13.3 Tikhonov Extended Kalman Inversion (TExKI)

Input: Initialization $u_0 = \hat{m}$, rule for choosing the step-sizes $\{\alpha_\ell\}_{\ell=0}^{L-1}$.

For $\ell = 0, 1, \dots, L-1$ do:

1. Set $K_\ell = \alpha_\ell \hat{C} H_\ell^\top (\alpha_\ell H_\ell \hat{C} H_\ell^\top + Q)^{-1}$, $H_\ell = Dh(u_\ell)$.
2. Set

$$u_{\ell+1} = u_\ell + K_\ell(z - h(u_\ell)). \quad (13.27)$$

Output: u_1, u_2, \dots, u_L .

When $\alpha_0 = 1$, the following linear-case result shows that TExKI reaches in one iteration the minimizer of a \mathbf{J}_{TP} objective appended with an additional regularization term.

Proposition 13.9. *Suppose that $G(u) = Au$ is linear and $\alpha_0 = 1$. Then the output of Algorithm 13.2 satisfies*

$$u_1 = \arg \min_u \left(\mathbf{J}_{\text{TP}}(u) + \frac{1}{2}|u - \hat{m}|_{\hat{C}}^2 \right),$$

where \mathbf{J}_{TP} is the Tikhonov-Phillips objective (13.2).

Proof. Notice that setting $H = \begin{bmatrix} A \\ I \end{bmatrix}$ we have

$$u_1 = \hat{m} + \hat{C} H^\top (H \hat{C} H^\top + Q)^{-1} (z - H \hat{m}).$$

Lemma 13.3 then implies that u_1 minimizes

$$\frac{1}{2}|z - Hu|_Q^2 + \frac{1}{2}|u - \hat{m}|_{\hat{C}}^2,$$

which implies the result. \square

Remark 13.10. It is illustrative to compare Propositions 13.5, 13.7, and 13.9. These results show that in a linear setting: (i) IExKF reaches in one iteration the minimizer of \mathbf{J}_{TP} , and that further iterates remain at the minimizer; (ii) ExKI reaches in one iteration the minimizer of \mathbf{J}_{TP} ; and (iii) TExKI reaches in one iteration the minimizer of a \mathbf{J}_{TP} objective appended with an additional regularization term. \diamond

13.4 Ensemble Kalman Methods

In this section we review three subfamilies of iterative methods that update an ensemble $\{u_\ell^{(n)}\}_{n=1}^N$ employing Kalman-based formulae, where $\ell = 0, 1, \dots$ denotes the iteration index and N is a fixed ensemble size. Each ensemble member $u_\ell^{(n)}$ is updated by optimizing an objective defined using the current ensemble $\{u_\ell^{(n)}\}_{n=1}^N$. The optimization is performed without evaluating derivatives by invoking a *statistical linearization* of a Gauss-Newton or Levenberg-Marquardt algorithm. In analogy with the previous section, the three subfamilies of ensemble methods we consider differ in the choice of the objective and in the choice of the optimization algorithm.

Given an ensemble $\{u_\ell^{(n)}\}_{n=1}^N$ we use the following notation for ensemble empirical means

$$m_\ell := \frac{1}{N} \sum_{n=1}^N u_\ell^{(n)}, \quad \bar{G}_\ell := \frac{1}{N} \sum_{n=1}^N G(u_\ell^{(n)}),$$

and empirical covariances and cross-covariances

$$\begin{aligned} \hat{C}_\ell^{uu} &:= \frac{1}{N} \sum_{n=1}^N (u_\ell^{(n)} - m_\ell)(u_\ell^{(n)} - m_\ell)^\top, \\ \hat{C}_\ell^{uy} &:= \frac{1}{N} \sum_{n=1}^N (u_\ell^{(n)} - m_\ell)(G(u_\ell^{(n)}) - \bar{G}_\ell)^\top, \\ \hat{C}_\ell^{yy} &:= \frac{1}{N} \sum_{n=1}^N (G(u_\ell^{(n)}) - \bar{G}_\ell)(G(u_\ell^{(n)}) - \bar{G}_\ell)^\top. \end{aligned}$$

Here and in what follows $(\hat{C}_\ell^{uu})^{-1}$ denotes the pseudoinverse of \hat{C}_ℓ^{uu} .

The overarching theme that underlies the derivation of the ensemble methods studied in this section is the use of statistical linearization to avoid evaluation of derivatives. The idea behind statistical linearization is this: if $G(u) = Au$ is linear, we have

$$\hat{C}_\ell^{uy} = \hat{C}_\ell^{uu} A^\top.$$

Thus, if \hat{C}_ℓ^{uu} is invertible, $A = (\hat{C}_\ell^{uy})^\top (\hat{C}_\ell^{uu})^{-1}$. Here and in what follows $(\hat{C}_\ell^{uu})^{-1}$ denotes the inverse of \hat{C}_ℓ^{uu} if this inverse exists, and the pseudoinverse otherwise. Noting that A is the derivative of $G(\cdot)$ in the linear case, this calculation motivates the following *approximation* in the general nonlinear case:

$$DG(u_\ell^{(n)}) \approx G_\ell := (\hat{C}_\ell^{uy})^\top (\hat{C}_\ell^{uu})^{-1}, \quad n = 1, \dots, N, \quad (13.28)$$

Note that (13.28) gives the same approximation of the derivative for every particle n , and indeed that it leads to an approximation that may be used at any point.

Other useful approximations follows from this. For example, note that the exact gradient of $J_{\text{DM}}(u)$ from (13.2) is given by

$$\nabla J_{\text{DM}}(u) = DG(u)^\top \Gamma^{-1}(y - G(u)).$$

This suggests the approximation, for G_ℓ given by (13.28),

$$\nabla J_{\text{DM}}(u_\ell^{(n)}) \approx G_\ell^\top \Gamma^{-1} (y - G(u_\ell^{(n)})), \quad (13.29a)$$

$$= (\hat{C}_\ell^{uu})^{-1} \hat{C}_\ell^{uy} \Gamma^{-1} (y - G(u_\ell^{(n)})). \quad (13.29b)$$

13.4.1 Iterative Ensemble Kalman Filter with Statistical Linearization (IEnKF-SL)

Given an ensemble $\{u_\ell^{(n)}\}_{n=1}^N$, consider the following Gauss-Newton update for each n :

$$u_{\ell+1}^{(n)} = u_\ell^{(n)} + \alpha_\ell v_\ell^{(n)}, \quad (13.30)$$

where $\alpha_\ell > 0$ is the step-size, and $v_\ell^{(n)}$ is the minimizer of the following (linearized) Tikhonov-Phillips objective (see (13.19))

$$J_{\text{TP},\ell}^{(n)}(v) = \frac{1}{2} |y - G(u_\ell^{(n)}) - G_\ell v|_\Gamma^2 + \frac{1}{2} |\hat{m} - u_\ell^{(n)} - v|_{\hat{C}}^2. \quad (13.31)$$

It is important to appreciate that we adopt the statistical linearization (13.28) in the above formulation. This couples the different objective functions $J_{\text{TP},\ell}^{(n)}$ indexed by ℓ . Applying Lemma 13.3, the minimizer $v_\ell^{(n)}$ of $J_{\text{TP},\ell}^{(n)}$ can be calculated as

$$v_\ell^{(n)} = C_\ell \left(G_\ell^\top \Gamma^{-1} (y - G(u_\ell^{(n)})) + \hat{C}^{-1} (\hat{m} - u_\ell^{(n)}) \right), \quad (13.32)$$

or, in an equivalent form,

$$v_\ell^{(n)} = K_\ell (y - G(u_\ell^{(n)})) + (I - K_\ell G_\ell) (\hat{m} - u_\ell^{(n)}), \quad (13.33)$$

where

$$C_\ell = (G_\ell^\top \Gamma^{-1} G_\ell + \hat{C}^{-1})^{-1},$$

$$K_\ell = \hat{C} G_\ell^\top (G_\ell \hat{C} G_\ell^\top + \Gamma)^{-1}.$$

Crucially each $v_\ell^{(n)}$ depends on all the $\{u_\ell^{(m)}\}_{m=1}^N$.

Combining (13.30) and (13.33) leads to the Iterative Ensemble Kalman Filter with Statistical Linearization (IEnKF-SL) algorithm. Discussion on how to choose the step-sizes adaptively can be found in Section 13.5.

Algorithm 13.4 Iterative Ensemble Kalman Filter with Statistical Linearization

Input: Initial ensemble $\{u_0^{(n)}\}_{n=1}^N$ sampled from $\mathcal{N}(\hat{m}, \hat{C})$, rule for choosing the step-sizes $\{\alpha_\ell\}_{\ell=0}^{L-1}$.

For $\ell = 0, 1, \dots, L-1$ do:

1. Set $K_\ell = \hat{C}G_\ell^\top (G_\ell \hat{C}G_\ell^\top + \Gamma)^{-1}$, $G_\ell = (\hat{C}_\ell^{uy})^\top (\hat{C}_\ell^{uu})^{-1}$.
2. Set

$$u_{\ell+1}^{(n)} = u_\ell^{(n)} + \alpha_\ell \left(K_\ell (y - G(u_\ell^{(n)})) + (I - K_\ell G_\ell)(\hat{m} - u_\ell^{(n)}) \right), \quad 1 \leq n \leq N. \quad (13.34)$$

Output: Ensemble means m_1, m_2, \dots, m_L .

Notice that IEnKF-SL is a natural ensemble-based version of the derivative-based IExKF Algorithm 13.1 with update (13.20). Other statistical linearizations and approximations of the Gauss-Newton scheme are possible.

13.4.2 Ensemble Kalman Inversion with Statistical Linearization (EnKI-SL)

Given an ensemble $\{u_\ell^{(n)}\}_{n=1}^N$, consider the following Levenberg-Marquardt update for each n :

$$u_{\ell+1}^{(n)} = u_\ell^{(n)} + v_\ell^{(n)}, \quad (13.35)$$

where $v_\ell^{(n)}$ is the minimizer of the following regularized (linearized) data-misfit objective (see (13.23))

$$J_{\text{DM},\ell}^{(n),\text{UC}}(v) = \frac{1}{2} |y - G(u_\ell^{(n)}) - G_\ell v|_\Gamma^2 + \frac{1}{2\alpha_\ell} |v|_{\hat{C}}^2, \quad (13.36)$$

and $\alpha_\ell > 0$ will be regarded as a step-size. Notice that we adopt the statistical linearization (13.28) in the above formulation. Applying Lemma 13.3, we can calculate the minimizer $v_\ell^{(n)}$ explicitly:

$$v_\ell^{(n)} = (G_\ell^\top \Gamma^{-1} G_\ell + \alpha_\ell^{-1} \hat{C}^{-1})^{-1} G_\ell^\top \Gamma^{-1} (y - G(u_\ell^{(n)})), \quad (13.37)$$

or, in an equivalent form,

$$v_\ell^{(n)} = \hat{C}G_\ell^\top (G_\ell \hat{C}G_\ell^\top + \alpha_\ell^{-1} \Gamma)^{-1} (y - G(u_\ell^{(n)})). \quad (13.38)$$

As in the preceding subsection, each $v_\ell^{(n)}$ depends on all the $\{u_\ell^{(m)}\}_{m=1}^N$. This leads to the Ensemble Kalman Inversion (EnKI-SL) with Statistical Linearization method. Discussion of how to choose the step-sizes adaptively can be found in Section 13.5.

Algorithm 13.5 Ensemble Kalman Inversion with Statistical Linearization

Input: Initial ensemble $\{u_0^{(n)}\}_{n=1}^N$ sampled from $\mathcal{N}(\widehat{m}, \widehat{C})$, rule for choosing the step-sizes $\{\alpha_\ell\}_{\ell=0}^{L-1}$.

For $\ell = 0, 1, \dots, L-1$ do:

1. Set $K_\ell = \widehat{C} G_\ell^\top (G_\ell \widehat{C} G_\ell^\top + \alpha_\ell^{-1} \Gamma)^{-1}$, $G_\ell = (\widehat{C}_\ell^{uy})^\top (\widehat{C}_\ell^{uu})^{-1}$.

2. Set

$$u_{\ell+1}^{(n)} = u_\ell^{(n)} + K_\ell (y - G(u_\ell^{(n)})), \quad 1 \leq n \leq N. \quad (13.39)$$

Output: Ensemble means m_1, m_2, \dots, m_L .

Notice that EnKI-SL is a natural ensemble-based version of the derivative-based ExKI Algorithm 13.2.

13.4.3 Tikhonov Ensemble Kalman Inversion with Statistical Linearization (TENKI-SL)

Recall that we define

$$z := \begin{bmatrix} y \\ \widehat{m} \end{bmatrix}, \quad h(u) := \begin{bmatrix} G(u) \\ u \end{bmatrix}, \quad Q := \begin{bmatrix} \Gamma & 0 \\ 0 & \widehat{C} \end{bmatrix}.$$

Then, given an ensemble $\{u_\ell^{(n)}\}_{n=1}^N$, we can define

$$\bar{h}_\ell := \frac{1}{N} \sum_{n=1}^N h(u_\ell^{(n)}),$$

and empirical covariances

$$\begin{aligned} \widehat{C}_\ell^{zz} &:= \frac{1}{N} \sum_{n=1}^N (h(u_\ell^{(n)}) - \bar{h}_\ell)(h(u_\ell^{(n)}) - \bar{h}_\ell)^\top, \\ \widehat{C}_\ell^{uz} &:= \frac{1}{N} \sum_{n=1}^N (u_\ell^{(n)} - m_\ell)(h(u_\ell^{(n)}) - \bar{h}_\ell)^\top. \end{aligned}$$

Furthermore, we define the statistical linearization H_ℓ :

$$Dh(u_\ell^{(n)}) \approx (\widehat{C}_\ell^{uz})^\top (\widehat{C}_\ell^{uu})^{-1} =: H_\ell. \quad (13.40)$$

Notice that

$$H_\ell = \begin{bmatrix} G_\ell \\ I \end{bmatrix},$$

with G_ℓ defined in (13.28).

Given an ensemble $\{u_\ell^{(n)}\}_{n=1}^N$, consider the following Levenberg-Marquardt update for each n :

$$u_{\ell+1}^{(n)} = u_\ell^{(n)} + v_\ell^{(n)},$$

where $v_\ell^{(n)}$ is the minimizer of the following regularized (linearized) Tikhonov-Phillips objective (see (13.26))

$$J_{\text{TP},\ell}^{(n),\text{UC}}(v) = \frac{1}{2} \|z - h(u_\ell^{(n)}) - H_\ell v\|_Q^2 + \frac{1}{2\alpha_\ell} \|v\|_{\hat{C}}^2, \quad (13.41)$$

and $\alpha_\ell > 0$ will be regarded as a step-size. We can calculate the minimizer $v_\ell^{(n)}$ explicitly, applying Lemma 13.3:

$$v_\ell^{(n)} = (H_\ell^\top Q^{-1} H_\ell + \alpha_\ell^{-1} \hat{C}^{-1})^{-1} H_\ell^\top Q^{-1} (z - h(u_\ell^{(n)})), \quad (13.42)$$

or, in an equivalent form,

$$v_\ell^{(n)} = \hat{C} H_\ell^\top (G_\ell \hat{C} H_\ell^\top + \alpha_\ell^{-1} Q)^{-1} (z - h(u_\ell^{(n)})). \quad (13.43)$$

Once again each $v_\ell^{(n)}$ depends on all the $\{u_\ell^{(m)}\}_{m=1}^N$.

This leads to Tikhonov Ensemble Kalman Inversion with Statistical Linearization (TEnKI-SL), described in Algorithm 13.6. Discussion on how to choose the step-sizes adaptively can be found in Section 13.5.

Algorithm 13.6 Tikhonov Ensemble Kalman Inversion with Statistical Linearization

Input: Initial ensemble $\{u_0^{(n)}\}_{n=1}^N$ sampled from $\mathcal{N}(m, P)$, rule for choosing the step-sizes $\{\alpha_\ell\}_{\ell=0}^{L-1}$.

For $\ell = 0, 1, \dots, L-1$ do:

1. Set $K_\ell = \hat{C} H_\ell^\top (G_\ell \hat{C} H_\ell^\top + \alpha_\ell^{-1} Q)^{-1}$, $H_\ell = (\hat{C}_\ell^{uz})^\top (\hat{C}_\ell^{uu})^{-1}$
2. Set

$$u_{\ell+1}^{(n)} = u_\ell^{(n)} + K_\ell (z - h(u_\ell^{(n)})), \quad 1 \leq n \leq N. \quad (13.44)$$

Output: Ensemble means m_1, m_2, \dots, m_L .

Notice that TEnKI-SL is a natural ensemble-based version of the derivative-based TExKI Algorithm 13.3.

13.5 Discussion and Bibliography

The presentation in this chapter follows the conceptual approach to this subject in the paper [51]: Kalman methods for inverse problems are studied from the optimization perspective, and classified in terms of the objective function they seek to minimize and the nonlinear least-squares optimization algorithm they are based on. For background on nonlinear least-squares optimization we refer to [227, 74] where, in particular, a detailed discussion on the adaptive choice of the step-size parameters can be found; note that the algorithms stated in this chapter have been agnostic regarding the step-size choice strategy as we have concentrated on the use of ideas from Kalman filtering within optimization. Furthermore, following the presentation in [51], we have considered only nonlinear least-squares objectives and quadratic regularizers. However, ensemble Kalman

methods for inverse problems that use other objective functions (or loss functions) and other regularizers are starting to emerge; in particular cross-entropy loss [176], logistic loss [241] and regularizers that promote sparsity [188, 278, 171] have all been considered.

There are a number of other ways in which Kalman filtering methods may be used to study inverse problems. The review article [42] emphasizes the Bayesian approach to inversion and, in particular, shows how ideas from the sequential Monte Carlo (SMC) [70] approach to Bayesian inversion can be adapted to the use of ensemble Kalman methods. This possibility is highlighted in the paper [257], which is focused on sequential data assimilation; note, however, that the analysis step (7.3) in sequential data assimilation requires solution of a Bayesian inverse problem and thus the ideas in that paper are relevant for inverse problems in general, beyond data assimilation. The reader interested in the use of SMC for inverse problems is directed to the papers [165, 23] and the references therein; the former paper demonstrates use of the methodology for an inverse problem arising from the Navier-Stokes equation, and the latter paper contains a simple proof of convergence of the particle filter in the context of SMC for inverse problems, following the analysis in [256] for particle filters in sequential data assimilation.

Another class of methods for inverse problems, which may be applied in both the optimization and Bayesian approaches, revolves around the idea of preconditioned gradient descent in ensemble Kalman methods for inversion; in particular use of the pre-conditioned gradient

$$\hat{C}_\ell^{uu} \nabla J_{\text{DM}}(u_\ell^{(n)}) \approx \hat{C}_\ell^{uy} \Gamma^{-1}(y - G(u_\ell^{(n)})).$$

which follows from (13.29). This leads to iterative optimization methods [152, 275, 276], based on gradient descent, and to Bayesian sampling methods [104, 105]. A key feature of the preconditioned gradient is that it leads to algorithms which are affine invariant [120], and hence to convergence rates which are uniform across wide classes of problems; see the review article [42] for further discussion.

Finally we note that Kalman methods are based on a Gaussian approximation, and hence on matching first and second order moments when studying Bayesian inversion. Given this it is natural to study Kalman methods for inverse problems which are applied to (possibly stochastic) dynamical systems whose long-term properties exactly solve the optimization or Bayesian approach to inversion in the linear-Gaussian setting; this idea is developed in [149, 148].

The gradient-based IExKF algorithm was developed in the control theory literature [156] without reference to the Gauss-Newton optimization method; the correspondence between both methods was established in [22]. Ensemble Kalman methods were also first introduced as filtering schemes for sequential data assimilation, as described in Chapter 10. Their use for state and parameter estimation and inverse problems was further developed in [12, 198, 279]. The idea of *iterating* these methods was considered in [53, 88, 257]. Ensemble Kalman methods are now popular in both inverse problems and data assimilation; they have also shown some potential in machine learning applications [125, 124, 176]. There are two main computational benefits in updating an ensemble of candidate reconstructions rather than a single estimate. First, the ensemble update can be performed without evaluating derivatives of G , effectively approximating them using

statistical linearization. This is important in applications where computing derivatives of G is expensive, or where the map G needs to be treated as a black-box. Second, the use of empirical rather than model covariances can significantly reduce the computational cost whenever the ensemble size N is smaller than the dimension d of the unknown u . Another advantage of the ensemble approach is that, for problems that are not strongly nonlinear, the spread of the ensemble may contain meaningful information on the uncertainty in the reconstruction. Statistical linearization has also been used within unscented Kalman methods, see [307, 147, 146].

In this chapter we have considered three families of ensemble algorithms characterized by a choice of objective function and optimization algorithm: (i) Tikhonov-Phillips and Gauss-Newton; (ii) data-misfit and Levenberg-Marquardt; and (iii) Tikhonov-Phillips and Levenberg-Marquardt. Each family of ensemble Kalman methods stems from a choice of objective and a derivative-based optimization scheme that is approximated with the ensemble. There is substantial freedom as to how to use the ensemble to approximate a derivative-based method. We have focused on randomized-maximum likelihood implementations [123, 168], but square-root approaches [12, 301] can also be considered.

Algorithms in the first family were first introduced in petroleum engineering and the geophysical sciences [1, 53, 88, 123, 192, 260] and were inspired by iterative, gradient-based, extended Kalman filters [21, 22, 156]. More challenging problems with strongly nonlinear dynamics are considered in [267]. In this chapter we have presented the Iterative IEnKF-SL as a prototypical example of an algorithm that belongs to this family. IEnKF-SL was introduced in [51] as a slight modification of the iterative ensemble Kalman algorithm proposed in [307]. One of the earliest applications of iterative ensemble Kalman methods for inversion in the petroleum engineering literature was proposed in [260], which considered the alternative characterization of the Gauss-Newton update (13.32). Moreover, instead of using a different preconditioner C_ℓ for each step, [260] used a fixed preconditioner.

Algorithms in the second family were introduced in the applied mathematics literature [150, 152] building on ideas from classical inverse problems [130]. Recent theoretical work has focused on developing continuous-time and mean-field limits, as well as various convergence results [30, 29, 47, 139, 78, 176, 275]. Methodological extensions based on Bayesian hierarchical techniques were introduced in [46, 48] and the incorporation of constraints has been investigated in [9, 49]. In this chapter we use EnKI-SL as a prototypical example of an algorithm that belongs to this subfamily. Its connection with the Ensemble Kalman Inversion algorithm from [152] is discussed in [51].

The third family, which has emerged more recently, combines explicit regularization through the Tikhonov-Phillips objective and an implicitly regularizing optimization scheme [50, 47]. In this chapter we use TEnKI-SL as a prototypical example of an algorithm that belongs to this subfamily.

Our presentation has focused on the derivation of Kalman formulae for the search direction update of Gauss-Newton and Levenberg-Marquardt algorithms and their ensemble approximations. All the algorithms studied in this chapter require to specify appropriate step-size parameters that determine the size of the updates along the search

direction. For gradient-based methods, there is abundant literature on the adaptive choice of step-sizes [227]. Gauss-Newton methods can be shown to converge when the step-sizes are chosen according to Armijo or Wolfe conditions; the line search is often performed with a backtracking strategy [227, 74]. When using Levenberg-Marquardt schemes for inverse problems it is important to ensure that the step-sizes, as well as the stopping criteria, provide sufficient implicit regularization to alleviate the ill-posedness of inverse problems [130]. For ensemble Kalman methods, the use and analysis of adaptive step-sizes is a topic of current research [47, 151]. In practice, ensemble methods are often run with short step-sizes, in which case the algorithms may be interpreted as being defined by discretization of (stochastic) differential equations, see e.g. [257, 51, 275]. Finally, we point out that the original description of some of the algorithms studied in this paper, e.g. EnKI and TEnKI in [152, 50], do not discuss the inclusion of step-size parameters. This would correspond to setting $\alpha_\ell = 1$ for all $\ell \geq 0$ in our terminology.

Chapter 14

Blending Inverse Problems and Machine Learning

In this chapter we study the use of machine learning in inverse problems. We have already seen ideas from machine learning, such as stochastic gradient descent (Chapter 3) and the variational formulation of Bayes theorem (Chapter 4). However, in this chapter we will embed machine learning into the formulation of the inverse problem itself.

The chapter is organized as follows: the first two sections discuss key ideas from machine learning; the next three show their application to inverse problems. Section 14.1 discusses the supervised learning task of approximating a map from input-output pairs. Three families of methods for function approximation are considered: neural networks, random features, and Gaussian processes. In Section 14.2 we focus on unsupervised learning. Given samples from a target pdf, we introduce a range of generative models that enable the generation of new approximate samples from the target pdf by transforming samples from an easy-to-sample reference pdf. In Section 14.3 we show how approximate forward maps, found using supervised learning, may be used to speed-up MCMC while retaining accurate posterior approximation. Section 14.4 investigates the use of unsupervised techniques to recast a Bayesian inverse problem with a given prior into an equivalent inverse problem with an easy-to-sample prior; in particular, this may be used when prior information is available only in the form of samples. Finally, Section 14.5 considers (unsupervised) transport methods to learn the map from prior to posterior. The chapter closes in Section 14.6 with extensions and bibliographical remarks.

14.1 Supervised Learning

This section is concerned with the *supervised learning* task of determining a function $\psi^\dagger : D \subseteq \mathbb{R}^d \rightarrow \mathbb{R}$ from data in the form of input-output pairs from the map. The codomain of ψ^\dagger may have finite cardinality (classification) or infinite cardinality (regression). We focus on regression since, as we will see in Subsection 14.3, this task arises naturally in the context of learning forward maps for inverse problems. We assume that we have available to us data in the form

$$\left\{ u^{(n)}, \psi^\dagger(u^{(n)}) + \sqrt{\lambda} \xi_i^{(n)} \right\}_{n=1}^N, \quad (14.1)$$

where $\xi^{(n)}$ is an i.i.d. mean zero noise process. The parameter $\lambda \geq 0$ allows us to consider noiseless data ($\lambda = 0$) and noisy data ($\lambda > 0$). Since the goal is to determine ψ^\dagger we are concerned with function approximation, and to that end we will study three approaches to parameterize and learn functions: neural networks (Subsection 14.1.1), random features (Subsection 14.1.2), and Gaussian processes (Subsection 14.1.3). We will concentrate on the noiseless case $\lambda = 0$, but will briefly mention the noisy case $\lambda > 0$ in the context of random features and Gaussian processes.

Throughout, we assume that the data $\{u^{(n)}\}_{n=1}^N$ are generated i.i.d. from pdf $\Upsilon(u)$, supported on $D \subseteq \mathbb{R}^d$. We let H_Υ denote the Hilbert space of real-valued functions on D with inner-product and induced norm

$$\langle \psi, \varphi \rangle_{H_\Upsilon} = \int_D \psi(u) \varphi(u) \Upsilon(u) du, \quad \|\psi\|_{H_\Upsilon}^2 = \langle \psi, \psi \rangle_{H_\Upsilon}.$$

Thus

$$\|\psi\|_{H_\Upsilon} = \left(\int_D \psi(u)^2 \Upsilon(u) du \right)^{\frac{1}{2}}. \quad (14.2)$$

If Υ is the uniform distribution on bounded domain $D \subseteq \mathbb{R}^d$, we write the Hilbert space as $H = L^2(D)$; the norm and inner-product are then denoted with H as suffix.

In practice, the pdf Υ is typically unknown but may be approximated by the empirical density Υ^N of the data $\{u^{(n)}\}_{n=1}^N$, given by

$$\Upsilon^N(u) = \frac{1}{N} \sum_{n=1}^N \delta(u - u^{(n)}).$$

We may then define an empirical approximation of $\|\psi\|_{H_\Upsilon}$ by replacing Υ by Υ^N in (14.2) to obtain

$$\|\psi\|_{H_\Upsilon^N} = \left(\frac{1}{N} \sum_{n=1}^N \psi(u^{(n)})^2 \right)^{\frac{1}{2}}.$$

The task of finding ψ^\dagger from data may be cast as a linear inverse problem, but this is not the connection to inverse problems that we will emphasize in this chapter; rather we will concentrate on the use of supervised learning, and variants, to formulate fast approximate Bayesian inverse methods, based on learning the log-likelihood or learning the forward model.

14.1.1 Neural Networks

A neural network is a parametric family of functions. By use of the data a value of the parameter may be chosen so as to determine an approximation of ψ^\dagger . To define a neural network we introduce $\Theta \subseteq \mathbb{R}^{d_\theta}$ and then $\psi : \mathbb{R}^d \times \Theta \rightarrow \mathbb{R}$ via the iteration

$$\psi_0(u; \theta) = u, \quad (14.3)$$

$$\psi_{\ell+1}(u; \theta) = \sigma(W_\ell \psi_\ell(u; \theta) + b_\ell), \quad \ell = 0, \dots, L-1, \quad (14.4)$$

$$\psi(u; \theta) = \beta^\top \psi_L(u; \theta). \quad (14.5)$$

In this definition, for $\ell \in \{0, \dots, L-1\}$, $W_\ell : \mathbb{R}^{d_{\ell+1} \times d_\ell}$, $b_\ell \in \mathbb{R}^{d_{\ell+1}}$ and $\beta \in \mathbb{R}^{d_L}$; together these matrices and vectors define θ (and d_θ). Note that $\psi_\ell : \mathbb{R}^{d_\ell} \rightarrow \mathbb{R}^{d_{\ell+1}}$ and $d_0 = d$. The *activation function* $\sigma : \mathbb{R} \rightarrow \mathbb{R}$ is a monotonic non-decreasing function, often $\sigma(u) = \max(u, 0)$; it is extended to a function $\mathbb{R}^s \rightarrow \mathbb{R}^s$, any integer s , elementwise.

An idealized approach to determining θ is to minimize the *risk*

$$\|\psi^\dagger - \psi(\cdot; \theta)\|_{H_Y}^2.$$

However, this requires knowing ψ^\dagger , which is of course not given, as well as the pdf Υ . Instead the optimal parameter θ^\star is chosen by *empirical risk minimization*:

$$\theta^\star = \operatorname{argmin}_{\theta \in \Theta} \|\psi^\dagger - \psi(\cdot; \theta)\|_{H_Y^N}^2. \quad (14.6)$$

The *empirical risk* is an empirical approximation of the risk $\|\psi^\dagger - \psi(\cdot; \theta)\|_{H_Y}^2$ and only requires knowledge of ψ^\dagger on the data points $\{u^{(n)}\}_{n=1}^N$; this is available to us under the assumption of noiseless data ($\lambda = 0$) in (14.1). The empirical risk is typically non-convex as a function of θ , with multiple saddle points and local minima; minimization may be attempted by using stochastic gradient descent (Chapter 3). We write $\psi^\star(u) := \psi(u; \theta^\star)$.

14.1.2 Random Features

Now consider a thought experiment in which, rather than optimizing over all of Θ , the parameters $\vartheta = \{W_\ell, b_\ell\}_{\ell=0}^{L-1}$ are chosen at random and optimization is performed only over β . In contrast to full optimization over θ , this leads to a quadratic optimization problem which is solved by inverting a linear system for β . To see this, note that, if $\varphi_i(u)$ is the i -th component of the \mathbb{R}^{d_L} -valued function ψ_L , then

$$\psi(u; \beta) := \sum_{i=1}^{d_L} \beta_i \varphi_i(u). \quad (14.7)$$

Here we view $\psi(\cdot; \beta)$ as parameterized by β , since the remaining elements ϑ of θ have been picked at random and then fixed. From ψ^\dagger we may define

$$\beta^\star = \operatorname{argmin}_{\beta \in \mathbb{R}^{d_L}} \|\psi^\dagger - \psi(\cdot; \beta)\|_{H_Y^N}^2 \quad (14.8)$$

and $\psi^\star(u) := \psi(u; \beta^\star)$.

The collection of functions $\{\varphi_i\}$ are random but not, in general, i.i.d. A variant on this idea is to define $B \subset \mathbb{R}^b$, place probability measure q on B , define functions $\varphi : \mathbb{R}^d \times B \rightarrow \mathbb{R}$ and seek

$$\psi(u; \beta) := \sum_{i=1}^{d_L} \beta_i \varphi(u; \vartheta_i), \quad \vartheta_i \sim q, \text{ i.i.d.}$$

Empirical risk minimization (14.8) again leads to a linear system for β . This minimization may be regularized and, in place of (14.8), β^\star is defined via

$$\beta^\star = \operatorname{argmin}_{\beta \in \mathbb{R}^{d_L}} J(\beta), \quad (14.9)$$

$$J(\beta) := \frac{1}{2} \|\psi^\dagger - \psi(\cdot; \beta)\|_{H_Y^N}^2 + \frac{\lambda}{2} |\beta|^2. \quad (14.10)$$

Again we write $\psi^*(u) := \psi(u; \beta^*)$. This regularization may be for instance adequate to deal with noisy data $\xi^{(n)} \sim \mathcal{N}(0, I)$ in (14.1) – see Remark 14.4 for a related discussion.

We refer to the functions $\varphi(\cdot; \vartheta)$ as *random features*. It is natural to ask how correlated these functions are at different points in D . To this end, we introduce a *kernel* $c : D \times D \rightarrow \mathbb{R}$ defined by

$$c(u, u') := \mathbb{E}^q[\varphi(u; \vartheta)\varphi(u'; \vartheta)], \quad (14.11)$$

where expectation is over $\vartheta \sim q$.

14.1.3 Gaussian Processes

The theory of Gaussian process regression starts from a kernel satisfying two key properties:

Definition 14.1. A kernel $c : D \times D \rightarrow \mathbb{R}$ is *symmetric* if $c(u, u') = c(u', u)$ for all $(u, u') \in D \times D$. It is *non-negative definite* if, for all $N \in \mathbb{N}$, all $\{u^{(i)}\}_{i=1}^N \subset D$ and all $e \in \mathbb{R}^N$,

$$\sum_{i=1}^N \sum_{j=1}^N c(u^{(i)}, u^{(j)}) e_i e_j \geq 0.$$

If equality implies that $e = 0$, the kernel is called *positive definite*. \diamond

A symmetric non-negative definite kernel may be viewed as a *covariance function* of a Gaussian random field and we will return to this perspective at the end of the subsection. From non-negative definite, symmetric c , we define the integral operator

$$(\mathcal{C}\varphi)(u) = \int_D c(u, u') \varphi(u') du'. \quad (14.12)$$

Provided that D is compact and c is continuous, symmetric and positive definite, \mathcal{C} is a positive definite compact operator on $L^2(D)$ and we may define the domain of the inverse of its square root as $K = D(\mathcal{C}^{-\frac{1}{2}})$; furthermore we define K^* the dual space of linear functionals on K ; thus $K \subset H = L^2(D; \mathbb{R}) \subset K^*$. We assume that K^* is rich enough that it contains Dirac measures in D (and hence pointwise evaluation) and define $\mathcal{C}^{-1} : K \rightarrow K^*$. It follows that, for all $u' \in D$,

$$\mathcal{C}^{-1}c(\cdot, u') = \delta_{u'}(\cdot). \quad (14.13)$$

We then seek to define our approximation to ψ^\dagger , function ψ^* , through the following minimization problem:

$$\psi^* = \operatorname{argmin}_{\psi \in K} J(\psi), \quad (14.14)$$

$$J(\psi) := \frac{1}{2} \|\psi^\dagger - \psi\|_{H_\Gamma^N}^2 + \frac{\lambda}{2} \|\mathcal{C}^{-\frac{1}{2}} \psi\|_H^2. \quad (14.15)$$

At first sight this appears to be an infinite dimensional optimization problem, over the whole of K . However, it has the following remarkable property, which is often referred to as the *representer theorem*, and demonstrates that the optimization problem is intrinsically finite dimensional:

Theorem 14.2. *Function ψ^* solving (14.14) has the form*

$$\psi^*(u) = \sum_{n=1}^N \alpha_n^* c(u, u^{(n)}). \quad (14.16)$$

Furthermore, the coefficients α^ solve the following quadratic minimization problem:*

$$\alpha^* = \operatorname{argmin}_{\alpha \in \mathbb{R}^N} A(\alpha), \quad (14.17)$$

$$A(\alpha) := \frac{1}{2} \left\| \psi^\dagger - \sum_{n=1}^N \alpha_n c(\cdot, u^{(n)}) \right\|_{H_Y^N}^2 + \frac{\lambda}{2} \sum_{n,r=1}^N \alpha_n \alpha_r c(u^{(n)}, u^{(r)}). \quad (14.18)$$

Proof. The Euler-Lagrange equations for objective function J in (14.14) yield

$$\lambda(C^{-1}\psi^*)(u) = \frac{1}{N} \sum_{n=1}^N (\psi^\dagger(u^{(n)}) - \psi^*(u^{(n)})) \delta_{u^{(n)}}.$$

Now note from (14.13) that $(C\delta_{u'})(u) = c(u, u')$. Thus applying C to the Euler-Lagrange equations shows that $\psi^*(u)$ is in the linear span of $\{c(\cdot, u^{(n)})\}_{n=1}^N$, establishing the first part of the result. For the second part, note that

$$\|C^{-\frac{1}{2}}\psi\|_H^2 = \langle \psi, C^{-1}\psi \rangle_H.$$

Substituting the established form (14.16) for $\psi^*(u)$ into this identity and using (14.13) reduces the regularization term proportional to λ to the desired form. \square

We define $C \in \mathbb{R}^{N \times N}$ to be the matrix with entries $C_{nr} = c(u^{(n)}, u^{(r)})$ and S to be its inverse, with entries S_{nr} ; notice that C is positive definite (and hence invertible) provided that the kernel c is positive definite. Then we have:

Corollary 14.3. *If $p^* \in \mathbb{R}^N$ is vector with entries $p_n^* = \psi^*(u^{(n)})$, then $p^* = C\alpha^*$ and*

$$p^* = \operatorname{argmin}_{p \in \mathbb{R}^N} J(p), \quad (14.19)$$

$$J(p) := \frac{1}{2} \sum_{n=1}^N |\psi^\dagger(u^{(n)}) - p_n|^2 + \frac{\lambda}{2} \sum_{n,r=1}^N p_n p_r S_{n,r}. \quad (14.20)$$

Remark 14.4. The minimization problem (14.14) corresponds to determining the mean of a posterior distribution of an infinite dimensional Bayesian inverse problem defined as follows. We place as prior on ψ a Gaussian random field with mean zero and covariance function $c(u, u')$. The likelihood is defined by assuming noisy data in (14.1), where $\xi^{(n)} \sim \mathcal{N}(0, I)$ i.i.d. and then the negative log-posterior density is given by $\lambda^{-1}J(\psi)$. The posterior mean, which is also a form of MAP estimator, then satisfies (14.14). We also remark that minimization of (14.9) also has a similar interpretation as a MAP estimator, but with respect to a Gaussian process with mean zero and covariance function a random approximation of $c(u, u')$. \diamond

14.1.4 Approximation Properties

All of the preceding three methods can, in principle, approximate continuous functions to arbitrary accuracy, over a compact set. Doing so requires sufficient data. Furthermore, in the case of neural networks, this also requires sophisticated optimization techniques to obtain close to optimal solutions; in contrast, the random features and Gaussian process approaches only require solution of linear systems, resulting from a quadratic optimization problem. Typical instances of the resulting approximation theory for the three supervised learning techniques typically shows that, for given $\delta > 0$, there is a volume of data N such that, with high probability with respect to the data,

$$\sup_{u \in D} |\psi^\dagger(u) - \psi^*(u)| < \delta. \quad (14.21)$$

Theory establishing results of this form is cited in the bibliography Section 14.6.

14.2 Unsupervised Learning

In this subsection we study a part of the methodology of unsupervised learning which is often referred to as *generative modeling*. We start by discussing the *measure transport* task of determining function $g : \mathbb{R}^{d_z} \rightarrow \mathbb{R}^d$ so that, given pdf ζ on \mathbb{R}^{d_z} and pdf Υ on \mathbb{R}^d , $g^\# \zeta = \Upsilon$; here $g^\#$ denotes the pushforward operation and so, explicitly, we are seeking g so that, if $z \sim \zeta$, then $g(z) \sim \Upsilon$. An important area of machine learning where this arises is in the *unsupervised learning* problem as follows. We have available to us data in the form

$$\{u^{(n)}\}_{n=1}^N, \quad (14.22)$$

assumed to be drawn i.i.d. from pdf Υ which is unknown to us. Hence we have access to the empirical density

$$\Upsilon^N(u) = \frac{1}{N} \sum_{n=1}^N \delta(u - u^{(n)}). \quad (14.23)$$

In unsupervised learning the goal is to understand the data set summarized by measure Υ^N . One approach is to study *clustering* within the data; we will not pursue this important topic because it is not of direct relevance to the solution of inverse problems, our focus in these notes. Instead we pursue the approach of *generative modeling*. Assume that ζ is Gaussian, then the aim is to find map g so that samples from Gaussian ζ , when pushed forward under g , will look like samples from Υ . We will also study relaxations of this problem, in which the Gaussian ζ is convolved with a Gaussian whose mean is function g .

As for supervised learning, the task of identifying g in the models described above must be undertaken empirically, since only Υ^N is available to us, not Υ .

14.2.1 Optimal Transport Maps

Although optimal transport does not lead to algorithms for inverse problems used in this chapter, it plays an important underpinning role in the theory of measure transport,

which does play a role in the algorithms used in this chapter. Given the two densities ζ, Υ on $\mathbb{R}^{d_z}, \mathbb{R}^d$ respectively, we define a *coupling* as a density π on $\mathbb{R}^{d_z} \times \mathbb{R}^d$ with the property that

$$\int_{\mathbb{R}^d} \pi(z, u) du = \zeta(z), \quad \int_{\mathbb{R}^{d_z}} \pi(z, u) dz = \Upsilon(u).$$

Thus the marginals of π deliver ζ and Υ . We denote the set of all such couplings by $\Pi_{\zeta, \Upsilon}$. Given a cost function $c : \mathbb{R}^{d_z} \times \mathbb{R}^d \rightarrow \mathbb{R}^+$ we define the Kantorovich formulation of the optimal transport problem as follows:

$$\pi^* = \operatorname{arginf}_{\pi \in \Pi_{\zeta, \Upsilon}} \int_{\mathbb{R}^{d_z} \times \mathbb{R}^d} c(z, u) \pi(z, u) dz du. \quad (14.24)$$

This notion of optimal transport may be used to define families of metrics on probability densities as follows. If $d_z = d$, so that ζ, Υ are both densities on the same space \mathbb{R}^d , then given a metric $d(\cdot, \cdot)$ on \mathbb{R}^d and an integer p , we define

$$W_p(\zeta, \Upsilon) = \left(\inf_{\pi \in \Pi_{\zeta, \Upsilon}} \int_{\mathbb{R}^d \times \mathbb{R}^d} d(z, u)^p \pi(z, u) dz du \right)^{\frac{1}{p}}. \quad (14.25)$$

This metric on probability measures has two key aspects: first, it relates the metric to an underlying metric on \mathbb{R}^d ; and second, it allows for a meaningful distance to be calculated between measures which are mutually singular. It is known as a Wasserstein- p distance.

Example 14.5. Let $p_i = \mathcal{N}(m_i, \Sigma_i)$ for $i = 1, 2$. It may be shown that, if the metric d induced by the Euclidean norm $|\cdot|$ is used, then

$$W_2(p_1, p_2)^2 = |m_1 - m_2|^2 + \operatorname{Tr}(\Sigma_1 + \Sigma_2 - 2(\Sigma_1^{\frac{1}{2}} \Sigma_2 \Sigma_1^{\frac{1}{2}})).$$

In particular, if p_2 is a Dirac measure at the origin then

$$W_2(p_1, p_2)^2 = |m_1|^2 + \operatorname{Tr}(\Sigma_1).$$

Thus, in the Wasserstein-2 metric Gaussian p_1 is close to a Dirac at the origin if the mean and covariance of p_1 are both small. In contrast, the total variation distance between Gaussian p_1 and a Dirac at the origin is maximal, and equal to 1, unless the two measures coincide ($m_1 = 0, \Sigma_1 = 0$) when it is 0. Similarly the Kullback-Leibler divergence becomes infinite as p_2 approaches a Dirac limit, from within the class of Gaussians – see Example 4.2.

Notice also that if p_1 and p_2 are Diracs at m_1 and m_2 , then $W_2(p_1, p_2) = |m_1 - m_2|$; thus closeness in the location of the mass locations m_1 and m_2 in Euclidean space translates into closeness of p_1 and p_2 in Wasserstein distance. \diamond

The connection of optimal transport to explicit transport maps is made clear in the Monge formulation of optimal transport. In this formulation we explicitly link Υ with a pushforward of ζ and identify the pushforward map which minimizes the cost:

$$g^* = \operatorname{arginf}_{g: g^* \zeta = \Upsilon} \int_{\mathbb{R}^{d_z}} c(z, g(z)) \zeta(z) dz. \quad (14.26)$$

Under certain smoothness assumptions, the Kantorovich formulation has solution within the Monge class. That is, the optimal coupling is constructed using the pushforward:

$$\pi^*(z, u) = \delta(u - g^*(z))\zeta(z).$$

Whilst optimal transport provides a deep mathematical structure within which to consider the measure transport problem, there are numerous applications where the optimality constraint on the transport confers few advantages over other transports. Furthermore, it makes the computational task of finding the transport quite difficult. For these reasons a number of other approaches to transport have been considered and we discuss some of them in the remaining subsections of this section.

14.2.2 Other Transport Approaches

Let π, π' be two pdfs on \mathbb{R}^d . We consider the task of finding invertible $g : \mathbb{R}^d \rightarrow \mathbb{R}^d$ with the property that $\pi \approx g^\# \pi'$; equivalently, since g is invertible, $\pi' \approx (g^{-1})^\# \pi$. We seek to determine a parameter such that g chosen from the parametric class $g : \mathbb{R}^d \times \Theta_g \mapsto \mathbb{R}^d$, with $\Theta_g \subseteq \mathbb{R}^{p_g}$, realizes this approximation. To this end we define

$$F(\theta_g) = d_{\text{KL}}(\pi \| g(\cdot; \theta_g)^\# \pi')$$

and set

$$\theta_g^* = \operatorname{argmin}_{\theta_g \in \Theta_g} F(\theta_g).$$

We define the resulting approximate pushforward map by $g^* = g(\cdot; \theta_g^*)$. Note that there exist perfect transport functions g_{perfect} (for example an optimal transport) for which $d_{\text{KL}}(\pi \| g_{\text{perfect}}^\# \pi') = 0$. We aim to get as close as possible to such solutions, within our parametric class, by minimizing F over θ_g .

The following lemma is useful in determining an explicit form of F for computational purposes. The proof is a straightforward consequence of change of variables.

Lemma 14.6. *Let π' be a probability density on \mathbb{R}^d and let $q \in C^1(\mathbb{R}^d, \mathbb{R}^d)$ be invertible everywhere on \mathbb{R}^d . Assume further that the determinant of the Jacobian of the inverse,*

$$\det D(q^{-1})(u) = \left(\det Dq(q^{-1}(u)) \right)^{-1},$$

is positive everywhere on \mathbb{R}^d . Then, for $u = q(z)$,

$$\int_{\mathbb{R}^d} \varphi(z) \pi'(z) dz = \int_{\mathbb{R}^d} (\varphi \circ q^{-1})(u) (\pi' \circ q^{-1})(u) \det D(q^{-1})(u) du.$$

Thus

$$q^\# \pi'(u) = (\pi' \circ q^{-1})(u) \det D(q^{-1})(u).$$

$$\log q^\# \pi'(u) = \log(\pi' \circ q^{-1})(u) - \log \det Dq(q^{-1}(u)). \quad (14.27)$$

Using the expression for the density of the pushforward we find that, for differentiable g ,

$$F(\theta_g) = \mathbb{E}^{u \sim \pi} [\log \pi(u) - \log g^\# \pi'(u)] \quad (14.28a)$$

$$= -\mathbb{E}^{u \sim \pi} [\log \pi' \circ g^{-1}(u; \theta_g) + \log \det D_u(g^{-1})(u; \theta_g)] + \text{const}, \quad (14.28b)$$

where the constant term is independent of g , and hence of θ_g ; it can be ignored for the purposes of minimization. Note also that, using (14.27), and neglecting the constant term, we may also write

$$F(\theta_g) = -\mathbb{E}^{u \sim \pi} [\log \pi' \circ g^{-1}(u; \theta_g) - \log \det D_u g(g^{-1}(u; \theta_g); \theta_g)]. \quad (14.29)$$

Remark 14.7. This approach can be implemented in the setting where $\pi = \Upsilon$ and $\pi' = \zeta$, detailed at the start of the section. In this setting $\pi = \Upsilon$ is only available empirically. Since F is defined as an expectation over π , this is readily approximated empirically. We thus find an approximate expression for π , known only through samples, as the image under g^* of π' . Once we have the map g^* we can generate new (approximate) samples from π by sampling π' and applying g^* . An important issue here is that we are interested in determining the optimal forward map g , but the optimization problem, for either choice of $F(\theta_g)$ in (14.28) or (14.29), necessarily involves g^{-1} . Thus g must be readily invertible. Subsection 14.2.6 addresses this issue in the context of normalizing flows.

We have introduced π and π' , rather than working with Υ and ζ from the outset, because the approach as outlined is useful in a different setting in Section 14.5. In Section 14.5 π is typically a known simple measure, from which samples are easily drawn, whereas π' is a more complicated measure which we wish to characterize and sample from; in such a setting, the objective is to determine $T = g^{-1}$ so that $\pi' = (g^{-1})^\# \pi$. Since (14.28) is expressed entirely in terms of $T = g^{-1}$, and not g itself, it is possible to approach this problem by directly parameterizing $T = g^{-1}$ rather than g . \diamond

14.2.3 Autoencoders

Autoencoders are primarily used as a technique for uncovering latent low-dimensional structure in high dimensional data. We introduce them here and then demonstrate in the next subsection that a natural probabilistic relaxation of the idea leads to generative models termed variational autoencoders.

Transport ideas may be used to (approximately) represent a complicated probability distribution, perhaps only known through samples, as the pushforward of a simpler measure. In this section we go a step further, by seeking a simpler measure which lives in a lower dimensional latent space. Autoencoders are one natural approach to such problems.

The basic idea of autoencoders is to find an approximate factorization of the identity which is accurate in the support of density Υ , but using only the empirical approximation of Υ by Υ^N . Let $f : \mathbb{R}^d \times \Theta_f \mapsto \mathbb{R}^{d_z}$ and $g : \mathbb{R}^{d_z} \times \Theta_g \mapsto \mathbb{R}^d$ where $\Theta_f \subseteq \mathbb{R}^{p_f}$ and $\Theta_g \subseteq \mathbb{R}^{p_g}$; in particular each of f and g can be a neural network, as defined in Subsection 14.1.1,

generalized to vector-valued output. Recalling that Id denotes the identity mapping on \mathbb{R}^d , and defining

$$F(\theta_f^*, \theta_g^*) = \left\| Id - g(f(\cdot; \theta_f); \theta_g) \right\|_{H_Y}^2$$

we consider the following optimization problem:

$$(\theta_f^*, \theta_g^*) = \operatorname{argmin}_{(\theta_f, \theta_g) \in \Theta_f \times \Theta_g} F(\theta_f^*, \theta_g^*). \quad (14.30)$$

We then define $f^*(u) = f(u, \theta_f^*)$ and $g^*(z) = g(z, \theta_g^*)$. Roughly speaking, and dropping the dependence on parameters for expository purposes, we are seeking functions f and g such that $g(f(u)) \approx u$. In practice the optimization is implemented empirically, and the norm on H_Y in F is replaced by the norm on H_Y^N .

This approach reduces the autoencoder to a particular form of supervised learning in which the inputs and outputs are equal, so we seek to approximate the identity, and in which we impose a specific structure on the class of approximating function – as composition of g with f . We refer to \mathbb{R}^{d_z} as the *latent space* and note that a primary application of the methodology is to identify latent spaces of dimension d_z which is much less than the dimension d of the data space. The approximate factorization of the identity found by composing g with f provides a way of moving between the data space and the latent space.

14.2.4 Variational Autoencoders

In the preceding subsection, note that $\zeta = (f^*)^\# \Upsilon$ gives the (approximate) distribution in the latent space, but that we cannot specify ζ ; mapping g (approximately) solves a measure transport problem from ζ to Υ , but choice of measure ζ is not within our control. It is natural to ask whether the methodology can be generalized to settings in which it is desirable to impose a specified distribution ζ . This leads to the topic of *variational autoencoders*.

To this end let π be a coupling of Υ and ζ and note that the following two identities hold:

$$\begin{aligned} \pi(u, z) &= \mathbb{P}(u|z)\zeta(z), \\ \pi(u, z) &= \mathbb{P}(z|u)\Upsilon(u). \end{aligned}$$

The idea of the variational autoencoder is to approximate the two conditional densities $\mathbb{P}(u|z), \mathbb{P}(z|u)$ appearing in these identities by parameterized families. A parametric choice is made to ensure that the two resulting approximate expressions for $\pi(u, z)$ are close. To be explicit we assume that

$$\begin{aligned} u|z &\sim \mathcal{N}(g(z; \theta_g), \sigma_g^2 I), \\ z|u &\sim \mathcal{N}(f(u; \theta_f), \sigma_f^2 I), \end{aligned}$$

noting that this is a relaxation of the setting for autoencoders. Invoking these Gaussian approximations for the conditionals we obtain the following two approximations for the

coupling density:

$$\begin{aligned}\pi_g(u, z) &= \frac{1}{Z_g} \exp\left(-\frac{1}{2\sigma_g^2}|u - g(z; \theta_g)|^2\right) \zeta(z), \\ \pi_f(u, z) &= \frac{1}{Z_f} \exp\left(-\frac{1}{2\sigma_f^2}|z - f(u; \theta_f)|^2\right) \Upsilon(u).\end{aligned}$$

A common choice is to assume that ζ is the density of a standard unit Gaussian; we make this assumption throughout what follows.

For simplicity, we consider the standard deviations σ_f, σ_g to be fixed, and determine the parameters of f and g . We do this by asking that π_f and π_g are close. If we measure closeness by means of Kullback-Leibler divergence, with π_f in the first argument, then using the Gaussian assumptions on the conditionals and on ζ leads to insightful explicit calculations. To see this, we first note that

$$d_{\text{KL}}(\pi_f \| \pi_g) = \mathbb{E}^{u \sim \Upsilon} \left[\mathbb{E}^{z \sim \mathbb{P}(z|u)} \left[\frac{1}{2\sigma_g^2} |u - g(z; \theta_g)|^2 \right] + d_{\text{KL}}(\mathbb{P}(\cdot|u) \| \zeta) \right] + \text{const},$$

where the constant is independent of the parameters we wish to learn and where $\mathbb{P}(z|u)$ and $\zeta(z)$ are given by their assumed Gaussian structure. Using the expression in Example 4.2 for the Kullback-Leibler divergence between two Gaussians we obtain

$$d_{\text{KL}}(\pi_f \| \pi_g) = \mathbb{E}^{u \sim \Upsilon} \left[\mathbb{E}^{z \sim \mathcal{N}(f(u; \theta_f), \sigma_f^2 I)} \left[\frac{1}{2\sigma_g^2} |u - g(z; \theta_g)|^2 \right] + \frac{1}{2} |f(u; \theta_f)|^2 \right] + \text{const}.$$

Noting that, $z \sim \mathcal{N}(f(u; \theta_f), \sigma_f^2 I)$ is the same in law as $f(u; \theta_f) + \sigma_f \xi$ where $\xi \sim \mathcal{N}(0, I)$ we may write this divergence as

$$d_{\text{KL}}(\pi_f \| \pi_g) = F(\theta_f, \theta_g) + \text{const}.$$

where

$$F(\theta_f, \theta_g) = \mathbb{E}^{u \sim \Upsilon} \left[\mathbb{E}^{\xi \sim \mathcal{N}(0, I)} \left[\frac{1}{2\sigma_g^2} |u - g(f(u; \theta_f) + \sigma_f \xi; \theta_g)|^2 \right] + \frac{1}{2} |f(u; \theta_f)|^2 \right]$$

and the constant term is independent of (θ_f, θ_g) .

This constitutes a regularized version of the standard autoencoder; in particular the preceding expression for the divergence clearly regularizes the basic concept that $g(f(u)) \approx u$ under density Υ .

Remark 14.8. In practice this is implemented with expectation over Υ approximated empirically by Υ^N . This leaves an optimization problem in which the objective is defined via expectation over ξ . Stochastic gradient descent from Chapter 3 may be used to tackle this problem. After training, approximate samples from Υ may be obtained by sampling $z \sim \zeta$ and then sampling $u|z \sim \mathcal{N}(g(z; \theta_g), \sigma_g^2)$. \diamond

14.2.5 Generative Adversarial Networks

The variational autoencoder trains a probabilistic model for u , by learning $\mathbb{P}(u|z)$ and specifying $\mathbb{P}(z)$. The generative adversarial network is another method for training such a probabilistic model, which also allows for low dimensional latent space. To be concrete we assume that it has the same structural form, namely

$$\begin{aligned} u|z &\sim \mathcal{N}(g(z; \theta_g), \sigma_g^2 I), \\ z &\sim \mathcal{N}(0, I). \end{aligned}$$

Thus samples from u are created from samples from z . We write the resulting density of u as Υ_g , with g for generative. It is desired that samples from Υ_g are similar to those specified by the data, which is drawn from density Υ .

The generative adversarial network starts by defining a *discriminator* $\mathbf{d} : \mathbb{R}^d \times \Theta_d \rightarrow [0, 1]$, to be thought of as taking values which are probabilities. Here $\Theta_d \subset \mathbb{R}^{p_d}$. It is instructive to think of $\mathbf{d}(u; \theta_d)$ as being the probability that u is drawn from the density Υ , and $1 - \mathbf{d}(u; \theta_d)$ as the probability of u being drawn from the generative model Υ_g . We then define $v : \Theta_g \times \Theta_d \rightarrow \mathbb{R}$ by

$$v(\theta_g, \theta_d) = \mathbb{E}^{u \sim \Upsilon} [\log \mathbf{d}(u; \theta_d)] + \mathbb{E}^{u \sim \Upsilon_g} [\log(1 - \mathbf{d}(u; \theta_d))].$$

The optimal parameter values are defined by

$$\begin{aligned} \theta'_d(\theta_g) &= \operatorname{argmax}_{\theta_d} v(\theta_g, \theta_d), \\ \theta_g^* &= \operatorname{argmin}_{\theta_g} v(\theta_g, \theta'_d(\theta_g)), \\ \theta_d^* &= \theta'_d(\theta_g^*). \end{aligned}$$

In the maximization step, the parameters of the discriminator are chosen to maximize v – the discriminator acts adversarially to try and find data under Υ_g which does not look like data under Υ . In the minimization step the generator acts to reduce v to try and make the two data sources look similar. Ideally, through an iterative process, a solution is found in which $\mathbf{d}(\cdot; \theta_d^*) \equiv \frac{1}{2}$, so that the data and generated data are indistinguishable. The value of θ_g^* defines the generative model once this indistinguishable state has been reached.

14.2.6 Normalizing Flows

The transport approach from Subsection 14.2.2 requires invertibility of the map g , and efficient computation of the determinant of the Jacobian. Invertibility of map g is also useful in other contexts. Normalizing flows address this issue; *normalizing* reflects the fact that distribution π' is often a Gaussian, whilst *flow* connotes the breaking up of map g into a sequence of simpler maps which are themselves parameterized, rather than parameterizing g itself.

To this end we introduce the iteration

$$v_{j+1} = H(v_j; \theta_g), \tag{14.31a}$$

$$v_0 = z, \tag{14.31b}$$

and let $J \in \mathbb{N}$ be defined so that $v_J = u$. Define $u = g(z)$ where $g = H \circ H \circ \dots \circ H$, the J -fold composition of H . We assume that $H(\cdot; \theta_g)$ is invertible, with inverse $H^{-1}(\cdot; \theta_g)$, and differentiable, with derivative $DH(\cdot; \theta_g)$. Assume that $z \sim \pi'$ and let $p_j(v_j)$ denote the density of v_j . Then the goal of normalizing flow is to choose parameter θ_g in H so that $p_J \approx \pi$ and hence (approximately) $u \sim \pi$; this is potentially a more straightforward task than working with a directly parameterized g , the approach described in Subsection 14.2.2.

Formula (14.27) shows that, since $v_j = H^{-1}(v_{j+1}; \theta_g)$,

$$\log p_{j+1}(v_{j+1}) = \log p_j(v_j) - \det DH(v_j; \theta_g).$$

Summing over j we obtain

$$\log p_J(v_J) = \log p_0(v_0) - \sum_{j=0}^{J-1} \det DH(v_j; \theta_g),$$

and hence

$$\log g^\# \pi'(u) = \log \pi'(z) - \sum_{j=0}^{J-1} \det DH(v_j; \theta_g), \quad (14.32)$$

where $u = g(z)$ and $v_j = g^{(j)}(z)$, the j -fold composition of g . Note that hence $v_j = (g^{-1})^{(J-j)}(u)$, the $(J-j)$ -fold composition of g^{-1} . In particular z is found as the J -fold composition of g^{-1} .

With these relationships defined between $(z, \{v_j\})$ and u , and noting that they are parameterized by θ_g , we generalize (14.29) to set

$$F(\theta_g) = -\mathbb{E}^{u \sim \pi} \left[\log \pi'(z) - \sum_{j=0}^{J-1} \log \det DH(v_j; \theta_g) \right]. \quad (14.33)$$

As before we set

$$\theta_g^* = \operatorname{argmin}_{\theta_g \in \Theta_g} F(\theta_g)$$

and define the resulting approximate pushforward map by $g^* = g(\cdot; \theta_g^*)$. Note that $g(\cdot; \theta_g^*)$ is found from the J -fold composition of $H(\cdot; \theta_g^*)$.

The continuum limit of normalizing flows leads to differential equations which map an initial probability distribution π' into probability distribution $g^\# \pi'$ at time $t = 1$. To this end we define

$$\frac{dv}{dt} = h(v; \theta_g), \quad (14.34a)$$

$$v(0) = z. \quad (14.34b)$$

Noting that $v(t)$ depends on z we define $g_t(z; \theta_g) = v(t)$ and $g(z; \theta_g) = g_1(z; \theta_g) = v(1)$. An advantage of the continuum perspective is that the inverse of map g is readily computed as follows. Define the equation

$$\frac{dw}{dt} = -h(w; \theta_g), \quad (14.35a)$$

$$w(0) = u. \quad (14.35b)$$

Then $g_t^{-1}(u; \theta_g) = w(t)$ and, in particular, $g^{-1}(u; \theta_g) = w(1)$.

Lemma 14.9. *Assume that, in (14.35), the initial condition satisfies $z \sim \pi'$. Then*

$$\log g^\# \pi'(u) = \log \pi'(z) - \int_0^1 \nabla \cdot h(v(s); \theta_g) ds. \quad (14.36)$$

Proof. This may be derived from the discrete normalizing flow, by setting $H(\cdot; \theta_g) = Id + \Delta t h(\cdot; \theta_g)$ where $J\Delta t = 1$. Note that this corresponds to an Euler approximation of the continuum picture in which $v_j \approx v(j\Delta t)$. Furthermore

$$\det DH = \det(I_d + \Delta t Dh) = 1 + \Delta t \text{Tr} Dh + \mathcal{O}(\Delta t^2).$$

Note that $\text{Tr} Dh = \nabla \cdot h$. Thus, substituting this expression for $\det DH$ into (14.32), expanding the logarithm in powers of Δt , summing over j and letting $\Delta t \rightarrow 0$ yields the desired result. \square

The continuum analog of (14.33) is then

$$F(\theta_g) = -\mathbb{E}^{u \sim \pi} \left[\log \pi'(z) - \int_0^1 \nabla \cdot h(v(s); \theta_g) ds \right],$$

where $z = g^{-1}(u; \theta_g)$ and $v(t) = g_{1-t}^{-1}(u; \theta_g)$. As before, up to an additive constant, $F(\theta_g) = d_{\text{KL}}(\pi \| g^\# \pi')$. Minimizing F over θ_g , to obtain θ_g^* , thus leads to $g^*(\cdot) = g(\cdot; \theta_g)$ and $(g^*)^\# \pi' \approx \pi$.

14.3 Learning the Forward Map

Recall the inverse problem (1.1) of finding u from y where

$$y = G(u) + \eta.$$

If the Bayesian approach is adopted, and MCMC is used to generate samples from the posterior, many evaluations of G may be required to evaluate the likelihood. When G is computationally expensive to evaluate, this may be prohibitive. The methods described in Section 14.1 can be used to approximate the (scalar-valued) likelihood l resulting from G , by an approximation l_δ with small error δ , uniformly over $D \subset \mathbb{R}^d$. Furthermore, the methods from Section 14.1 can all be generalized to approximate (vector-valued) G by a uniform approximation over $D \subset \mathbb{R}^d$, G_δ , which in turn results in a uniform approximation l_δ of the likelihood. If carefully designed, then the machine learning approximation of the likelihood will be much faster to evaluate than the true likelihood and, because of the approximation properties, will result in accurate posterior inference, with errors of size δ . Such results rely on error bounds of the form (14.21) which (with high probability) can be obtained with a number N of evaluations of the forward model which is orders of magnitude smaller than the number of evaluations required within MCMC. The resulting method can thus be very efficient.

We now establish that the resulting approximate posterior is indeed close to the truth, using error bounds of the form (14.21) within a modification of the well-posedness theory from Chapter 1.

We denote by

$$l(u) = \nu(y - G(u)) \quad \text{and} \quad l_\delta(u) = \nu(y - G_\delta(u))$$

the true and approximate likelihoods. Thus we may define the true and approximate posterior distributions by

$$\pi^y(u) = \frac{1}{Z} l(u) \rho(u) \quad \text{and} \quad \pi_\delta^y(u) = \frac{1}{Z_\delta} l_\delta(u) \rho(u);$$

here $Z, Z_\delta > 0$ are the corresponding normalizing constants. To prove our result about the closeness between the true posterior and the machine-learned posterior we specify our assumptions.

Assumption 14.10. *The prior distribution is supported on bounded open set $D \subset \mathbb{R}^d$. There exist $\delta^+ > 0$ and $K_1, K_2 < \infty$ such that, for all $\delta \in (0, \delta^+)$,*

- (i) $\sup_{u \in \mathbb{R}^d} |\sqrt{l(u)} - \sqrt{l_\delta(u)}| \leq K_1 \delta;$
- (ii) $\sup_{u \in \mathbb{R}^d} (|\sqrt{l(u)}| + |\sqrt{l_\delta(u)}|) \leq K_2.$

This assumption follows from (14.21) if it is assumed that l is uniformly bounded on D . Furthermore results of the form (14.21) typically require continuity of l on D . Using the assumption we may state the approximation result for the machine-learned posterior. When combined with Lemma 1.11, the following theorem guarantees that expectations computed with respect to the machine-learned posterior commit an error of order δ , the magnitude of the error in the approximate likelihood.

Theorem 14.11 (Effect of Machine-Learned Likelihood on Posterior). *Under Assumption 14.10 we have*

$$d_H(\pi^y, \pi_\delta^y) \leq c\delta, \quad \delta \in (0, \Delta),$$

for some $\Delta > 0$ and some $c \in (0, +\infty)$ independent of δ .

As in the proof of the well-posedness Theorem 1.15, we first show a lemma which characterizes the normalization constants and their approximation in the small δ limit.

Lemma 14.12. *Under Assumption 14.10 there exist $\Delta > 0$, $c_1, c_2 \in (0, +\infty)$ such that*

$$|Z - Z_\delta| \leq c_1 \delta \quad \text{and} \quad Z, Z_\delta > c_2, \quad \text{for } \delta \in (0, \Delta).$$

Proof. Since $Z = \int l(u) \rho(u) du$ and $Z_\delta = \int l_\delta(u) \rho(u) du$, we have

$$\begin{aligned} |Z - Z_\delta| &= \left| \int (l(u) - l_\delta(u)) \rho(u) du \right| \\ &\leq \left(\int |\sqrt{l(u)} - \sqrt{l_\delta(u)}|^2 \rho(u) du \right)^{1/2} \left(\int |\sqrt{l(u)} + \sqrt{l_\delta(u)}|^2 \rho(u) du \right)^{1/2} \\ &\leq \left(\int K_1^2 \delta^2 \rho(u) du \right)^{1/2} \left(\int K_2^2 \rho(u) du \right)^{1/2} \\ &\leq K_1 K_2 \delta, \quad \delta \in (0, \delta^+). \end{aligned}$$

Therefore, for $\delta \leq \Delta := \min\{\frac{Z}{2K_1K_2}, \delta^+\}$, we have

$$Z_\delta \geq Z - |Z - Z_\delta| \geq \frac{1}{2}Z.$$

The lemma follows by taking $c_1 = K_1K_2$ and $c_2 = \frac{1}{2}Z$. □

Proof of Theorem 14.11. Following proof of the well-posedness Theorem 1.15, we decompose the total error into two contributions, reflecting respectively the difference between Z and Z_δ , and the difference between the likelihoods l and l_δ :

$$d_H(\pi^y, \pi_\delta^y) \leq \frac{1}{\sqrt{2}} \left\| \sqrt{\frac{l\rho}{Z}} - \sqrt{\frac{l\rho}{Z_\delta}} \right\|_{L^2} + \frac{1}{\sqrt{2}} \left\| \sqrt{\frac{l\rho}{Z_\delta}} - \sqrt{\frac{l_\delta\rho}{Z_\delta}} \right\|_{L^2}.$$

Using Lemma 14.12 we have, for $\delta \in (0, \Delta)$,

$$\begin{aligned} \left\| \sqrt{\frac{l\rho}{Z}} - \sqrt{\frac{l\rho}{Z_\delta}} \right\|_{L^2} &= \left| \frac{1}{\sqrt{Z}} - \frac{1}{\sqrt{Z_\delta}} \right| \left(\int l(u)\rho(u) du \right)^{1/2} \\ &= \frac{|Z - Z_\delta|}{(\sqrt{Z} + \sqrt{Z_\delta})\sqrt{Z_\delta}} \\ &\leq \frac{c_1}{2c_2} \delta, \end{aligned}$$

and

$$\left\| \sqrt{\frac{l\rho}{Z_\delta}} - \sqrt{\frac{l_\delta\rho}{Z_\delta}} \right\|_{L^2} = \frac{1}{\sqrt{Z_\delta}} \left(\int |\sqrt{l(u)} - \sqrt{l_\delta(u)}|^2 \rho(u) du \right)^{1/2} \leq \sqrt{\frac{K_1^2}{c_2}} \delta.$$

Therefore

$$d_H(\pi^y, \pi_\delta^y) \leq \frac{1}{\sqrt{2}} \frac{c_1}{2c_2} \delta + \frac{1}{\sqrt{2}} \sqrt{\frac{K_1^2}{c_2}} \delta = c\delta,$$

with $c = \frac{1}{\sqrt{2}} \frac{c_1}{2c_2} + \frac{1}{\sqrt{2}} \sqrt{\frac{K_1^2}{c_2}}$ independent of δ . □

14.4 Learning the Prior

Recall the inverse problem of finding $u \in \mathbb{R}^d$ from $y \in \mathbb{R}^k$ when related by (1.1): $y = G(u) + \eta$. Under the assumptions of Theorem 1.2, this leads to the posterior distribution given by (1.2):

$$\pi(u) = \frac{1}{Z} \nu(y - G(u)) \rho(u);$$

we have dropped the explicit dependence of the posterior on y for notational convenience. Now consider a setting in which the prior $\rho(u)$ is not known explicitly and only given through samples. Assume further that $\rho = (g^\dagger)^\# \rho'$, where $g^\dagger : \mathbb{R}^{d_z} \rightarrow \mathbb{R}^d$ and ρ' is a probability density on \mathbb{R}^{d_z} . We have the following useful result:

Lemma 14.13. *Let $d_z = d$ and assume that g^\dagger is invertible. Define*

$$\pi'(z) = \frac{1}{Z} \nu(y - G(g^\dagger(z))) \rho'(z).$$

It follows that $\pi = (g^\dagger)^\# \pi'$.

Proof. From Lemma 14.6, with $u = g^\dagger(z)$,

$$\begin{aligned} (g^\dagger)^\# \pi'(u) &= (\pi' \circ (g^\dagger)^{-1})(u) \det D((g^\dagger)^{-1})(u) \\ &= \frac{1}{Z} \nu(y - G(u)) (\rho' \circ (g^\dagger)^{-1})(u) \det D((g^\dagger)^{-1})(u) \\ &= \frac{1}{Z} \nu(y - G(u)) (g^\dagger)^\# \rho'(u) \\ &= \frac{1}{Z} \nu(y - G(u)) \rho(u), \\ &= \pi(u) \end{aligned}$$

as required. \square

A similar result may be established even if $d_z < d$. Hence, if pair (g^\dagger, ρ') are known, then the original Bayesian inverse problem for π on \mathbb{R}^d may be converted to one for π' on \mathbb{R}^{d_z} ; pushforward of π' under g^\dagger yields solution to the original problem. For this reason we concentrate on this inverse problem in z -space and the effect of having learned g^\dagger from data, and hence know it only approximately.

In practice we typically specify ρ' to be a simple measure such as a unit Gaussian. By means of unsupervised learning methods, such as those outlined in Subsection 14.2, we have access to an approximation g^* to g^\dagger . An assumption such as the following can be reasonably expected to hold for many of these methods, if sufficient data is employed, with high probability. However little analysis of this kind is currently available. We will proceed on the basis that the assumption holds.

Assumption 14.14. *Assume that probability density ρ' is supported on compact set $D \subset \mathbb{R}^{d_z}$. Then, for any $\delta > 0$, there is $\theta_g^* \in \Theta_g$ such that*

$$\sup_{z \in D} |g^\dagger(z) - g^*(z)| < \delta. \quad (14.37)$$

In what follows, we denote by g_δ any function g^* for which upper error bound (14.37) holds. We define

$$l(z) = \nu(y - G(g^\dagger(z))) \quad \text{and} \quad l_\delta(z) = \nu(y - G(g_\delta(z))),$$

the true and approximate likelihoods in the z -space formulation of the inverse problem. In z -space we also define the true and approximate posterior distributions defined by

$$\pi'(z) = \frac{1}{Z} l(z) \rho'(z) \quad \text{and} \quad \pi'_\delta(z) = \frac{1}{Z_\delta} l_\delta(z) \rho'(z),$$

where $Z, Z_\delta > 0$ are the corresponding normalizing constants.

Theorem 14.15 (Effect of Machine-Learned Prior on Posterior). *Let Assumption 14.14 hold and assume that ν, G are C^1 functions, uniformly on compact sets, and that g is bounded on D . Then we have*

$$d_H(\pi', \pi'_\delta) \leq c\delta, \quad \delta \in (0, \Delta),$$

for some $\Delta > 0$ and some $c \in (0, +\infty)$ independent of δ .

Proof. The proof is identical to the proof of Theorem 14.11 after noting that Assumption 14.14, together with the boundedness of g and the C^1 properties of ν, G , imply Assumption 14.10, in z -space. \square

14.5 Learning the Prior to Posterior Map

Consider Bayes theorem written as map relating prior ρ to posterior π via the relation

$$\begin{aligned} \pi(u) &= \frac{1}{Z} l(u) \rho(u), \\ Z &= \mathbb{E}^{u \sim \rho} [l(u)]. \end{aligned}$$

This is a nonlinear map on the space of measures. We now ask whether we can realize this nonlinear map via an invertible transport T on the state-space \mathbb{R}^d with the property $\pi = T^\# \rho$. Specifically, in the notation of Subsection 14.2.2, we seek to find $\theta_g \in \Theta_g$ to minimize

$$F(\theta_g) = d_{\text{KL}}(\rho \| T^{-1}(\cdot; \theta_g)^\# \pi).$$

From (14.28), with $g = T^{-1}$, we deduce that

$$F(\theta_g) = -\mathbb{E}^{u \sim \rho} [\log \pi \circ T(u; \theta_g) + \log \det D_u T(u; \theta_g)] + \text{const},$$

Using the expression for the posterior in terms of the prior, and noting that Z is constant, we may write

$$F(\theta_g) = -\mathbb{E}^{u \sim \rho} [\log \rho \circ T(u; \theta_g) + \log l \circ T(u; \theta_g) + \log \det D_u T(u; \theta_g)] + \text{const}. \quad (14.38)$$

As usual we identify θ_g^* with the argmin of F and then employ transport map $T^* = T(\cdot; \theta_g^*)$. For simplicity we have sought the posterior as transport from the prior. This is natural because prior measures are often straightforward to sample, and hence $F(\theta_g)$ can be evaluated by Monte Carlo, for example. However it may be computationally expedient to seek π which is the pushforward of a different, easy-to-sample, reference measure.

14.6 Discussion and Bibliography

The subject of neural network function approximation, the core task of supervised learning, is overviewed in [76]. Universal approximation theorems may be found in [65, 242]. The use of random features was popularized as a methodology, and analyzed rigorously, in the collection of papers [247, 249, 248]. Gaussian processes are described

in [316] and kernel-based methods more generally are described in [231]. Error estimates for interpolation using Gaussian processes are developed in [315]. The link between regression and Bayesian inversion with Gaussian process priors is developed in depth in [61, 312]. A definition of MAP estimator in infinite dimensions, appropriate for the discussion in Remark 14.4 may be found in [67]. We have articulated a specific link between neural networks and random features; a related concept underpins the subject of the *neural tangent kernel* [155].

The subject of optimal transport is overviewed and systematically developed in [308]; computational methodology is overviewed and developed in [240]. The idea of conducting unsupervised learning with (generative adversarial networks) GANs was introduced in [118]. Autoencoders have a long history; see [119, 140, 277] and the citations therein. Triangular transport maps are overviewed as a method for sampling in [208].

The idea of learning regularizers from data, to define objective functions for the optimization approach to inversion, is overviewed in [14]. The paper [285] provides a framework for the subject which employs structured factorizations of data matrices to learn semidefinite regularizers. The paper [200] develops an adversarial approach to the problem.

The idea of learning prior probabilistic models from data is described in [235] where generative adversarial networks are used to determine a mapping from a Gaussian to the space of prior data samples. Many methods of this type reduce the dimension of the unknown parameter space, determining a latent space of low effective dimension. A different approach to learning this mapping is to use invertible maps [172] and the work on normalizing flows [296, 286]; see [16] for application of invertible maps to prior construction for inversion. This idea can be combined with variational inference to solve sampling problems in general, and inverse problems in particular [261, 295, 102, 230]. The use of triangular transport maps for Bayesian inference was introduced in [87].

Using emulators to speed-up forward model evaluations, for example in the context of likelihood evaluation in Bayesian inversion, was first introduced as a systematic methodology in [266], and taken further in the realm of Bayesian model error estimation in [169]. The paper [291] studies the use of Gaussian processes for emulation, and derives errors bounds quantifying the effect of emulation error on the posterior; the methodology is developed for a range of applications in the geosciences in [57]. A specific application of the idea in climate science may be found in [84]. Data-driven discretizations of forward models for Bayesian inversion are studied in [25].

The topic of clustering is overviewed in [310]. The paper [219] describes an underlying mathematical framework, based on eigenvalue perturbation theory. Understanding large data limits of spectral clustering methods is a subject developed in [311, 141]. The use of graph Laplacians, which underpin spectral clustering, in the solution of inverse problems, is undertaken in [106, 86, 109, 132, 272, 134]. The use of various machine-learning inspired approximation methods in the solution of PDEs may be found in [251, 54, 218, 175].

Chapter 15

Blending Data Assimilation and Machine Learning

In Part II of these notes we considered the data assimilation problem of estimating a time-evolving state in the setting where the dynamics governing the state-observation system is known. It is natural to ask how to extend this to settings where the dynamical model is itself unknown. This final chapter is devoted to the problem of estimating a time-evolving state and the dynamics governing its evolution from a window of partial and noisy observations of the state. Estimating jointly the state and mathematical model governing the dynamics is important in data assimilation applications where available stochastic dynamics models are inaccurate or expensive to evaluate. The accuracy of data assimilation can be improved, for instance, by estimating parameters in the model dynamics or by learning a neural network model correction; the efficiency of data assimilation can be improved by leveraging machine-learned surrogate models that are cheap to evaluate.

This chapter describes two algorithmic frameworks to blend data assimilation techniques for estimating the state with machine learning techniques for recovering model parameters or training surrogate models. After introducing the problem setting in Section 15.1, Section 15.2 describes the expectation-maximization framework and an algorithmic implementation based on Monte Carlo integration and gradient descent. Section 15.3 considers auto-differentiable Kalman filters, which enable blending Kalman filtering algorithms with gradient descent and auto-differentiation methods. Section 15.4 closes with extensions and bibliographical remarks. The material in this chapter brings together many topics covered in these notes, including optimization (Chapter 3), variational formulations of Bayes theorem (Chapter 4), Monte Carlo methods (Chapters 5 and 6), Kalman filtering algorithms (Chapters 8 and 10), and parameterizations of functions for machine learning (Chapter 14).

15.1 The Setting

Consider stochastic dynamics and data models given by

$$v_{j+1} = \Psi_{\vartheta}(v_j) + \xi_j, \quad \xi_j \sim \mathcal{N}(0, \Sigma_{\beta}) \text{ i.i.d.}, \quad (15.1)$$

$$y_{j+1} = H v_{j+1} + \eta_{j+1}, \quad \eta_j \sim \mathcal{N}(0, \Gamma) \text{ i.i.d.}, \quad (15.2)$$

with $v_0 \sim \mathcal{N}(m_0, C_0)$ independent of the independent i.i.d. sequences $\{\xi_j\}$ and $\{\eta_j\}$. We assume that $v_j \in \mathbb{R}^d$ and $y_j \in \mathbb{R}^k$. The observation matrix H and noise covariance Γ

in (15.2) are assumed to be known. The stochastic dynamics in (15.1) are defined in terms of a deterministic map Ψ_ϑ and Gaussian additive noise with covariance Σ_β , where $\theta := \{\vartheta, \beta\}$ are model parameters. We denote the Markov kernel for the dynamics by $\mathbb{P}(\cdot | v_j, \theta) := \mathcal{N}(\Psi_\vartheta(v_j), \Sigma_\beta)$ and are interested in finding θ so that this Markov kernel approximates that of an unknown, ground-truth stochastic dynamics model of the form

$$v_{j+1} = \Psi^\dagger(v_j) + \xi_j, \quad \xi_j \sim \mathcal{N}(0, \Sigma^\dagger), \quad 1 \leq j \leq J. \quad (15.3)$$

Once θ is found, the signal $\{v_j\}$ can be estimated using the filtering and smoothing algorithms in Part II of these notes with stochastic dynamics (15.1) and data model (15.2). The role of the parameter β is to enable estimating the unknown covariance Σ^\dagger . We consider three motivating examples for the interpretation of the parameter ϑ , of the parameterized map Ψ_ϑ , and of the relationship between the map Ψ_ϑ and the ground-truth deterministic map Ψ^\dagger .

Example 15.1 (Parameterized Dynamics). $\Psi^\dagger = \Psi_{\vartheta^\dagger}$ is parameterized, but the true parameter ϑ^\dagger is unknown and needs to be estimated. For instance, Ψ^\dagger may be defined by time-discretization of a parameterized system of differential equations and we may be interested in estimating ϑ^\dagger from observations $\{y_j\}$. \diamond

Example 15.2 (Fully-Unknown Dynamics). There are settings in which Ψ^\dagger is fully unknown and ϑ represents the parameters of a neural network, random features, or Gaussian process surrogate model Ψ_ϑ for Ψ^\dagger ; see Chapter 14 for background on these parameterizations of functions. The goal is to find an accurate surrogate model Ψ_ϑ . Even if Ψ^\dagger is fully known, a surrogate model, or *emulator*, may be much cheaper to evaluate, enabling the use of large sample size for particle filters or ensemble Kalman methods. Similar computational considerations motivated learning the forward map for inverse problems in Chapter 14. \diamond

Example 15.3 (Model Correction). Ψ^\dagger is unknown, but we have access to an inaccurate model $\Psi^{\text{approx}} \approx \Psi^\dagger$. Here ϑ represents the parameters of a neural network, random features, or Gaussian process $\Psi_\vartheta^{\text{correction}}$ used to correct the inaccurate model Ψ^{approx} . The goal is to learn ϑ so that $\Psi_\vartheta := \Psi^{\text{approx}} + \Psi_\vartheta^{\text{correction}}$ approximates Ψ^\dagger accurately. Learning model corrections is important in applications where available models have moderate predictive accuracy. For instance, fine scales of the state may not be resolved accurately due to computational constraints and we may be interested in learning from data a surrogate model which accounts for the unresolved scales of the system. \diamond

For a given and fixed integer J , we define, following the notation in Chapter 7,

$$V := \{v_0, \dots, v_J\}, \quad Y := \{y_1, \dots, y_J\}.$$

Note that $V \in \mathbb{R}^{d(J+1)}$ and $Y \in \mathbb{R}^{kJ}$. In contrast to the supervised learning setting in Chapter 14, here we do not assume to have direct data $\{v^{(n)}, \Psi^\dagger(v^{(n)})\}_{n=1}^N$ to learn the map Ψ^\dagger . Instead, we assume to have only access to data Y obtained from indirect and noisy measurement of a trajectory V from the signal. However, this new learning task can also be cast as an optimization problem, and to that end we adopt a *maximum*

likelihood estimation approach to estimate θ . That is, we seek to find θ that maximizes the likelihood function of θ given the observed data Y :

$$\mathbb{P}(Y|\theta) = \int \mathbb{P}(V, Y|\theta) dV = \int \mathbb{P}(Y|V) \mathbb{P}(V|\theta) dV. \quad (15.4)$$

In the last equation we used that $\mathbb{P}(Y|V, \theta) = \mathbb{P}(Y|V)$; here and throughout this chapter integrals are over $\mathbb{R}^{d(J+1)}$ unless otherwise noted. Evaluating the likelihood function $\mathbb{P}(Y|\theta)$ is challenging due to the unobserved, or *latent*, variable V . Therefore, in practice we may seek to maximize a lower bound or an approximation of the likelihood function.

Whilst evaluating the likelihood is often challenging, we will use in the sequel that the joint distribution of V and Y admits the characterization

$$\begin{aligned} \log \mathbb{P}(V, Y|\theta) &= \log \mathbb{P}(Y|V) + \log \mathbb{P}(V|\theta) \\ &= -\frac{1}{2} \sum_{j=0}^{J-1} |y_{j+1} - H v_{j+1}|_{\Gamma}^2 - \frac{1}{2} \det \log(\Sigma_{\beta}) \\ &\quad - \frac{1}{2} |v_0 - m_0|_{C_0}^2 - \frac{1}{2} \sum_{j=0}^{J-1} |v_{j+1} - \Psi_{\vartheta}(v_j)|_{\Sigma_{\beta}}^2 + c, \end{aligned} \quad (15.5)$$

where c is a constant independent of V , Y and θ . The next two sections consider two algorithmic frameworks to approximately compute the maximum likelihood estimator.

15.2 The Expectation-Maximization Framework

The expectation-maximization (EM) algorithm is a general-purpose approach to maximum likelihood estimation with latent variables. We derive it here in general terms and then specify it to the problem of joint estimation of state and dynamics model parameters θ . Central to the abstract derivation of the EM algorithm is the following lower bound of the log-likelihood function, obtained using Jensen inequality:

$$\begin{aligned} \log \mathbb{P}(Y|\theta) &= \log \int \mathbb{P}(V, Y|\theta) dV \\ &= \log \int \frac{\mathbb{P}(V, Y|\theta)}{q(V)} q(V) dV \\ &\geq \int \log \left(\frac{\mathbb{P}(V, Y|\theta)}{q(V)} \right) q(V) dV =: \mathcal{L}(q, \theta), \end{aligned}$$

where q is any pdf over the latent variables V with compatible support. In fact, the following theorem shows that the difference between $\log \mathbb{P}(Y|\theta)$ and $\mathcal{L}(q, \theta)$ is given by the Kullback-Leibler divergence $d_{\text{KL}}(q \| \mathbb{P}(V|Y, \theta))$, which is always non-negative. Notice that the proof is identical to that of the variational formulation of Bayes theorem in Chapter 4.

Theorem 15.4 (Likelihood Characterization for EM Framework). *It holds that*

$$\log \mathbb{P}(Y|\theta) = \mathcal{L}(q, \theta) + d_{\text{KL}}(q \| \mathbb{P}(V|Y, \theta)).$$

Proof. Using the definition of $\mathcal{L}(q, \theta)$, product rule, and the definition of the Kullback-Leibler divergence in Chapter 4, we have

$$\begin{aligned}\mathcal{L}(q, \theta) &= \int \log \left(\frac{\mathbb{P}(V, Y | \theta)}{q(V)} \right) q(V) dV \\ &= \int \log \left(\frac{\mathbb{P}(V | Y, \theta)}{q(V)} \right) q(V) dV + \int \log \mathbb{P}(Y | \theta) q(V) dV \\ &= -d_{\text{KL}}(q \| \mathbb{P}(V | Y, \theta)) + \log \mathbb{P}(Y | \theta),\end{aligned}$$

as desired. \square

Theorem 15.4 motivates an iterative approach to maximize the log-likelihood function $\log \mathbb{P}(Y | \theta)$, which is equivalent to maximizing the likelihood $\mathbb{P}(Y | \theta)$ since the logarithm is an increasing function. Given the current iterate θ_ℓ , we obtain the next iterate $\theta_{\ell+1}$ in two steps, maximizing in turn the two components of the lower bound:

1. First, we find $q_\ell(V)$ that maximizes the lower bound $\mathcal{L}(q, \theta_\ell)$ over pdf q . From Theorem 15.4,

$$\log \mathbb{P}(Y | \theta_\ell) = \mathcal{L}(q, \theta_\ell) + d_{\text{KL}}(q \| \mathbb{P}(V | Y, \theta_\ell)),$$

and it follows that maximizing $\mathcal{L}(q, \theta_\ell)$ or minimizing $d_{\text{KL}}(q \| \mathbb{P}(V | Y, \theta_\ell))$ over q are equivalent. Since the Kullback-Leibler divergence is minimized when both arguments agree, we obtain that $q_\ell(V) = \mathbb{P}(V | Y, \theta_\ell)$.

2. Second, we obtain $\theta_{\ell+1}$ by maximizing the lower bound $\mathcal{L}(q_\ell, \theta)$ over θ . Note that

$$\mathcal{L}(q_\ell, \theta) = \int \log \mathbb{P}(V, Y | \theta) \mathbb{P}(V | Y, \theta_\ell) dV + c, \quad (15.6)$$

where c is independent of θ . Hence, the quantity to maximize is the expected value of the joint log-density $\log \mathbb{P}(V, Y | \theta)$ with respect to $q_\ell(V) = \mathbb{P}(V | Y, \theta_\ell)$.

Combining these two steps gives the EM framework, summarized in Algorithm 15.1 below. Figure 15.1 illustrates how each new iterate is obtained by maximizing a lower bound on the log-likelihood.

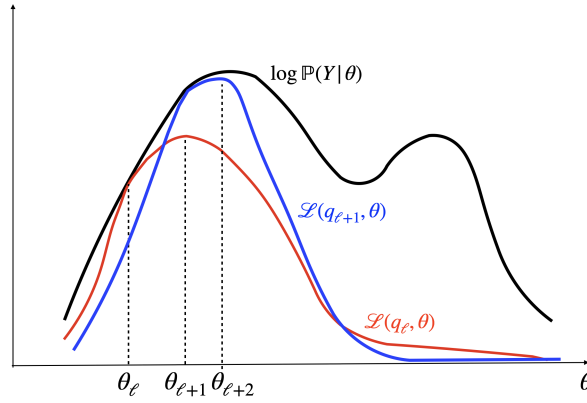


Figure 15.1 Iterates of the EM algorithm. The blue and red lines represent log-likelihood lower bounds as functions of θ . Notice that they lie below the likelihood, but $\mathbb{P}(Y|\theta_\ell) = \mathcal{L}(q_\ell, \theta_\ell)$ since by design $d_{\text{KL}}(q_\ell \| \mathbb{P}(V|Y, \theta_\ell)) = 0$ for all $\ell \geq 0$.

Algorithm 15.1 Expectation Maximization

- 1: **Input:** Initialization θ_0 .
- 2: For $\ell = 0, 1, \dots, L - 1$ do the following expectation and maximization steps:
- 3: **E-Step:** Compute

$$\mathbb{E}^{V \sim \mathbb{P}(V|Y, \theta_\ell)} [\log \mathbb{P}(V, Y|\theta)] = \int \log \mathbb{P}(V, Y|\theta) \mathbb{P}(V|Y, \theta_\ell) dV.$$

- 4: **M-Step:** Compute

$$\theta_{\ell+1} = \arg \max_{\theta} \mathbb{E}^{V \sim \mathbb{P}(V|Y, \theta_\ell)} [\log \mathbb{P}(V, Y|\theta)].$$

- 5: **Output:** Parameter θ^L .
-

The following result shows that the EM framework has the desirable property that the likelihood function increases monotonically along iterates θ_ℓ .

Theorem 15.5 (Monotonic Increase of Likelihood along EM Iterates). *Let $\{\theta_\ell\}_{\ell=0}^{L-1}$ be the iterates of the EM Algorithm 15.1. Then, for $0 \leq \ell \leq L - 1$, it holds that*

$$\log \mathbb{P}(Y|\theta_\ell) \leq \log \mathbb{P}(Y|\theta_{\ell+1}). \quad (15.7)$$

Proof. Let $q_\ell(V) = \mathbb{P}(V|Y, \theta_\ell)$. Using the log-likelihood characterization in Theorem

15.4, it holds that

$$\begin{aligned}
\log \mathbb{P}(Y|\theta_{\ell+1}) &= \mathcal{L}(q_\ell, \theta_{\ell+1}) + d_{\text{KL}}(q_\ell \| \mathbb{P}(V|Y, \theta_{\ell+1})) \\
&\geq \mathcal{L}(q_\ell, \theta_\ell) + d_{\text{KL}}(q_\ell \| \mathbb{P}(V|Y, \theta_{\ell+1})) \\
&\geq \mathcal{L}(q_\ell, \theta_\ell) + d_{\text{KL}}(q_\ell \| \mathbb{P}(V|Y, \theta_\ell)) \\
&= \log \mathbb{P}(Y|\theta_\ell).
\end{aligned}$$

The first inequality follows because $\theta_{\ell+1} = \arg \max_\theta \mathcal{L}(q_\ell, \theta)$; the second because $d_{\text{KL}}(q_\ell \| \mathbb{P}(V|Y, \theta_\ell)) = 0$ since $q_\ell = \mathbb{P}(V|Y, \theta_\ell)$, while $d_{\text{KL}}(q_\ell \| \mathbb{P}(V|Y, \theta_{\ell+1})) \geq 0$. \square

Remark 15.6. As a consequence of Theorem 15.5 it is possible to deduce —under mild assumptions— that the iterates θ_ℓ of the EM algorithm converge, as $\ell \rightarrow \infty$, to a local maximizer of the likelihood function. It is important to note, however, that the expectation in the E-step and the optimization in the M-step are often intractable. Monte Carlo, filtering, or smoothing algorithms may be employed to approximate the E-step, and optimization algorithms to approximate the M-step. Such approximations can cause loss of monotonicity and convergence guarantees. \diamond

Let us now return to the problem of jointly estimating state and dynamics. To illustrate the application of the EM algorithm in this setting, we consider Monte Carlo methods for the E-step and gradient descent optimization for the M-step.

For the E-step, recall equation (15.5) to see that

$$\mathbb{E}^{V \sim \mathbb{P}(V|Y, \theta_\ell)} \left[\log \mathbb{P}(V, Y|\theta) \right] = -\frac{1}{2} \log \det(\Sigma_\beta) - \frac{1}{2} \int \sum_{j=0}^{J-1} |v_{j+1} - \Psi_\vartheta(v_j)|_{\Sigma_\beta}^2 \mathbb{P}(V|Y, \theta_\ell) dV + c, \quad (15.8)$$

where c is independent of θ . Thus, given (approximate) samples $\{V^{(n)}\}_{n=1}^N$ from $\mathbb{P}(V|Y, \theta_\ell)$, we may use Monte Carlo integration to approximate

$$\mathbb{E}^{V \sim \mathbb{P}(V|Y, \theta_\ell)} \left[\log \mathbb{P}(V, Y|\theta) \right] \approx -\frac{1}{2} \log \det(\Sigma_\beta) - \frac{1}{2} \frac{1}{N} \sum_{n=1}^N \sum_{j=0}^{J-1} |v_{j+1}^{(n)} - \Psi_\vartheta(v_j^{(n)})|_{\Sigma_\beta}^2. \quad (15.9)$$

For the M-step, we notice that given ϑ , the above expression can be explicitly maximized over β ; however, to optimize over ϑ we need to resort to optimization methods. The following algorithm summarizes an EM implementation for learning dynamics and states using Monte Carlo and gradient descent.

Algorithm 15.2 Expectation-Maximization with Monte Carlo and Gradient Descent

- 1: **Input:** Initialization $\theta^0 = (\vartheta^0, \beta^0)$. Rule to choose gradient descent step-sizes $\{\alpha_i\}_{i=1}^{\mathcal{I}}$.
- 2: For $\ell = 0, 1, \dots, L-1$ do the following expectation and maximization steps:
- 3: **E-Step:** Obtain (approximate) samples $\{V^{(n)}\}_{n=1}^N$ from $\mathbb{P}(V|Y, \theta_\ell)$.
- 4: **M-Step:**
- 5: Set

$$\Sigma_{\beta^{\ell+1}} = \frac{1}{NJ} \sum_{n=1}^N \sum_{j=0}^{J-1} \left(v_{j+1}^{(n)} - \Psi_{\vartheta^\ell}(v_j^{(n)}) \right) \left(v_j^{(n)} - \Psi_{\vartheta^\ell}(v_j^{(n)}) \right)^\top$$

and define

$$J(\vartheta, \{V^{(n)}\}_{n=1}^N) := \frac{1}{NJ} \sum_{n=1}^N \sum_{j=0}^{J-1} |v_{j+1}^{(n)} - \Psi_{\vartheta}(v_j^{(n)})|_{\Sigma_{\beta^{\ell+1}}}^2.$$

- 6: Initialize $\vartheta^{\ell,0} = \vartheta^\ell$.
 - 7: For $i = 0, \dots, \mathcal{I}-1$ do:
 - 8: $\vartheta^{\ell,i+1} = \vartheta^{\ell,i} - \alpha_i \nabla J(\vartheta^{\ell,i}, \{V^{(n)}\}_{n=1}^N)$.
 - 9: Set $\vartheta^{\ell+1} = \vartheta^{\ell,\mathcal{I}}$.
 - 10: **Output:** Approximation θ^L to the maximum likelihood estimator.
-

The signal $\{v_j\}$ can be estimated by performing data assimilation with the stochastic dynamics and data models (15.1) and (15.2) with learned parameter ϑ^L and covariance model Σ_{β^L} .

Remark 15.7. In analogy to the supervised learning task studied in Chapter 14, equation (15.8) may be conceptually interpreted as defining a risk for the parameter θ ; here the distribution $\mathbb{P}(V|Y, \theta_\ell)$, which represents our available knowledge on the distribution of the latent variable V given data Y and parameter estimate θ^ℓ , plays an analogous role to Υ in Chapter 14. Then, (15.9) can be interpreted as an empirical risk, defined via approximate samples $V^{(n)} \sim \mathbb{P}(V|Y, \theta_\ell)$. These samples may be obtained, for instance, using the MCMC methods described in Chapter 6. Alternately, ensemble Kalman methods may be employed, with the proviso that, as discussed in Chapter 10, they can yield accurate posterior samples only in approximately linear-Gaussian settings. Finally, notice that the implementation of the EM framework in Algorithm 15.2 treats differently the parameters ϑ and β in the M-step. This is because optimization of the empirical risk over Σ_β admits a closed form solution, but optimization algorithms such as gradient descent are needed to optimize ϑ for general parameterization Ψ_ϑ of the dynamics. \diamond

15.3 Auto-Differentiable Kalman Filters

In Chapter 10 we studied extended and ensemble Kalman filtering algorithms that combine a Gaussian approximation

$$\mathbb{P}(v_{j+1}|Y_j, \theta) \approx \mathcal{N}(\hat{m}_{j+1}(\theta), \hat{C}_{j+1}(\theta)) \quad (15.10)$$

for the predictive distribution with a linear-Gaussian data model to derive an approximation

$$\mathbb{P}(v_{j+1}|Y_{j+1}, \theta) \approx \mathcal{N}(m_{j+1}(\theta), C_{j+1}(\theta)) \quad (15.11)$$

of the filtering distribution. These Gaussian approximations can be accurate if the noise in the dynamics and the observations are small, or the map Ψ_θ is approximately linear. In this section we show how the Gaussian ansatz (15.10) can be leveraged to produce a Kalman-based approximation of the log-likelihood function $\log \mathbb{P}(Y|\theta)$ and thereby an algorithm for maximum likelihood estimation. The derivation rests upon the following characterization of the log-likelihood function under a Gaussian ansatz.

Theorem 15.8 (Likelihood Characterization under Gaussian Predictive Distribution). *Suppose that, for each $0 \leq j \leq J-1$, the predictive distribution $\mathbb{P}(v_{j+1}|Y_j, \theta)$ of the stochastic dynamics and data models (15.1) and (15.2) is Gaussian with mean $\hat{m}_{j+1}(\theta)$ and covariance $\hat{C}_{j+1}(\theta)$. Then the log-likelihood function admits the following characterization*

$$\log \mathbb{P}(Y|\theta) = -\frac{1}{2} \sum_{j=0}^{J-1} |y_{j+1} - H\hat{m}_{j+1}(\theta)|_{S_{j+1}(\theta)}^2 - \frac{1}{2} \sum_{j=0}^{J-1} \log \det(S_{j+1}(\theta)), \quad (15.12)$$

where $S_{j+1}(\theta) = H\hat{C}_{j+1}(\theta)H^\top + \Gamma$.

Proof. We have

$$\log \mathbb{P}(Y|\theta) = \sum_{j=0}^{J-1} \log \mathbb{P}(y_{j+1}|Y_j, \theta),$$

where we use the convention that $Y_0 := \emptyset$ so that conditioning to Y_0 does not provide any information. Now conditioning in the data model

$$y_{j+1} = Hv_{j+1} + \eta_{j+1},$$

we see that

$$\begin{aligned} \mathbb{E}[y_{j+1}|Y_j] &= \mathbb{E}[Hv_{j+1} + \eta_{j+1}|Y_j] = H\hat{m}_{j+1}(\theta), \\ \text{Cov}[y_{j+1}|Y_j] &= \text{Cov}[Hv_{j+1} + \eta_{j+1}|Y_j] = H\hat{C}_{j+1}(\theta)H^\top + \Gamma. \end{aligned}$$

Moreover, $\mathbb{P}(y_{j+1}|Y_j)$ is Gaussian. The result follows. \square

Thus, for any value of θ , we may obtain an *approximation* of the log-likelihood $\log \mathbb{P}(Y|\theta)$ by running a Kalman filtering algorithm, obtaining predictive means and covariances $\hat{m}_{j+1}(\theta), \hat{C}_{j+1}(\theta)$, for $0 \leq j \leq J-1$, and using (15.12). Moreover, an approximation of the log-likelihood gradient at θ can be obtained auto-differentiating through our Kalman-based likelihood estimate. Automatic-differentiation involves repeated application of chain rule on elementary operations and enables computing derivatives accurately to working precision. Auto-differentiable Kalman filters use these estimates of the log-likelihood gradients to conduct gradient descent. The procedure is summarized in Algorithm 15.3.

Algorithm 15.3 Auto-Differentiable Kalman Filter

- 1: **Input:** Initialization θ^0 , rule to choose step-sizes $\{\alpha_\ell\}_{\ell=0}^{L-1}$.
- 2: For $\ell = 0, 1, \dots, L-1$ do the following Kalman filtering and gradient descent steps:
- 3: **Kalman Filtering:** Run a Kalman filtering algorithm to obtain predictive means and covariances $\hat{m}_{j+1}(\theta^\ell), \hat{C}_{j+1}(\theta^\ell)$, for $0 \leq j \leq J-1$. Set

$$J(\theta^\ell) := \frac{1}{2} \sum_{j=0}^{J-1} |y_{j+1} - H\hat{m}_{j+1}(\theta^\ell)|_{S_{j+1}(\theta^\ell)}^2 + \frac{1}{2} \sum_{j=0}^{J-1} \log \det(S_{j+1}(\theta^\ell)).$$

- 4: **Gradient Descent:** Auto-differentiate the map $\theta^\ell \mapsto J(\theta^\ell)$ to obtain a gradient estimate $\nabla J(\theta^\ell)$. Set

$$\theta^{\ell+1} = \theta^\ell - \alpha_\ell \nabla J(\theta^\ell). \quad (15.13)$$

- 5: **Output:** Approximation θ^L to the maximum likelihood estimator.
-

The signal $\{v_j\}$ can be estimated by performing data assimilation with the stochastic dynamics and data models (15.1) and (15.2) with learned parameter θ^L .

Remark 15.9. Notice that in the EM Algorithm 15.2 each posterior sample $\{V^{(n)}\}_{n=1}^N$ is used to perform \mathcal{I} gradient descent steps in the M-Step, with the goal of maximizing the lower bound $\mathcal{L}(q_\ell, \theta)$. In contrast, in the auto-differentiable Kalman filter Algorithm 15.3, each run of a Kalman filtering algorithm is used to produce an estimate of the log-likelihood gradient, and a gradient descent is taken. \diamond

15.4 Discussion and Bibliography

In this chapter we have introduced two computational frameworks for joint state and parameter estimation: the EM algorithm and auto-differentiable filters. Both frameworks find the parameters in the dynamics by approximating the maximum likelihood estimator, and then use a filtering or smoothing algorithm to recover the state. This final section provides bibliographical context for the algorithms considered

in this chapter, and briefly discusses other computational methods that do not stem from a maximum likelihood formulation.

The EM framework for maximum likelihood estimation was introduced in [72]. Embedding of the EnKF and the ensemble Kalman smoother (EnKS) into the EM algorithm was proposed in [297, 305, 82, 246], with a focus on estimation of error covariance matrices. The E-step is approximated with an EnKS under the Monte Carlo EM framework [314]. In addition, [34, 220] incorporate machine learning techniques in the M-step to train neural network surrogate models. The paper [31] proposes Bayesian estimation of model error statistics, together with a neural network emulator for the dynamics. On the other hand, [306, 58] consider online EM methods for error covariance estimation with EnKF. Although gradient information is used during the M-step to train the surrogate model [34, 220, 31], these methods do not auto-differentiate through the EnKF.

Our presentation of auto-differentiable Kalman filters follows [55], which proposes and analyzes an approach for joint state and parameter estimation that leverages gradient information of an EnKF estimate of the likelihood. EnKFs for derivative-free maximum likelihood estimation are studied in [289, 246]. An empirical comparison of the likelihood computed using the EnKF and other filtering algorithms is made in [44]; see also [131, 210]. The paper [83] uses EnKF likelihood estimates to design a pseudo-marginal MCMC method for Bayesian inference of model parameters. The works [288, 290] propose online Bayesian parameter estimation using the likelihood computed from the EnKF under a certain family of conjugate distributions.

While our discussion has focused on ensemble Kalman methods, particle filters can also be employed for joint state and parameter estimation. Particle filters give an unbiased estimate of the data likelihood [69, 13]. Based upon this likelihood estimate, a particle MCMC Bayesian parameter estimation method is designed in [13]. Although particle filter likelihood estimates are unbiased, they suffer from two potential drawbacks that limit their applicability to some problems. First, their variance can be large, as they inherit the weight degeneracy of importance sampling in high dimensions [284, 5, 268, 271] —see Chapters 11 and 12 for further background on this subject. Second, while the forecast and analysis steps of particle filters can be auto-differentiated, the resampling steps involve discrete distributions that cannot be handled by the reparameterization trick, as discussed in [55]. For this reason, previous differentiable particle filters omit auto-differentiation of the resampling step [217, 202, 187], introducing a bias.

An alternative to maximum likelihood estimation is to optimize a lower bound of the data log-likelihood with variational inference [27, 173, 252]. The posterior distribution over the latent states is approximated with a parametric distribution and is jointly optimized with model parameters defining the dynamics model. In this direction, variational sequential Monte Carlo methods [217, 202, 187] construct the lower bound using a particle filter. Moreover, the proposal distribution of the particle filter is parameterized and jointly optimized with model parameters. Although variational sequential Monte Carlo methods provide consistent data log-likelihood estimates, they suffer from the same two potential drawbacks as likelihood-based particle filter methods.

A recent work [154] proposes blending variational sequential Monte Carlo and EnKF with an importance sampling-type lower bound estimate, which is effective if the state dimension is small. Other works that build on the variational inference framework include [177, 253, 99]. An important challenge is to obtain suitable parameterizations of the posterior, especially when the state dimension is high. For this reason, a restrictive Gaussian parameterization with a diagonal covariance matrix is often used in practice [177, 99].

Another alternative approach to maximum likelihood estimation is to concatenate state and parameters into an augmented state-space, and employ the data assimilation methods in Part II of these notes in the augmented state-space. This approach requires one to design a pseudo-dynamic for the parameters, which can be challenging when certain types of parameters (e.g., error covariance matrices) are involved [288, 71] or if the dimension of the parameters is high. The use of EnKF for joint learning of state and model parameters by *state augmentation* was introduced in [12].

Beyond the problem of joint parameter and state estimation, the development of data-driven frameworks for learning dynamical systems is a very active research area. We refer to [39, 122, 133, 250] for recent methods that do not rely on the EM algorithm, auto-differentiation of filtering methods, or variational inference.

Bibliography

- [1] S. I. Aanonsen, G. Nævdal, D. S. Oliver, A. C. Reynolds, and B. Vallès. The ensemble Kalman filter in reservoir engineering—a review. *Spe Journal*, 14(03): 393–412, 2009.
- [2] H. Abarbanel. *Predicting The Future: Completing Models Of Observed Complex Systems*. Springer, 2013.
- [3] S. Agapiou, S. Larsson, and A. M. Stuart. Posterior contraction rates for the Bayesian approach to linear ill-posed inverse problems. *Stochastic Processes and their Applications*, 123(10):3828–3860, 2013.
- [4] S. Agapiou, M. Burger, M. Dashti, and T. Helin. Sparsity-promoting and edge-preserving maximum a posteriori estimators in non-parametric Bayesian inverse problems. *Inverse Problems*, 34(4):045002, 2017.
- [5] S. Agapiou, O. Papaspiliopoulos, D. Sanz-Alonso, and A. M. Stuart. Importance sampling: Intrinsic dimension and computational cost. *Statistical Science*, 32(3): 405–431, 2017.
- [6] S. Agrawal, H. Kim, D. Sanz-Alonso, and A. Strang. A variational inference approach to inverse problems with gamma hyperpriors. *arXiv preprint arXiv:2111.13329*, 2021.
- [7] Ö. D. Akyildiz and J. Míguez. Convergence rates for optimised adaptive importance samplers. *Statistics and Computing*, 31(2):1–17, 2021.
- [8] O. al Ghattas and D. Sanz-Alonso. Non-asymptotic analysis of ensemble Kalman updates: effective dimension and localization. *arXiv*, 2022.
- [9] D. J. Albers, P.-A. Blancquart, M. E. Levine, E. E. Seylabi, and A. M. Stuart. Ensemble Kalman methods with constraints. *Inverse Problems*, 35(9):095007, 2019.
- [10] B. Anderson and J. B. Moore. *Optimal Filtering*. Prentice-Hall Information and System Sciences Series, 1979.
- [11] E. C. Anderson. Monte Carlo methods and importance sampling. *Lecture Notes for Statistical Genetics*, 2014.

- [12] J. L. Anderson. An ensemble adjustment Kalman filter for data assimilation. *Monthly Weather Review*, 129(12):2884–2903, 2001.
- [13] C. Andrieu, A. Doucet, and R. Holenstein. Particle Markov chain Monte Carlo methods. *Journal of the Royal Statistical Society: Series B (Statistical Methodology)*, 72(3):269–342, 2010.
- [14] S. Arridge, P. Maass, O. Öktem, and C.-B. Schönlieb. Solving inverse problems using data-driven models. *Acta Numerica*, 28:1–174, 2019.
- [15] M. Asch, M. Bocquet, and M. Nodet. *Data Assimilation: Methods, Algorithms, and Applications*, volume 11. SIAM, 2016.
- [16] M. Asim, M. Daniels, O. Leong, A. Ahmed, and P. Hand. Invertible generative models for inverse problems: mitigating representation error and dataset bias. In *International Conference on Machine Learning*, pages 399–409. PMLR, 2020.
- [17] A. Bain and D. Crisan. *Fundamentals of Stochastic Filtering*, volume 60. Springer Science & Business Media, 2008.
- [18] G. Bal. Introduction to Inverse Problems. *Lecture Notes-Department of Applied Physics and Applied Mathematics, Columbia University, New York*, 2012.
- [19] P. Bassiri, C. Holmes, and S. Walker. A general framework for updating belief distributions. *Journal of the Royal Statistical Society: Series B (Statistical Methodology)*, 78(5):1103–1130, 2016.
- [20] T. Bayes. An essay towards solving a problem in the doctrine of chances. *Philosophical transactions of the Royal Society of London*, 53:370–418, 1763.
- [21] B. M. Bell. The iterated Kalman smoother as a Gauss–Newton method. *SIAM Journal on Optimization*, 4(3):626–636, 1994.
- [22] B. M. Bell and F. W. Cathey. The iterated Kalman filter update as a Gauss–Newton method. *IEEE Transactions on Automatic Control*, 38(2):294–297, 1993.
- [23] A. Beskos, A. Jasra, K. J. H. Law, R. Tempone, and Y. Zhou. Multilevel Sequential Monte Carlo Samplers. *Stochastic Processes and their Applications*, 127(5):1417–1440, 1994.
- [24] P. Bickel, B. Li, and T. Bengtsson. Sharp failure rates for the bootstrap particle filter in high dimensions. In *Pushing the limits of contemporary statistics: Contributions in honor of Jayanta K. Ghosh*, pages 318–329. Institute of Mathematical Statistics, 2008.
- [25] D. Bigoni, Y. Chen, N. Garcia Trillos, Y. Marzouk, and D. Sanz-Alonso. Data-driven forward discretizations for Bayesian inversion. *Inverse Problems*, 36(10):105008, 2020.

-
- [26] C. H. Bishop, B. J. Etherton, and S. J. Majumdar. Adaptive sampling with the ensemble transform Kalman filter. Part I: Theoretical aspects. *Monthly Weather Review*, 129(3):420–436, 2001.
 - [27] C. M. Bishop. *Pattern Recognition and Machine Learning*, volume 128. Springer, 2006.
 - [28] D. M. Blei, A. Kucukelbir, and J. D. McAuliffe. Variational inference: A review for statisticians. *Journal of the American Statistical Association*, 112(518):859–877, 2017.
 - [29] D. Blömker, C. Schillings, and P. Wacker. A strongly convergent numerical scheme from ensemble Kalman inversion. *SIAM Journal on Numerical Analysis*, 56(4): 2537–2562, 2018.
 - [30] D. Blömker, C. Schillings, P. Wacker, and S. Weissmann. Well posedness and convergence analysis of the ensemble Kalman inversion. *Inverse Problems*, 35(8): 085007, 2019.
 - [31] M. Bocquet, J. Brajard, A. Carrassi, and L. Bertino. Bayesian inference of chaotic dynamics by merging data assimilation, machine learning and expectation-maximization. *arXiv preprint arXiv:2001.06270*, 2020.
 - [32] L. Bottou, F. E. Curtis, and J. Nocedal. Optimization methods for large-scale machine learning. *SIAM Review*, 60(2):223–311, 2018.
 - [33] S. Boyd, S. P. Boyd, and L. Vandenberghe. *Convex Optimization*. Cambridge University Press, 2004.
 - [34] J. Brajard, A. Carrassi, M. Bocquet, and L. Bertino. Combining data assimilation and machine learning to emulate a dynamical model from sparse and noisy observations: a case study with the lorenz 96 model. *Journal of Computational Science*, 44:101171, 2020.
 - [35] M. Branicki, A. J. Majda, and K. J. H. Law. Accuracy of some approximate Gaussian filters for the Navier–Stokes equation in the presence of model error. *Multiscale Modeling & Simulation*, 16(4):1756–1794, 2018.
 - [36] C. Brett, K. Lam, K. J. H. Law, D. McCormick, M. Scott, and A. M. Stuart. Accuracy and stability of filters for dissipative PDEs. *Physica D: Nonlinear Phenomena*, 245(1):34–45, 2013.
 - [37] J. Bröcker. Existence and uniqueness for four-dimensional variational data assimilation in discrete time. *SIAM Journal on Applied Dynamical Systems*, 16(1): 361–374, 2013.
 - [38] S. Brooks, A. Gelman, G. Jones, and X. Meng. Handbook of Markov chain Monte Carlo. *CRC Press*, 2011.

- [39] S. L. Brunton and J. N. Kutz. *Data-driven Science and Engineering: Machine Learning, Dynamical Systems, and Control*. Cambridge University Press, 2019.
- [40] M. F. Bugallo, V. Elvira, L. Martino, D. Luengo, J. Miguez, and P. M. Djuric. Adaptive importance sampling: The past, the present, and the future. *IEEE Signal Processing Magazine*, 34(4):60–79, 2017.
- [41] R. E. Caflisch. Monte Carlo and quasi-Monte Carlo methods. *Acta Numerica*, 7: 1–49, 1998.
- [42] E. Calvello, S. Reich, and A. M. Stuart. Ensemble Kalman Methods: A Mean Field Perspective. *arXiv*, 2022.
- [43] D. Calvetti and E. Somersalo. *An Introduction to Bayesian Scientific Computing: Ten Lectures on Subjective Computing*, volume 2. Springer Science & Business Media, 2007.
- [44] A. Carrassi, M. Bocquet, A. Hannart, and M. Ghil. Estimating model evidence using data assimilation. *Quarterly Journal of the Royal Meteorological Society*, 143(703):866–880, 2017.
- [45] A. Carrassi, M. Bocquet, L. Bertino, and G. Evensen. Data assimilation in the geosciences: An overview of methods, issues, and perspectives. *Wiley Interdisciplinary Reviews: Climate Change*, 9(5), 2018.
- [46] N. K. Chada. Analysis of hierarchical ensemble Kalman inversion. *arXiv preprint arXiv:1801.00847*, 2018.
- [47] N. K. Chada and X. T. Tong. Convergence acceleration of ensemble Kalman inversion in nonlinear settings. *arXiv preprint arXiv:1911.02424*, 2019.
- [48] N. K. Chada, M. A. Iglesias, L. Roininen, and A. M. Stuart. Parameterizations for ensemble Kalman inversion. *Inverse Problems*, 34(5):055009, 2018.
- [49] N. K. Chada, C. Schillings, and S. Weissmann. On the incorporation of box-constraints for ensemble Kalman inversion. *Foundations of Data Science*, 1(4): 433, 2019.
- [50] N. K. Chada, A. M. Stuart, and X. T. Tong. Tikhonov regularization within ensemble Kalman inversion. *SIAM Journal on Numerical Analysis*, 58(2):1263–1294, 2020.
- [51] N. K. Chada, Y. Chen, and D. Sanz-Alonso. Iterative ensemble Kalman methods: A unified perspective with some new variants. *Foundations of Data Science*, 3(3): 331–369, 2021.
- [52] S. Chatterjee and P. Diaconis. The sample size required in importance sampling. *The Annals of Applied Probability*, 28(2):1099–1135, 2018.

-
- [53] Y. Chen and D. Oliver. Ensemble randomized maximum likelihood method as an iterative ensemble smoother. *Mathematical Geosciences*, 44(1):1–26, 2002.
 - [54] Y. Chen, B. Hosseini, H. Owhadi, and A. M. Stuart. Solving and learning nonlinear PDEs with Gaussian processes. *Journal of Computational Physics*, 447:110668, 2021.
 - [55] Y. Chen, D. Sanz-Alonso, and R. Willett. Auto-differentiable ensemble Kalman filters. *SIAM Journal on Mathematics of Data Science*, 4(2):801–833, 2022.
 - [56] N. Chopin and O. Papaspiliopoulos. *An Introduction to Sequential Monte Carlo*. Springer, 2020.
 - [57] E. Cleary, A. Garbuno-Inigo, S. Lan, T. Schneider, and A. M. Stuart. Calibrate, emulate, sample. *Journal of Computational Physics*, 424:109716, 2021.
 - [58] T. J. Cocucci, M. Pulido, M. Lucini, and P. Tando. Model error covariance estimation in particle and ensemble Kalman filters using an online expectation–maximization algorithm. *Quarterly Journal of the Royal Meteorological Society*, 147(734):526–543, 2021.
 - [59] S. Cotter, M. Dashti, and A. M. Stuart. Approximation of Bayesian inverse problems for PDE’s. *SIAM Journal on Numerical Analysis*, 48(1):322–345, 2010.
 - [60] S. L. Cotter, G. O. Roberts, A. M. Stuart, and D. White. MCMC methods for functions: modifying old algorithms to make them faster. *Statistical Science*, pages 424–446, 2013.
 - [61] P. Craven and G. Wahba. Smoothing noisy data with spline functions. *Numerische mathematik*, 31(4):377–403, 1978.
 - [62] D. Crisan and A. Doucet. A survey of convergence results on particle filtering methods for practitioners. *Signal Processing, IEEE Transactions on*, 50(3):736–746, 2002.
 - [63] D. Crisan and B. Rozovskii. *The Oxford Handbook of Nonlinear Filtering*. Oxford University Press, 2011.
 - [64] D. Crisan, P. Moral, and T. Lyons. Discrete filtering using branching and interacting particle systems. *Université de Toulouse. Laboratoire de Statistique et Probabilités [LSP]*, 1998.
 - [65] G. Cybenko. Approximation by superpositions of a sigmoidal function. *Mathematics of control, signals and systems*, 2(4):303–314, 1989.
 - [66] M. Dashti and A. M. Stuart. Bayesian approach to inverse problems. *Handbook of Uncertainty Quantification*, pages 311–428, 2017.

- [67] M. Dashti, K. J. H. Law, A. M. Stuart, and J. Voss. MAP estimators and their consistency in Bayesian nonparametric inverse problems. *Inverse Problems*, 29(9):095017, 2013.
- [68] B. De Finetti. *Theory of Probability: A Critical Introductory Treatment*, volume 6. John Wiley & Sons, 2017.
- [69] P. Del Moral. *Feynman-Kac Formulae: Genealogical and Interacting Particle Systems with Applications*. Springer Science & Business Media, 2004.
- [70] P. Del Moral, A. Doucet, and A. Jasra. Sequential Monte Carlo samplers. *Journal of the Royal Statistical Society: Series B (Statistical Methodology)*, 68(3):411–436, 2006.
- [71] T. DelSole and X. Yang. State and parameter estimation in stochastic dynamical models. *Physica D: Nonlinear Phenomena*, 239(18):1781–1788, 2010.
- [72] A. P. Dempster, N. M. Laird, and D. B. Rubin. Maximum likelihood from incomplete data via the EM algorithm. *Journal of the Royal Statistical Society: Series B (Methodological)*, 39(1):1–22, 1977.
- [73] Ö. Deniz Akyildiz. Global convergence of optimized adaptive importance samplers. *arXiv preprint arXiv:2201.00409*, 2022.
- [74] J. E. Dennis Jr and R. B. Schnabel. *Numerical Methods for Unconstrained Optimization and Nonlinear Equations*. SIAM, 1996.
- [75] A. V. der Vaart. *Asymptotic Statistics*. Cambridge University Press, 1998.
- [76] R. DeVore, B. Hanin, and G. Petrova. Neural network approximation. *Acta Numerica*, 30:327–444, 2021.
- [77] J. Dick, F. Y. Kuo, and I. H. Sloan. High-dimensional integration: the quasi-monte carlo way. *Acta Numerica*, 22:133, 2013.
- [78] Z. Ding and Q. Li. Ensemble Kalman sampling: mean-field limit and convergence analysis. *arXiv preprint arXiv:1910.12923*, 2019.
- [79] J. L. Doob. Application of the theory of martingales. *Le calcul des probabilités et ses applications*, pages 23–27, 1949.
- [80] A. Doucet, S. Godsill, and C. Andrieu. On sequential Monte Carlo sampling methods for Bayesian filtering. *Statistics and Computing*, 10(3):197–208, 2000.
- [81] A. Doucet, N. d. Freitas, and N. Gordon. An introduction to sequential Monte Carlo methods. In *Sequential Monte Carlo methods in practice*, pages 3–14. Springer, 2001.

-
- [82] D. Dreano, P. Tandeo, M. Pulido, B. Ait-El-Fquih, T. Chonavel, and I. Hoteit. Estimating model-error covariances in nonlinear state-space models using Kalman smoothing and the expectation–maximization algorithm. *Quarterly Journal of the Royal Meteorological Society*, 143(705):1877–1885, 2017.
 - [83] C. Drovandi, R. G. Everitt, A. Golightly, D. Prangle, et al. Ensemble MCMC: accelerating pseudo-marginal MCMC for state space models using the ensemble Kalman filter. *Bayesian Analysis*, 2021.
 - [84] O. R. Dunbar, A. Garbuno-Inigo, T. Schneider, and A. M. Stuart. Calibration and uncertainty quantification of convective parameters in an idealized GCM. *Journal of Advances in Modeling Earth Systems*, 13(9):e2020MS002454, 2021.
 - [85] M. M. Dunlop. Multiplicative noise in Bayesian inverse problems: Well-posedness and consistency of MAP estimators. *arXiv preprint arXiv:1910.14632*, 2019.
 - [86] M. M. Dunlop, D. Slepčev, A. M. Stuart, and M. Thorpe. Large data and zero noise limits of graph-based semi-supervised learning algorithms. *Applied and Computational Harmonic Analysis*, 49(2):655–697, 2020.
 - [87] T. A. El Moselhy and Y. M. Marzouk. Bayesian inference with optimal maps. *Journal of Computational Physics*, 231(23):7815–7850, 2012.
 - [88] A. Emerick and A. Reynolds. Investigation of the sampling performance of ensemble-based methods with a simple reservoir model. *Computational Geosciences*, 17(2):325–350, 2013.
 - [89] H. England, M. Hanke, and A. Neubauer. *Regularization of Inverse Problems*. Springer Science and Business Media, 1996.
 - [90] O. Ernst, B. Sprungk, and H. Starkloff. Analysis of the ensemble and polynomial chaos Kalman filters in Bayesian inverse problems. *SIAM/ASA Journal on Uncertainty Quantification*, 3(1):823–851, 2015.
 - [91] G. Evensen. Sequential data assimilation with a nonlinear quasi-geostrophic model using Monte Carlo methods to forecast error statistics. *Journal of Geophysical Research: Oceans*, 99(c5):10143–10162, 1995.
 - [92] G. Evensen. *Data Assimilation: the Ensemble Kalman Filter*. Springer Science and Business Media, 2009.
 - [93] G. Evensen and P. V. Leeuwen. Assimilation of Geosat altimeter data for the Agulhas current using the ensemble Kalman filter with a quasigeostrophic model. *Monthly Weather Review*, 124(1):85–96, 1996.
 - [94] G. Evensen and P. J. Van Leeuwen. An ensemble Kalman smoother for nonlinear dynamics. *Monthly Weather Review*, 128(6):1852–1867, 2000.

- [95] G. Evensen, F. C. Vossepoel, and P. J. van Leeuwen. *Data Assimilation Fundamentals: A Unified Formulation of the State and Parameter Estimation Problem*. Springer, 2022.
- [96] A. Farchi and M. Bocquet. Comparison of local particle filters and new implementations. *Nonlinear Processes in Geophysics*, 25(4):765–807, 2018.
- [97] S. E. Fienberg. When did Bayesian inference become “Bayesian”? *Bayesian Analysis*, 1(1):1–40, 2006.
- [98] M. Fisher, J. Nocedal, Y. Trémolet, and S. Wright. Data assimilation in weather forecasting: a case study in PDE-constrained optimization. *Optimization and Engineering*, 10(3):409–426, 2009.
- [99] M. Fraccaro, S. Kamronn, U. Paquet, and O. Winther. A disentangled recognition and nonlinear dynamics model for unsupervised learning. *arXiv preprint arXiv:1710.05741*, 2017.
- [100] J. Franklin. Well-posed stochastic extensions of ill-posed linear problems. *Journal of Mathematical Analysis and Applications*, 31(3):682–716, 1970.
- [101] M. Frei and H. R. Künsch. Bridging the ensemble Kalman and particle filters. *Biometrika*, 100(4):781–800, 2013.
- [102] M. Gabrié, G. M. Rotskoff, and E. Vanden-Eijnden. Efficient Bayesian sampling using normalizing flows to assist Markov chain Monte Carlo methods. *arXiv preprint arXiv:2107.08001*, 2021.
- [103] D. Gamerman and H. Lopes. Markov chain Monte Carlo: stochastic simulation for Bayesian inference. *CRC Press*, 2006.
- [104] A. Garbuno-Inigo, F. Hoffmann, W. Li, and A. M. Stuart. Interacting Langevin diffusions: Gradient structure and ensemble Kalman sampler. *SIAM Journal on Applied Dynamical Systems*, 19(1):412–441, 2020.
- [105] A. Garbuno-Inigo, N. Nüsken, and S. Reich. Affine invariant interacting Langevin dynamics for Bayesian inference. *SIAM Journal on Applied Dynamical Systems*, 19(3):1633–1658, 2020.
- [106] N. Garcia Trillos and D. Sanz-Alonso. Continuum limits of posteriors in graph Bayesian inverse problems. *SIAM Journal on Mathematical Analysis*, 50(4):4020–4040, 2018.
- [107] N. Garcia Trillos and D. Sanz-Alonso. The Bayesian update: variational formulations and gradient flows. *Bayesian Analysis*, 15(1):29–56, 2020.
- [108] N. Garcia Trillos, Z. Kaplan, and D. Sanz-Alonso. Variational characterizations of local entropy and heat regularization in deep learning. *Entropy*, 21(5):511, 2019.

-
- [109] N. Garcia Trillos, Z. Kaplan, T. Samakhoana, and D. Sanz-Alonso. On the consistency of graph-based Bayesian semi-supervised learning and the scalability of sampling algorithms. *Journal of Machine Learning Research*, 21(28):1–47, 2020.
 - [110] A. Gelb, J. F. Kasper, R. A. Nash, C. F. Price, and A. A. Sutherland. *Applied Optimal Estimation*. MIT Press, 1974.
 - [111] A. Gelman, J. B. Carlin, H. S. Stern, D. B. Dunson, A. Vehtari, and D. B. Rubin. *Bayesian Data Analysis*. Chapman and Hall/CRC, 2013.
 - [112] M. Ghil, S. Cohn, J. Tavantzis, K. Bube, and E. Isaacson. Applications of estimation theory to numerical weather prediction. In *Dynamic Meteorology: Data Assimilation Methods*, pages 139–224. Springer, 1981.
 - [113] A. Gibbs and F. Su. On choosing and bounding probability metrics. *International Statistical Review*, 70(3):419–435, 2002.
 - [114] M. Giles. Multilevel Monte Carlo methods. *Acta Numerica*, 24:259–328, 2015.
 - [115] E. Gine and R. Nickl. *Mathematical Foundations of Infinite-dimensional Statistical Models*. Cambridge University Press, 2015.
 - [116] M. Giordano and R. Nickl. Consistency of Bayesian inference with Gaussian process priors in an elliptic inverse problem. *Inverse Problems*, 36(8):085001, 2020.
 - [117] F. Gland, V. Monbet, and V. Tran. Large sample asymptotics for the ensemble Kalman filter. *PhD Thesis*, 2009.
 - [118] I. Goodfellow, J. Pouget-Abadie, M. Mirza, B. Xu, D. Warde-Farley, S. Ozair, A. Courville, and Y. Bengio. Generative adversarial nets. *Advances in Neural Information Processing Systems*, 27, 2014.
 - [119] I. Goodfellow, Y. Bengio, and A. Courville. *Deep Learning*. MIT press, 2016.
 - [120] J. Goodman and J. Weare. Ensemble samplers with affine invariance. *Communications in applied mathematics and computational science*, 5(1):65–80, 2010.
 - [121] G. A. Gottwald and A. J. Majda. A mechanism for catastrophic filter divergence in data assimilation for sparse observation networks. *Nonlinear Processes in Geophysics*, 20(5):705–712, 2013.
 - [122] G. A. Gottwald and S. Reich. Supervised learning from noisy observations: Combining machine-learning techniques with data assimilation. *Physica D: Nonlinear Phenomena*, 423:132911, 2021.
 - [123] Y. Gu and D. S. Oliver. An iterative ensemble Kalman filter for multiphase fluid flow data assimilation. *Spe Journal*, 12(04):438–446, 2007.
 - [124] P. A. Guth, C. Schillings, and S. Weissmann. Ensemble Kalman filter for neural network based one-shot inversion. *arXiv preprint arXiv:2005.02039*, 2020.

- [125] E. Haber, F. Lucka, and L. Ruthotto. Never look back-A modified EnKF method and its application to the training of neural networks without back propagation. *arXiv preprint arXiv:1805.08034*, 2018.
- [126] M. Hairer, A. M. Stuart, and J. Voss. Signal processing problems on function space: Bayesian formulation, stochastic PDEs and effective MCMC methods. In *The Oxford Handbook of Nonlinear Filtering*, pages 833–873. Oxford University Press, 2011.
- [127] M. Hairer, A. M. Stuart, J. Voss, and P. Wiberg. Analysis of SPDEs arising in path sampling. Part I: The Gaussian case. *Communications in Mathematical Sciences*, 3(4):587–603, 2013.
- [128] M. Hairer, A. M. Stuart, and S. J. Vollmer. Spectral gaps for a Metropolis–Hastings algorithm in infinite dimensions. *The Annals of Applied Probability*, 24(6):2455–2490, 2014.
- [129] J. Hammersley and D. Handscomb. Percolation processes. *Monte Carlo Methods*, pages 134–141, 1964.
- [130] M. Hanke. A regularizing Levenberg-Marquardt scheme, with applications to inverse groundwater filtration problems. *Inverse Problems*, 13(1):79–95, 1997.
- [131] A. Hannart, A. Carrassi, M. Bocquet, M. Ghil, P. Naveau, M. Pulido, J. Ruiz, and P. Tandeo. Dada: data assimilation for the detection and attribution of weather and climate-related events. *Climatic Change*, 136(2):155–174, 2016.
- [132] J. Harlim, D. Sanz-Alonso, and R. Yang. Kernel methods for Bayesian elliptic inverse problems on manifolds. *SIAM/ASA Journal on Uncertainty Quantification*, 8(4):1414–1445, 2020.
- [133] J. Harlim, S. W. Jiang, S. Liang, and H. Yang. Machine learning for prediction with missing dynamics. *Journal of Computational Physics*, 428:109922, 2021.
- [134] J. Harlim, S. W. Jiang, H. Kim, and D. Sanz-Alonso. Graph-based prior and forward models for inverse problems on manifolds with boundaries. *Inverse Problems*, 38(3):035006, 2022.
- [135] A. Harvey. *Forecasting, Structural Time Series Models and the Kalman Filter*. Cambridge University Press, 1964.
- [136] W. K. Hastings. Monte Carlo sampling methods using Markov chains and their applications. *Biometrika*, 57(1):97–109, 1970.
- [137] K. Hayden, E. Olson, and E. Titi. Discrete data assimilation in the Lorenz and 2D Navier–Stokes equations. *Physica D: Nonlinear Phenomena*, 240(18):1416–1425, 2011.

-
- [138] T. Helin and M. Burger. Maximum a posteriori probability estimates in infinite-dimensional Bayesian inverse problems. *Inverse Problems*, 31(8):085009, 2015.
 - [139] M. Herty and G. Visconti. Kinetic methods for inverse problems. *Kinetic & Related Models*, 12(5):1109, 2019.
 - [140] G. E. Hinton and R. Zemel. Autoencoders, minimum description length and helmholtz free energy. *Advances in Neural Information Processing Systems*, 6, 1993.
 - [141] F. Hoffmann, B. Hosseini, A. A. Oberai, and A. M. Stuart. Spectral analysis of weighted Laplacians arising in data clustering. *Applied and Computational Harmonic Analysis*, 56:189–249, 2022.
 - [142] B. Hosseini. Well-posed Bayesian inverse problems with infinitely divisible and heavy-tailed prior measures. *SIAM/ASA Journal on Uncertainty Quantification*, 5(1):1024–1060, 2017.
 - [143] B. Hosseini and N. Nigam. Well-posed Bayesian inverse problems: Priors with exponential tails. *SIAM/ASA Journal on Uncertainty Quantification*, 5(1):436–465, 2017.
 - [144] P. L. Houtekamer and J. Derome. Methods for ensemble prediction. *Monthly Weather Review*, 123(7):2181–2196, 1995.
 - [145] P. L. Houtekamer and H. Mitchell. Data assimilation using an ensemble Kalman filter technique. *Monthly Weather Review*, 126(3):796–811, 1998.
 - [146] D. Z. Huang and J. Huang. Unscented Kalman inversion: efficient Gaussian approximation to the posterior distribution. *arXiv preprint arXiv:2103.00277*, 2021.
 - [147] D. Z. Huang, T. Schneider, and A. M. Stuart. Unscented Kalman inversion. *arXiv preprint arXiv:2102.01580*, 2021.
 - [148] D. Z. Huang, J. Huang, S. Reich, and A. M. Stuart. Efficient derivative-free Bayesian inference for large-scale inverse problems. *arXiv preprint arXiv:2204.04386*, 2022.
 - [149] D. Z. Huang, T. Schneider, and A. M. Stuart. Iterated Kalman methodology for inverse problems. *Journal of Computational Physics*, 463:111262, 2022.
 - [150] M. A. Iglesias. A regularizing iterative ensemble Kalman method for PDE-constrained inverse problems. *Inverse Problems*, 32(2):025002, 2016.
 - [151] M. A. Iglesias and Y. Yang. Adaptive regularisation for ensemble Kalman inversion. *Inverse Problems*, 37(2):025008, 2021.

- [152] M. A. Iglesias, K. J. H. Law, and A. M. Stuart. Ensemble Kalman methods for inverse problems. *Inverse Problems*, 29(4):045001, 2014.
- [153] M. A. Iglesias, K. Lin, and A. M. Stuart. Well-posed Bayesian geometric inverse problems arising in subsurface flow. *Inverse Problems*, 30(11):114001, 2014.
- [154] T. Ishizone, T. Higuchi, and K. Nakamura. Ensemble Kalman variational objectives: nonlinear latent trajectory inference with a hybrid of variational inference and ensemble Kalman filter. *arXiv preprint arXiv:2010.08729*, 2020.
- [155] A. Jacot, F. Gabriel, and C. Hongler. Neural tangent kernel: Convergence and generalization in neural networks. *Advances in Neural Information Processing Systems*, 31, 2018.
- [156] A. Jazwinski. *Stochastic Processes and Filtering Theory*. Courier Corporation, 2007.
- [157] A. Johansen and A. Doucet. A note on auxiliary particle filters. *Statistics and Probability Letters*, 78(12):1498–1504, 2008.
- [158] M. I. Jordan, Z. Ghahramani, T. S. Jaakkola, and L. K. Saul. An introduction to variational methods for graphical models. *Machine learning*, 37(2):183–233, 1999.
- [159] H. Kahn. *Use of different Monte Carlo sampling techniques*. Rand Corporation, 1955.
- [160] H. Kahn and A. W. Marshall. Methods of reducing sample size in Monte Carlo computations. *Journal of the Operations Research Society of America*, 1(5): 263–278, 1953.
- [161] J. Kaipio and E. Somersalo. *Statistical and Computational Inverse Problems*. Springer Science & Business Media, 160, 2006.
- [162] R. Kalman. A new approach to linear filtering and prediction problems. *Journal of Basic Engineering*, 82(1):35–45, 1960.
- [163] R. Kalman and R. Bucy. New results in linear filtering and prediction theory. *Journal of Basic Engineering*, 83(1):95–108, 1961.
- [164] E. Kalnay. *Atmospheric Modeling, Data Assimilation and Predictability*. Cambridge University Press, 2003.
- [165] N. Kantas, A. Beskos, and A. Jasra. Sequential Monte Carlo methods for high-dimensional inverse problems: a case study for the Navier Stokes equations. *SIAM Journal on Uncertainty Quantification*, 2(1):464–489, 2014.
- [166] R. Kawai. Adaptive importance sampling Monte Carlo simulation for general multivariate probability laws. *Journal of Computational and Applied Mathematics*, 319:440–459, 2017.

-
- [167] D. Kelly and A. M. Stuart. Ergodicity and accuracy of optimal particle filters for Bayesian data assimilation. *Chinese Annals of Mathematics, Series B*, 40(5): 811–842, 2019.
 - [168] D. Kelly, K. J. H. Law, and A. M. Stuart. Well-posedness and accuracy of the ensemble Kalman filter in discrete and continuous time. *Nonlinearity*, 27(10):2579, 2014.
 - [169] M. C. Kennedy and A. O’Hagan. Bayesian calibration of computer models. *Journal of the Royal Statistical Society: Series B (Statistical Methodology)*, 63(3):425–464, 2001.
 - [170] J. Kiefer and J. Wolfowitz. Stochastic estimation of the maximum of a regression function. *The Annals of Mathematical Statistics*, 23(3):462–466, 1952.
 - [171] H. Kim, D. Sanz-Alonso, and A. Strang. Hierarchical ensemble Kalman methods with sparsity-promoting generalized gamma hyperpriors. *arXiv preprint arXiv:2205.09322*, 2022.
 - [172] D. P. Kingma and P. Dhariwal. Glow: Generative flow with invertible 1x1 convolutions. *Advances in Neural Information Processing Systems*, 31, 2018.
 - [173] D. P. Kingma and M. Welling. Auto-Encoding Variational Bayes. In *2nd International Conference on Learning Representations*, 2014.
 - [174] B. Knapik, A. van der Vaart, and J. van Zanten. Bayesian inverse problems with Gaussian priors. *Annals of Statistics*, 39(5):2626–2657, 2011.
 - [175] N. Kovachki, Z. Li, B. Liu, K. Azizzadenesheli, K. Bhattacharya, A. Stuart, and A. Anandkumar. Neural operator: Learning maps between function spaces. *arXiv preprint arXiv:2108.08481*, 2021.
 - [176] N. B. Kovachki and A. M. Stuart. Ensemble Kalman inversion: A derivative-free technique for machine learning tasks. *Inverse Problems*, 35(9):095005, 2019.
 - [177] R. Krishnan, U. Shalit, and D. Sontag. Structured inference networks for non-linear state space models. In *Proceedings of the AAAI Conference on Artificial Intelligence*, 2017.
 - [178] E. Kwiatkowski and J. Mandel. Convergence of the square root ensemble Kalman filter in the large ensemble limit. *SIAM/ASA Journal on Uncertainty Quantification*, 3(1):1–17, 2015.
 - [179] S. P. Lalley. Beneath the noise, chaos. *The Annals of Statistics*, 27(2):461–479, 1999.
 - [180] S. Lasanen. Non-Gaussian statistical inverse problems. Part I: Posterior distributions. *Inverse Problems & Imaging*, 6(2):215–266, 2012.

- [181] S. Lasanen. Non-Gaussian statistical inverse problems. Part II: Posterior convergence for approximated unknowns. *Inverse Problems & Imaging*, 6(2):267, 2012.
- [182] J. Latz. On the well-posedness of Bayesian inverse problems. *SIAM/ASA Journal on Uncertainty Quantification*, 8(1):451–482, 2020.
- [183] K. J. H. Law and V. Zankin. Sparse online variational Bayesian regression. *arXiv preprint arXiv:2102.12261*, 2021.
- [184] K. J. H. Law, A. Shukla, and A. M. Stuart. Analysis of the 3DVAR filter for the partially observed Lorenz’63 model. *Discrete and Continuous Dynamical Systems*, 34(3):1061–1078, 2014.
- [185] K. J. H. Law, A. M. Stuart, and K. Zygalakis. *Data Assimilation*. Springer, 2015.
- [186] K. J. H. Law, D. Sanz-Alonso, A. Shukla, and A. M. Stuart. Filter accuracy for the Lorenz 96 model: Fixed versus adaptive observation operators. *Physica D: Nonlinear Phenomena*, 325:1–13, 2016.
- [187] T. A. Le, M. Igl, T. Rainforth, T. Jin, and F. Wood. Auto-encoding sequential Monte Carlo. *arXiv preprint arXiv:1705.10306*, 2017.
- [188] Y. Lee. l_p regularization for ensemble Kalman inversion. *SIAM Journal on Scientific Computing*, 43(5):A3417–A3437, 2021.
- [189] P. V. Leeuwen, Y. Cheng, and S. Reich. *Nonlinear Data Assimilation*. Springer, 2015.
- [190] M. S. Lehtinen, L. Paivarinta, and E. Somersalo. Linear inverse problems for generalised random variables. *Inverse Problems*, 5(4):599, 1989.
- [191] M. E. Levine and A. M. Stuart. A framework for machine learning of model error in dynamical systems. *arXiv preprint arXiv:2107.06658*, 2021.
- [192] G. Li and A. C. Reynolds. An iterative ensemble Kalman filter for data assimilation. In *SPE annual technical conference and exhibition*. Society of Petroleum Engineers, 2007.
- [193] C. Lieberman, C. Willcox, and O. Ghattas. Parameter and state model reduction for large-scale statistical inverse problems. *SIAM Journal on Scientific Computing*, 32(5):2535–2542, 2010.
- [194] T. Lindvall. *Lectures on the Coupling Method*. Springer, 2002.
- [195] J. S. Liu. *Monte Carlo Strategies in Scientific Computing*. Springer Science & Business Media, 2008.
- [196] A. Lorenc. Analysis methods for numerical weather prediction. *Quarterly Journal of the Royal Meteorological Society*, 112(474):1177–1194, 1986.

-
- [197] A. C. Lorenc, S. P. Ballard, R. S. Bell, N. B. Ingleby, P. L. F. Andrews, D. M. Barker, J. R. Bray, A. M. Clayton, T. Dalby, D. Li, et al. The Met. Office global three-dimensional variational data assimilation scheme. *Quarterly Journal of the Royal Meteorological Society*, 126(570):2991–3012, 2000.
 - [198] R. Lorentzen, R. Fjelde, J. FrØyen, A. Lage, G. Naevdal, and E. Vefring. Underbalanced and low-head drilling operations: Real time interpretation of measured data and operational support. *SPE Annual Technical Conference and Exhibition*, 2001.
 - [199] Y. Lu, A. M. Stuart, and H. Weber. Gaussian approximations for probability measures on \mathbb{R}^d . *SIAM/ASA Journal on Uncertainty Quantification*, 5(1):1136–1165, 2017.
 - [200] S. Lunz, O. Öktem, and C.-B. Schönlieb. Adversarial regularizers in inverse problems. *Advances in Neural Information Processing Systems*, 31, 2018.
 - [201] D. MacKay. *Information Theory, Inference and Learning Algorithms*. Cambridge University Press, 2003.
 - [202] C. J. Maddison, D. Lawson, G. Tucker, N. Heess, M. Norouzi, A. Mnih, A. Doucet, and Y. W. Teh. Filtering variational objectives. *arXiv preprint arXiv:1705.09279*, 2017.
 - [203] A. J. Majda and J. Harlim. *Filtering Complex Turbulent Systems*. Cambridge University Press, 2012.
 - [204] J. Mandel, L. Cobb, and J. D. Beezley. On the convergence of the ensemble Kalman filter. *Applications of Mathematics*, 56(6):533–541, 2011.
 - [205] J. Martin, L. Wilcox, C. Burstedde, and G. Omar. A stochastic Newton MCMC method for large-scale statistical inverse problems with application to seismic inversion. *SIAM Journal on Scientific Computing*, 34(3):A1460–A1487, 2012.
 - [206] L. Martino, V. Elvira, and F. Louzada. Effective sample size for importance sampling based on discrepancy measures. *Signal Processing*, 131:386–401, 2017.
 - [207] Y. Marzouk and D. Xiu. A stochastic collocation approach to Bayesian inference in inverse problems. *Communications in Computational Physics*, 6(4):826–847, 2009.
 - [208] Y. Marzouk, T. Moselhy, M. Parno, and A. Spantini. Sampling via measure transport: An introduction. *Handbook of Uncertainty Quantification*, pages 1–41, 2016.
 - [209] J. Mattingly, A. Stuart, and D. Higham. Ergodicity for PDE’s and approximations: locally Lipschitz vector fields and degenerate noise. *Stochastic Processes and Their Applications*, 101(2):185–232, 2002.

- [210] S. Metref, A. Hannart, J. Ruiz, M. Bocquet, A. Carrassi, and M. Ghil. Estimating model evidence using ensemble-based data assimilation with localization—The model selection problem. *Quarterly Journal of the Royal Meteorological Society*, 145(721):1571–1588, 2019.
- [211] N. Metropolis, A. W. Rosenbluth, M. N. Rosenbluth, A. H. Teller, and E. Teller. Equation of state calculations by fast computing machines. *The Journal of Chemical Physics*, 21(6):1087–1092, 1953.
- [212] S. Meyn and R. Tweedie. *Markov Chains and Stochastic Stability*. Springer Science and Business Media, 2012.
- [213] E. L. Miller and W. C. Karl. Fundamentals of Inverse Problems. *Not yet published*, 2003.
- [214] T. P. Minka. Expectation propagation for approximate Bayesian inference. *arXiv preprint arXiv:1301.2294*, 2013.
- [215] A. Moodey, A. Lawless, R. Potthast, and P. V. Leeuwen. Nonlinear error dynamics for cycled data assimilation methods. *Inverse Problems*, 29(2):025002, 2013.
- [216] M. Morzfeld, D. Hodyss, and C. Snyder. What the collapse of the ensemble Kalman filter tells us about particle filters. *Tellus A: Dynamic Meteorology and Oceanography*, 69(1):1283809, 2017.
- [217] C. Naesseth, S. Linderman, R. Ranganath, and D. Blei. Variational sequential Monte Carlo. In *International Conference on Artificial Intelligence and Statistics*, pages 968–977. PMLR, 2018.
- [218] N. H. Nelsen and A. M. Stuart. The random feature model for input-output maps between Banach spaces. *SIAM Journal on Scientific Computing*, 43(5): A3212–A3243, 2021.
- [219] A. Ng, M. Jordan, and Y. Weiss. On spectral clustering: Analysis and an algorithm. *Advances in Neural Information Processing Systems*, 14, 2001.
- [220] D. Nguyen, S. Ouala, L. Drumetz, and R. Fablet. Em-like learning chaotic dynamics from noisy and partial observations. *arXiv preprint arXiv:1903.10335*, 2019.
- [221] R. Nickl. Bernstein–von Mises theorems for statistical inverse problems I: Schrödinger equation. *Journal of the European Mathematical Society*, 22(8): 2697–2750, 2020.
- [222] R. Nickl. *Bayesian Non-linear Statistical Inverse Problems*. 2022. URL http://www.statslab.cam.ac.uk/~nickl/Site/_files/lecturenotes.pdf.
- [223] R. Nickl and G. Paternain. On some information-theoretic aspects of non-linear statistical inverse problems. *arXiv preprint arXiv:2107.09488*, 2021.

-
- [224] R. Nickl and J. Söhl. Bernstein–von Mises theorems for statistical inverse problems II: compound Poisson processes. *Electronic Journal of Statistics*, 13(2):3513–3571, 2019.
- [225] R. Nickl, S. van de Geer, and S. Wang. Convergence rates for penalised least squares estimators in PDE-constrained regression problems. *SIAM/ASA Journal on Uncertainty Quantification*, 8(1):374–413, 2020.
- [226] F. Nielsen and V. Garcia. Statistical exponential families: A digest with flash cards. *arXiv preprint arXiv:0911.4863*, 2009.
- [227] J. Nocedal and S. Wright. *Numerical Optimization*. Springer Science & Business Media, 2006.
- [228] D. Oliver, A. Reynolds, and N. Liu. *Inverse Theory for Petroleum Reservoir Characterization and History Matching*. Cambridge University Press, 2008.
- [229] L. Oljaca, J. Brocker, and T. Kuna. Almost sure error bounds for data assimilation in dissipative systems with unbounded observation noise. *SIAM Journal on Applied Dynamical Systems*, 17(4):2882–2914, 2018.
- [230] G. Ongie, A. Jalal, C. A. Metzler, R. G. Baraniuk, A. G. Dimakis, and R. Willett. Deep learning techniques for inverse problems in imaging. *IEEE Journal on Selected Areas in Information Theory*, 1(1):39–56, 2020.
- [231] H. Owhadi and C. Scovel. *Operator-Adapted Wavelets, Fast Solvers, and Numerical Homogenization: From a Game Theoretic Approach to Numerical Approximation and Algorithm Design*, volume 35. Cambridge University Press, 2019.
- [232] H. Owhadi, C. Scovel, T. J. Sullivan, M. McKerns, and M. Ortiz. Optimal uncertainty quantification. *SIAM Review*, 55(2):271–345, 2013.
- [233] H. Owhadi, C. Scovel, and T. J. Sullivan. Brittleness of Bayesian inference under finite information in a continuous world. *Electronic Journal of Statistics*, 9(1):1–79, 2015.
- [234] H. Owhadi, C. Scovel, and T. J. Sullivan. On the brittleness of Bayesian inference. *SIAM Review*, 57(4):566–582, 2015.
- [235] D. V. Patel and A. A. Oberai. GAN-Based Priors for Quantifying Uncertainty in Supervised Learning. *SIAM/ASA Journal on Uncertainty Quantification*, 9(3):1314–1343, 2021.
- [236] D. Paulin, A. Jasra, D. Crisan, and A. Beskos. On concentration properties of partially observed chaotic systems. *Advances in Applied Probability*, 50(2):440–479, 2018.

- [237] D. Paulin, A. Jasra, D. Crisan, and A. Beskos. Optimization based methods for partially observed chaotic systems. *Foundations of Computational Mathematics*, 19(3):485–559, 2019.
- [238] G. A. Pavliotis. *Stochastic Processes and Applications: Diffusion Processes, the Fokker-Planck and Langevin Equations*, volume 60. Springer, 2014.
- [239] K. Petersen and M. Pedersen. *The matrix cookbook*. Technical University of Denmark, 2008.
- [240] G. Peyré, M. Cuturi, et al. Computational optimal transport: with applications to data science. *Foundations and Trends® in Machine Learning*, 11(5-6):355–607, 2019.
- [241] J. Pidstrigach and S. Reich. Affine-invariant ensemble transform methods for logistic regression. *arXiv preprint arXiv:2104.08061*, 2021.
- [242] A. Pinkus. Approximation theory of the MLP model in neural networks. *Acta numerica*, 8:143–195, 1999.
- [243] F. Pinski, F. Simpson, A. M. Stuart, and H. Weber. Algorithms for Kullback–Leibler approximation of probability measures in infinite dimensions. *SIAM Journal on Scientific Computing*, 37(6):A2733–A2757, 2015.
- [244] F. Pinski, F. Simpson, A. M. Stuart, and H. Weber. Kullback–Leibler approximation for probability measures on infinite dimensional spaces. *SIAM Journal on Mathematical Analysis*, 47(6):4091–4122, 2015.
- [245] M. Pitt and N. Shephard. Filtering via simulation: Auxiliary particle filters. *Journal of the American Statistical Association*, 94(446):590–599, 1999.
- [246] M. Pulido, P. Tandeo, M. Bocquet, A. Carrassi, and M. Lucini. Stochastic parameterization identification using ensemble Kalman filtering combined with maximum likelihood methods. *Tellus A: Dynamic Meteorology and Oceanography*, 70(1):1–17, 2018.
- [247] A. Rahimi and B. Recht. Random features for large-scale kernel machines. *Advances in Neural Information Processing Systems*, 20, 2007.
- [248] A. Rahimi and B. Recht. Uniform approximation of functions with random bases. In *2008 46th Annual Allerton Conference on Communication, Control, and Computing*, pages 555–561. IEEE, 2008.
- [249] A. Rahimi and B. Recht. Weighted sums of random kitchen sinks: Replacing minimization with randomization in learning. *Advances in Neural Information Processing Systems*, 21, 2008.

-
- [250] M. Raissi, P. Perdikaris, and G. E. Karniadakis. Multistep neural networks for data-driven discovery of nonlinear dynamical systems. *arXiv preprint arXiv:1801.01236*, 2018.
 - [251] M. Raissi, P. Perdikaris, and G. E. Karniadakis. Physics-informed neural networks: A deep learning framework for solving forward and inverse problems involving nonlinear partial differential equations. *Journal of Computational physics*, 378: 686–707, 2019.
 - [252] R. Ranganath, S. Gerrish, and D. Blei. Black box variational inference. In *Artificial intelligence and statistics*, pages 814–822. PMLR, 2014.
 - [253] S. S. Rangapuram, M. Seeger, J. Gasthaus, L. Stella, Y. Wang, and T. Januschowski. Deep state space models for time series forecasting. In *Proceedings of the 32nd international conference on neural information processing systems*, pages 7796–7805, 2018.
 - [254] H. Rauch, C. Striebel, and F. Tung. Maximum likelihood estimates of linear dynamic systems. *AIAA Journal*, 3(8):1445–1450, 1965.
 - [255] F. Rawlins, S. P. Ballard, K. J. Bovis, A. M. Clayton, D. Li, G. W. Inverarity, A. C. Lorenc, and T. J. Payne. The Met Office global four-dimensional variational data assimilation scheme. *Quarterly Journal of the Royal Meteorological Society: A journal of the atmospheric sciences, applied meteorology and physical oceanography*, 133(623):347–362, 2007.
 - [256] P. Rebeschini and R. V. Handel. Can local particle filters beat the curse of dimensionality? *Annals of Applied Probability*, 25(5):2809–2866, 2015.
 - [257] S. Reich. A dynamical systems framework for intermittent data assimilation. *BIT Numerical Mathematics*, 51(1):235–249, 2017.
 - [258] S. Reich. Data assimilation: the Schrödinger perspective. *Acta Numerica*, 28: 635–711, 2019.
 - [259] S. Reich and C. Cotter. *Probabilistic Forecasting and Bayesian Data Assimilation*. Cambridge University Press, 2015.
 - [260] A. C. Reynolds, M. Zafari, and G. Li. Iterative forms of the ensemble Kalman filter. In *ECMOR X-10th European conference on the mathematics of oil recovery*, pages cp–23. European Association of Geoscientists & Engineers, 2006.
 - [261] D. Rezende and S. Mohamed. Variational inference with normalizing flows. In *International conference on machine learning*, pages 1530–1538. PMLR, 2015.
 - [262] H. Robbins and S. Monro. A stochastic approximation method. *The Annals of Mathematical Statistics*, 22(3):400–407, 1951.

- [263] C. Robert and G. Casella. *Monte Carlo Statistical Methods*. Springer Science & Business Media, 2013.
- [264] G. O. Roberts, J. S. Rosenthal, et al. Optimal scaling for various Metropolis-Hastings algorithms. *Statistical Science*, 16(4):351–367, 2001.
- [265] E. K. Ryu and S. P. Boyd. Adaptive importance sampling via stochastic convex programming. *arXiv preprint arXiv:1412.4845*, 2014.
- [266] J. Sacks, W. J. Welch, T. J. Mitchell, and H. P. Wynn. Design and analysis of computer experiments. *Statistical Science*, 4(4):409–423, 1989.
- [267] P. Sakov, D. S. Oliver, and L. Bertino. An iterative EnKF for strongly nonlinear systems. *Monthly Weather Review*, 140(6):1988–2004, 2012.
- [268] D. Sanz-Alonso. Importance sampling and necessary sample size: An information theory approach. *SIAM/ASA Journal on Uncertainty Quantification*, 6(2):867–879, 2018.
- [269] D. Sanz-Alonso and A. M. Stuart. Long-time asymptotics of the filtering distribution for partially observed chaotic dynamical systems. *SIAM/ASA Journal on Uncertainty Quantification*, 3(1):1200–1220, 2015.
- [270] D. Sanz-Alonso and A. M. Stuart. Gaussian approximations of small noise diffusions in Kullback-Leibler divergence. *Communications in Mathematical Sciences*, 15(7):2087–2097, 2017.
- [271] D. Sanz-Alonso and Z. Wang. Bayesian update with importance sampling: Required sample size. *Entropy*, 23(1):22, 2021.
- [272] D. Sanz-Alonso and R. Yang. The SPDE approach to Matérn fields: graph representations. *arXiv preprint arXiv:2004.08000*, 2020.
- [273] S. Särkkä. *Bayesian Filtering and Smoothing*, volume 3. Cambridge University Press, 2013.
- [274] L. J. Savage. *The Foundations of Statistics*. Courier Corporation, 1972.
- [275] C. Schillings and A. M. Stuart. Analysis of the ensemble Kalman filter for inverse problems. *SIAM Journal on Numerical Analysis*, 55(3):1264–1290, 2017.
- [276] C. Schillings and A. M. Stuart. Convergence analysis of ensemble kalman inversion: the linear, noisy case. *Applicable Analysis*, 97(1):107–123, 2018.
- [277] J. Schmidhuber. Deep learning in neural networks: An overview. *Neural networks*, 61:85–117, 2015.
- [278] T. Schneider, A. M. Stuart, and J.-L. Wu. Imposing sparsity within ensemble Kalman inversion. *arXiv preprint arXiv:2007.06175*, 2020.

-
- [279] J.-A. Skjervheim, G. Evensen, J. Hove, and J. G. Vabø. An ensemble smoother for assisted history matching. In *SPE Reservoir Simulation Symposium*. OnePetro, 2011.
 - [280] I. H. Sloan and H. Woźniakowski. When are quasi-Monte Carlo algorithms efficient for high dimensional integrals? *Journal of Complexity*, 14(1):1–33, 1998.
 - [281] R. C. Smith. *Uncertainty Quantification: Theory, Implementation, and Applications*, volume 12. SIAM, 2013.
 - [282] C. Snyder. Particle filters, the optimal proposal and high-dimensional systems. *Proceedings of the ECMWF Seminar on Data Assimilation for Atmosphere and Ocean*, pages 1–10, 2011.
 - [283] C. Snyder, T. Bengtsson, and M. Morzfeld. Performance bounds for particle filters using the optimal proposal. *Monthly Weather Review*, 143(11):4750–4761, 2015.
 - [284] C. Snyder, T. Bengtsson, P. Bickel, and J. L. Anderson. Obstacles to high-dimensional particle filtering. *Monthly Weather Review*, 136(12):4629–4640, 2016.
 - [285] Y. S. Soh and V. Chandrasekaran. Learning semidefinite regularizers. *Foundations of Computational Mathematics*, 19(2):375–434, 2019.
 - [286] Y. Song, J. Sohl-Dickstein, D. P. Kingma, A. Kumar, S. Ermon, and B. Poole. Score-based generative modeling through stochastic differential equations. *arXiv preprint arXiv:2011.13456*, 2020.
 - [287] A. S. Stordal, H. A. Karlsen, G. Nævdal, H. J. Skaug, and B. Vallès. Bridging the ensemble Kalman filter and particle filters: the adaptive Gaussian mixture filter. *Computational Geosciences*, 15(2):293–305, 2011.
 - [288] J. R. Stroud and T. Bengtsson. Sequential state and variance estimation within the ensemble Kalman filter. *Monthly Weather Review*, 135(9):3194–3208, 2007.
 - [289] J. R. Stroud, M. L. Stein, B. M. Lesht, D. J. Schwab, and D. Beletsky. An ensemble Kalman filter and smoother for satellite data assimilation. *Journal of the American Statistical Association*, 105(491):978–990, 2010.
 - [290] J. R. Stroud, M. Katzfuss, and C. K. Wikle. A Bayesian adaptive ensemble Kalman filter for sequential state and parameter estimation. *Monthly Weather Review*, 146(1):373–386, 2018.
 - [291] A. Stuart and A. Teckentrup. Posterior consistency for Gaussian process approximations of Bayesian posterior distributions. *Mathematics of Computation*, 87(310):721–753, 2018.
 - [292] A. M. Stuart. Inverse problems: a Bayesian perspective. *Acta Numerica*, 19:451–559, 2010.

- [293] A. M. Stuart and A. R. Humphries. *Dynamical Systems and Numerical Analysis*, volume 2. Cambridge University Press, 1998.
- [294] T. J. Sullivan. *Introduction to Uncertainty Quantification*, volume 63. Springer, 2015.
- [295] H. Sun and K. L. Bouman. Deep probabilistic imaging: Uncertainty quantification and multi-modal solution characterization for computational imaging. *arXiv preprint arXiv:2010.14462*, 9, 2020.
- [296] E. G. Tabak and E. Vanden-Eijnden. Density estimation by dual ascent of the log-likelihood. *Communications in Mathematical Sciences*, 8(1):217–233, 2010.
- [297] P. Tandeo, M. Pulido, and F. Lott. Offline parameter estimation using EnKF and maximum likelihood error covariance estimates: Application to a subgrid-scale orography parametrization. *Quarterly journal of the royal meteorological society*, 141(687):383–395, 2015.
- [298] A. Tarantola. *Inverse Problem Theory and Methods for Model Parameter Estimation*. SIAM, 2015.
- [299] A. Tarantola. Towards adjoint-based inversion for rheological parameters in nonlinear viscous mantle flow. *Physics of the Earth and Planetary Interiors*, 234: 23–34, 2015.
- [300] A. N. Tikhonov and V. Y. Arsenin. *Solutions of Ill-posed Problems*. Washington, Winston & Sons, 1977.
- [301] M. K. Tippett, J. L. Anderson, C. H. Bishop, T. M. Hamill, and J. S. Whitaker. Ensemble square root filters. *Monthly Weather Review*, 131(7):1485–1490, 2003.
- [302] S. Tokdar, S. Kass, and R. Kass. Importance sampling: a review. *Wiley Interdisciplinary Reviews: Computational Statistics*, 2(1):54–60, 2010.
- [303] X. T. Tong, A. J. Majda, and D. Kelly. Nonlinear stability of the ensemble Kalman filter with adaptive covariance inflation. *Nonlinearity*, 29(2):54–60, 2015.
- [304] X. T. Tong, A. J. Majda, and D. Kelly. Nonlinear stability and ergodicity of ensemble based Kalman filters. *Nonlinearity*, 29(2):657, 2016.
- [305] G. Ueno and N. Nakamura. Iterative algorithm for maximum-likelihood estimation of the observation-error covariance matrix for ensemble-based filters. *Quarterly Journal of the Royal Meteorological Society*, 140(678):295–315, 2014.
- [306] G. Ueno and N. Nakamura. Bayesian estimation of the observation-error covariance matrix in ensemble-based filters. *Quarterly Journal of the Royal Meteorological Society*, 142(698):2055–2080, 2016.

-
- [307] S. Ungarala. On the iterated forms of Kalman filters using statistical linearization. *Journal of Process Control*, 22(5):935–943, 2012.
 - [308] C. Villani. *Optimal Transport: Old and New*, volume 338. Springer, 2009.
 - [309] C. R. Vogel. *Computational Methods for Inverse Problems*. SIAM, 2002.
 - [310] U. Von Luxburg. A tutorial on spectral clustering. *Statistics and Computing*, 17(4):395–416, 2007.
 - [311] U. Von Luxburg, M. Belkin, and O. Bousquet. Consistency of spectral clustering. *The Annals of Statistics*, pages 555–586, 2008.
 - [312] G. Wahba. *Spline Models for Observational Data*. SIAM, 1990.
 - [313] M. J. Wainwright and M. I. Jordan. *Graphical Models, Exponential Families, and Variational Inference*. Now Publishers Inc, 2008.
 - [314] G. C. Wei and M. A. Tanner. A Monte Carlo implementation of the EM algorithm and the poor man’s data augmentation algorithms. *Journal of the American statistical Association*, 85(411):699–704, 1990.
 - [315] H. Wendland. *Scattered Data Approximation*, volume 17. Cambridge University Press, 2004.
 - [316] C. K. Williams and C. E. Rasmussen. *Gaussian Processes for Machine Learning*, volume 2. MIT press Cambridge, MA, 2006.

Alphabetical Index

Symbols

3DVAR, 117–121, 123, 143, 145, 147
4DVAR, 117, 121–123
 strong constraint, 121
 weak constraint, 121, 122

A

analysis, 99–101, 106–109, 119, 127–130, 135, 136, 143, 147, 150, 151
approximation, 174, 190, 191
auto-differentiation, 193, 201–203
autocorrelation, 81
autoencoder, 181–183, 191
 variational, 181, 182, 184

B

Bayes formula, 3, 15, 27, 135, 137
Bayes theorem, 14, 16, 17, 39, 55, 61–63, 66, 77, 97–100, 107, 136, 140, 144, 145, 173, 190, 193, 195
Bayesian, 3, 13, 15, 17, 18, 21, 26–28, 31, 37, 41, 44, 53, 55, 63, 91, 103, 117, 155, 170, 186, 191, 202
 brittleness, 28
 hierarchical, 40
 inference, 28, 32, 55, 191, 202
 inverse problem, 13, 17, 18, 26, 27, 53, 62, 65, 88, 96, 98, 173, 177, 189
 inversion, 31, 37, 39, 169, 174, 191
 statistics, 27
Bernoulli, 86, 90
Bernstein-von Mises theorem, 37
BPF, 136, 138–141, 143, 145, 150, 151
burn-in, 81

C

Cauchy-Schwarz inequality, 19, 21, 73, 99
clustering, 178, 191
coupling, 85, 87, 91, 179, 180, 182, 183
credible intervals, 15

D

data assimilation, 2–4, 15, 16, 18, 21, 37, 62, 67, 95, 102, 103, 115, 123, 155, 169, 193, 199, 201
data model, 95–97, 102, 103, 105, 115, 118, 119, 121, 146, 193, 194, 199–201
data-misfit, 155, 156, 158, 159, 161, 166, 170
detailed balance, 83, 84, 88, 89
Dirac, 3, 4, 15, 32, 66, 77, 135–137, 143, 148, 176, 179
dirac, 179
discrete Gronwall inequality, 25, 26, 121, 141
distance, 13, 18, 45, 55, 56, 72, 179
 between random probability measures, 65, 67, 138, 145
 Hellinger, 13, 18–21, 56, 57, 72, 101
 total variation, 13, 18–21, 56, 65, 72, 81, 87, 91, 95, 101, 179
 Wasserstein, 179
divergence, 55, 56, 60, 61, 76, 183
 χ^2 , 65, 71, 72, 74, 75, 150, 151
 Kullback-Leibler, 55, 56, 58, 61, 62, 72, 179, 183, 195, 196
dynamical system, 3, 103, 118, 121, 123, 128, 135, 136, 141, 142, 147, 151, 203

dynamics, 101–103, 106, 109, 115, 117, 119–121, 125, 136, 142, 143, 145, 170, 193–195, 198, 200–202
 deterministic, 102, 119, 121
 linear, 105, 106
 stochastic, 3, 135, 136, 143, 146

E

EM, 195–198, 202, 203
 EnKF, 125, 128, 129, 132, 202, 203
 EnKI, 171
 EnKI-SL, 158, 166, 167
 ergodicity, 79, 81, 85, 87, 90, 91
 ExKF, 125–128, 132
 ExKI, 158, 162, 163, 167
 expectation-maximization, 195, 199
 exponential family, 63

F

filtering, 18, 76, 95, 96, 99, 101, 102, 105, 115, 117, 118, 132, 135, 136, 143, 150, 151, 169, 193, 194, 198, 201–203
 distribution, 96, 99, 101, 102, 105, 106, 108, 111, 115, 117, 125, 128, 130, 133, 135, 138, 143, 200
 map, 137
 update, 137, 143
 forward
 error, 18
 map, 173, 181
 model, 2, 3, 13, 17, 21, 24, 27, 29, 37, 51, 117, 155, 174, 186, 191
 problem, 2
 uncertainty quantification, 28
 forward Euler method, 24

G

Gauss-Newton, 115, 155–160, 164–166, 169–171
 Gaussian, 3, 15, 27, 29, 30, 32, 33, 36, 37, 40, 42–45, 53, 55, 57, 59–63, 68, 71, 75, 85, 88, 89, 91, 103, 105, 106, 109, 111–113, 130, 135, 147, 150,

151, 156, 176–179, 183, 184, 189, 191, 194, 200, 203
 ansatz, 135, 200
 approximation, 15, 16, 29, 37, 57–59, 61, 62, 102, 125, 132, 169, 182, 200
 elimination, 113
 mixture, 15
 process, 173, 174, 176–178, 190, 191, 194
 truncated, 88
 generative adversarial network, 184, 191
 generative model, 27, 178, 184
 GOPF, 145, 146, 148, 151
 gradient descent, 39, 46, 47, 52, 193, 198, 199, 201
 stochastic, 39, 49, 50, 52, 59, 173, 183

I

i.i.d., 40, 45, 50, 52, 66, 67, 70, 81, 86, 90, 95, 105, 111, 120, 125, 129, 136, 137, 141, 143, 146, 148, 174, 175, 177, 178, 193
 IEnKF-SL, 158, 165, 166, 170
 IExKF, 158, 160–163, 166, 169
 ill-posed, 2, 158, 171
 importance sampling, 3, 5, 37, 65–67, 70–74, 76, 77, 135, 138, 145, 202, 203
 innovation, 108
 invariant distribution, 77–81, 83, 85–87
 inverse problem, 2–4, 17, 18, 21, 23, 26, 27, 29, 31, 37, 39, 46, 53, 55, 62, 65, 74, 88, 95, 96, 98, 108, 150, 155, 158, 159, 168–171, 173, 174, 178, 186, 188, 189, 191

J

Jensen inequality, 72, 195

K

Kalman filter, 102, 105, 106, 108, 109, 111, 115, 117–119, 126–130, 133, 135, 147
 auto-differentiable, 193, 200, 201
 ensemble, 5, 125, 128, 129, 151, 155, 200

-
- extended, 5, 125–127, 155, 200
 - iterative ensemble, 158, 165, 166, 170
 - iterative extended, 158, 160, 161
 - Kalman gain, 108, 109, 119, 127, 129, 159
 - Kalman inversion
 - ensemble, 158, 166, 167
 - extended, 158, 161, 162
 - Tikhonov ensemble, 158, 167, 168
 - Tikhonov extended, 158, 162, 163
 - Kalman smoother, 105, 111–113, 115
 - ensemble, 202
- L**
- Laplace distribution, 40, 42, 43
 - latent, 181, 182, 184, 191, 195, 202
 - Lebesgue, 4, 40, 42, 88, 90
 - Levenberg-Marquardt, 155–159, 161, 162, 164, 166, 167, 170, 171
 - likelihood, 3, 4, 14, 18, 21, 29, 31, 37, 40, 61, 66, 77, 88, 89, 97–100, 106, 130, 133, 144–146, 150, 174, 177, 186–189, 191, 195–198, 200, 202
 - randomized maximum, 132, 170
 - linear-Gaussian setting, 29, 31, 37, 40, 74, 105, 107, 108, 111, 113, 115, 130, 135, 150, 159, 169, 199
 - Lipschitz, 23, 24, 27, 50, 99, 138
 - loss, 31, 32, 39–41, 57, 60, 97, 98, 155, 169
- M**
- machine learning, 3, 4, 173, 178, 186, 193, 203
 - MAP estimator, 15, 16, 27, 30, 31, 39–42, 44, 45, 53, 113, 115, 117, 121, 156, 177, 191
 - Markov chain, 50, 52, 77–79, 81, 85–87, 91, 100, 106, 136
 - Monte Carlo, 3, 77
 - sampling, 77, 79
 - Markov inequality, 34
 - Markov kernel, 77–79, 82, 83, 85, 90, 136, 137, 144–146, 194
 - maximum likelihood estimation, 194, 195, 199–202
 - MCMC, 3, 5, 77, 79–81, 91, 173, 186, 199, 202
 - Metropolis-Hastings, 77, 81–85, 87, 88, 90
 - model error, 102, 103, 191
 - Monte Carlo, 60, 65–72, 74–77, 79, 81, 135, 145, 193, 198, 199, 202, 203
- N**
- neural network, 173, 174, 178, 181, 190, 191, 193, 194, 202
 - non-Gaussian, 27, 29, 53, 135
 - nonlinear least-squares, 155, 156, 161, 168
 - normalizing flow, 181, 184–186, 191
- O**
- objective, 31, 40–44, 47, 49–51, 59, 121, 122, 128, 155–166, 168, 170, 177, 183, 191
 - function, 50
 - observation, 2, 3, 16, 97, 100–103, 105, 106, 108, 109, 118, 120, 123, 135, 143, 146, 147, 150, 151, 193, 194
 - function, 98, 105, 117, 120, 121, 125, 128, 136, 139, 143, 145, 146
 - noise, 13, 17, 29, 31, 32, 35–37, 119, 151, 200
 - perturbed, 130
 - ODE, 23, 24
 - OPF, 143–147, 149–151
 - optimal transport, 179, 180, 191
 - Kantorovich, 179
 - Monge, 179
 - optimization, 2, 3, 15, 31, 37, 39, 41, 46, 49, 51–53, 55, 62, 109, 117, 118, 121, 128, 132, 155, 156, 158, 159, 162, 164, 168–170, 193, 198, 199
 - ordinary differential equation, 23, 103
- P**
- particle filter, 135, 142, 147–149, 151, 202
 - bootstrap, 135–138, 141, 143
 - Gaussianized optimal, 145, 148
 - optimal, 143, 148
 - pCN, 77, 81, 85, 87–91

- positive definite, 4, 29, 32, 46–50, 52, 57–60, 95, 102, 105–107, 113–115, 176
- posterior, 3, 5, 13–17, 22, 24, 27–37, 39–45, 55, 57, 61–63, 65, 66, 68, 71, 75, 77, 79, 88, 90, 91, 103, 108, 117, 150, 173, 177, 186–191, 202, 203
- consistency, 33–35, 37
- mean estimator, 15, 16, 30–32, 113
- prediction, 99–101, 106–108, 119, 126–130, 132, 135, 136, 143, 145, 147, 151
- prior, 3, 4, 14–16, 27–29, 31, 32, 34, 36, 37, 39–41, 53, 57, 61, 65, 66, 71, 75, 77, 88, 96–98, 103, 135, 150, 156, 173, 177, 187, 188, 190, 191
- proposal, 83, 88, 150
- distribution, 70, 72, 74, 76, 77, 150
- kernel, 81–83, 88, 89, 91
- pushforward, 178–181, 185, 189, 190
- R**
- random features, 173–176, 178, 190, 191, 194
- random walk Metropolis proposal, 91
- regularization, 27, 31, 53, 155, 156, 158, 168, 170, 171, 177
- representer theorem, 176
- resampling, 141, 142, 145, 147–151, 202
- S**
- sampling, 15, 16, 63, 91, 138, 143, 145, 148, 181, 191
- sequential importance resampling, 76, 135, 136
- sequential Monte Carlo, 169
- signal, 96, 102, 103, 117, 119, 122, 125, 194, 199, 201
- small noise limit, 17, 29, 31–35, 37, 62, 125, 151
- smoothing, 18, 21, 95–99, 101, 102, 105, 111, 115, 117, 121, 132, 135, 143, 194, 198, 201
- distribution, 96–98, 101, 105, 111–113, 117, 121
- state, 3, 83, 85, 86, 97, 102, 103, 105, 106, 108, 109, 118, 119, 121, 123, 128, 133, 169, 193–195, 198, 201–203
- state augmentation, 203
- state-space, 85, 91, 108, 130–132, 147, 190, 203
- continuous, 85, 87
- finite, 5, 85, 87, 90
- statistical linearization, 155, 164–167, 170
- stochastic dynamics model, 95–97, 100, 102, 105, 118, 119, 138, 142, 151, 193, 194, 199, 201
- supervised learning, 173, 174, 178, 190, 194
- T**
- target distribution, 62, 65–68, 70, 72, 74–77, 79, 81–85, 88, 89, 91, 150
- TEnKI, 171
- TEnKI-SL, 158, 168
- TExKI, 158, 163, 168
- Tikhonov-Phillips, 155, 156, 158–163, 165, 168, 170
- transport, 180, 181, 184, 190, 191
- measure, 178, 180, 182
- optimal, 178
- U**
- unsupervised learning, 173, 178, 189, 191
- V**
- variational, 53, 117
- autoencoder, 181, 182, 184
- Bayes method, 191
- Bayesian method, 62, 202, 203
- characterization of total variation, 20, 87
- data assimilation, 123
- formulation of Bayes theorem, 61–63, 173, 193, 195
- W**
- weak convergence, 4, 32, 56
- well-posed, 2, 3, 13, 17, 18, 21–23, 27, 95, 98, 101, 186–188, 190
- Woodbury matrix identity, 109, 159